VOLUME 1

NOVEL ROUTES TO HIGH PURITY OXIDES

BY

JEFFREY ADAMS

being a thesis submitted for the degree of Doctor of Philosophy in the Chemistry Department of the University of Glasgow.

FEBRUARY 1991

ProQuest LLC.
789 East Eisenhower Parkway
P.O. Box 1346
Ann Arbor, MI 48106 – 1346

VOLUME 1

CONTENTS

CHAPTER TWO:

ELECTRON MICROSCOPY

CHAPTER THREE:

EXPERIMENTAL

ACKNOWLEDGEMENT

I would like to thank my supervisors Dr. Thomas Baird (University of Glasgow) and Prof. Paul S. Braterman (University of North Texas) for their help, guidance and encouragement throughout the course of my research work. I must also thank Dr. David L. Segal (UKAEA Harwell Laboratory), Prof. James A. Cairns (University of Dundee) and Dr. John R. Fryer (University of Glasgow) for their valuable advice and suggestions.

Thanks are also due to the members of the electron microscopy centre, both past and present, for their useful discussions. Particular thanks must go to Dr. Martin J.F. Shevlin and Dr. Laura J. Butterly for their assistance with the transmission electron microscopes, Dr. Laurence Tetley and Ms Margaret Mullin for their assistance with the scanning electron microscopes, and especially to Mr. David Thom for his technical assistance and advice.

I would also like to express my gratitude to Mr. George Bruce for his assistance with the x-ray diffraction and Mr. George McCulloch for his assistance with the IR spectroscopy and thermogravimetric analysis.

I would also like to acknowledge the financial support given to me by the United Kingdom Atomic Energy Authority and the Science and Engineering Research Council.

DECLARATION

This thesis is a record of the work carried out by the author in the Department of Chemistry of the University of Glasgow, under the supervision of Dr. T. Baird and Prof. P.S. Braterman.

No part of this work has been submitted in any previous application for a degree.

Some of the work described in this thesis was presented at the Materials Research Society International Conference "Better Ceramics Through Chemistry III", held in Reno, Nevada in April 1988. This has subsequently been published in the conference proceedings;

"An Electron Microscopy Study of the Alkaline Hydrolysis Products of Tetraethoxysilane", Adams, J., Baird, T., Braterman, P.S., Cairns, J.A. and Segal, D.L., Mater. Res. Soc. Symp. Proc. 121, "Better Ceramics Through Chemistry III", (Brinker, C.J., Clark, D.E., Ulrich, D.R., Eds.), Mater. Res. Soc., Pittsburgh, (1988). p 361-366.

ABBREVIATIONS AND SYMBOLS

Within this thesis a number of abbreviations and symbols have been used to simplify the writing and to allow the use of mathematical formulae. A key to the meaning of the abbreviations and symbols used is given below. This is organised in the following fashion. First the abbreviations are listed then the symbols. In each case the list is in alphabetical order with those of the roman alphabet followed by those in the greek and then those which do not belong to either.

ABBREVIATIONS

cps	Counts per second
CRT	Cathode Ray Tube
DCCA	Drying Control Chemical Additive
EDS	Energy Dispersive Spectrometry
EELS	Electron Energy Loss Spectrometry
EPMA	Electron Probe Microanalysis
F	In relation to product morphology indicates fused
FTIR	Fourier Transform IR Spectrometry
HREM	High resolution electron microscopy
I	In relation to product morphology indicates irregular
IR	Infrared
log	Logarithm to the base ten

n	In relation to stereochemistry indicates normal
NA	Not Available
NMR	Nuclear Magnetic Resonance Spectrometry
OS	Over the Scale
PCTF	Phase Contrast Transfer Function
PVA	Polyvinyl Alcohol
RS	In relation to product morphology indicates roughly spherical
s	In relation to stereochemistry indicates secondary
S	In relation to product morphology indicates spherical
SAXS	Small angle x-ray scattering
SEM	Scanning Electron Microscope
S_N^1	Nucleophilic Substitution with one step
S_N^2	Nucleophilic Substitution with two steps
sym	Symmetrical
t	In relation to stereochemistry indicates tertiary
TBOS	Tetrabutylorthosilicate
TEM	Transmission Electron Microscope
TEOS	Tetraethylorthosilicate
TGA	Thermogravimetric Analysis
XRD	X-ray Diffraction

SYMBOLS

$A(s)$	Aperture Function
$A_f(u,v)$	Amplitude distribution in the back focal plane
$A_i(x,y)$	Amplitude distribution in the image plane

$A_o(x,y)$	Amplitude distribution of the transmitted wave at the exit plane of the specimen
C_c	Coefficient of chromatic aberration
C_s	Coefficient of spherical aberration
d	Periodicities or lattice spacing
D	Distance from optical axis at point where diffracted beam strikes the fluorescent screen
d_{min}	Scherzer cut-off
e	Charge on the electron
Et	Ethyl group
$E_\alpha(s)$	Envelope function due to partial coherence
$E_\epsilon(s)$	Envelope function due to chromatic fluctuations
F	Fourier transform
f_o	Focal length of the objective lens
$f_m(x_m)$	Relative frequency per unit interval in diameter
h	Planck's constant
$\hbar$	Planck's Constant divided by 2
h k l	Miller indices
i	Phase nature of object
I	In relation to electron microscopy indicates current supplied to lens
I	In relation to x-ray diffraction indicates intensity of diffracted beam
I_o	Intensity of strongest diffracted x-ray beam
I(r)	Intensity distribution in image plane
J_o	Zero order Bessel function
J_1	First order Bessel function

K_{α}	X-ray radiation produced by transition of an electron from the 2p orbital to the 1s orbital
L	Effective distance between diffracting lattices and fluorescent screen
m	Mass of the electron
M	In electron microscopy indicates magnification of the lens
M	In relation to chemical formulae indicates metal atom
n	In relation to size distribution is the number of measurements
n	Integer
n_m	In relation to size distribution is the number of measurements within an interval
OEt	Ethoxy group
OR	Alkoxy group
P	Integer
pH	Negative log to the base ten of the hydrogen ion activity
pK_b	Negative log to the base ten of the dissociation constant of the base
r	Indicates real space coordinates
R	Alkyl group
s	In electron microscopy indicates reciprocal space coordinates
s	In relation to stereochemistry indicates secondary
S_n	Adjusted root mean square deviation

$\sin\chi(s)$	Phase contrast transfer function
$\sin\chi(s)_{\alpha.\epsilon}$	PCTF modified for partial coherence and chromatic fluctuations
T_c	Temperature at which material becomes superconducting
u,v	Coordinates perpendicular to the optical axis in the back focal plane
V	Voltage supplied to lens
w	Relativistically corrected accelerating voltage
w/w	Weight for weight
x	Measured value
x	In relation to chemical formulae indicates an integer
x_m	Measured diameter
X_n	Arithmetic mean from n measurements of x
x,y	Coordinates perpendicular to the optical axis in the object plane
α	Specimen illumination angle
$\alpha(s)$	Scattering angle pertaining to reciprocal space coordinates (s)
δ	Interaction constant
$\delta(s)$	Primary undeviated wave amplitude
γ_{SL}	Interfacial energy of the solid liquid interface
γ_{sv}	Interfacial energy of the solid vapour interface
Δf	Defocus value of lens
$\Delta f'$	Optimum defocus value of lens
ΔI	Fluctuation in current

ΔV	Fluctuation in voltage
Δx	Interval in diameter
ϵ	Focal variation due to high voltage and current fluctuations
θ	Angle of incidence of x-ray beam
λ	Wavelength of the x-ray or electron beam
π	Mathematical constant pi
$\varphi(r)$	Electrostatic potential within the sample
$\chi(s)$	Instrumental phase adjustment factor
$\psi(\underline{r})$	Wave function
$\psi_D(s)$	Scattered wave amplitude in the back focal plane
$\psi_o(r)$	Transmitted amplitude of objective wave
∇^2	The Laplacian

SUMMARY

Advances in the applications of ceramic material presently being introduced require products with chemical and physical properties tailored to the particular application. To attain the high standards necessary, a number of new methods of producing ceramics have been developed. One of these, organo-sol-gel processing, is the subject of the work described here. Silica is produced by the hydrolysis of tetraethylorthosilicate and the properties of the product are related to the reaction conditions leading to its production. Because the reaction is catalysed by both acid and base, the results are significantly different in each case, the two systems are dealt with separately. Under base catalysis the product morphology may be of interest as a support for metal catalysts so a third section deals with the incorporation of nickel compounds within the silica.

The first section of the thesis deals with reactions prepared under neutral or acidic conditions. These conditions lead to the formation of clear rigid gels. The material was studied both during and after completion of the reaction by x-ray diffraction, infrared spectroscopy, thermogravimetric analysis, microanalysis, transmission electron microscopy and electron diffraction. The x-ray diffraction results were those of amorphous material and did not alter significantly on alteration of the reaction composition. Similarly the microanalysis and TGA results were not sensitive to alterations in the reaction conditions. The infrared spectra suffered from a similar problem giving the spectra of silica with

little difference, but in a few cases peaks corresponding to carbonyl groups appear and may indicate the catalytic activity of the silica. TEM and electron diffraction were the most useful techniques.

A number of sample preparation methods were used including dispersion in water or organic solvents, preparation of films, freeze drying, thin sectioning, removal of small areas by contact and staining with uranyl acetate. These all gave similar results where the product appeared to be small particles which form chains and 3D networks or material which forms plate-like areas of sample which appeared layered in nature. A number of these areas, especially the latter type, appeared crystalline when examined by electron diffraction but the patterns do not correspond to any known form of silica; this may indicate the formation of a crystalline hydrated silica. However it is not possible to determine the extent to which the preparation method influenced the observed morphology.

The second section deals with the production of silica when the reaction is carried out under basic conditions. The reaction produced three distinct types of product; weak gels, colloidal dispersions and precipitates. The material was studied both during and after completion of the reaction by techniques including infrared spectroscopy, transmission and scanning electron microscopy. The product morphologies included small particles which aggregate to form 3D networks thus forming a gel, large particles of irregular shape which precipitate out of the reaction, and particles of spherical or near spherical shape with

diameters up to 400nm. The size of these particles altered depending on the reaction conditions used to form them. Comparison of the size variation and particle growth rates with variations predicted from possible effects of the concentration changes on the rates of reaction and solvent properties indicate a possible nucleation and growth mechanism. The effect of including an ionic salt or polymer in the reaction support the growth mechanism proposed. Reactions employing tetrabutylorthosilicate in place of the tetraethylorthosilicate produced particles of diameter up to 1.2μm. The alteration with size, both within the tetrabutylorthosilicate reactions and in comparison with the tetraethylorthosilicate reactions, again supports the proposed mechanism. The observations also included SEM which indicated the solids formed by settling of spheres correspond to the structure of natural opal providing a dense solid with an iridescent sheen.

The third section deals with the deposition of nickel complexes within the silica spheres as they grow. The original method was to deposit nickel bis(dimethylglyoximate) formed from the reaction of diacetyl, hydroxylamine and a nickel salt. However the presence of the ionic nickel salt altered the morphology of the silica and a nickel hydroxylamine chloride complex was precipitated, thus leading to the formation of particles including nickel hydroxylamine complex and silica. Alteration of the reaction to eliminate all chloride irons prevented the formation of the nickel hydroxylamine chloride complex and and allowed nickel bis(dimethylglyoximate) to be deposited. However examination of the product showed this to be

unsuitable as a source of nickel due to the sublimation of nickel bis(dimethylglyoximate).

Subsequent methods deposited the nickel hydroxylamine chloride complex on the silica but this again altered the morphology of the silica. By delaying the addition of reagents to deposit the nickel complex the silica was produced as spherical particles with a coating of nickel complex on the outer surface. In all cases the products were calcined in air to determine the calcination products and the location of the nickel. The reaction products and the calcination products were characterised by x-ray diffraction, infrared spectroscopy, microanalysis, TGA, and TEM. The same techniques were employed to follow the decomposition of the nickel complexes.

1. INTRODUCTION

1.1 INTRODUCTION

In the introductory chapter of their book Kingery, Bowen and Ulmann (1976) define ceramics as "solid articles which have as their essential component, and are composed in large part of, inorganic nonmetallic material", a definition which includes pottery, porcelain, refractories, clays, nonmetallic magnetic materials, glasses, cements, abrasives, high temperature superconductors and a large number of other materials and industrial products. This wide range of materials indicates the importance of ceramics in both industry and every day life.

In the recent past the production of ceramics was largely a matter of trial and error with procedures and compositions unchanging from those known to give an adequate product. This approach to the production of ceramics has several drawbacks. The first is that the effort and cost of development of one ceramic can not be used as a basis for the development of a new product (Barringer and Bowen, 1985). The second drawback is that the lack of understanding inherent in such a system make it impossible to predict properties. Therefore it would be necessary to produce and test every possible composition in order to find the available and optimum properties of ceramics. This is, of course, not possible and therefore there are probably many useful ceramics as

yet undiscovered. An excellent example of this was the recent discovery of ceramic oxides which became superconducting at relatively high temperatures (Bednorz and Müller, 1986) a property not previously imagined.

The trial and error production techniques were due to a lack of knowledge of the underlying structures and processes occurring. However the more advanced and technologically demanding applications of ceramics now being employed require products with chemical and physical properties tailored to the application, and production methods which can supply well characterised ceramics of predetermined structure, composition and properties. These requirements have lead to the development of a number of processes for the production of precursors to ceramics, for example (Segal, 1989(a)) polymer pyrolysis, hydrothermal reactions, pyrolysis of metal alkoxides, flame hydrolysis and sol-gel processing, which give greater control of the product. However these processes are, compared to the history of ceramics, relatively new and as yet not fully understood. Although these new production techniques are still an area of active research there are a large number of industrial applications already (Klein, 1988; Segal, 1989(a)).

1.2 COLLOIDAL DISPERSIONS

A colloidal dispersion (Everett, 1988; Hunter, 1987) is a system in which one component (the disperse or discontinuous phase) is uniformly distributed throughout the second component (the dispersion medium or continuous phase) where the dispersed

phase has at least one dimension in the range 1-1000nm.

This is an extremely important state of matter and covers a large number of materials. Depending on whether the dispersed phase and the dispersion medium are solid, liquid or gas the resultant dispersion could be sols, aerosols, gels, foam or emulsion. Examples of such dispersions include smoke, fog, mist, aerosol sprays, paint, some alloys, blood, milk, bone, expanded plastic, certain glasses and many more.

The work of this project will deal mainly with sols - dispersions of solid particles in a liquid medium - and therefore the following discussion will be based on that system although it is generally applicable to most colloidal systems.

These dispersions are stable (they do not settle due to gravity) because of several forces which interact within the system. The first of these is the London or Van der Waals force. In any atom or molecule the electron cloud undergoes fluctuations and these fluctuations give rise to a temporary dipole. This dipole will create an electric field which will polarise any neighbouring atoms creating a secondary dipole. The interaction of these dipoles causes an attractive electrostatic force between the two atoms.

The second force which occurs is the Born repulsion. The force arises from the interaction of the electron clouds of the molecules as they come close to one another. This gives rise to a repulsive force between the two molecules which falls off rapidly with separation and is extremely large when the electron clouds interpenetrate.

In dealing with particles in the colloidal size range it is necessary to take account of the fact that they are not single atoms or molecules. This is done by calculating the interaction of each molecule in one particle with each molecule in the other particle in relation to the two forces described above.

The last force which is normally a consideration is electrostatic repulsion. In many sols the particles have a charged surface. This can occur in a number of ways:

(a) **Ionisation of surface groups.** If the solid material contains acidic or basic groups they will, depending on the pH of the solution, ionise to produce a positive or negative charge. For example silica particles have Si-OH groups on the surface which under basic conditions ionise to form $Si-O^-$ and give the surface a negative charge. The magnitude of the surface charge depends on the acid/base strength of the surface groups and the pH of the solution. It is possible to reduce the surface charge to zero (the point of zero charge) by varying the pH.

(b) **Differential solution.** If one of the ions which makes up the solid dissolves in the solution preferentially it will leave an excess of the oppositely charged ions on the surface and thus produce a surface charge.

(c) **Isomorphous substitution.** If one of the ions in the solid can be replaced by an ion with a different charge then the neutrality of the surface will be destroyed. This can occur in

(d) **Charged crystal surfaces.** In producing the colloid it is possible that a crystal is broken and species are exposed which can form a charge. This again occurs in clays.

(e) **Specific ion absorption.** Surfactant ions may be absorbed onto the surface and thus produce a charge on the surface.

In the work carried out in this project the main charge forming process which is involved in the ionisation of the surface groups.

In electrolyte solution the electric charge on the surface of the particle causes a higher concentration of ions of an opposite charge near the surface. This is called the diffuse electrical double layer and the thickness of this double layer depends on the concentration of the electrolyte solution.

This charge on the particle surface causes a repulsive force between the particles. This can be considered as arising from the interaction of the double layers as they approach and, as they hold the same charge, the interaction will be repulsive. It can also be considered that as the particles approach, the double layers which balanced the charge of the particles no longer properly shield the charges on the particles and an electrostatic repulsion becomes apparent.

When all of the forces between the particles are considered together an interaction potential curve can be obtained. The form of this varies with the system but a common form is shown (fig.1.1).

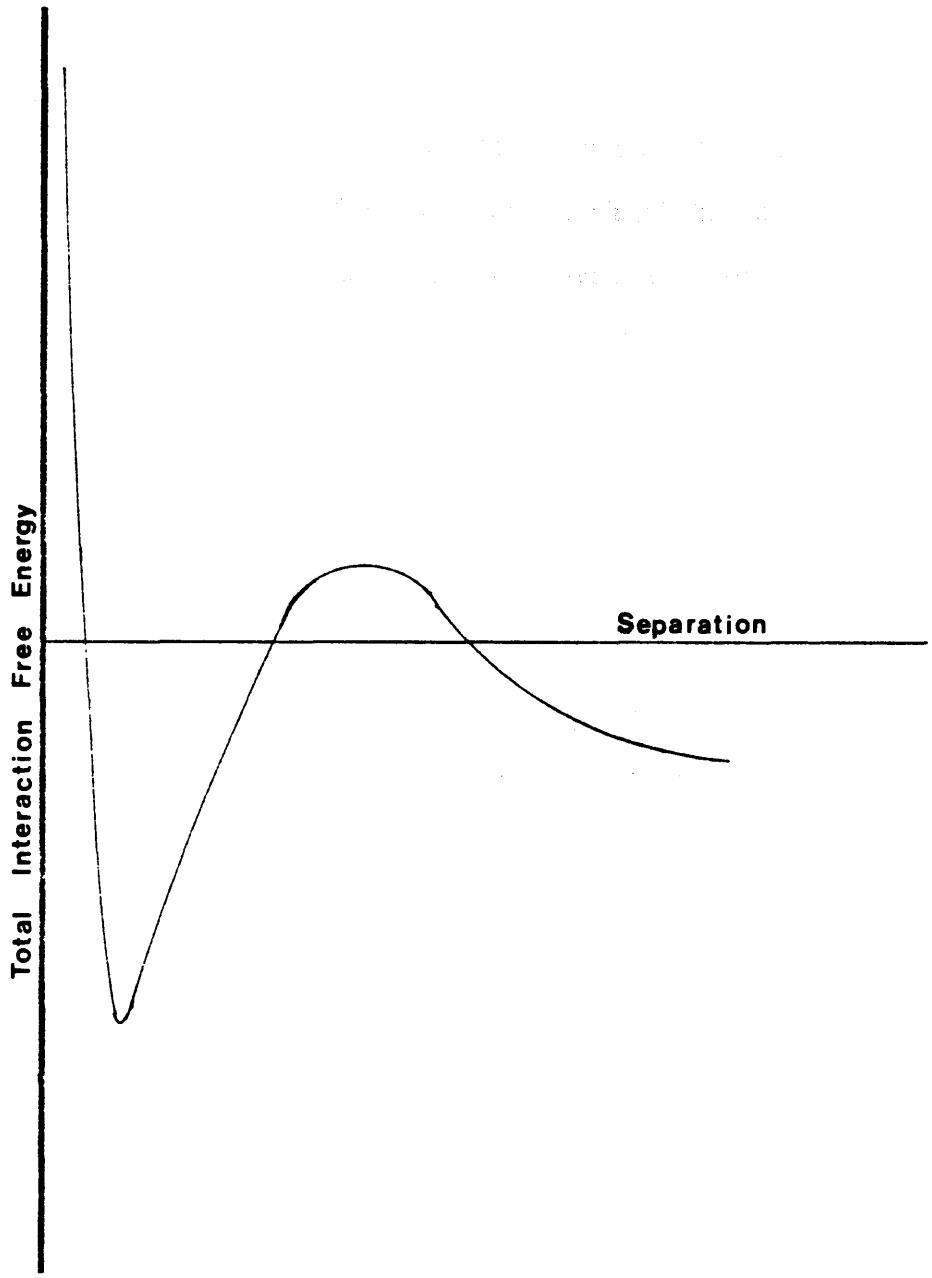

Fig. 1.1: Potential energy curve for approaching colloidal particles.

From this it is clear that there is a barrier to the close approach of the particles due to the Born repulsion. At further separation there is a minimum caused by the London forces and at further separation still there is a second barrier caused by the double layer interaction. If this barrier is much higher that the thermal energy held by the particles it is unlikely that any will surmount it and fall into the minimum and the suspension will be stable. If however the barrier is low or (as is possible) does not exist the particles enter the primary minimum, thus are then very difficult to separate.

In many cases a secondary minimum occurs at slightly greater separation than the barrier but particles which aggregate in this region can be separated by mechanical means, changing the composition of the liquid or even by Brownian motion of the solution.

The height of the energy barrier is affected by the concentration of the electrolyte. Increasing the concentration of the electrolyte decreases the thickness of the diffuse double layer and thus lowers the height of the barrier. Thus by increasing the electrolyte concentration the colloid can be made unstable and will coagulate.

Although the above discussion outlines the forces which occur in a colloidal system under the conditions most often used in this project there is one other stabilising effect which can arise. This is a repulsive force which occurs because of absorbed layers on the colloidal particles (Napper, 1982). If the absorbed layer is a polymer then, as the particles approach, the polymer

layers on the particles will interpenetrate. This has two effects (a) because of the high concentration of polymer in the interparticle region, osmotic effects will cause liquid to diffuse into the region and (b) the interpenetration of the polymer chains causes a reduction in the entropy of the system, and leads to an increase in the free energy and thus promotes separation. The actual value of the repulsion depends on a large number of factors such as the amount of polymer and how it attaches to the surface.

The above discussion describes why colloidal dispersions such as sols are stable. However when this stability is destroyed the product is often a gel. A gel is a solid which contains a fluid, such that both the solid and fluid components are highly dispersed and the solid provides a sufficient structural framework to provide rigidity. This is often formed when the attractive forces between the disperse phase are strong enough to provide a rigid structure. The disperse phase may be solid particles or polymer molecules and the attractive forces may be Van der Waals attraction or chemical bonds.

1.3 SOL-GEL PROCESSING

1.3.1 INTRODUCTION

Sol-gel processing is a method of producing oxides and less commonly carbides and nitrides which involves the formation of, or use of sols and/or gels.

Although techniques which would now be termed sol-gel

processes were used as early as the 1930s (Geffcken and Berger, 1939; Ewell and Insley, 1935) it is generally accepted that sol-gel processing as an independent process appeared in the early 1960s. At this time the oxide fuel for nuclear reactors was prepared by conventional ceramic processing techniques involving mixing powders, granulating, pressing and sintering at ≈1600°C. These operations did not lend themselves to the remote operation in shielded facilities necessary in the nuclear industries and the radioactive dust produced was a serious problem.

Research at nuclear establishments and associated industries (Hermans, 1964; Ferguson et al, 1964) developed sol-gel processing as a method of producing nuclear fuel which eliminated the radioactive dust hazard and could easily be remotely handled. It also had the advantages that the product could be sintered at 1100°C and that the shape of the oxide product could be determined. Therefore the product could be formed as spherical particles which were suitable for vibrocompaction of fuel rods (Segal, 1984).

The processes which had been developed were what are now termed conventional or aqueous sol-gel processing. This interest in advanced methods of preparing ceramic materials led to the organo sol-gel process. This process stems from work carried out on the preparation of minerals (Roy, 1956; Roy and Roy, 1955) in which metal alkoxides were used to form oxides. The results of this work showed that this system had considerable promise for the formation of ceramic materials. This led to the adoption of the alkoxide based reaction by persons working in the sol-gel field.

In fact this process is so versatile that since 1980 nearly all of the publications in the field of sol-gel processing have related to organo sol-gel processing (Segal, 1985(a))

1.3.2 CONVENTIONAL SOL-GEL PROCESSING

The process can be represented schematically as follows (Woodhead, 1972)

Starting Material ⟶ Dispersible Oxide ⟶ Sol ⟶ Gel ⟶ Oxide

In describing the process it is easiest to examine the main steps individually.

There are many methods of preparing inorganic sols but those of most frequent use in this process are the following.

1. Solvent Extraction

In this method aqueous solutions of hydrolysable cations are reacted with long chain amines. These amines are dissolved in water immiscible solvents and react to remove the anion as the hydrolytic acid. For example (Woodhead, 1975) titanium (IV) chloride reacts

$$pTiCl_{4(aq)} + pnH_2O \longrightarrow [Ti(OH)_nCl_{4-n}]_p + HCl$$

By mixing the aqueous solution with a solution of Primene JMT (Rohm & Hass product, $R_3C\text{-}NH_2$, $C_{18}<R<C_{22}$) in an immiscible organic phase eg 1,1,1-trichloroethane the hydrolytic acid, in this case

hydrochloric, is removed from the aqueous phase as, in this case, the amine chloride and the hydrolysis reaction promoted. When the hydrolysis has proceeded sufficiently (and the anion concentration fallen) the insoluble oxide separates out.

This method has been used (Segal, 1980; Woodhead, 1984) in the formation of sols of Cr(III), Al(III), Fe(III), and Zr(IV).

2. Deaggregation

It has long been known (and used in analytical chemistry) that the hydroxides of many transition metals and group III, IV, V metals such as aluminium precipitate out of aqueous solutions as a gelatinous mass. This mass is constituted of small primary particles of colloidal dimensions. Thus, by reacting an appropriate solution of the element with a basic solution, commonly ammonium hydroxide, colloidal particles of the hydroxide or hydrous oxide are formed. Addition of acid to the precipitate establishes an electrostatic repulsion between the particles by the absorption of H^+ ions onto the surface. This causes the particles to deaggregate and form a sol in a process usually called peptisation.

This technique has been employed for the production of sols of alumina (Ramsay and Daish, 1978), titania, indium oxide (Segal and Woodhead, 1986), ceria (Woodhead, 1974) and thoria (Hermans, 1964).

3. Thermal Decomposition of Salts.

A number of metal salts decompose on heating to give the oxide or

hydroxide which can then be dispersed in water to give a sol. Examples of this type of salt are hydrated thorium nitrate and thorium oxalate (Ferguson et al, 1964; Woodhead, 1972).

These are the main methods of forming oxide or hydrous oxide sols for the aqueous sol-gel process. It is at this point of the process that a number of properties of the product can be determined. For example if the sol is prepared in such a manner that the particles are aggregated to some extent this aggregation will prevent dense packing in the gel and the final product will have a higher porosity and lower density for a given firing temperature than if the sol particles were not aggregated (Woodhead, 1984; Nelson et al, 1981; Ramsay and Avery, 1986). It is also possible, by mixing two different sols at this stage, that mixed oxide ceramics can be formed (Segal and Woodhead, 1986).

If colloidal carbon is mixed with the sol at this point careful heating in an argon or carbon dioxide atmosphere can produce metal carbides (Ferguson et al, 1964) or with further heating in nitrogen and/or ammonia can lead to metal nitrides (Woodhead, 1984).

The next step in the process is to convert the sol to a gel and this can be done in a number of methods depending on the desired product. However the different methods can be classified into two main groups (a) the removal of water and (b) destabilisation of the sol, usually by removing the stabilising ion.

The simplest method of gelling the sol by dehydration is to evaporate the liquid by drying in trays at up to 105°C (Ferguson

et al, 1964). However this gives a fragmented material which is not often desirable. A more desirable product is spherical particles and these can be formed by a number of gelling techniques (Segal, 1984; Woodhead, 1984).

1. **Chemical Dehydration**

The aqueous sol is dispersed in an immiscible hydrophilic solvent, such as 2-ethyl hexanol, as small droplets. Water transfers from the sol droplets to the solvent causing the sol to convert to gel. The size of the product particles can be controlled by the method of initially preparing the sol droplets. This technique can produce spherical particles with diameters in the range 10 - 1000μm (Woodhead, 1972).

2. **External Gelation**

Again the aqueous sol is dispersed in an immiscible solvent. By adding a long chain amine or passing ammonia gas through the solvent the anion is removed from the sol droplets, the sol is destablished and forms a gel. This technique is suitable for the preparation of spherical particles in the 5 - 50μm size range (Segal and Woodhead, 1986).

3. **Internal Gelation**

In this case a weak base such as hexamethylenetetramine is added to the sol before it is dispersed in the organic solvent. Upon heating the base gives off ammonia gas which causes gelling in a similar manner to that in external gelation (Segal, 1989(a)).

It is also possible to form the gel by drawing or extruding the sol. This occurs because of the much greater surface area of the new form (Woodhead and Segal, 1984)

The last step in the process is the conversion of the gel to the final product. This is normally done by heating in air but the rates of heating must be carefully controlled to prevent destroying the shape formed in the gelling stage. In the case of carbides and nitrides it is also necessary to heat in a suitable atmosphere eg carbon dioxide or argon.

1.3.3 ORGANO SOL-GEL PROCESSING

The above discussion gives an outline of what is normally termed conventional or aqueous sol-gel processing. There is however, another closely related sol-gel process referred to as organo or alkoxide sol-gel processing. In this form of the process the sol and/or gel are derived from the hydrolysis of metal-organic species. This is usually metal alkoxides but any compound in which organic groups are bonded to a metal via an oxygen may be used, including acetates and acetylacetonates (Guglielmi and Carturan, 1988). In the present work the emphasis is on metal alkoxides, thus the subsequent discussion will be centred on these. The relevant properties and chemical reactivities of meal alkoxides will be discussed in more detail later but at present it is sufficient to know that they hydrolyse to form the metal oxide or hydrous oxide.

In this process hydrolysis is achieved by dissolving the metal alkoxide in alcohol (they are not soluble in water) and adding water and if necessary a catalyst. The reaction leads to the production of oxide by the formation of M-OH and subsequently M-O-M bonds. As will be seen later the final form of the oxide can vary considerably depending on the reaction conditions used. It can range from polymeric gels, colloidal dispersions, colloidal gels to precipitates.

Once the sol and/or gel has been formed it can be processed in a similar manner to those prepared from conventional sol-gel processing. However this variation of the processing has several advantages over the conventional process. The first of these is that metal alkoxides are often liquids and can be purified. The second is that mixed oxides can be produced by mixing the alkoxides rather than the colloidal dispersions. This leads to mixing on a molecular level and much greater homogeneity in the product. A further advantage is the avoidance of the more complicated sol-and gel-forming techniques described above.

1.3.4 ADVANTAGES

The use of sol-gel processing provides a number of advantages, some of which have already been mentioned, including;

1. **Dust free processing.** The use of "liquid" reagents greatly reduces the production of dust. This is an obvious advantage if

the dust is a health hazard or is radioactive such as in the nuclear industries.

2. **Control of physical properties.** By control of the structure of the colloidal dispersion (particle size and degree of aggregation) the density and porosity of the final product can be determined (Nelson et al, 1981). In the case of gels derived from alkoxides the density, pore size, surface area, index of refraction, strength and hardness can be controlled by the production conditions, addition of drying control chemical additives, and the heat treatment of the product. This can allow the formation of bodies with the desired shape and properties and even allows the production of monolithic bodies with physical property gradients within it (Hench et al, 1986; Hench, 1986; Yamane et al, 1986).

3. **Predetermined product shape.** The gel product can be made in shapes such as spheres or fibres of predetermined size by the control of the sol-gel transition or by appropriate treatment of the gel. Examples include the formation of silica, alumina, titania, zirconia and silicon carbide fibres by drawing from solution (LaCourse, 1984; Sakka, 1984) or unidirectional freezing of gels (Sakka, 1984). Spherical particles are produced by many of the gelling techniques previously outlined. It is also possible to prepare bodies of a specific shape by casting the sol into a mould (Hench, 1986).

4. **Control of size.** Powders can be prepared in desired size fractions and shapes thus minimising crushing and grinding processes. In the case of conventional sol-gel processing the appropriate control in the gelation stage can form particles of a desired size as previously noted. Similarly in the case of organo sol-gel processes spherical particles can be produced to a predetermined size with small standard deviation (Stöber et al, 1968; Jean and Ring, 1986(a); Bogush et al, 1988(a)). These submicron spherical particles are of interest in the field of ceramics as will be discussed later.

5. **Low temperature processing.** Because much of the oxide network, including that of mixed oxides, is formed by the reaction at lower temperature and because of the small and uniform pore sizes produced the required density can often be obtained at lower temperatures than used in conventional processing techniques (Bouquin et al, 1987; Yoldas, 1977). This has the obvious advantage of energy savings but also allows processing to avoid particular temperatures which may cause problems such as crystallization or degradation of a component such as fibres in composites (Uhlmann et al, 1984). Within the area of glass production it allows restrictions such as critical cooling rate to be avoided.

6. **Intimate mixing.** For multicomponent oxides the mixing at colloidal or in the organo process molecular level allows more

homogeneous mixing and a lower temperature for processing (Wu et al, 1984).

7. **Novel Compositions.** Preparation of mixed oxide compounds with novel compositions or compounds which are difficult to prepare by conventional methods (MacKenzie, 1985, 1988).

8. **High Purity.** In the case of alkoxide sol-gel processing many of the precursors eg tetraethylorthosilicate and titanium isopropoxide are liquids and can be purified by distillation (Segal, 1985(b)). For example distillation of tetraethylorthosilicate has been shown to lower transition metal impurities, already at part per billion levels, by factors between two and ten depending on the element involved (Segal, 1985(b)). This leads to a very high purity product because the other reagents used can also be purified. This method also avoids the contamination which can occur during crushing and heating at high temperatures.

9. **Mixed organic-inorganic materials.** In the organo sol-gel process the use of metal alkoxides which have non-hydrolysable organic species attached to the metal will lead to mixed organic-inorganic material because these groups will still be attached to the metal in the final gel. This will lead to the formation of material with properties between plastics and glasses (Schmidt and Seiferling, 1986). If this organic material can be polymerized a second polymer phase may be produced in the product. This has

been used to produce non-brittle silicate material (Schmidt, 1984) and for material which forms monoliths without large shrinkage (Schmidt, 1984). The inclusion of organic groups can also be used to produce silicon carbide fibres (Lee and Hench, 1986).

An interesting variation on this principle is the alteration of the organic material so that it can then be used to accommodate a further type of material. An example of this is the inclusion of amine groups into organic material attached to the silicon in organotrialkoxysilanes. These then act to solvate a guest ionic species allowing a third phase to be present (Charbouillot et al, 1988).

10. **Carbides and Nitrides.** Metal carbides and nitrides such as silicon carbide, tungsten carbide and aluminium nitride provide materials with desirable properties such as high refractory and chemically resistant nature, extreme hardness, high thermal conductivity and electrical properties which have found uses in the field of abrasives, cutting tools and reinforcing materials. These materials can be produced by both the organo and conventional sol-gel processes. In the conventional process addition of colloidal carbon at the sol stage means the gel can be calcined in carbon dioxide to form metal carbides. Further heating in an ammonia atmosphere will lead to the production of metal nitrides. In the organo sol-gel process inclusion of non-hydrolysable organic groups leads to their retention in the final gel. This can then be converted to the carbide by heating in an argon atmosphere (Fox et al, 1986) and converted to the nitride in

a similar fashion to that in the conventional process or by heating the gel in ammonia (Brown and Pantano, 1984).

11. **Multi-phase systems.** Sol-gel processing can be used to produce materials containing two or more phases which have maximum interpenetration of the separate phases. This includes two separate crystalline phases of the same material or separate phases of different materials. This can be done by forming the gel monolith and then causing the precipitation of the second phase within the monolith or by mixing the appropriate sols (Roy et al, 1984). This technology has been used to prepare photosensitive materials such as silver chloride in silica (Roy et al, 1984) and ceramic metal composites (Roy et al, 1984; Roy, 1987). An interesting use of this technology is the incorporation of photochromatic dyes into the polymerising material (Levy et al, 1989) where it has been shown that alteration of the polymerising material changes the response of the photochromatic dye. Also for the preparation of composites containing silica gel and organic polymers eg composites of silica, silicon carbide and polymethylmethacrylate which have high strain values before cracking (Pope and MacKenzie, 1986(a)).

A more recent, and exciting, multi-phase system produced by sol-gel processes incorporates homogeneous catalysts into a silica gel. Homogeneous catalysts consist of metals, such as ruthenium, with a number of ligands which usually include organic groups. By altering one of the organic groups so that it has a silicon alkoxide entity included, and then hydrolysing it with the silicon

alkoxide the organic group will be incorporated into the silica framework. These organic groups act as anchors for the catalyst species so that the benefits of homogeneous and heterogeneous catalysts are combined (Schubert et al, 1988).

Although these have been discussed individually in practice they are used together. For example the ability to prepare fibres has been linked to the ability to produce homegeneous mixed oxides to produce high temperature superconductor fibres (Kozuka et al, 1988)

1.3.5 DISADVANTAGES

It can be seen from the above discussion that such processes provide many advantages in the field of ceramics. However there are also a number of problems associated with these processes.

1. **Cost.** The cost of the large volumes of solvents and many of the precursor compounds is high which leads to a high final product cost. The processing of the material is also expensive.
2. **Processing time.** The time involved in processing can be much longer than that in conventional systems.
3. **Large shrinkage.** In an attempt to reduce the surface energy of the system a gel will shrink to reduce the solid-liquid interface. This is the basis of the phenomenon of syneresis. Also, once the solvent has begun to evaporate there appears a number of pressures within the system due to the differences between the energy of solid-vapour and solid-liquid interfaces (Scherer, 1986(a)) and these also tend to cause shrinkage. In the

case of Alkoxide derived gels the condensation of hydroxyl groups brought near each other also promotes contraction.

4. **Cracking.** During drying pressures develop within a gel. The capillary pressure developed within a pore is inversely proportional to the pore radius. Therefore the presence of pores of different diameters tends to produce different capillary pressures which generate stresses within the gel. If the stress exceeds the strength of the gel the gel will crack. (Zelinski and Uhlmann, 1984).

5. **Fire Hazard.** In the case of organo sol-gel processing there is the hazard of handling large quantities of flammable material.

6. **Batch Processing.** At present sol-gel processes are usually carried out in batches were continuous processing would be more efficient.

7. **Organic Residues.** The gel contains a significant amount of organic material which must be removed carefully during heating.

However, many of these restraints are being overcome eg continuous processing systems (Ring, 1987), and gels which dry without cracking (Orcel and Hench, 1984). The high cost of this technology, whilst it can not be overcome, does not act as a deterrent to its use but merely directs the applications of the process to those areas where it is commercially viable. These are areas where the high value of the products and/or precursors or stringent requirements for properties or performance of the

product render the added costs of sophisticated processing acceptable.

1.3.6 APPLICATIONS

Even with the restraints mentioned above the process has been employed successfully in a wide number of fields. A brief outline of some of these fields is given below.

1. **Nuclear Fuel Pellets.**

As described previously, conventional processing techniques posed several problems to operators of nuclear installations. Sol-gel processing allowed preparation of mixed thorium-uranium oxide fuels without powder mixing, reduced dust hazards and allowed sintering at lower temperatures. An added advantage was the ability to fabricate the product as spherical particles which were suitable for vibrocompacting into the fuel rods (Ferguson et al, 1964).

2. **Fibres**

Ceramic fibres are of use as reinforcing agents in ceramic composites. The conventional method of preparing ceramic fibres is by drawing from high temperature melts, but this is not convenient for materials which have high melting points or which are immiscible in the liquid state. Sol-gel processing allows the formation of fibres by drawing from alkoxide solutions or extrusion of the gel (Sakka and Kamiya, 1982; Sakka, 1984; Matsuzaki et al, 1989). The gel fibres can then be calcined at several hundred degrees thus avoiding the problems outlined above.

3. Coatings

It has already been described how stresses which occur during drying cause cracking in gels. However it has been shown (Zelinski and Uhlmann, 1984) that the drying rate which can be accommodated without cracking is inversely proportional to the thickness of the body being dried. Therefore the problem of cracking is avoided when thin layers are applied to a substrate. When this is considered in conjunction with the fact that the dipping route permits the coating of complex shapes and that very small amounts of material are used (and thus the precursor cost is not a consideration) the application of sol-gel processing to coating technology appears promising.

In fact the application of sol-gel processing to coating is one of the main areas of its use with a number of different reasons for coatings. A few of the applications are;

A. Coatings to give particular optical properties. Examples of these include the application of antireflective or protective coatings to solar cells to give higher efficiency (Brinker and Harrington, 1981; Ashley and Reed, 1986; Reed and Ashley, 1986) and the application of coating window glass to prevent the transmission of infra-red radiation (Dislich, 1985; Arfsten, 1984). Both with obvious use in energy production and conservation.

B. Coatings to enhance oxidation and abrasion resistance. Examples include the deposition of silica and ceria on stainless

steel (Nelson et al, 1981) or germania silica layers on silicon carbide (Schlichting and Neumann, 1982) to prevent oxidation.

C. Coatings to alter surface chemistry. An example is the application of coatings of porous oxides to act as catalyst supports. For example silica or alumina coatings on steel (Cairns et al, 1984). In this case the ability to control the porosity of the oxide is a great advantage.

D. Coatings of conducting or semiconducting materials. Coatings of these materials are of use for heating windows, antifogging devices, photocells and solar cells. Examples include the deposition of thin films of cadmium stannate (Dislich and Hinz, 1982). It is also possible that the coating of thin films will be used in the production of microelectronic devices (Carman and Pantano, 1986).

E. Coatings of glass to give a particular colour. This is often done by coating with a material including transition metal oxides (Sakka, 1985). This is used frequently in automotive and architectural glasses. The incorporation of transmission or rare earth metals, such as cobalt, into gels has been used in the formation of optical filters (Wang and Hench, 1986).

As well as the direct application of sol-gel processing to prepare coatings, it is also possible to prepare free flowing powders of the required size, shape and composition for use in

plasma spraying (Scott and Woodhead, 1982).

This small selection of the coating applications os sol-gel processing indicates the usefulness of this field.

4. Glass Preparation.

Sol-gel processing is applied to glass formation by (a) melting powders produced by sol gel processes, (b) sintering or hot pressing gel derived powders or (c) heat treating gels to produce monoliths. The advantages of gel derived material as precursors for melting is the homogeneity of the material which leads to lower and shorter melting times and uniform composition (Roy, 1969).

In the case of sintering or hot pressing the important factors are the removal of any organic material and the collapse of the pore system. In this field the ability to control porosity is an advantage and the ability to produce submicron spherical particles which pack to give a body with a uniform pore network have been used to produce glasses (Optiz, 1987; Sacks and Tseng, 1984(a), 1984(b)) This has the advantage of lower processing temperatures and very high purity which is essential for certain uses of glass ie optical fibres.

It is possible to prepare monolithic glass bodies by drying and heat treating of gels derived from sol-gel processing (Cheng and Hench, 1988; Li and Hench, 1988). This has to be carried out with care to prevent the cracking described earlier. However the use of drying control chemical additives such as formamide and oxalic acid (Orcel and Hench, 1984; Woodhead and Segal, 1984)

relaxes the requirements by strengthening the gel and making the pore size distribution more uniform thus reducing the stresses and making the gel more able to withstand them. This process has the advantage that the sol can be cast into a mould of the required shape and monolithic shaped bodies can be prepared. This becomes more attractive when the body can be prepared with a desired colour (Wang and Hench, 1986), desired physical properties including gradients of these properties (Woodhead and Segal, 1984) and a more uniform microstructure than conventionally pressed glass (Mukherjee and Zarzycki, 1976). However the most interesting advantage of the process is that it allows the production of glasses with novel compositions ie those which can not be prepared by conventional methods. For example those which crystallise on cooling or mixed oxides within the liquid immiscibility zone (Zelinski and Uhlmann, 1984).

5. Production of mixed oxide ceramics.

The intimate or molecular mixing available in sol-gel processing has been employed for the formation of oxide ceramics containing more than one metallic element. These include mixed V_2O_5 - GeO_2 glasses (Hou and Sakka, 1989), mixed B_2O_3 - SiO_2 and MgO - B_2O_3 - SiO_2, ZnO - B_2O_3 - SiO_2 glasses (Tohge and Minami, 1989), conducting ceramics such as In_2O_3 - SnO_2 (Segal and Woodhead, 1986) and more recently high T_c oxide superconductors (Horowitz et al, 1989). This technology is often linked to the application of coatings for example coatings of lithium niobate (Eichorst and Payne, 1988).

6. Controlled microstructure.

The process can be used to produce material with predetermined structures. Examples include the formation of alumina with uniformly dispersed zirconia for use as an abrasive (Zelinski and Uhlmann, 1984) and the preparation of the desired crystalline form in titania and alumina by seeding the sols (Messing et al, 1986(a)).

The above discussion is a brief outline of some of the main applications of sol-gel processing at present and an indication of the important place this process is now attaining in the field of ceramic synthesis. The importance of this can be seen from the increase in the publications relating to sol-gel processing (Dislich, 1985), the success of the recent Materials Research Society symposia dealing with this area (Brinker et al, 1984(a), 1986(a), 1988(a)) and recent publications (Dislich, 1985; Ulrich, 1988; Wenzel, 1985; MacKenzie, 1985) predict a bright future for the technology. However to fulfil the full potential of the process more work is necessary to understand the underlying chemistry.

1.4 MONODISPERSE PARTICLES

It has previously been described how sol-gel processing involves the formation of a sol and its subsequent conversion to a gel. However the process may also be used to prepare sols without transformation to a gel. If all of the particles within the suspension are the same size they are referred to as monodisperse.

of fields and, as a large part of this thesis will be devoted to the production of these particles, it is appropriate to outline the production and application of these particles.

1.4.1 APPLICATION

Much of the importance of monodisperse particles, especially spherical particles, relates to the fact that they are simple well defined systems. For this reason they are ideal as model systems for the development of theories explaining the behaviour of colloidal and other systems. The ability to produce such systems allows the evaluation of the theories and provides the ability to carry out experiments to develop further theories. Examples include the adhesion of particles to surfaces (Kuo and Matijevic, 1980), evaluation of small angle neutron scattering theories (Ottewill, 1982) and nitrogen absorption theories (Lecloux et al, 1986).

These particles also have an important place in the science of ceramics. The first area of application is similar to those mentioned above, in that it is the ability to use the monodisperse powders as well defined systems for the development of theories. For example green compacts formed from monodisperse powders have been used in the study of sintering and densification in ceramics (Sacks and Tseng, 1984(a)).

The second area of application of these powders is as starting material for the production of ceramic bodies in a process which has been termed (Iler, 1986) the Densely Packed Uniform Colloid Process. Conventional processes for the

production of ceramics from powders have a number of problems associated with them. The first of these is that the powders are complex and not easily characterised (Barringer and Bowen, 1985). Therefore it is difficult to generate material with reproducible tolerances and this means that a proportion of the product bodies must be rejected, the cost of which may be as high as 50% of the total manufacturing cost (Barringer et al, 1984). It is also the case that the powders contain a large range of particle sizes and agglomerates of particles (Barringer et al, 1984). These lead to green bodies with inhomogeneous packing, a large pore size distribution and variation in the number of interparticle contacts. This causes the product to contain variations in microstructure, the formation of cracks and warping and necessitates longer and higher temperature sintering (Barringer and Bowen, 1985; Sacks and Tseng, 1984(b)).

If instead of conventional powders, spherical monodisperse colloidal powders are used these problems can be overcome (Barringer and Bowen, 1985; Barringer et al, 1984). The particles form dense packed bodies with the largest possible number of interparticle contacts and a uniform pore size distribution. This is close to the ideal green body described by Barringer (Barringer et al, 1984) and leads to lower sintering time and temperature, uniform shrinkage, no warping or cracking and a uniform microstructure (Barringer and Bowen, 1985). The use of colloidal particles also overcomes one of the problems of sol-gel processing. The larger scale of the colloidal system reduces the capillary stresses and thus reduces the tendency to crack. This

capillary stresses and thus reduces the tendency to crack. This makes the colloidal system useful for the preparation of larger bodies and thicker coatings (Barringer et al, 1984).

The above discussion gives the impression that the use of monodisperse particles overcomes all the problems of ceramic production and provides a perfect green body. This is not the case, there are several difficulties with this method. The first of these is the ability to produce monodisperse colloidal powders. With modern synthetic techniques many such materials can be produced and this is not a serious hindrance. Some of these methods will be outlined below. It is then necessary to convert these powders or suspensions to a dense packed green body. This can usually be achieved by controlling conditions such as pH and electrolyte concentration so that the particles repel each other thus allowing the particles to form an ordered compact (Barringer and Bowen, 1985).

Even when the above conditions have been met and an ordered compact has been formed, it is not perfect. The packing within the ordered bodies made from monodisperse powders include defects similar to those observed in atomic packing for example vacancies, dislocations and grain boundaries (Sacks and Tseng, 1984(b)). They also contain flaws such as foreign bodies and aggregates of primary particles (Chappell et al, 1986) which are not specific to monodisperse particles. It has also been noted that the regions of order only extend over tens of microns before grain or domain boundaries occur (Milne, 1986) and that areas of disordered packing and large voids occur (Milne, 1986). The reason for the

voids and disordered regions have not been established but it may be related to the conditions necessary to produce the ordered packing not being met.

Even with these flaws the bodies prepared from monodisperse powders are much closer to the ideal than those prepared from "normal" powders. This has lead to the use of this technology for the production of glasses and ceramics eg high purity silica glass for use in production of optical fibres (Optiz, 1987).

1.4.2 PRODUCTION

Although at the beginning of this discussion it was mentioned that these materials could be produced by the techniques employed in sol-gel processing there are a large number of methods of forming monodisperse powders (Sugimoto, 1987). These methods are broadly classified as homogeneous or heterogeneous (Sugimoto, 1987).

In a homogeneous system there is only one phase present and the concentration of the monomer builds up in solution in that phase until it precipitates from the solution. This covers a number of techniques including redox reactions, precipitation by poor solvent, decomposition of compounds, hydrolysis in organic or aqueous media and the reaction of ions or chelates.

In heterogeneous systems there are a number of phases present before precipitation of the colloidal material. This class includes reactions in aerosols, emulsion polymerisation, and phase transformation.

Several of these techniques have found application in the formation of colloidal oxides (Matijevic, 1984) and more specifically the formation of oxides for use in ceramics (Matijevic, 1987). The first of these is by reaction in aerosols where droplets of a liquid reagent containing the required metal are generated. These droplets are then reacted with a vapour leading to the production of solid particles. This can be done by forming small droplets of a metal alkoxide or hydrolysable liquid eg titanium tetrachloride and then reacting these liquids with water vapour thus forming particles of the oxide (Matijevic, 1981; Visca and Matijevic, 1979). The particles are spherical and the size determined by the size of droplets in the aerosol.

The next technique, and that already referred to as applying the sol-gel methods, is homogeneous precipitation. This process has been qualitatively described in the case of the formation of monodisperse sulphur sols by LaMer (LaMer and Dinegar, 1950). In this process the concentration of the material to be precipitated is increased in solution. This is usually achieved by means of a chemical reaction, for example LaMer produced molecularly dispersed sulphur by the decomposition of sodium thiosulphate in acid. At some point the concentration of material reaches the critical supersaturation, at which point self nucleation occurs and small particles of solid appear. These small particles then grow by diffusion and in doing so reduce the concentration of precipitating material in solution. The growth continues until the concentration of material in solution is in equilibrium with that in the solid state. This system is illustrated in fig. 1.2.

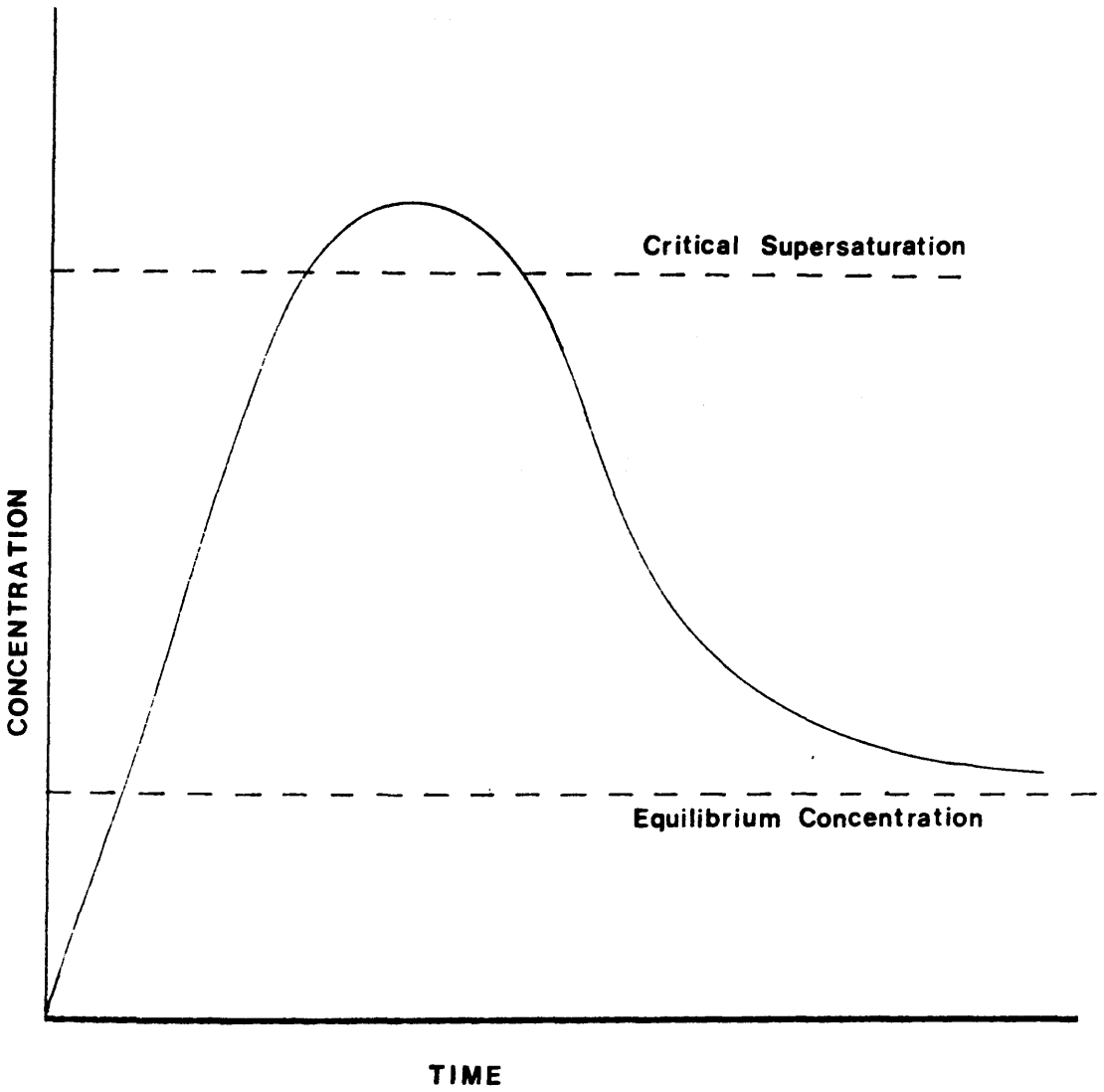

Fig 1.2: Illustration of the LaMer nucleation and growth model.

The production of monodisperse particles from this method requires that only one short burst of nucleation occurs and then all particles grow at the same rate. Should for example, the rate of production of material be faster than the rate of removal by growth, the system will continue at, or re-attain, the critical supersaturation and more particles will be produced. Because the particles produced in such a subsequent nucleation burst, or at later times in a single nucleation period, are formed at a later time they do not grow to the same size as those formed earlier and a range of particle sizes are found. This technique may cover the precipitation of oxides by the hydrolysis of metal alkoxides and thus includes what could be termed sol-gel processes. The formation of monodisperse particles from the hydrolysis of alkoxides is one of the most common ways of producing them and has been used for the production of silica (Stöber et al, 1968), titania (Jean and Ring, 1986(a)), zirconia (Fegley and Barringer, 1984) and a number of others.

The third technique for forming monodisperse particles which has found application in this field is the flame oxidation or flame hydrolysis of compounds containing the required metal. This can use compounds such as chlorides (Dorn et al, 1987) eg silicon tetrachloride. This technique is the source of some of the commercially available colloidal silica powders eg Cab-O-Sil (trademark of the Cabot Corp.) is prepared by flame oxidation of silicon tetrachloride. However the purity of this material is not high enough for use in optical fibre production (Rabinovich et al, 1986).

It is also worthy of note that in the case of silica, which is the compound under study, there is a further source of monodisperse colloids; sodium silicate. This is a complex compound most commonly produced by the fusion of silica with sodium sulphate or carbonate (Iler, 1979; Barby et al, 1977). It has the formula $Na_2O.SiO_2$ with large variations in the ratio of the two components.

The compound is normally supplied as an aqueous solution in which the silica forms polymeric ions or small charged particles. The system being stabilised by the presence of the sodium ions (Iler, 1979). However if the sodium is removed the system will gel or, in dilute systems, form a colloidal dispersion of silica. This can be done by altering the pH to the appropriate value and removing some of the sodium ions by electrodialysis or by using ion exchange resin.

Sodium silicate is the source of a number of commercially available silica dispersions for example Syton (trademark the Monsanto Chemical Company) and Ludox (trademark the Du Pont Company) ranges of products. However silica suspensions prepared in this fashion generally contain particles in the range 5-30nm (Du Pont, 1988(a), 1988(b); Monsanto, 1986) which are well below the optimum 0.1-1μm diameter range quoted by Barringer (Barringer and Bowen, 1985; Barringer et al, 1984) for preparation of ceramics. They also contain significant amounts of sodium salts or in some cases aluminium compounds as stabilisers (Iler, 1979; Du Pont, 1988(a), 1988(b); Monsanto, 1986). Therefore these products do not offer the same purity as dispersions formed from

some of the other methods especially sol-gel reactions.

It must be noted however that although the above drawbacks occur, certain companies trade in dispersions with the particle sizes above 0.1μm eg Syton X30 (trademark Monsanto Chemical Company) (Iler, 1979). Monsanto also trade in dispersions produced from the hydrolysis of silicon alkoxides (Monsanto, 1986).

Although there are several other methods of preparing monodisperse colloidal oxide particles (Matijevic, 1981) only those above have found general application for the formation of oxides for the production of ceramics.

In all of the above described techniques, except those based on sodium silicate, the starting material is volatile and may be purified by distillation and therefore the produce ceramic will be of high purity. However there are drawbacks with these techniques. In the case of reaction with aerosols and flame oxidation a suitable volatile precursor must be available. This can, especially in the case of reaction in aerosols, reduce the number of metals which can be used. Also in the case of flame oxidation monodisperse particles are only formed if a laser is used as the heat source (Scherer, 1985).

It can be seen from the foregoing discussion that monodisperse particles offer a route to the production of ceramics that overcome a number of the problems of conventional powder processing. In many areas the use of monodisperse powders is complimentary to the use of sol-gel processing but the two

techniques merge when the sol-gel techniques are used to form the monodisperse particles.

1.5 METAL ALKOXIDES

Metal alkoxide is the name applied to a broad class of compounds of the general formula $M_x(OR)_n$ where M is a metal or metalloid element, O is oxygen and R is an alkyl group (OR being an alkoxy group) and n and x are integers. These were first reported in 1846 (Ebelman and Bouquet, 1846; Ebelman, 1846) for silicon and boron and are now known for most metallic and metalloid elements spanning a large number of alkoxy groups in each case. As would be expected with such a large class of compounds the range of chemical and physical properties is large.

1.5.1 NOMENCLATURE

The range and history of these compounds has led to a varied nomenclature (Bradley et al, 1978) which must be outlined to clarify the later discussion. Metal alkoxides can be viewed from a number of standpoints and this leads to a number of approaches to naming a particular alkoxide. The alkoxide can be viewed as the product of the reaction between a metal and an alcohol ie sodium with methanol and thus named as the salt-sodium methoxide. However the compounds can also be considered as esters which leads to many alkoxides being names as orthoesters eg orthosilicates such as tetraethylorthosilicate. In general the alkoxides of

alkoxides of highly electropositive metals such as sodium and magnesium, which can react with alcohols, are referred to as alkoxides where those of less electropositive, or electronegative, elements such as silicon and titanium are referred to as orthoesters. However these guidelines are not rigidly held and it is not unusual for compounds expected to be named ester to be discussed as alkoxides eg silicon ethoxide, depending on the circumstances.

In certain cases extra derivation of the compound can be envisaged and this leads to further possible names. For example silicon alkoxides can be viewed as derivatives of silane and thus referred to as alkoxysilanes eg tetraethoxysilane.

In the remainder of this thesis these compounds shall, as far as possible be referred to according to the above guidelines but may be simplified by abbreviating the names eg tetraethylorthosilicate will often be referred to as TEOS.

1.5.2 SYNTHESIS

The large number of elements which form metal alkoxides and the range of properties of those elements leads to the expectation of a wide variety of possible syntheses. While this is the case, these syntheses can generally be classified into a number of broad types of reaction.

The first of these is the reaction of the metal with the appropriate alcohol. This can be illustrated:

$$M + n\,ROH \longrightarrow M(OR)_n + n/2\ H_2$$

Due to the weak acid nature of the alcohol proton the synthesis works as written only for strongly electropositive elements such as sodium (Ethyl Corpn., 1955).

This type of synthesis can also be used for less electropositive metals, eg magnesium and beryllium, if a catalyst such as iodide (Turova et al, 1959) is added. Other variations involve the use of the metal as an amalgam (Gladstone and Tribe, 1881) and the addition of small amounts of alkoxide to activate the reaction (Brown and Mazadiyasni, 1970).

The second class of reactions is the reaction of metal halides with the alcohol. For example;

$$SiCl_4 + 4C_2H_5OH \longrightarrow Si(OC_2H_5)_4 + 4\ HCl$$

This type of synthesis, which is believed to occur by coordination of the alcohol followed by elimination of HCl (Sidgwick, 1924), is used for less electropositive metals, such as lanthanum and thorium and electronegative elements such as silicon, phosphorus and boron (Ebelman and Bouquet, 1846; Bradley et al, 1952; Doak and Freedman, 1961). Again the reaction is linked to the electropositive character of the metal with the reactivity of the chlorides within a group of the periodic table being greater with more electropositive elements.

A common variation used in this type of synthesis is to add a base to the reaction to remove the hydrogen chloride and drive the reaction to completion eg ammonia (Mehrotra and Pant, 1962) or sodium alkoxide (Hyde and Curry, 1955). Less common variations

include the addition of other bases eg pyridine (Koetzsch, 1968).

It is also possible to produce alkoxides by the reaction of the metal oxide or hydroxide with alcohol. This can be illustrated:

$$M(OH)_n + nROH \longrightarrow M(OR)_n + nH_2O$$

$$MO_n + 2mROH \longrightarrow M(OR)_{2n} + nH_2O$$

This type of synthesis has been used for alkoxides of several metals including sodium (Jones and Hughs, 1934) and boron (Etridge and Sugden, 1928).

Although these indicate the broad classes of reactions which are most commonly used to prepare metal alkoxides there exist other methods which have been applied to specific cases, for example the formation of chromium trimethoxide by the photooxidation of aryltricarbonyl chromium in methanol (Brown et al, 1966). There are also methods such as alcohol exchange (Shiihavam et al, 1961; Backer, 1938) and transesterification (Backer, 1938; Mehrotra, 1953) which allow the conversion of one alkoxide to a different alkoxide of the same metal.

The above discussion gives a brief outline of the common methods of synthesis of metal alkoxides but does not go into any detail of the practical aspects or difficulties, nor does it deal with the formation of double (those with two different metal atoms) or mixed (those with different alkyl groups) alkoxides

which although used in sol-gel processing are not employed in this project and are beyond the scope of this thesis.

1.5.3 PROPERTIES

The physical and chemical properties of metal alkoxides is a large subject which is a field of research in itself. Therefore only those properties which are of direct importance to the application of alkoxides to this project will be outlined.

The first, and in relation to this project, the most important feature is the chemical nature of the M-O-C bond. Because of the strongly electronegative nature of the oxygen atom the bond is highly polar and thus the central atom is susceptible to nucleophilic attack (Bradley et al, 1978). This makes the compounds easily hydrolysable leading to the hydroxide or hydrated oxide and this is the basis of the work discussed later. The mechanism of the hydrolysis reaction is discussed later in relation to the alkoxides used in this project.

The second property of alkoxides which has direct affect is that many are volatile. This property is dependent on a number of features such as molecular size, nature of the alkoxide group and the nature of the central atom. These are related to the tendency of the alkoxides to oligomerise (Sidgwick, 1924; Jones and Hughs, 1934; Etridge and Sugden, 1928) and thus lower the volatility. Thus features such as long or branched alkyl chains which hinder oligomerization increase the volatility (Uhlmann et al, 1984). Silicon alkoxides, which are the subject of this work, are

monomeric and volatile which allows the easy purification by distillation which is of importance to the uses within this project.

1.6 HYDROLYSIS OF ALKOXIDES

The hydrolysis of metal alkoxides has already been mentioned in the section dealing with alkoxides and here it will be discussed in more detail. As most of the work in this project is carried out on tetraethylorthosilicate this will be used as the basis for the discussion. The hydrolysis of TEOS can be written simply as

$$Si(OEt)_4 + 2H_2O \longrightarrow SiO_2 + 4EtOH$$

where Et indicates an ethyl group. However the hydrolysis is in fact achieved by three reactions occurring concurrently.

$$\equiv Si\text{-}OR + H_2O \longrightarrow \equiv Si\text{-}OH + ROH$$

hydrolysis

$$\equiv Si\text{-}OR + HO\text{-}Si\equiv \longrightarrow \equiv Si\text{-}O\text{-}Si\equiv + ROH$$

alcohol condensation

$$\equiv Si\text{-}OH + HO\text{-}Si\equiv \longrightarrow \equiv Si\text{-}O\text{-}Si\equiv + H_2O$$

water condensation

R is an alkyl group

With the reverse reactions being esterification, alcoholysis and hydrolysis respectively.

Thus the apparently simple hydrolysis reaction is more complicated than it first appears and in fact it has been shown (Assink and Kay, 1988) that there are fifteen possible silicon environments which would lead to 165 possible reaction rates (Kay and Assink, 1988). As the molecular structure and thus ultimately the macroscopic structure of the product depend on these reactions and their relative rates it is necessary to outline what is occurring during the reaction.

1.6.1 HYDROLYSIS REACTION

Before any condensation occurs it is necessary for hydrolysis to occur. This is clear from the fact that alkoxides are stable compounds when anhydrous. Therefore the hydrolysis step will be dealt with first.

It has been mentioned that the Si-O bond is polar causing the silicon atom to be susceptible to nucleophilic attack. This is the basis of the hydrolysis reaction. The silicon atom in the alkoxide is attacked by the oxygen in water. This has been shown by the use of isotopically labelled water (Khaskin, 1952). In the most basic analysis this is the reaction, but the rate and mechanism of the reaction can be affected by a number of factors.

The first of these is the actual structure of the alkoxide with steric and inductive effects determining the stability of the compound. The larger of the two is the steric factor (Vorankov et

al, 1978) where complication of the alkoxy group reduces the rate of hydrolysis. Therefore alkoxy groups with long or branched alkyl chains will reduce the rate of hydrolysis by hindering the approach of the nucleophile. The structure of the alkoxide also affects the rate by the inductive effects of the substituents. If the substituents are electron releasing they will tend to stabilise a transition state with a positive charge and similarly electron withdrawing groups will stabilise negatively charged transition states. Therefore the groups attached to the silicon can affect the reaction rate and it will become clear later in the discussion that this has an important effect during the reaction.

The second factor is the presence of a catalyst. The reaction has been shown to be catalysed by acid and base (Aelion et al, 1950) and a number of other materials such as halide compounds (Pope and MacKenzie, 1986(b)). In the case of mineral acids the anion also has an effect on the rate of the reaction (Pope and MacKenzie, 1986(b)). The reason for the catalytic effect of materials like halides is believed to be the ability to increase the coordination number of the silicon, forming five coordinate intermediates which are unstable and very susceptible to nucleophilic attack. The reason for the acid and base catalysis is based on the production of hydroxide or hydronium ions which are believed to take part in both the hydrolysis and condensation reactions.

The mechanism of the reaction is believed to differ in acid and base catalysed systems and this is supported by the kinetic data available. That is that the inductive effects indicate a

positive transition state in the acid catalysed state and a negatively charged transition state in the base catalysed state. The actual mechanisms involved are still a matter of debate but it is generally agreed that the reaction occurs by nucleophilic substitution involving a five coordinate transition state.

Under acidic conditions two possible mechanisms have been proposed. In the first of these the first stage of the reaction is the protonation of an alkoxy group. This reduces the electron density on the silicon and make it more susceptible to nucleophilic attack. Then the silicon is attacked by the oxygen on a water molecule leading to a five coordinate species. The transition state then decays by the protonated alkoxy group leaving as the alcohol resulting in the replacement of an alkoxy group by a silanol. It has also been proposed (Keefer, 1984) that the reaction occurs by the electrophilic reaction mechanism where a positively charged hydronium ion approaches the alkoxide with the ion being attracted to the electron density on the oxygen atoms in the alkoxy groups. The ion then forms a transition state where the oxygen in the hydronium is partially bonded to the silicon and the hydrogens are partially bonded to the oxygens on the alkoxy groups. The transition state then decays by the removal of one of the protonated alkoxy groups as the alcohol and the oxygen from the hydronium remaining as a silanol group (see fig. 1.3).

Under the basic conditions the reaction is believed to occur by the nucleophilic attack of hydroxyl anion on the silicon to form a five coordinate transition state. The transition state

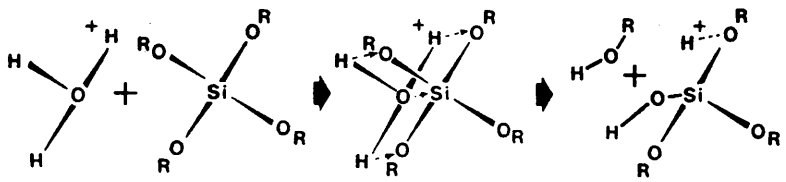

Fig 1.3: Acid catalysed hydrolysis mechanism

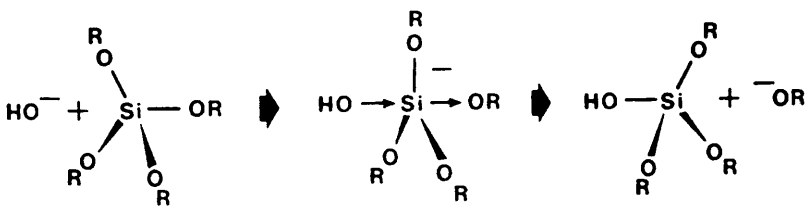

Fig. 1.4: Base catalysed hydrolysis mechanism

then decays by an alkoxy group leaving as an alkoxide anion and the hydroxyl remaining as the silanol group (see fig. 1.4). It should be noted that in this mechanism the attacking group is on the opposite side of the silicon to the leaving group. Therefore the reaction will cause inversion of the molecule. This will make it difficult for hydrolysis to occur in a molecule if it is part of a large species.

The mechanisms outlined above indicate why acid and base act as catalysts for the reactions. These also indicate why the reaction should be affected by the solvent used to carry out the reaction. The polarity of the solvent determines its ability to solvate species in solution and the availability of labile protons determines its ability to hydrogen bond. If the solvent is able to hydrogen bond to hydronium or hydroxide ions it would reduce their catalytic activity. The ability to solvate charged species can also affect the stability of the transition state and thus the rate of reaction. In the case of alcohol solvents where the alcohol is not that corresponding to the alkoxy groups on the alkoxide there is also the possibility of ligand exchange which could have a great affect on the reaction.

1.6.2 CONDENSATION REACTION

As previously mentioned the condensation reaction occurs by one of two reactions, that producing water and that producing alcohol. Again the rates of the reactions can be affected by a number of factors, the first of which is again the structure of

the species involved. It is believed that the complication of the alkoxy groups present on the condensing species will reduce the rate (Vorankov et al, 1978) but because of the complexity of the species present in the reactions at the time condensation is occurring it has not been proved.

The second factor is the presence of catalysts, again acid or base. The rate of condensation has been studied with varying acid/base content (Pohl and Osterholtz, 1985) and showed that the condensation is catalysed by both. The reason for this catalysis can be seen from the reaction mechanism.

The most commonly accepted mechanism for the condensation is that proposed by Iler (1979) for the condensation of silicic acid in aqueous systems. In this the silicon atom in one species undergoes nucleophilic attack by a deprotonated silanol group on another species. This forms a five coordinate species which decays by a hydroxyl anion or alkoxide anion leaving the attacked species thus forming and Si-O-Si bond (see fig. 1.5).

Again it can be seen that in a similar fashion to the hydrolysis reaction this mechanism can be affected by the solvent. In studies of the effect of solvent on the condensation reaction (Artaki et al, 1986) it was shown that the solvent can have a large effect on the reaction and structure of the polymer produced. This is in part the reason for the effect of drying control chemical additives (DCCA's). The basis of this effect is

the polarity and availability of labile protons. Highly polar protic solvents can hydrogen bond to the nucleophile and thus deactivate it thus slowing the reaction for base catalysed systems. Highly polar aprotic solvents may also slow the reaction by stabilising the reactants with respect to the transition state.

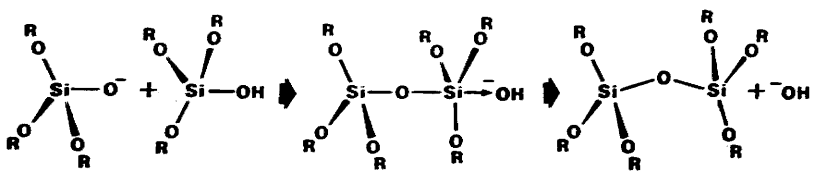

Fig. 1.5: Mechanism of condensation reaction in silicate polymers.

1.6.3 STRUCTURE-REACTION RELATIONSHIP

It was previously mentioned that the reactions occurring during the hydrolysis of the alkoxide must be the basis of the different macroscopic structures found in the system. This has been supported by numerous studies which show the basic structure and properties of the product vary with varying reaction conditions. However the above discussion, outlining the reactions occurring, does not make clear how these could have any great effect on the structure. This is because it deals with each reaction in isolation where in the real situation the reactions are all occurring at the same time, and it is the relative rates and the interactions of the different species produced which lead to the different structures.

The way in which these interactions vary the structure has been described by a number of authors (Brinker et al, 1982; Keefer, 1984). The basis of the differences lies in the differences in the reaction in the different reaction conditions.

In the model proposed by Keefer (1984), when an alkoxide is hydrolysed in alkaline solution, the hydrolysis step occurs by nucleophilic attack on the silicon by a hydroxide ion. This type of attack will be sensitive to the electron density on the silicon and also to steric and inductive effects of the substituents. Because of their bulk and electron donating properties alkoxy

groups will hinder the hydrolysis so that tetraethylorthosilicate will be hydrolysed slower than the products of its hydrolysis. Therefore in alkaline hydrolysis once hydrolysis of a molecule begins it will tend to go to completion and produce orthosilicic acid. As in conditions with pH above 2 the condensation step occurs by the reaction of a deprotonated and protonated silanol group it would be expected that more highly cross-linked polymers would be formed.

In acid catalysed hydrolysis Keefer (1984) proposed that the reaction proceeds by the electrophilic attack of a hydronium ion on the silicate species. Therefore the rate of attack will be greatest on the silicate species with the highest electron density ie that with the highest number of alkoxy groups. This is the reverse of the trend in alkaline hydrolysis. Also the monomer has a higher statistical chance of reacting simply because it has a higher number of alkoxide groups. These arguments would indicate the tetraalkoxide monomer would be most rapidly hydrolysed, then the end groups on polymer chains, and the slowest would be the middle group on the chains. Therefore acid catalysis tends not to produce orthosilicic acid and condensation is likely to occur between species which are not completely hydrolysed. This leads to a less highly cross-linked polymer.

Brinker (Brinker et al, 1982, 1984(c), 1986(b)) proposed a model for the effect of reaction conditions on the structure which depended on the relative rate of the hydrolysis and condensation reactions. In the case where the hydrolysis reaction is much faster than the condensation reaction it was proposed that the

condensation reaction exerts control over the structure. This control is based on the fact the reaction mechanism requires a deprotonated silanol group. In any reaction the silanol which will be deprotonated will be the most acidic and this is determined by the other substituents on the silicon atom. The acidity of the silanol increases as the electron donating ability of the other groups attached to the silicon decrease. Therefore the replacement of an alkoxy group with a silanol or a silanol with a -O-Si bond will increase the acidity of a silanol attached to the same silicon atom. Hence the most acidic protons and therefore the most likely species to undergo condensation as the deprotonated silanol will be the most cross-linked. Similarly the least likely to be deprotonated will be the least acidic species. So that in conditions where the hydrolysis is rapid compared to the condensation, the condensation reaction will occur preferentially between the most cross-linked polymer and the least cross-linked monomer thus tending to produce more highly cross-linked polymers.

When the condensation reaction is much faster than the hydrolysis reaction Brinker proposes the structure is determined by the hydrolysis reaction. The acidic hydrolysis reaction depends on an electrophilic attack on the alkoxide oxygen which will not be sensitive to electronic effects but will be sensitive to steric effects. Therefore the rate of hydrolysis would be monomer > chain ends > middle of chain. The silanols on the weakly cross-linked species then condense to form less highly cross-linked polymers.

It can be seen that the two models above are quite similar and the product from the different type of reaction are the same in both cases. However the authors point out that these are fairly extreme conditions and many of the conditions employed to carry out these reactions do not fit precisely into one category. Keefer (1984) also points out that the mechanisms which he proposes only bias the reaction to one type of product but that other conditions may override this bias. For example although base catalysed reactions are expected to form dense highly cross-linked polymers, a low water content will inhibit the hydrolysis reaction but tend to accelerate the condensation reaction. This will lead to condensation occurring between species which are not fully hydrolysed and thus produce less highly cross-linked products.

Therefore the initial reaction conditions alter the basic structure of the polymers formed by the reaction. As the reactions proceed the polymers grow by the addition of monomers by condensation and as they grow larger they interpenetrate other polymers present and link by condensation. Thus the clusters grow larger until a single polymer stretches across the volume of the reaction and this is often termed the sol to gel transition (Scherer, 1987). In the case of base catalysed reactions where the product polymers tend to be highly cross-linked there tends to be less interaction between the different polymers. This leads to the formation of particulate species in the base catalysed system. The actual form of the polymer interaction leading to the gel and a suitable model to describe it are still a matter of debate

(Zarzycki, 1986; Scherer, 1987; Pope and MacKenzie, 1988). However it is clear that the structure of the gel will be determined by the structures of the polymers which produce it and therefore on the reaction parameters forming the polymers. A more detailed discussion of the formation of polymers and gels is given in a number of sources (Scherer, 1987; Brinker, 1988; Brinker et al, 1988(b)).

The above discussion indicates how variation of the basic conditions of the reaction can alter the rates, mechanism and product structure. Studies and understanding of these features are further complicated by the fact that the conditions change during the reaction. As the reaction proceeds the alkoxide and water concentrations fall and the alcohol concentration rises. Then as the condensation reaction occurs the water concentration rises again. Further, the reaction also produces silanol groups which are acidic, so that under base catalysis the silanol groups will react with the base and reduce the pH. Again as the condensation reaction occurs the silanol groups are destroyed and the pH will rise again (LaCourse et al, 1983).

1.6.4 GEL TO GLASS CONVERSION

Having produced the gel from the reaction the next stage of the production process is the conversion of the gel to a glass. Although this is referred to as a single step it is in fact a number of processes. These involve the drying of the gel and then the heating of the gel to convert the dry gel to a glass. The

latter step involving the removal of residual organic material and hydroxyl species, elimination of pores and shrinkage and densification of the material. The processes occurring from the conversion of the wet gel to the final glass product have been described in detail by several authors (Kawaguchi et al, 1986; Scherer, 1987; James, 1988). Because the work in this thesis did not deal with the conversion of the dry gel to the glass these processes will not be outlined further.

The one step which will be of direct importance to the work described here is the drying of gels, because any examination of the gel in an electron microscope would require its drying. The processes which occur during the drying of a gel are complicated and have been greatly elucidated by the work of Scherer (1986(a), 1986(b), 1987, 1988(a), 1988(b)).

The drying of gels produces a number of difficulties. These are generally caused by the interfacial energy between the different phases present. As the solvent begins to evaporate the surface of the solid phase becomes exposed. Because the interfacial energy of the solid-vapour (γ_{SV}) and the solid-liquid (γ_{SL}) differ, a number of changes occur. The specific energy of γ_{SV} there is greater than that of γ_{SL} there is a greater tendency for the dry region to shrink. A further possible result of this difference is that the liquid spreads along the outside of a pore to reduce the vapour-solid interface, this induces a pressure difference which can act to draw the pore walls closer together. Also because the capillary pressures in the system depend on the

diameter of the pore, any difference in pore diameter leads to pressure differences in the gel.

Because of the different sources of pressure and their complex interrelation the drying of the gel is a difficult process. If the conditions are not controlled carefully the pressures will warp or crack the gel. The system is further complicated by the active species on the surface of the material, such as alkoxy or silanol groups, which promote shrinkage because this would allow their reaction. Further, because the solvent is a mixture of liquids which have different evaporation rates there may be composition gradients in the liquid phase, adding another complicating factor.

The above, very brief, outline of the drying processes indicate that it is one of the most complicated and time consuming steps in the production of monolithic bodies. However some of these difficulties can be overcome by the use of drying control chemical additives which appear to thicken the solid phase, making more able to endure the pressures, and reducing the spread of pore sizes, reducing the pressure differences. The drying process and the shrinkage involved also greatly alter the structure, making observations difficult.

1.7 SILICA

Silicon and oxygen between them constitute 75.2% of the earth's crust, including terrestrial waters and the atmosphere

(Stark and Wallace, 1982). It is therefore not surprising to find that the combination of these elements is one of the most frequently found, both as pure silica (silicon dioxide) or combined with other elements.

The basic unit found in the combinations of silicon and oxygen is a silicon atom in the centre of a tetrahedron which has four oxygen atoms, one at each of the four corners of the tetrahedron. These tetrahedra link by a neighbouring silicon sharing from one to three of the oxygen atoms in an adjacent tetrahedron. This leads to the formation of strands, planes and networks of tetrahedra (West, 1985; Adams, 1981; Wells, 1984). If the ordering of the tetrahedra is regular and symmetrical the material is crystalline. If not the material is amorphous such as a glass or vitreous silica. In the case of silica there is a number of crystal types, listed in table 1.1, with the A.S.M.T. index where available. The large number of crystalline forms indicates the large number of possible regular arrangements of the tetrahedra. It should be noted that some of these crystal forms, such as stishovite and coesite, are only produced under the extreme conditions of volcanoes or meteor craters (Iler, 1979) and are therefore not expected to be observed normally.

These silica structures are commonly found in the earth in mineral such as quartz, chalcedony and opal or with impurities within the structure in materials such as amethyst, citrine, agate, onyx and carnelian (Kirkaldy, 1973; Iler, 1979).

α-Quartz (A.S.T.M. file 5-490)

β-Quartz (A.S.T.M. file 11-252)

α-Cristobalite (A.S.T.M. file 11-695)

β-Cristobalite (A.S.T.M. file 4-359)

Coesite (A.S.T.M. file 14-654)

Keatite (A.S.T.M. file 13-26)

Melanophlogite (A.S.T.M. file 16-331)

Silica-O (A.S.T.M. file 12-708)

Silica-W

Silica-X (A.S.T.M. file 16-380)

Silicalite

Stishovite (A.S.T.M. file 15-26)

Tridymite S-1 (A.S.T.M. file 18-1170)

Tridymite S-II

Tridymite S-III

Tridymite S-IV (A.S.T.M. file 18-1169)

Tridymite S-V

Tridymite S-VI

Tridymite M-I

Tridymite M-II

Tridymite M-III

Table 1.1: Crystalline forms of silica with XRD index where available.

Where some of the silicon atoms have been replaced with other metal such as aluminium, then a charge imbalance occurs and other metals are required to balance the charge. These other metals often occur between the layers of the tetrahedra. This is the basis of a large number of minerals including clays and aluminosilicate minerals such as feldspar, garnet and olivine.

As well as the large natural occurrence of silica and silicate minerals, and possibly because of it, there has been a long association with man. The earliest tools, and first step to a technological civilisation, were based on flint. The earliest man-made containers were prepared from clays. Similarly many of the early artworks were prepared from clay or from processes involving clays. It has ever been suggested that silicate minerals were necessary precursors for the formation of carbon-based life (Cairns-Smith, 1982).

Although more elements and ceramic materials are available today silica is still a very important part of the ceramics industry. Many glasses are either pure silica or a mixture of silica with other materials and silica is still an important component in many ceramics. Silica is also used as a piezoelectric material, desiccant, selective absorbent, insulator, chromatographic support, thickening agent and anticaking agent in food as well as many others (Greenwood and Earnshaw, 1984; Iler, 1979).

One specific use of silica which will be of importance in this work is that as a support for catalyst. Many catalysts in use today are based on the reactions that occur on the surfaces of

metal. The most efficient way of having the metal present is as extremely small particles dispersed on an inert support. Silica is one of the most commonly used materials for this purpose. In particular silica is used as a support for small particles of nickel. These nickel on silica catalysts are used in a number of reactions including methanation and reforming reactions (Satterfield, 1980).

Because of this central role in the field of ceramics and the availability of suitable and easily handled alkoxides of silicon much of the work in sol-gel processing has been in the production of silica. Therefore the work described within this thesis will be on the production of silica.

1.8 AIMS OF THE PROJECT

The aims of the work described in this thesis were to produce silica by the hydrolysis of silicon alkoxides and to study the product by electron microscopy and other techniques. By doing so the morphology and properties of the product could be related to the reaction conditions leading to their formation, thus illuminating the processes occurring during the reaction.

A further aim was, that having an understanding of the processes controlling the production of the product and its morphology, this knowledge could be used to control the morphology during the production of a material in which the morphology of the silica was possibly important. The product targeted here was a

catalyst with nickel within the silica, the aim being to incorporate the nickel just below the surface of the silica so that the properties of the catalyst could be altered.

2. ELECTRON MICROSCOPY

2.1 INTRODUCTION

The discovery of the light microscope by Galileo in 1610 allowed the study of materials not previously observable, and thus provided great impetus in a number of scientific fields. From the very first microscope a large number of alterations have been made to improve the resolution. However there is one limit which could not be overcome - the wavelength of the light used (Jenkins and White, 1981). This limit is based on the Rayleigh criterion which states that two point objects can only be resolved by an optical instrument when the central maxima of the diffraction pattern of one, lies no closer than the first minima to the centre of the diffraction pattern of the second. Therefore the dependence on the wavelength, and this limits the theoretical resolution of light microscopes to the region of 200nm. The actual resolution being much lower.

It was not until the hypothesis of wave particle duality (de Broglie, 1924) and its experimental confirmation (Davison and Germer, 1927; Thomson and Reid, 1927) that a practical method of overcoming this limit became evident. The theory would indicate that an accelerated electron had a wavelength much smaller than that of visible light, and therefore a microscope employing accelerated electrons would have a resolution much better than that of a light microscope. However Ruska (1980) has explained that the above argument was only pointed out to him after the

initial work on the electron microscope had been carried out. In fact the initial investigations of imaging (Knoll and Ruska, 1932) were based on the work of Busch (1926, 1927) which treated electrons as classical charged particles.

The work of Knoll and Ruska led to the production of the first transmission electron microscope (TEM) in 1931 and the first high resolution instrument was built by the same pioneers in 1933. This instrument was capable of resolving 50nm, a great advance on light microscopes. Since this time the development has continued to the present state of the technology which is far beyond the vision of the originators, Knoll and Ruska.

Modern electron microscopes such as those at Glasgow are capable of routinely achieving resolution of 0.3nm. Instruments which employ higher accelerating voltages such as the Cambridge 600kV microscope (Cosslett et al, 1979) can achieve atomic resolution, for suitable specimens, and have achieved lattice resolution of less than 0.1nm (Hall and Hines, 1970; Murata et al, 1976; Iijima, 1977; Fryer, 1983; Marks and Smith, 1983; Smith et al, 1983(a), 1985). This ability allows the detailed study of structure in many fields (Murata et al, 1976; Hirsch et al, 1965; Fryer and Smith, 1984; Buseck, 1985) making the electron microscope one of the most important research tools in existence. In recognition of this fact Ruska gained the Nobel prize for physics in 1986.

The history of electron microscopy has been well documented (Ruska, 1980; Mulvey, 1967; Goodman, 1981; Cosslett, 1981(a), 1981(b), 1987; Hawkes, 1985) and the electron optical theories and

development of the instrument have been extensively reviewed (Hirsch et al, 1965; Zworykin et al, 1945; Hillier and Vance, 1945; Cosslett 1951; Magnan, 1961; Hall, 1966; Hawkes, 1972; Grivet, 1972; Cowley, 1979; Geiss, 1979; Spence, 1980; Wischnitzer, 1981; Watt, 1985) with practical techniques used in modern day microscopy described by Kay (1965).

2.2 PRINCIPLES OF THE ELECTRON MICROSCOPE

Transmission electron microscopes are designed to operate in a similar fashion to light microscopes. In both there is a source of illumination which is focused onto the sample being examined. The illuminating agent then passes through the sample, interacting with it. The wave exiting from the sample is then magnified and projected to produce a magnified image which can be studied. The differences between the two systems arise from the use of the beam of electrons as the illumination source in TEM.

Therefore the source of illumination must be a source of electrons rather than visible light and, because electrons can not be focused by glass lenses, magnetic or electrostatic lenses must be used. These are magnetic or electrical fields designed to alter the path of an electron in an analogous fashion to the alteration of a ray of light in a glass lens. As the electron beam is not visible it could not be directly observed and the image must be projected onto a fluorescent screen for examination. Because electrons have a low penetrating power, and can only travel significant distances in a vacuum, it is necessary to have thin

samples and the column of the microscope must be kept under a vacuum of 10^{-3} Pa or less.

The main features of a modern transmission electron microscope are shown schematically in fig. 2.1 and the operation in the transmission mode is depicted in fig. 2.2.

The source of illumination is the electron gun, in which electrons are generated and focussed into a fine beam. The source of electrons is an electrically heated cathode emitter at a selected negative potential. Owing to its high melting point, low vapour pressure, and high mechanical strength tungsten is normally used as the emitter in the form of a hairpin filament (Hall, 1966; Haine and Cosslett, 1961). An increase in source brightness can be obtained by using special pointed tungsten filaments (Wolfe and Joy, 1971) or from lanthanum hexaboride cathodes (Ahmed, 1971; Batson et al, 1976; Yonezawa et al, 1977). Also field emission cathodes (Crewe et al, 1968) can replace electrical heating with similar benefits.

The electrons produced in the gun are then accelerated by the potential difference between the filament and an anode plate kept at earth potential. The beam is then focused onto the sample by the condenser lens system with a field limiting aperture. A double condenser lens is normally used for high resolution studies. The first lens produces a highly demagnified image of the electron source. This beam of reduced cross section is then projected onto the specimen by the second condenser lens. This system gives a very small minimum spot size, with the advantage of enhanced brightness over a small area. After the beam emerges

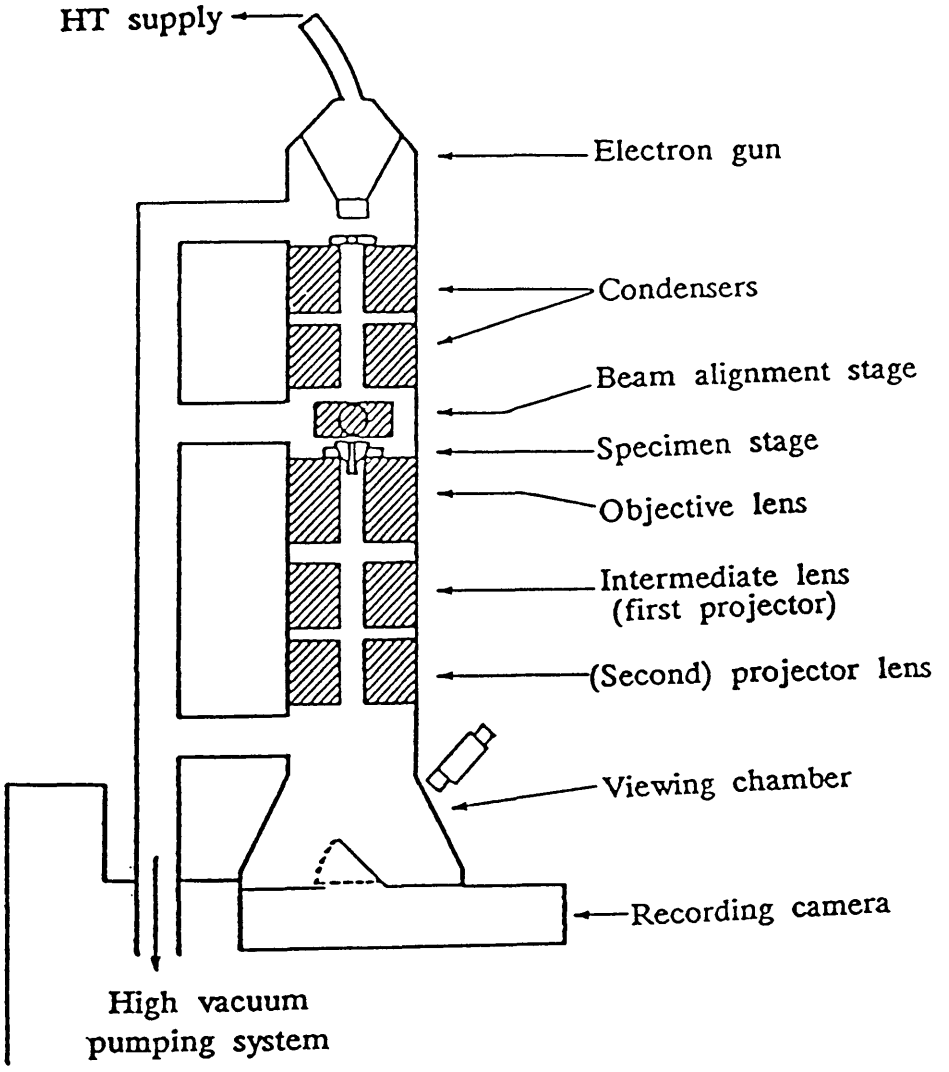

Fig 2.1: Schematic diagram of a transmission electron microscope.

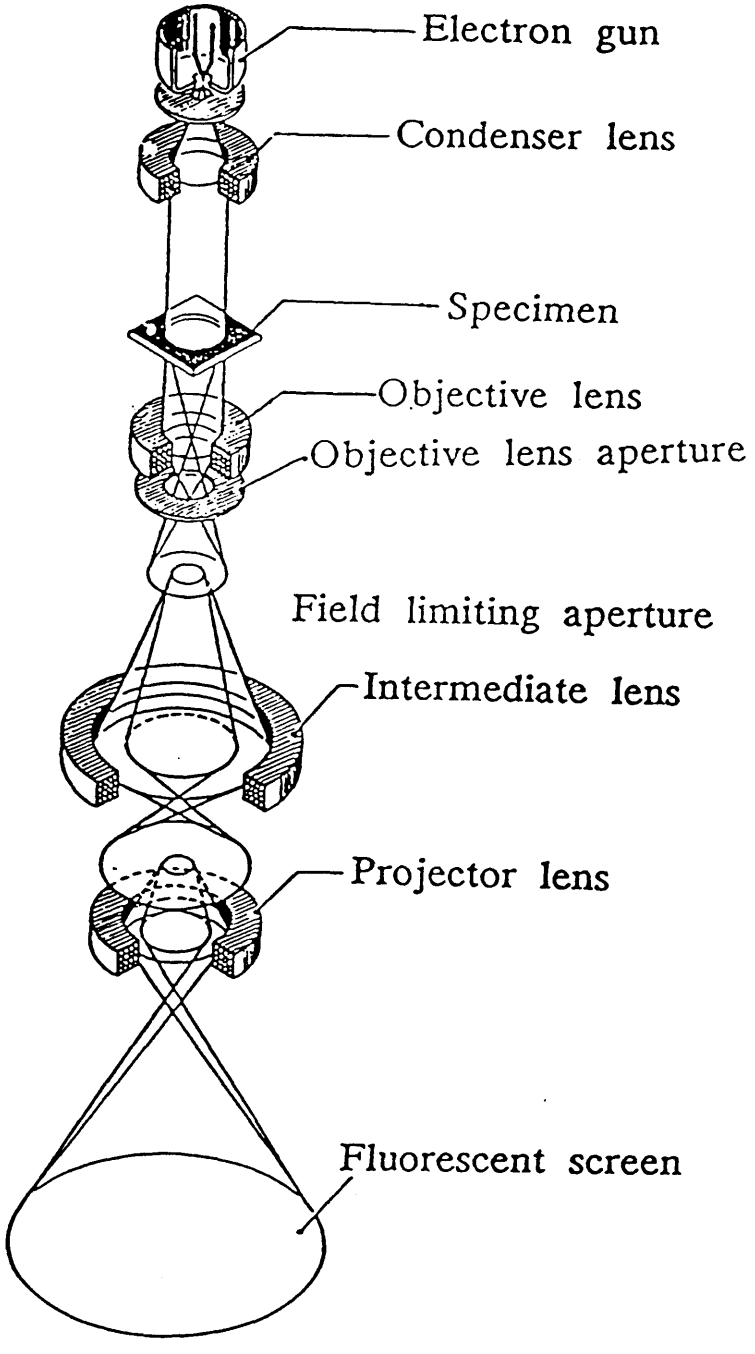

Fig. 2.2: Operation of the TEM in the transmission mode.

from the specimen the image is magnified and projected onto a fluorescent screen by a lens system consisting of an objective, intermediate and projector lenses. The image can then be recorded on a photographic plate positioned beneath a movable section of the fluorescent screen. The magnification is determined by the excitation of the intermediate lens, the brightness by control of the excitation of the condenser lens and the focus is controlled by the objective lens.

The objective lens detects, transmits and magnifies the modified electron beam and therefore its performance is critical to the overall performance of the microscope. Light microscopes employ a series of converging and diverging lenses to compensate for individual lens defects. However the nature of electrostatic and electromagnetic lenses is always converging and as such the lens defects can not be compensated for in the same manner as light microscopes. Therefore high resolution electron microscopes require an objective lens designed and constructed to an extremely high standard. Even with this, the defects still occur and this has a great effect on the performance of the microscope which will be detailed later.

The intermediate and projector lenses, although less critical to the overall performance, transmit and further magnify the modified electrons from the objective lens.

The information which can be recovered from TEM is contained in the electrons scattered during the passage through the sample. The information desired is represented by perturbations in the electron waves. Electron optical defects can cause similar

perturbations. However if these are suppressed to a lower level than the specimen perturbations then meaningful resolution may result, although the lens aberrations can make interpretation difficult.

The work in this project was carried out on JEOL JEM 100C and 1200EX transmission electron microscopes, the electron source being either a tungsten hairpin filament or a lanthanum hexaboride cathode. In the case of the JEM 1200EX the accelerating voltage is 120kV and therefore the electron would have a wavelength of 0.003nm. This should allow direct observation of atomic detail, but as will be made clear later lens aberrations limit the performance of the microscope.

2.3 BEAM SPECIMEN INTERACTION

The basis of all information gained from electron microscopy is the interaction of a beam of high-energy electrons with the specimen. The possible interactions are summarised in fig. 2.3 and it can be seen that there are a number of signals generated. All of these signals can be used to gain information about the specimen. Those which are of use in TEM are indicated. The others are used for scanning electron microscopy or analytical techniques such as energy dispersive spectrometry (EDS), electron energy loss spectrometry (EELS), electron probe microanalysis (EPMA) and several others (Williams, 1984).

The electron microscope is based on the interaction between the electron beam and the electrostatic potential within the

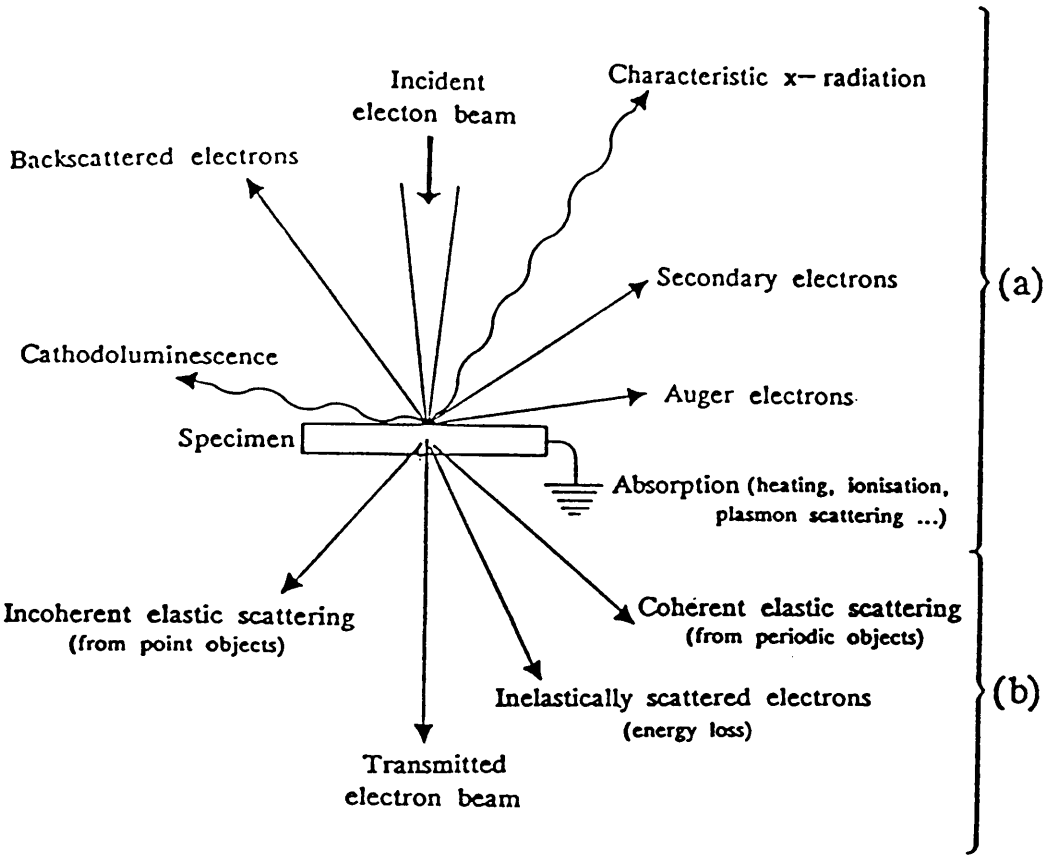

(a) Scanning or Analytical Electron Microscopy

(b) Conventional or Scanning Transmission Electron Microscopy

Fig.2.3: Schematic representation of the information resulting from the interaction of the electron beam with the specimen.

specimen (Coulomb interaction). Almost all of the incident electrons pass through (assuming the sample is thin) with only those passing close to atoms being deflected. This situation can be described quantum mechanically by Schrodinger's wave equation (Schrödinger, 1926).

$$\hbar^2\nabla^2/\ 2m\psi(r) \ -\!\!-\ e\varphi(\underline{r}) \ = \ -i\hbar d\varphi(\underline{r})/\ dt$$

In which $\psi(r)$ is the wave function such that $|\psi(r)\ |^2$ is the probability that an electron will be present in a unit volume. The electrostatic potential is described by $\varphi(\underline{r})$, m is the mass of the electron and e is the charge of the electron. Solving this equation for electrons of a single energy describes the effect of the specimen on the incident electrons. The two dominant scattering mechanisms are:

(a) Elastic scattering occurs when the electrons of the probe interact with the nuclei in the specimen and are deflected without loss of energy. The scattering angles are related, in crystalline samples, to the geometry of the crystal lattice and to the electron wavelength.

(b) Inelastic scattering occurs when the electrons of the probe interact with the orbital electrons of the specimen and are deflected with a loss of energy.

Increasing the atomic number, of the specimen nuclei, or increasing specimen thickness increases the elastic scattering of

electrons. If elastic scattering occurs at large angles to the optical axis of the incident electron beam, or an aperture is inserted such that the electrons scattered greater than the aperture angle are cut out then image contrast arises as "mass thickness" contrast or amplitude contrast, or for specimens with a periodic nature "diffraction contrast". In such cases, areas of specimen from which elastically scattered electrons have been removed appear dark in the image.

In inelastic scattering small deflections are imparted to the electrons along with the alteration to their energy and hence their wavelengths. Recombination of these inelastically scattered electrons with similarly altered unscattered electrons results in increased or decreased intensities in the image contrast, depending on the relative phases of the interacting waves. This phenomena is referred to as inelastic phase contrast. Elastic phase contrast correspondingly can be obtained if the aperture allows transmission of the phase-altered elastically scattered electrons. Amplitude is again increased or decreased to allow recombination of these with the undeviated electrons. If the elastically scattered electrons arise from a periodic structure in the specimen then a related periodicity in the image may be obtained. This information may only be obtained for periodicities normal to the electron beam. This is the basis of "lattice imaging" in high resolution TEM.

Small periodicities normal to the electron beam produce widely elastically scattered electrons. These will be transmitted by sufficiently large objective aperture, but will be focused at

off-axis parts of the objective lens, as a consequence of the lens aberrations which thus severely effect phase contrast image retrieval and interpretation.

Thin specimens (<10nm) are the only ones for which elastic and inelastic phase contrast effects can easily be interpreted. Electrons entering a thin specimen can be imagined to undergo only a single scattering event and conform to the kinematic approximation (Hirsch et al, 1965; Whelan, 1959). Multiple scattering of the electrons occurs in thicker specimens and a more rigorous and accurate treatment has been developed to account for scattered amplitudes and phases in this case (Cowley and Moodie, 1957).

2.4 IMAGE FORMATION

The interaction of the electron beam with the specimen leads to the formation of a transmitted wave at the exit surface of the specimen. This transmitted wave may be interpreted as being the sum of the unscattered wave and a set of scattered waves. The next process of importance is the propagation of this transmitted electron wave along the optical axis of the microscope and the formation of an image.

The principle is the same as that of Abbé theory (Abbé, 1873) for gratings and light optics. If the scattered and unscattered beams can be made to recombine so combining their phase and amplitude, then a lattice image of the planes which are diffracting may be resolved directly (phase contrast).

Alternatively amplitude contrast is obtained by deliberately excluding the diffracted beams from the imaging process by use of suitably sized apertures placed in the back focal plane of the objective lens.

The Abbé theory of imaging may be conveniently translated to mathematical form for specimens in which only single scattering events occur (Cowley, 1975). As indicated in fig 2.4 the distribution of wave amplitude in the back focal plane $A_f(x,y,)$ at the exit surface of the specimen by a Fourier transform

$$A_f(u,v) = F[A_o(x,y)]$$

where x,y and u,v are coordinates perpendicular to the optical axis in the object and back focal planes of the objective lens respectively.

The waves will then propagate to the image plane where they interfere to give an amplitude distribution $A_i(x,y)$. This may be represented by a second Fourier transform

$$A_i(x,y) = F[A_f(u,v)] = F(F[A_o(x,y)])$$

This formation expresses the imaging process ie, the operation of obtaining the amplitude and phase distribution in the image, given that in the object, can be regarded as two successive Fourier transforms.

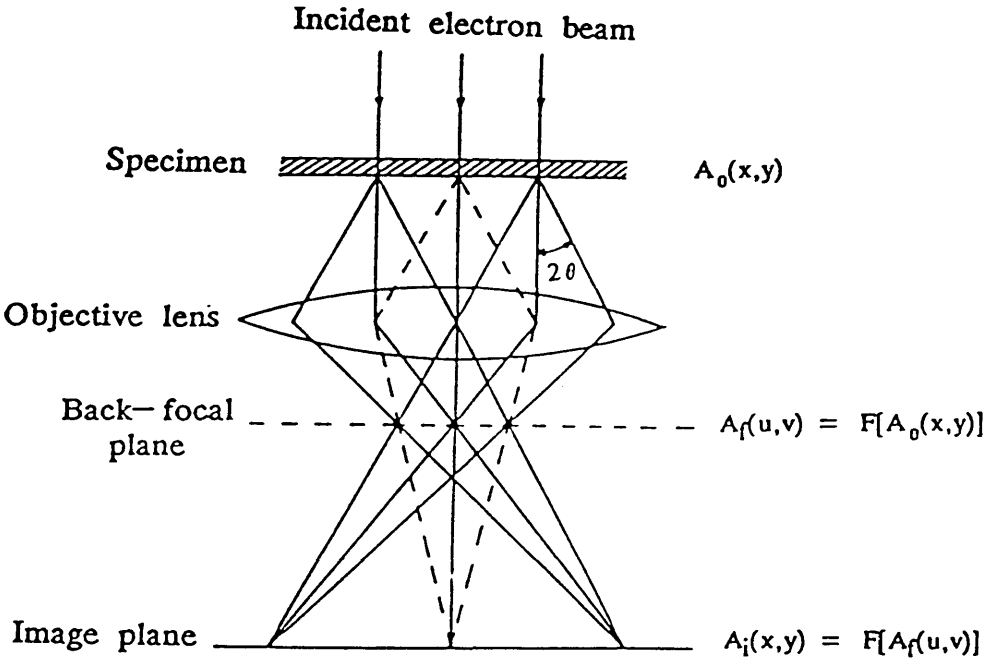

Fig. 2.4: Schematic diagram of the formation of an image by the objective lens of a TEM

2.4.1 LENS ABERRATIONS

The above discussion on image formation is based on an ideal system where all of the exit wave takes part in the imaging process and the lens system perfectly reproduces a magnified image of this wave. Unfortunately this is not the case, the lenses are not perfect and these imperfections have a direct effect on the operation of the microscope. Also the interaction of the incident wave with the sample scatters some of the electrons. The electrons scattered at large angles (those scattered by small periodicities) will not take part in the imaging process because they will be removed by the apertures, or at extreme values by the microscope column.

The imperfections are lens aberrations which are analogous to those obtained in light optical systems. There are several aberrations which occur, many of which can be reduced or eliminated by careful construction of the lenses. The aberrations which are of greatest importance to the image formation are:-

(a) Spherical aberration. Because of the nature of electron-field geometries, and the coincidence of the component electron rays, electrons originating at different points on the object are focused at slightly different points along the optical axis.

(b) Astigmatism. This problem is most troublesome in the objective lens although the condenser lens system is also

affected. This occurs because the focal length of a lens is longer in one plane direction than another normal plane direction. This can be due to inaccuracies in manufacture, inhomogeneities in the soft iron pole piece or can be caused by contamination within the microscope column, causing distorting fields due to charging. The latter can be minimised by maintaining extreme cleanliness on all surfaces, especially apertures, which are exposed to the electron beam. A compensating field is applied to correct astigmatism, this is established when the grain of carbon support film appears symmetrical, or a symmetrical fresnel fringe is obtained around a hole in "holey" carbon film (Haine and Mulvey, 1954).

(c) Chromatic Aberration. The above aberrations are based on problems in the lenses, there are also problems caused by the electron beam. These are basically due to velocity differences within the electron beam ie the electrons do not have a uniform energy or velocity. Therefore the lenses have different effects depending on the energy of the electron, that is the focal length depends on the energy of the electron.

The differences in velocity can arise from a number of effects. These are (i) the energy distribution of the electrons emitted from the source, due to different work functions on different crystal faces; (ii) instability of the electrical power supply and (iii) electron-electron repulsion at the beam cross-over (the Boersch effect).

In practice the use of a low beam current can reduce the

Boersch effect and the use of single crystal emitters can reduce the energy distribution of the beam.

2.4.2 RESOLUTION

The process of image formation and the effect of the electron optical system was considered in detail by Scherzer (1949) who developed a wave mechanical formulation of image formation. This formulation took account of the interaction of the electron beam with the specimen and subsequent effects of the optical system in transforming the propagated wave to the image plane.

The specimen is regarded as a weak phase object (Grinton and Cowley, 1971; Lynch and O'Keefe, 1972), single scattering conditions apply and scattered amplitudes are considered to be much smaller than those in the primary wave. Thus in mathematical terms, for a coherent, monoenergetic plane electron wave of unit amplitude the effect of passage through the object can be represented by the equation

$$\psi_o(r) = \exp[i\delta\varphi(r)] \qquad (i)$$

where ψ_o is the transmitted amplitude of the objective wave (o)

r represents real space coordinates

i indicates the phase nature of the object

δ is the interaction constant $\pi/w\lambda$, where w and λ are the relativistically corrected accelerating voltage and electron wavelength respectively

If the approximation of the weak phase object holds, then the higher order terms in $\delta\varphi(r)$ can be neglected and the equation becomes

$$\psi_o(r) = 1 + i\delta\varphi(r) \qquad \text{(ii)}$$

As described earlier the Fourier transforms of this object wave gives the transmitted amplitude in the back focal plane of the objective lens.

However electromagnetic lenses are not perfect and the electrical and mechanical defects are accounted for by the inclusion of a phase modulator, $\chi(s)$, where (s) denotes reciprocal space coordinates. The objective aperture is also situated in the back focal plane of the objective lens and therefore an aperture function A(s) is inserted, with values of one inside the aperture, and zero elsewhere. Thus the scattered wave amplitude in the back focal plane is given by

$$\psi_D(s) = F[\psi_o(r)] \exp[i\chi(s)] A(s) \qquad \text{(iii)}$$

Under single scattering conditions, the resultant amplitude distribution is given by the difference between the primary undeviated wave amplitude, $\delta(s)$, and the elastically scattered

amplitude distribution represented by equation (iii). Substituting for $\psi_o(r)$ from (ii), and performing the Fourier transform operation for all (s) inside the objective aperture gives;

$$\psi_D(s) = \delta(s) - [\delta\varphi(r)\sin\chi(s) - i\delta\varphi(r)\cos\chi(s)] \quad \text{(iv)}$$

A second (inverse) transform of (iv) corresponds to the image plane and gives the resultant amplitude distribution;

$$\psi(r) = 1 - F[\delta\varphi(r)\sin\chi(s) - i\delta\varphi(r)\cos\chi(s)] \quad \text{(v)}$$

and the intensity distribution in the image plane (that observed on the micrograph) is given by

$$1(r) = \psi\,\psi^*$$

$$= 1 - 2\delta\varphi(r)^* F\sin\chi(s) \quad \text{(vi)}$$

where $*$ indicates a convolution integral. Equation (vi) represents the intensity distribution in the image plane, within the limits of the weak phase approximation (Grinton and Cowley, 1971; Lynch and O'Keefe, 1972) used in its derivation. The diffracted amplitudes were shown to be modified by an instrumental function. More correctly the instrumental transfer function modulates the phase of the diffracted waves. However, in the case of a weak phase object the imaginary terms are second order, so that the

image intensity, calculated from the modulated diffraction amplitudes holds good but only for these kinematic conditions. Despite these limitations equation (vi) demonstrated the importance of $\sin\chi(s)$, called the Phase Contrast Transfer Function (PCTF), which determines the transfer of object information to the image plane. For a perfect lens $\sin\chi(s) = 1$, and equation (vi) becomes

$$I(r) = 1 - 2\delta\varphi(r) \qquad \text{(vii)}$$

and the object and the image are linearly related. The defects present in the magnetic lenses preclude this possibility. However, an instrumental phase adjustment factor $\chi(s)$, first derived by Scherzer (1949) takes account of the phase delays introduced by (i) the spherical aberration of the objective lens and (ii) the phase delay introduced by altering the focus of the objective lens so that the image plane is moved along the z-axis by Δf the defocus (Heinrich, 1964).

$$\chi(s) = 2\pi/\lambda\ [\Delta f\alpha(s)^2/2 - C_s\,\alpha(s)^4/4] \qquad \text{(viii)}$$

where $\alpha(s)$ is the scattering angle pertaining to reciprocal space coordinates (s)

C_s is the spherical aberration coefficient of the objective lens

Δf is the lens defocus

The final image contrast is therefore dependent on the oscillatory function $\sin\chi$, having different values at different spatial frequencies, depending on the scattering angle for the particular frequency, the defocus value and the spherical aberration of the objective lens. Fig 2.5 shows sin plotted against reciprocal periodicity ($1/d\ nm^{-1}$) assuming coherent illumination over a range of defocus values. The diagram pertains to the JEOL JEM 100C microscope operated at 100kV. The polepiece spherical aberration constant was C_s = 0.67mm with an aperture of 50μm.

For most applications, it is desirable to operate the microscope at defocus values where the appropriate transfer function value is identical and near unity over the maximum range of spatial frequencies, without contrast reversal. This "optimum defocus" value $\Delta f'$ first found by Scherzer (1949) is given by;

$$\Delta f' = 1.2\ [C_s \lambda]^{1/2} \qquad \text{(ix)}$$

For the 100C microscope $\Delta f'$ is equal to 60nm, as shown in fig 2.5. Fig 2.6 shows the resolution loss with increasing C_s value for the optimum defocus value at 100kV.

The Scherzer cut-off d_{min}, was calculated (Eisenhandler and Siegel, 1966) as

$$d_{min} = 0.65 C_s^{0.25} \lambda^{0.75} \qquad \text{(x)}$$

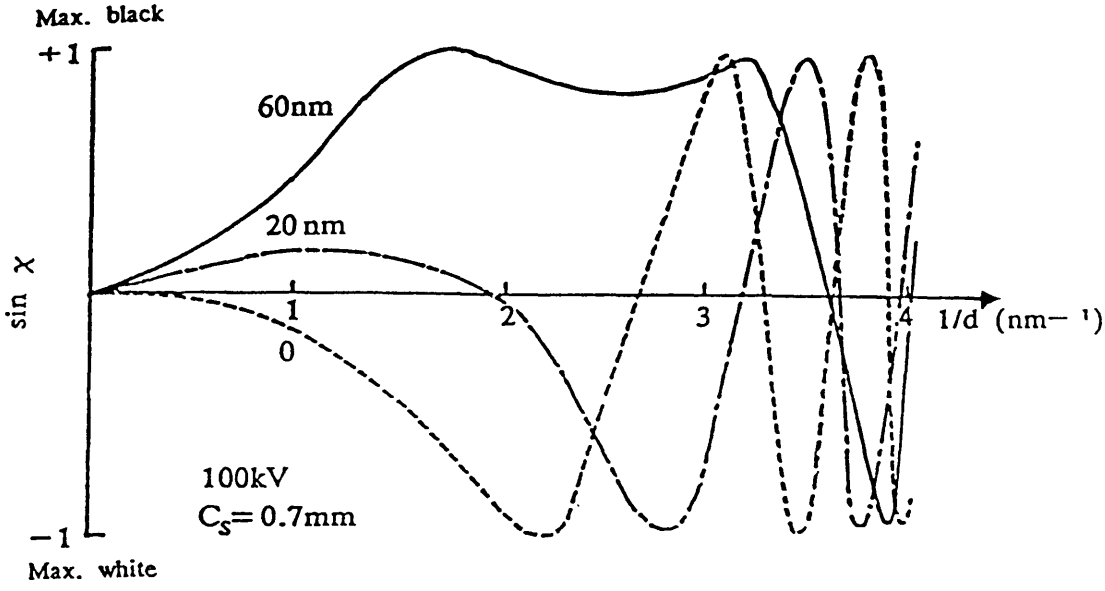

Fig. 2.5: Phase Contrast Transfer Function for a range of defocus values, Δf=0, 20 and 60nm underfocus with a 50 μm aperture cut off.

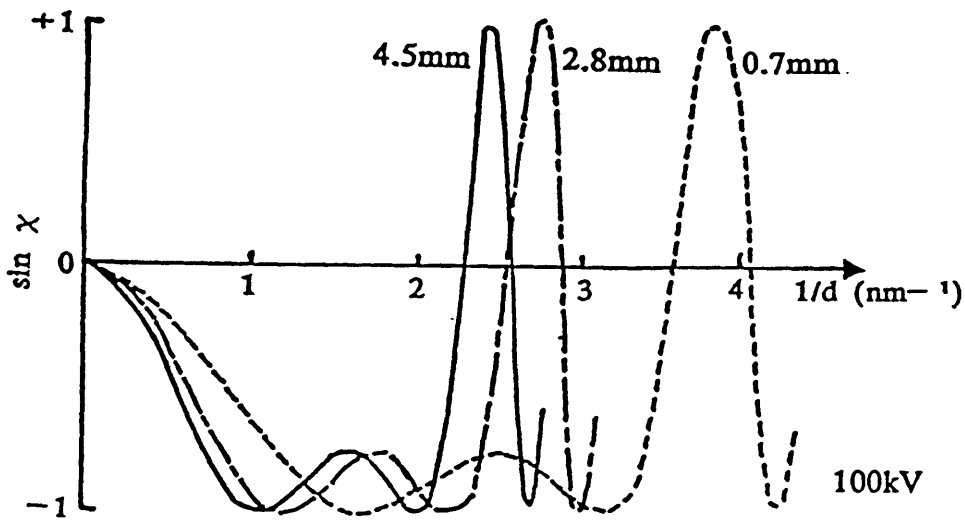

Fig. 2.6: Optimum defocus phase contrast transfer curves for increasing spherical aberation ceofficients C_s = 4.5, 2.8, 0.7mm.

and is the largest value of d for which $\sin\chi = 0$ at the optimum defocus.

The optimum defocus defines the limit of the most faithful reproduction over the maximum range of spatial frequencies. However smaller structures can be resolved in good contrast if the appropriate defocus value is selected. For example in fig 2.5 a structural periodicity of 0.29nm ($0.34nm^{-1}$) would be imaged at high contrast at 20nm defocus or in reverse contrast at zero defocus. However, greater care is required in image interpretation as the absence of detail from other periodicities can lead to spurious effects and thus erroneous observations.

As stated above the inclusion of the PCTF accounts for the effect of spherical aberration and defocus on the transfer of the exit wave to the image plane. However these are not the only instrumental factors which affect this process. It was assumed that the electrons were monochromatic and that the source had perfect spatial and temporal coherence. These assumptions are not justified and a more complete treatment of the transfer theory must account for these. This has been achieved by including envelope functions (Hanzen, 1971; Hanzen and Trepte, 1971; Misell, 1973; Frank, 1973; Boerchia and Bonhomme, 1974).

If the electron source approximates to a small disc-shape as determined by the final condenser lens aperture, and if chromatic aberration is assumed to arise from sinusoidal modulation of the finite energy electrons by the high voltage system and objective lens current, then the phase contrast transfer function can be further modified:-

$$\sin\chi_{\alpha\epsilon}(s) = \sin\chi(s) \cdot E_{\alpha}(s) \cdot E_{\epsilon}(s)$$

where: $E_{\alpha}(s)$ is the envelope function representing damping of the PCTF due to partial coherence

$E_{\epsilon}(s)$ represents the PCTF modification due to chromatic fluctuations

The mathematical form of these envelope functions has been described (Frank, 1973) and are

$$E_{\alpha}(s) = \frac{2J_1[2\pi\alpha(C_s\alpha^3\Delta f\alpha)/\lambda]}{2\pi\alpha[(C_s\alpha^3-\Delta f\alpha)/\lambda]} \qquad \text{(xii)}$$

and $$E_{\epsilon}(s) = J_o(\pi\lambda.\epsilon/d^2) \qquad \text{(xiii)}$$

where: J_o and J_1 are the zero order and first order Bessel functions respectively.

α is the specimen illumination angle

ϵ is the focal variation due to high voltage (V) and lens current (I) fluctuations

and $$\epsilon = (\Delta V/V + 2\Delta I/I)\, Cc \qquad \text{(xiv)}$$

C_c is the chromatic aberration coefficient

Fig. 2.7: shows respective particle coherence envelope functions and increased resolution loss for larger illumination angles. Fig. 2.8 shows the optimum defocus PCTF modified for illumination angle α= 1 milliradian.

Fig. 2.9 shows the envelope functions due to chromatic fluctuations for several focal variations (ϵ). The calculations are made for JEOL 100C taking $\epsilon \leq 500$nm as calculated from equation (xiv), with $\Delta V/V \leq 2 \times 10^{-6}$ min^{-1}, $\Delta I/I \leq 1 \times 10^{-6}$ min^{-1} and C_c = 1.1mm. Fig. 2.10 shows the optimum defocus PCTF modified for chromatic focal variation ϵ = 500nm.

The above theory, the phase contrast theory, provides a basic outline of the events occurring within the microscope and the effect these have on the image forming process. However the assumptions made in the kinematic approximation are not realistic. In real specimens multiple scattering of electrons occur and therefore a true description of the interaction of the electron with the specimen requires a more rigorous theory. This has been provided in the dynamical treatment (Cowley and Moodie, 1957; Lynch and O'Keefe, 1972; Allpress et al, 1972; Cowley, 1975) which will provide accurate phases and amplitudes of the scattered waves.

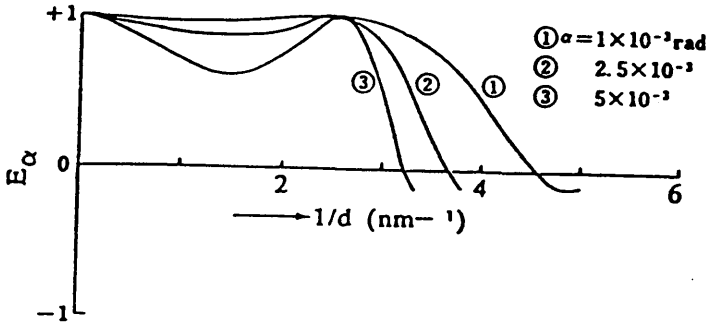

Fig. 2.7: Partial coherence envelope function for various specimen illumination angles (α).

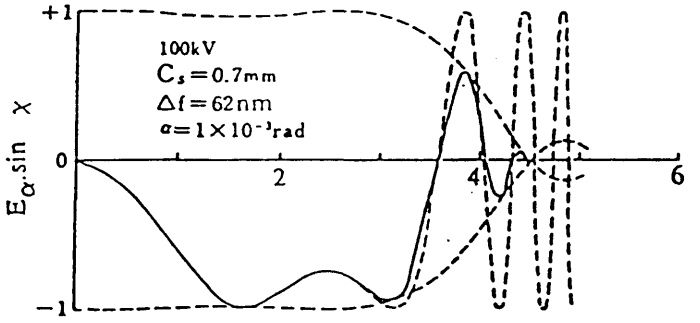

Fig. 2.8: Optimum defocus phase contrast transfer function modified for specimen illumination angle α= 1m.rad.

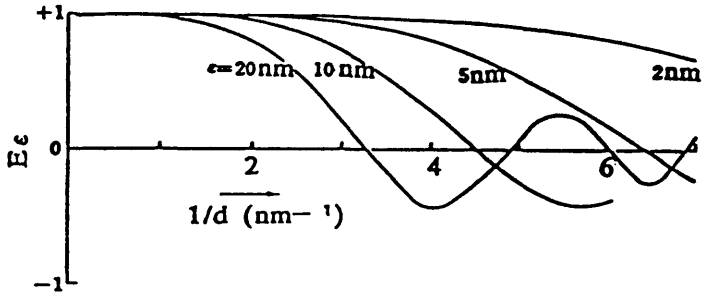

Fig.2.9: Envelope function due to chromatic fluctuations for several focal variations (ϵ).

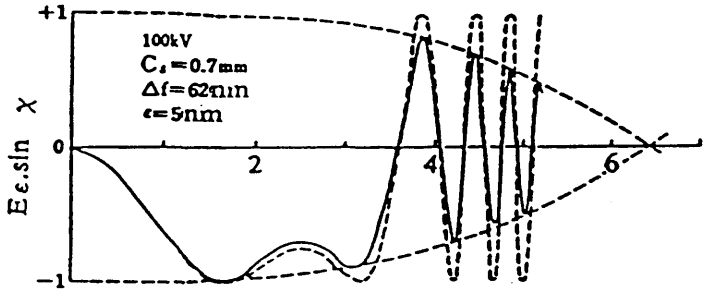

Fig. 2.10: Optimum defocus phase contrast transfer function modified for focal variation ϵ = 5nm.

2.4.3 LIMITING FACTORS

The discussion above described how the electron optical system can affect the resolution of the microscope. However the aberrations in the magnetic lenses and coherence affects already mentioned are not the only factors which can affect the performance of the electron microscope. Some of the other limitations are described below.

2.4.3a SPECIMEN CONTAMINATION

The build up of amorphous, usually carbonaceous material on the specimen, enhanced by the electron beam, obscures fine structure in the specimen and causes a general loss of clarity. The residual atmosphere inside the column of the microscope will contain atmospheric gases including hydrocarbon compounds. These may have originated from vacuum pumping fluids, vacuum sealing gaskets, and any removable parts which are handled by the operator. Under normal conditions there will be a thin layer of hydrocarbon absorbed on all surfaces within the column, including the specimen. Electron bombardment polymerizes the surface film and permanently fixes it in place. The depleted surface layer of hydrocarbon is replenished by continued condensation of vapour and by diffusion of freshly condensed material inwards across the surface from the outside of the electron bombarded area. Thus, a permanent deposit grows on the specimen surface whenever it is

under examination. The deposit is referred to as "contamination" and its rate of formation as the "contamination rate".

Modern electron microscopes reduce this problem by the attachment of anti-contaminators or by maintaining an extremely high and clean vacuum by the use of dry pumps such as sputter-ion and turbomolecular systems. Anti-contaminators normally take the form of liquid-nitrogen cooled jackets around the specimen area, to remove organic and other contaminant vapours by preferential condensation.

2.4.3b SPECIMEN STABILITY

Most material undergo some form of alteration when bombarded by electrons in the microscope. To the extent that such alterations affect the integrity of the information sought from the specimen, they are referred to as "radiation damage", but, when the effects prove incidental to the information sought they are largely ignored.

Radiation damage affects all types of material in the microscope. The affect of radiation damage in organic materials can totally destroy the structure being examined (Holland et al, 1983) and as such as prohibitive to their study. Although inorganic materials are generally more stable radiation damage still occurs (Holland et al, 1983; Burton et al, 1947; Hobbs, 1979; Dahmen et al, 1987; Sharma et al, 1987; Smith et al, 1987). This damage occurs by one of two mechanisms; (a) "knock-on" displacement where the electron beam interacts with the cores of

atoms in the specimen (Seitz and Koehler, 1956) or (b) radiolytic mechanism where the electron beam transfers energy to the electrons in the specimen leading to bond breaking and structure alteration (Hobbs, 1987)

To minimise radiation damage a large number of techniques have been developed. These include the use of image intensifiers and low beam doses (English and Venables, 1971), minimum dose systems which allow focus in other areas of the sample and then the examined area is brought into the photograph area only long enough to expose the plate (Williams and Fisher, 1970). These techniques can also be aided by the use of x-ray film which has a much shorter exposure period (Fryer, 1978; Fryer et al, 1980).

2.4.3c MECHANICAL STABILITY

Mechanical stability, mainly in the form of residual drift in the specimen stage, can adversely affect the microscope performance, especially during high resolution imaging. This problem can be made worse by high beam doses causing local heating which in turn produces differential thermal expansion which causes drift.

2.5 ELECTRON DIFFRACTION

The above discussion on image formation in the electron microscope explained that the objective lens forms the Fourier transform of the exit wave in its back focal plane. Where the

specimen contains a periodic structure, and the planes of this structure are near parallel to the incident electron beam, the Fourier transform will have a regular structure - the diffraction pattern. This gives information about the crystal structure within the sample and can be used to identify the material.

The process of image formation means that the diffraction pattern is always present in the microscope. In the transmission mode (fig. 2.2) the intermediate lens is set so that the objective lens image acts as the object and is propagated to the fluorescent screen. In the diffraction mode (fig. 2.11) the setting of the intermediate lens is altered so that the back focal plane of the objective lens acts as the object and the diffraction pattern is propagated to the fluorescent screen.

The above description explains how the diffraction pattern can be obtained on the fluorescent screen. However it is possible to obtain the diffraction pattern from a small area of the sample rather than the whole area under illumination. This allows the study and identification of small particles or regions of interest within the specimen. This can be achieved by employing selected area diffraction which was pioneered by Boersch (1936) and Le Poole (1947). Fig. 2.12 shows a ray diagram illustrating the formation of the diffraction pattern. It can be seen that the diffraction pattern of the whole illuminated area is formed in the plane at C and the image produced in plane D. If an aperture is inserted in plane D, the rays passing down the column will be limited.

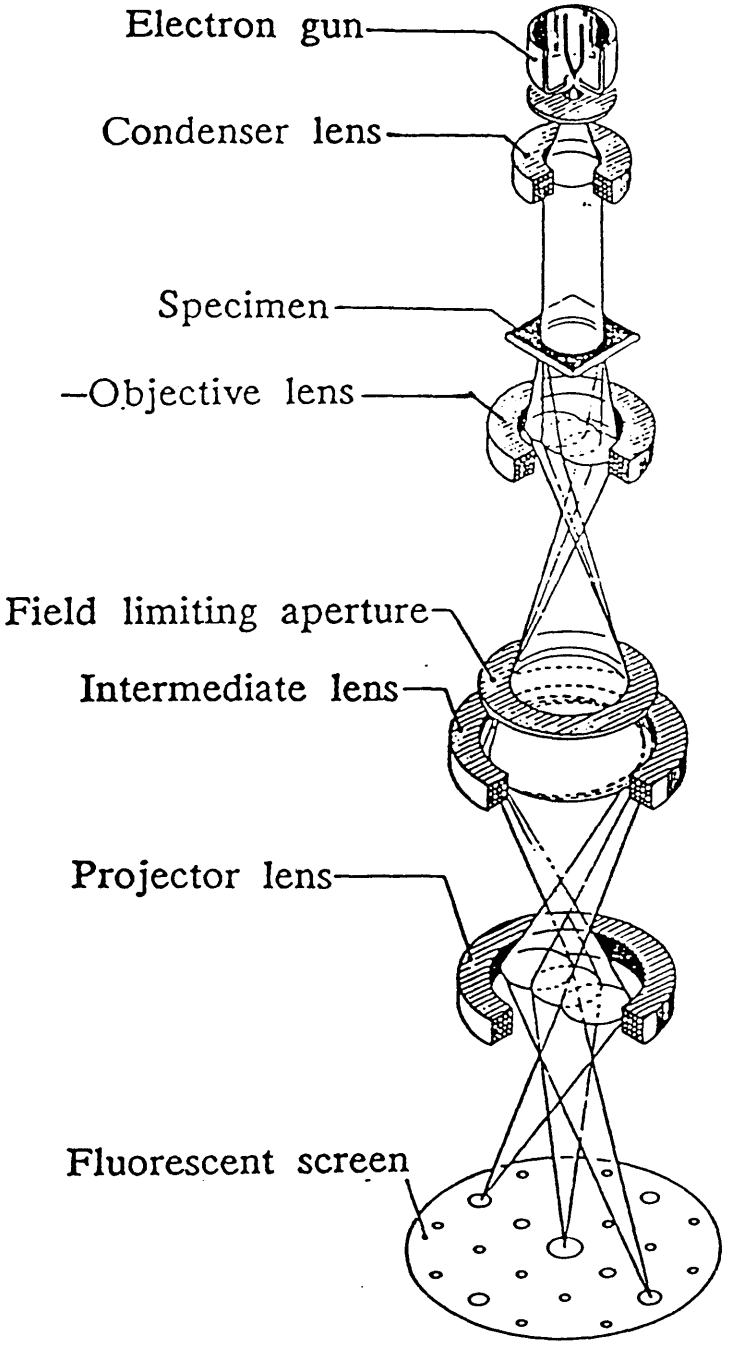

Fig.2.11: Operation of the TEM in the diffraction mode.

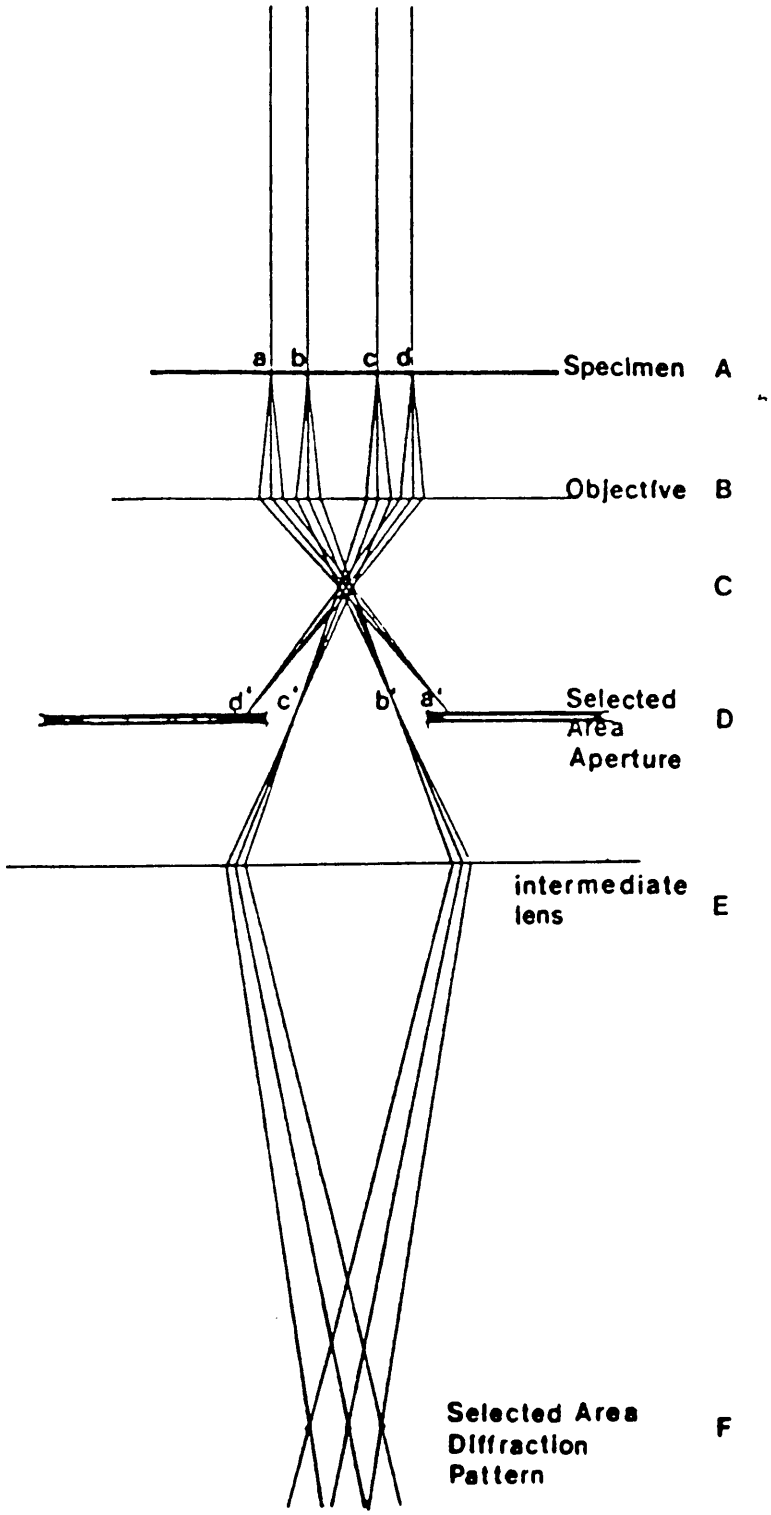

Fig.2.12: Ray diagram illustration of selected area diffraction.

Therefore any electrons which do not originate from an area on the specimen corresponding to the demagnified image of the selected area aperture are stopped. Thus the diffraction pattern formed at F by the intermediate lens is composed only of those electrons which originate within the selected area. Plane F is the image plane of the intermediate lens so the diffraction pattern will act as the object for the projector lens system and will thus be transferred to the fluorescent screen.

The aperture inserted in the plane at D can typically be as small as 20μm with an objective lens magnification of fifty this corresponds to a selected area of 0.4μm. However, these diagrams are for perfect thin lenses and magnetic lenses are not perfect. Due to the effect of spherical aberration electrons scattered from areas other than the selected area can be included in the diffraction pattern which appears on plane F. The significance of the contribution of these electrons depends on the angle at which the electrons pass through the objective lens (Agar, 1960). Thus the area of the specimen contributing to the diffraction pattern varies for each spot and increases with increasing scattering angle. If this effect is to remain negligible for the scattering angles typically encountered, the selected area on the specimen should exceed for example 1μm for a lens aberration of 3.33mm and 100KeV electrons.

In the diffraction mode the electron microscope can be considered as a simple electron diffraction camera. Fig.2.13 shows the evolution of a diffraction pattern from a set of planes

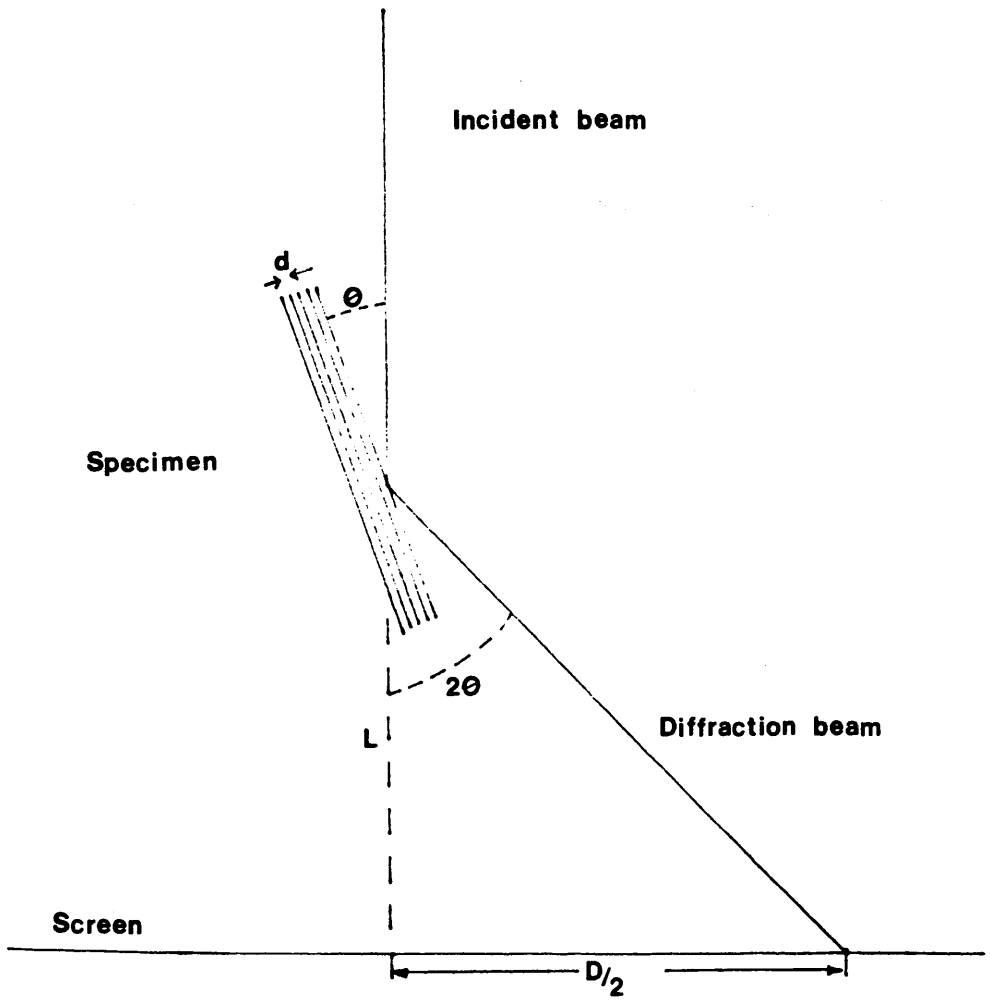

Fig. 2.13: The TEM as a simple diffraction camera.

with a regular periodic spacing, d, at angle, θ, to the incident electron beam. From the diagram

$$\tan 2\theta = D/2L \qquad \text{(xv)}$$

and using Bragg's law for the diffraction

$$2d \sin\theta = n\lambda \qquad \text{(xvi)}$$

for the first order diffraction n = 1. The angle θ is usually less than 3°, and therefore the approximation

$$\tan 2\theta = 2 \sin\theta = 2\theta \qquad \text{(xvii)}$$

is valid. Then by substituting this in equation (xvi) gives the relation

$$D\,d = 2\lambda L \qquad \text{(xviii)}$$

The wavelength, λ, of the electron is set by the operating voltage of the electron microscope. Similarly the value of L is set by the operating conditions of the microscope. It is equivalent to the distance between the diffracting planes and the fluorescent screen and is given by

$$L = f_o M_1 M_2 M_3 \qquad \text{(xix)}$$

where f_o is the focal length of the objective lens, and M_1 M_2 M_3 are the magnifications of the intermediate and projector lenses.

The above expression (xviii) indicates the spacing of the spot or ring in the diffraction pattern is related to the d-spacing of the periodic structure which is diffracting the electrons and a constant, the camera constant, which is set by the conditions in the microscope. This constant is generally found by using a standard of known diffraction pattern. Unknown diffraction patterns are identified by comparison of the spacings with tabulated x-ray data in the A.S.T.M. index (1965). To obtain accurate electron diffraction results, the diffraction mode must be precisely set up, in particular, the specimen height and post specimen lens current must be standardised for correlation of measurements. Even with these limitations, lattices spacings can be obtained to an optimum 1% accuracy. However it has been noted (Andrews et al, 1967) that there is a linear variation in the camera constant with ring diameter due to the decreasing validity of equation (xvii) for large angles. It is also the case that in x-ray diffraction the sample is rotated which does not occur in election diffraction. Therefore the intensities of the electron diffraction pattern may not match those of the x-ray pattern because certain planes may preferentially be in the orientation necessary to diffract the electron beam.

The diffraction pattern contains the structural data, periodicies and orientations for the plane projected normal to the electron beam. Forumulae are available which allow calculation of the interplanar spacing, angle between planes, zone axes and

angles between zone axes for common crystal systems (Andrews et al, 1967; Beetson, 1972). Displacement and changes in intensities in the diffraction pattern give information about changes within the specimen (Hirsch et al, 1965) and the rate at which the diffraction pattern fades gives information about the radiation stability of the sample (Fryer, 1979).

2.6 SCANNING ELECTRON MICROSCOPY

The theoretical basis of the scanning electron microscope is almost as old as that of the transmission electron microscope, first being suggested by Knoll (1935) in 1935. Working models were in existence a few years later (Von Ardenne, 1938; Zworykin et al, 1942). However it was not until the 1950's and 60's that research and development (Zworykin et al, 1942; Smith and Oatley, 1955; Oatley et al, 1965) improved the instrument to the standards now achieved and the SEM became commercially available. The main use of the SEM is to produce a three dimensional image of the surface of the material under observation but many of the processes shown in fig. 2.3 can be used to gain other information.

2.6.1 PRINCIPLES OF THE SEM

When a beam of high energy electrons interact with a solid a large number of effects occur (fig. 2.3). One of these effects is the formation of secondary electrons. The electrons emitted from the surface actually include elastically and inelastically

backscattered electrons and secondary electrons. Therefore the energy distribution of the emitted electrons ranges from zero to that of the incident beam. It is not possible to completely separate inelastically backscattered and secondary electrons but those electrons with energy below 50eV are considered to be secondary (Rudberg, 1934).

The yield of secondary electrons from a solid is dependent on a number of factors. These include the energy of the incident beam, the work function of the solid (Sixtus, 1929) and the angle of incidence of the electron beam (Müller, 1937).

The principle of the scanning electron microscope is illustrated in fig. 2.14. A beam of electrons is generated in the electron gun and accelerated through a potential, usually between 2.5 and 50kV. A series of magnetic lenses then focus the beam into a fine beam probe on the surface of the specimen. The probe is then scanned across the sample by deflecting coils working in two dimensions.

An electron detector then collects the electrons emitted from the surface, mainly secondary electrons, and conveys the current to an amplifier. The output from the amplifier is then used to modulate a cathode ray tube (CRT) which is scanned synchronously with the scan of the sample. The variation of imaging current, normally secondary electrons, which reach the scintillation detector, depends on varying details on the surface on the specimen.

The image contrast is affected by the surface morphology and especially the angle the incident electrons strike the specimen,

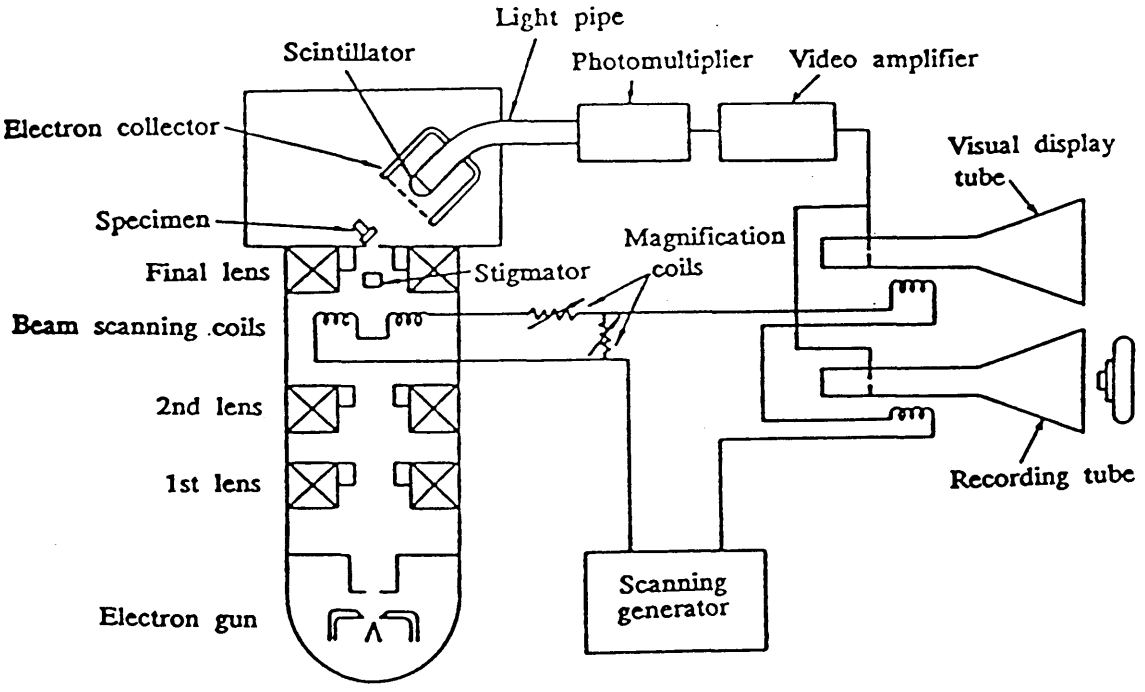

Fig. 2.14: Schematic diagram of the SEM.

the density of the specimen (which determines the penetration of the electron beam), the chemistry and crystal structure of the material (which affects the work function) and by any charging of the surface. Therefore the image attained on the screen of the CRT reflects corresponding factors about the specimen, especially the surface topography (Everhart et al, 1959).

Reflected electrons have high emission velocities and as such their paths to the detector is essentially a straight line, while those of secondary electrons can be deflected by magnetic fields and are generally curved. Consequently reflected electrons will only yield information on parts of the sample for which there is a straight line path between the point of reflectance and the detector. Secondary electrons are not subject to this limitation and will provide far more detail about rough surfaces. Normally, the collector is set up for the detection of secondary electrons and the reflected ones are ignored as far as possible. The superiority of the secondary electrons for revealing detail has been demonstrated (Everhart et al, 1959).

3. EXPERIMENTAL

3.1 MATERIALS

The reagents used to carry out experimental work in this project were as follows. In all reactions using tetraethylorthosilicate it was supplied by BDH as the general purpose reagent grade (98% purity). In reactions using an acid catalyst, concentrated hydrochloric acid was used as Pronalys Analytical grade (35.5 - 37.5% aqueous solution) supplied by May and Baker. Where base catalysis was required both ammonia and ethylamine were used. The concentrated ammonia solution was supplied by Hopkins and Williams as the Analar grade (density 0.88g/ml, 35% w/w aqueous solution) and the ethylamine was supplied by BDH as the anhydrous Analar reagent (99.5% purity).

In reactions aimed at producing material other than pure silica additional reagents were used. In the experiments to determine the effect of the presence of a salt on the reaction the salt used was lithium chloride which was supplied by BDH as a general laboratory reagent (98.5% assay). In reactions which were to determine the effect of the presence of the polymer absorbed on the surface, the polymer employed was polyvinyl alcohol which was supplied by BDH as the general purpose reagent, the approximate molecular weight being 125,000 g/mol.

In reactions to deposit nickel on the silica produced by the hydrolysis reactions, a number of chemicals were used. The first of these was diacetyl (2,3-butanedione) which was a BDH general

purpose reagent (99% assay). Hydroxylamine hydrochloride was supplied as the Aldrich standard reagent grade (99% assay). Nickel chloride hexahydrate was supplied by BDH as a general laboratory reagent (97% assay). In a number of reactions related to the deposition of nickel, dimethylglyoxime was used. This was supplied by BDH as the Analar grade reagent (99.0% purity).

Where the nickel deposition reactions were altered to remove chloride ions, the following reagents were used. Nickel perchlorate hexahydrate was supplied by BDH as a general laboratory reagent (98% assay). Silver nitrate was supplied by Johnstone Matthey Chemicals Ltd, as the standard grade (63% silver assay). Perchloric acid was used as the Pronalys Analytical grade (60 - 62% w/w aqueous solution) supplied by May and Baker. The last reagent used in these reactions was Amberlite IRA 400 Ion Exchange Resin supplied by Hopkins and Williams as the analytical grade, chloride form, 14-52 mesh with an exchange capacity of 1.4 meq/g when wet and 3.8 meq/g when dry (meg = milliequivalent).

In reactions employing tetrabutylorthosilicate the reagent was supplied by Aldrich as the standard reagent grade (97% purity) and was the tetra-n-butylorthosilicate.

In all reactions which employed water the water was distilled. The reactions were normally carried out using ethanol as a solvent because water and TEOS are immiscible. The ethanol was used both as the Analar reagent grade and the technical reagent. The reactions carried out in acid or neutral conditions were prepared using Analar grade ethanol (99.86% purity) supplied by James Burroughs which had been redistilled under nitrogen, the

nitrogen being fed into the liquid through an air leak via a drying train. The reactions which were carried out under conditions of base catalysis employed technical grade ethanol supplied by James Burroughs Ltd. (99.5% purity).

In reactions to standardise the reagents several other materials were used. The concentrated nitric acid (70% w/w aqueous solution) was supplied by May and Baker as the Pronalys grade. Copper Sulphate was supplied as copper sulphate pentahydrate, Analar grade (99% assay) by BDH. Methyl orange and phenolphthalein indicators were supplied as the standard grade by BDH. Accurately known amounts or solutions of hydrochloric acid and sodium hydroxide were prepared from Volucon concentrated volumetric solutions supplied by May and Baker, any dilution necessary was with distilled water.

Sample preparation techniques which employed staining used uranyl acetate supplied as the general purpose reagent (98% purity) by BDH. In several methods of sample preparation organic solvents were employed. These were diethyl ether supplied as the Pronalys AR grade (99% purity) by May and Baker, toluene supplied as the Analar reagent grade (99.5% purity) by BDH, n-hexane supplied as the general reagent grade (95% purity) by Koch-Light Ltd, and chloroform supplied as the general laboratory grade (98% purity) by May and Baker.

3.1.1 STANDARDISATION

To determine accurate values of properties of the reagents which could lie within a range of values standardisation

experiments were carried out.

The first of these was to standardise the strength of the ammonia solutions. This was done by accurately pipetting 20ml of the concentrated ammonia solution into a 1 litre volumetric flask and making up the volume to one litre with distilled water. Then 10ml samples of this solution were titrated against 1M hydrochloric acid solution using methyl orange indicator. This indicator was used because of the weak base nature of ammonia and strong acid nature of hydrochloric acid. The titration was carried out five times and the average result used to determine the molarity of the ammonia solution. Although the results varied with different samples of the ammonia it was usually found to be in the region of 28% w/w rather than the 35% w/w stated by the supplier. The 28% w/w corresponds well to the values quoted for concentrated ammonia solutions in reference books (Stark and Wallace, 1982).

The density of the ammonia solution could be determined by accurately measuring the mass contained in a volumetric flask. Therefore the mass of a given volume and the ammonia contained within it were known and thus the water contained within the volume could also be calculated, hence the water content was determined.

The standardisation of the ethylamine was complicated by the fact that it has a low boiling point (16.6°C at 760 torr). This raised the possibility that the ethylamine would evaporate during the time taken for the titration and thus affect the accuracy of the standardisation. To overcome this problem it was necessary to

alter the technique so that the ethylamine would rapidly be converted to a non-volatile form. Therefore the procedure was as follows. An ice bath was prepared and in it was placed a flask containing 0.1 moles of hydrochloric acid in solution and a small amount of methyl orange indicator. This indicator was used because ethylamine is a weak base and hydrochloric acid a strong acid. Once this had cooled 5ml of the ethylamine was pipetted into the flask and allowed to react with the hydrochloric acid. Once the reaction had taken place the excess hydrochloric acid in solution was titrated against 1M sodium hydroxide solution. The results of these titrations indicate the ethylamine to be 15.64M. This value is almost exactly the theoretical value calculated from the physical properties of the liquid ie 15.18M. Therefore, as there were likely to be inaccuracies in the standardisation it was decided to use the theoretical value in the calculation of reaction compositions.

The standardisation of the hydrochloric acid was carried out by pipetting 10ml of the acid into a flask and titrating against 4M sodium hydroxide solution using phenolphthalein indicator. This indicator was used because of the strong acid - strong base nature of the titration. The procedure being carried out five times and the average value being used.

The density of the ethanol, both technical and Analar grades, was determined by accurately measuring the mass of ethanol in a volumetric flask. The density of both the grades corresponded closely to that of pure ethanol (Weast, 1972).

Analysis to determine the water content of the technical

grade ethanol made use of the fact that copper sulphate normally exists as the pentahydrate (Greenwood and Earnshaw, 1984). Therefore anhydrous copper sulphate will absorb water to form the pentahydrate.

Anhydrous copper sulphate was produced by calcination of copper sulphate pentahydrate in a furnace at 400°C for three hours. Once cool an amount of this material was accurately weighed into a beaker and a known volume of technical grade ethanol was added. The mixture was stirred for fifteen minutes and the solid recovered either by evaporation or filtration. After drying the mass of the solid was determined.

The water present in the ethanol would have been used to convert the anhydrous copper sulphate to the pentahydrate form. Thus the mass increase between the anhydrous sample and the ethanol treated sample is the mass of water present in the ethanol.

The recovered material is then calcined to 400°C for three hours to reconvert to the anhydrous form. The mass is then measured in order to account for any loss during the recovery stage.

The use of perchloric acid and nitric acid solutions did not require the exact strength to be known. Therefore these reagents were not standardised.

3.1.2 TEM EXAMINATION

The reagents described above were to be used to carry out reactions with the intention of studying the reaction mixture and

products by transmission electron microscopy (TEM). It was therefore necessary to determine if any of the reagents (other than the alkoxides) included material which would be observed in the microscope.

Therefore samples of the reagents were prepared for examination in the transmission electron microscope. This was done by depositing drops of the reagents on copper electron microscope grids, which had previously been coated with carbon. In all samples some material was observed on the grids, but usually only a small amount. The most contaminated material was the ethanol which contained fibre like particles some of which gave an electron diffraction pattern. It was not clear whether the contamination was due to the alcohol or part of the production process of the grids on which the samples were studied. However the examination of the reagents meant that the contamination observed would not be mistaken for the sample in later studies.

3.1.3 GLASSWARE

All glassware used to carry out a reaction was thoroughly cleaned with lisoprol detergent, ethanol and diethyl either to remove any contamination. No strongly acid or base cleaning agents were used because of the possibility of residues affecting the reaction. After cleaning, the glassware was placed in an oven at >150°C to dry before use.

The majority of reactions were carried out in new, calibrated, dark glass containers. These were individually

calibrated by using a burette to accurately add the required volume to the container, and marking the calibration with a diamond tipped pen. After use, all of the containers were disposed of because the reaction caused the contamination of the inside of the glass with silica which could not easily be removed.

3.2 HYDROLYSIS REACTIONS

3.2.1 REACTION PREPARATION

The reactions carried out to produce pure silica were carried out in two separate manners. Those carried out under neutral conditions and acid catalysis were prepared to specific molar ratios of reagents. In these, the exact amount of each reagent could be calculated beforehand. The quantity of water had to be calculated carefully to account for the water which was contained in the other reagents. The reaction mixtures were then prepared by mixing the required amount of water, acid and ethanol in the reaction vessel (all volumes measured by pipette). Then the required volume of TEOS would be pipetted in, the vessel sealed and shaken. The vessel was then left for the reaction to take place.

In the case of reactions carried out with base catalysis the reactions were prepared to give certain concentrations of the reagents rather than molar ratios. This raised a number of problems the largest of which was the fact that the amounts of reagents could not be calculated. This problem arises because the

volumes of all the reagents are not additive. For example 50ml of water added to 50ml ethanol does not have a total volume of 100ml. This in turn means that although the quantity of TEOS and base can be calculated the volume of water required can not be accurately determined because the volume of ethanol required to make the volume up to the calibration mark, and therefore the water content added in the ethanol, can not be predicted.

To overcome this problem the volume of reagents required was calculated assuming that the volumes were additive. This will miscalculate the volume of ethanol required but the error should be fairly small, and as the water content in the ethanol is low the error in the water concentration would also be small.

Therefore the reactions were carried out as follows. The calculated volumes of base and water were mixed in the reaction vessel. Then 80% of the calculated volume of ethanol was added and the reaction mixed. The TEOS was then pipetted into the vessel and the volume made up to the calibration mark by addition of ethanol from a known volume of ethanol. The vessel would then be sealed and shaken. Because the ethanol used to make up the volume was removed from the known volume, the total amount of ethanol added to the reaction could be calculated. Therefore the actual composition of the reaction mixture could be calculated. After the initial preparation of a particular composition it was possible to add all of the ethanol at the first stage and forego the second ethanol addition because the exact value would be known.

The actual length of time the reactions were allowed to

continue varied considerably. The product of the reaction was then recovered by one of a number of methods depending on the type of product. If the product was a gel, the material was left for the solvent to evaporate but this was a slow process. In some reaction conditions the product is in the form of a precipitate which can be filtered off easily, either under vacuum or not. If the reaction forms a colloidal dispersion there were a number of methods of recovering the product. The first method attempted was to filter the suspension under vacuum. This method fails, because, due to the size of the product, much of the material comes through the filter and during the filtration process the filter becomes clogged making this method unsuitable. The next method was to centrifuge the reaction mixture. This was a very poor method of separating the product because it had to be done in batches and required a large amount of time for the material to settle. It often required several hours to recover a few grams of product. It is also possible to leave the reaction vessel open to the atmosphere for the solvent to evaporate. This is slow, often taking several weeks, but the mixture can be left unattended during this period so is not very demanding on effort. The fastest and easiest method of recovering the product was by means of a rotary evaporator which removes the solvent under reduced pressure. This was relatively fast and left a dry powder.

Where reactions made use of tetrabutylorthosilicate the same methods as those described above were employed with the only variation being that tetrabutylorthosilicate replaced TEOS. In the reactions using ethylamine as the base the only variations

were that ethylamine replaced the ammonia, and because of this the reaction mixture was cooled in an ice bath prior to the addition of the ethylamine, and the TEOS, to prevent evaporation of the ethylamine.

3.2.2 POLYMER INCLUSION

To observe the effect of the presence of polymers on the morphology of the product, reactions were carried out containing polyvinyl alcohol. The reactions were carried out as follows. A concentrated solution of polyvinyl alcohol (PVA) was prepared by dissolving 15g polyvinyl alcohol in 100ml hot water. This was then allowed to cool forming a fairly viscous solution of PVA. Reactions were then prepared in the same manner as for normal reactions except the PVA solution was used as the source of water. The reactions were prepared to correspond to compositions which produce different types of product morphology so that the effect on different morphologies could be examined.

3.2.3 SALT INCLUSION

To observe the effect of an ionic salt on the reaction, reactions were prepared with compositions which normally produce a specific type of product morphology but with the variation that a small amount of salt is added. Therefore the reaction would be prepared by mixing the ethanol, distilled water and the

concentrated ammonia solution in a flask equipped with a magnetic stirrer. Then the required amount of the salt is added and allowed to dissolve. The salt used in these experiments was lithium chloride because it is soluble in ethanol. The TEOS is then added and the reaction sealed with Nescofilm and left stirring.

3.3 NICKEL DEPOSITION

The attempts to deposit nickel on or within the silica structure during the alkoxide hydrolysis were carried out in three basic fashions. The first two were based on the formation of nickel bis(dimethylglyoximate) during the reaction producing the silica. This compound can be formed in a number of methods. The method decided on for this experiment was the reaction of diacetyl and hydroxylamine to form dimethylglyoxime which then reacts with nickel ions to form nickel bis(dimethylglyoximate). The reason for this method of production was that the nickel bis(dimethylglyoximate) would then be produced by homogeneous nucleation, giving better control of the product (Gordon and Salesin, 1961). However during the reactions a problem arose in that a precipitate formed in place of nickel bis(dimethylglyoximate). To overcome this the second method of production was developed. In this, all chloride ions were replaced by perchlorate ions and thus the precipitate was avoided. The third method of depositing nickel was based on forming a nickel complex other than nickel bis(dimethylglyoximate) during

the reaction. The complex used was that which precipitated out during reactions to form nickel bis(dimethylglyoximate) in the presence of chloride ions.

3.3.1 CHLORIDE BASED DEPOSITION

To carry out the reaction it was decided to mix the reagents in two vessels so that neither vessel included all the essential elements of any one reaction. Therefore the required quantities of nickel chloride hexahydrate, hydroxylamine hydrochloride, ammonia and distilled water were mixed with ethanol in a flask equipped with a magnetic stirrer. Typically this included 2.75g nickel chloride hexahydrate, 3.62g hydroxylamine hydrochloride, 300ml ethanol, 5ml concentrated ammonia solution and 66.25ml distilled water. In a separate container the required amounts of diacetyl, TEOS and a quantity of ethanol were mixed. This normally included 2.00g diacetyl, 25ml TEOS and 50ml ethanol. To begin the reactions the second mixture was added to the flask containing the other reagents and the flask sealed with Nescofilm and left stirring.

The reaction was allowed to carry on for periods up to three days, at which time the product was recovered by filtration under vacuum and then dried in an oven at 90°C. To test if all of the nickel ions in the reaction had been converted to a solid within the product some of the filtered solution was added to a solution of dimethylglyoxime. If nickel were present a bright red precipitate would form. No such precipitate was observed.

3.3.2 PERCHLORATE BASED DEPOSITION

The second method of production was based on the same idea as the first, but to overcome precipitate problems which arose in the above reaction, it was decided to remove all of the chloride ions and replace them with perchlorate ions which are unlikely to form a precipitate. To do this it was necessary to convert the hydroxylamine hydrochloride to the perchlorate form. This was accomplished in the following manner.

Amberlite IRA 400 ion exchange resin was converted from the chloride to the hydroxide form by steeping it in concentrated ammonia solution for two weeks, with regular changes of the ammonia solution. Once the resin had been converted it was washed with distilled water. The material was washed until the solution coming off of the resin included no chloride ions as tested by reaction with silver nitrate solution. The resin was then ready for use. To convert the hydroxylamine hydrochloride to the hydroxide form it was dissolved in distilled water and allowed to react with the ion exchange resin. In a typical reaction 3.52g of hydroxylamine hydrochloride dissolved in 20ml distilled water was reacted with an excess of exchange resin (12.5g would be required but 25g was used). This converted all of the molecules to the hydroxide form. The liquid was then removed from the resin, the resin washed and the washings added to the solution. The hydroxylamine was then converted to the perchlorate form by reaction of the solution with perchloric acid until the solution had been neutralised (as determined with pH paper).

The reaction was carried out slowly and carefully because of the hazards involved in the use of perchloric acid (Muse, 1972). The second alteration necessary to convert all of the chloride ions present in the reaction to perchlorate ions was the replacement of nickel chloride with nickel perchlorate. Because of the strongly oxidising nature of perchlorates (Sax, 1984), and the resultant risk in adding such materials to flammable organic solvents, the perchlorate was added in aqueous solution to reduce the risk.

The reaction was then carried out by mixing the nickel perchlorate hexahydrate solution, the hydroxylamine perchlorate solution, ethanol and ammonia in a flask. Typically 4.12g of nickel perchlorate hexahydrate dissolved in distilled water (the total volume of water to prepare the hydroxylamine and nickel perchlorate solution was 60ml), 10ml concentrated ammonia solution and 300ml ethanol. To the flask was added a mixture of TEOS, ethanol and diacetyl. Typically 25ml TEOS and 2.08g diacetyl dissolved in 67.5ml ethanol. The flask would then be sealed with Nescofilm and left stirring.

The reaction was left for twenty four hours after which time the reaction was filtered under vacuum to recover the product, which was then dried in an oven at 90°C. To test if all of the nickel ions in the reaction had been converted to a solid within the product some of the solution was added to a solution of dimethylglyoxime. If nickel were present a bright red precipitate would form. No such precipitate was observed.

3.3.3 NICKEL COMPLEX DEPOSITION

The basis of this method was the controlled deposition of a nickel complex which had unexpectedly appeared in the previous methods when chloride ions were present. To do this a similar method to that used in the chloride based deposition of nickel bis(dimethylglyoximate) was used. The reaction was carried out by mixing the required amounts of distilled water, hydroxylamine hydrochloride, nickel chloride hexahydrate and ethanol in a flask with a flask with a magnetic stirred. This would normally be 3.65g hydroxylamine hydrochloride, 2.68g nickel chloride hexahydrate, 60ml distilled water and 367.5ml ethanol. Then the ammonia, typically 10ml concentrated ammonia solution, was added to the reaction. The reaction was left for a few moments and then the 25ml of TEOS were pipetted into the reaction and the flask sealed with Nescofilm and left stirring.

In an attempt to deposit the nickel complex closer to the outer edge of the silica the above reaction was varied slightly so that the complex did not appear until later in the reaction. This was done by mixing the ethanol, distilled water, and concentrated ammonia solution in a flask with a magnetic stirrer. The quantities were 367.5ml ethanol, 66ml distilled water, 5ml concentrated ammonia solution. Then 25ml TEOS was added to start the formation of the silica. After one hour, a solution of 2.73g nickel chloride hexahydrate in 20ml distilled water with 5ml concentrated ammonia solution included was added dropwise to the reaction.

In both cases the reaction was allowed to continue for twenty four hours after which time the product was recovered by filtering under vacuum. To test if all of the nickel ions in the reaction had been converted to a solid within the product some of the solution was added to a solution of dimethylglyoxime. If nickel were present a bright red precipitate would form. No such precipitate was observed.

3.4 CALCINATION

Samples to be calcined were weighed into fused silica crucibles with lids and placed in a furnace with a thermostat temperature control. The control was set and the furnace allowed to come to temperature. Once at temperature the sample was left in the furnace for two hours. The furnace would then be turned off and the sample left in the furnace until it cooled. All samples were calcined in an air atmosphere. After calcination the mass was determined so that the mass loss during calcination could be calculated.

3.5 SAMPLE PREPARATION AND EXAMINATION

3.5.1 TRANSMISSION ELECTRON MICROSCOPY (TEM)

Samples for examination in the transmission electron microscopes were prepared by a number of methods depending on the

nature of the sample. In the case of reactions prepared by hydrolysis under base catalysis the product was often particulate in nature. Therefore samples were prepared by one of two methods. The first was to dilute a small volume of the reaction mixture in distilled water and then use a stretched pasteur pipette to place some of this dispersion onto a carbon-coated microscope grid. The second method was to disperse some of the solid product in distilled water by placing it in an ultrasonic bath for ten minutes. Some of the resulting suspension was then placed on carbon-coated copper grids using a stretched pasteur pipette. In both cases the grids were placed in an oven at approximately 30°C to dry.

In the case of reactions which were aimed at producing the deposition of nickel, the samples could not be prepared using the ultrasonic bath because this is capable of removing particles from the surface of the silica. Therefore samples of these reactions were prepared by grinding some of the product in an agate mortar and pestle with a small volume of distilled water. Some of the suspension produced was then transferred to carbon-coated copper grids using a stretched pasteur pipette. Again the grids were placed in an oven at approximately 30°C to dry.

In the case of acid catalysed gels the preparation of samples which represented the structure of the gel and could be studied in the TEM was a problem. In an attempt to prepare such samples a number of techniques were tried. These were:

A. to disperse the gelled material in a solvent (water was rarely used as this was one of the reagents). To do this, small

pieces of gel were placed in small bottles of anhydrous diethyl ether, n-hexane, Analar ethanol, toluene and chloroform and in each case the bottle was placed in the ultrasonic bath for ten minutes. In all cases the sample dispersed to some extent. The dispersions thus produced were then transferred to carbon-coated copper grids and allowed to dry.

B. to use forceps to touch carbon-coated copper grids against the surface of the gel in question. Small amounts of the gel attached to the surface of the grid and therefore provided a sample.

C. to prepare a sample of the reactions before it gelled. To do this a small amount of the reaction mixture was removed from the reaction and mixed with a solvent, most commonly ethanol or n-hexane. The suspension thus produced was placed onto carbon-coated copper grids and allowed to dry.

D. to prepare a sample of the reaction mixture by dropping pure reaction mixture onto the grid at times when the mixture was not very viscous.

E. dipping uncoated copper grids into the reaction mixtures, removing them and allowing them to dry.

F. placing the reaction mixture on top of a bath of organic solvent, normally chloroform or toluene, and lifting some of the material off with copper grids.

G. In an attempt to prepare samples without greatly affecting the gel structure it was decided to freeze-dry samples. This was done by placing a piece of wet gel on top of a glass microscope slide on top of a brass block which had been cooled to liquid nitrogen temperature (-196°C). This was inside the vacuum chamber of a coating unit which was rapidly evacuated. The idea being that freeze-drying may remove the solvent without collapsing the gel structure. Samples of the freeze dried material could then be prepared by grinding it and picking it up on carbon-coated copper grids.

The samples were examined in JEOL JEM 100C and 1200EX electron microscopes operated at accelerating voltages of 100 kV and 120 kV respectively. The images were recorded on photographic film (Ilford EM film).

3.5.2 THIN SECTIONS

To obtain information about the internal structure of materials they could be examined as thin sections. This technique has been described in detail elsewhere (Reid, 1974; Watt, 1985) but a brief outline is as follows. The material to be studied was embedded in araldite resin and the resin allowed to dry. Once dry the block is cut into very thin sections using a microtome equipped with a diamond or glass knife. These thin sections were placed on copper microscope grids allowing them to be studied in the transmission electron microscope.

3.5.3 SPECIMEN STAINING

In an attempt to obtain samples of gel suitable for TEM examination, but with an increase in contrast and more observable detail, sample staining was carried out. This is a common technique in biological electron microscopy (Meek, 1970; Lewis and Knight, 1982). The essence of this technique is the absorption of heavy metal atoms into the sample. The metals used include rubidium (in the form of salts), osmium (as osmium tetraoxide) and uranium (most commonly as uranyl acetate). Because of the high atomic masses and resultant high atomic scattering factor the areas in which they are present appear darker in the image, thus providing increased contrast throughout the sample but especially in areas where the metal is absorbed to a greater extent. It was therefore possible that the staining would make the areas of gel appear darker and make the pore structure within the gel more prominent.

To prepare the stained samples small pieces of gel were soaked in saturated uranyl acetate solution. The gel was then removed from the solution and washed several times with distilled water to remove any excess uranyl acetate present. The samples were then prepared by dispersing some of the gel in distilled water in an ultrasonic bath and dropping some of the suspension onto carbon-coated copper electron microscope grids. Samples were also prepared by touching the gel with carbon coated copper

electron microscope grids. Both methods correspond to methods described in section 3.5.1.

3.5.4 TIME SAMPLING

To follow the evolution of product morphology during the lifetime of a reaction it was necessary to sample the reaction mixture at set times. For such a technique to work it would be necessary to stop the reaction at the time of sampling.

Therefore at the predetermined times after the reaction had begun by the addition of TEOS, samples of approximately 0.2ml were removed using a pasteur pipette. This was then added to 2ml of ethanol to stop the reaction, and the suspension was shaken. Some of this suspension was then placed on carbon-coated copper grids using a stretched pasteur pipette. These grids were then studied in the transmission electron microscope.

The sample preparation technique is essentially the same as that used by Jean and Ring (1986(b)) for the study of the growth of titania. In a second paper (Jean and Ring, 1986(a)) the method was altered by adding a small amount of para-hydroxybenzoic acid to the diluting alcohol to sequester all of the unreacted alkoxide but this alteration was not adopted because it adds to a further parameter which may alter the results.

3.5.5 SIZE DETERMINATION

Where the product was particulate in nature the particle size could be determined. This was done by studying the product in the transmission electron microscope. Then the diameters of at least one hundred individual particles were measured. The data thus obtained was used to calculate (Barford, 1967) the arithmetic mean and the adjusted root mean square deviation, S_n.

Where S_n is given by

$$S_n^2 = \Sigma(x-X_n)^2/n-1$$

Where:- x is the measured value

X_n is the arithmetic mean

n is the number of measurements

This technique for obtaining the mean particle size has been used by several workers (Jean and Ring, 1986(a), 1986(b); Bogush and Zukoski, 1987; Bogush et al, 1988(a)) but it has been shown (Jean and Ring, 1986(b)) that this type of particle shrinks when exposed to heat and dried. Similarly it has been shown (Van Helden et al, 1981; McDonald et al, 1977; Catone and Matijevic, 1981) that particles shrink when exposed to the electron beam in the microscope; the shrinkage has been estimated at 5% (Van Helden et al, 1981). The size determined by this method would thus be the dried size, the difference probably being due to the swelling of the particles in solution due to their polymeric nature (Jean

and Ring, 1986(b)).

Other, in situ, techniques such as dynamic laser light scattering (Harris and Byres, 1988) and photon correlation spectroscopy (Jean and Ring, 1986(b)) measure the size of the particles present in the reaction. However such techniques do not take account of the particle morphology or of aggregation of particles in the reaction. This leads to a distortion of the results which has led to the assertion that TEM is the best method for particle sizing (Jean and Ring, 1986(b)).

Where a visual representation of the particle size distribution is required this will be presented as a normalised histogram. (Barford, 1967). Here the relative frequency per unit interval in diameter is plotted against the diameter intervals. This is done such that the height of the rectangles $f_m(x_m)$ obeys the equation

$$[x_m - x_{m-1}] \quad f_m(x_m) \quad = \quad n_m/n$$

where $x_m - x_{m-1}$ is the interval diameter

n_m is the number of measurements within the interval

n is the total number of measurements

and n_m/n is the relative frequency of obtaining a measurement

$$x_{m-1} < x \leq x_m$$

Although the intervals in diameter, Δx, need not remain the same within the histogram those used within this thesis will normally be the same.

In the histograms presented the diameter intervals will be indicated by the labelling of the upper diameter included in the interval. Due to space restrictions it may not be possible to label every interval but these can be determined from the interval values given and the labelled intervals.

The diagrams will also include, n, the total number of measurements.

3.5.6 SCANNING ELECTRON MICROSCOPY (SEM)

Samples for study in the scanning electron microscope were prepared by converting the material to a powder, if it were not so already. This was done by gently grinding in an agate mortar and pestle. The powder was then mounted on aluminium stub spindles using carbon paint. To prevent charging effects the samples were coated with gold in a Polaron E5000 SEM coating unit.

The samples were examined on a Philips 501B Scanning electron microscope and a Cambridge Instruments Stereoscan 90SEM. The images were recorded on Ilford 120mm roll film for the Philips and Polaroid film for the Cambridge Instruments.

3.5.7 X-RAY POWDER DIFFRACTION

Several samples of both pure silica reactions and more commonly samples which include nickel were examined by powder x-ray diffraction (XRD). Samples which were not in the form of a powder were converted to a powder by grinding in an agate mortar and pestle. Two methods of mounting the samples were used. In the first the powder was mounted on an adhesive tape, rolled into a cylinder and placed in the XRD equipment. In the second method the powder was packed into a cavity mount and placed in the equipment. The equipment used was a Philips X-Ray diffractometer including a PW 1050/35 goniometer, PW 1140 generator and a PW 1370/00 measuring panel.

The sample was rotated through angles of 3°-65° while being exposed to the x-ray beam. The angle through which the sample was rotated was equivalent to the two theta angle in the Bragg equation. The x-ray radiation used was of two types, copper K_α which has a wavelength, λ, of 0.154178nm and cobalt K_α which has a wavelength of 0.1790260nm. The resulting x-ray diffraction patterns were recorded on a chart recorder operating at 1000 cps full scale deflection. The lattice spacings, d, could then be calculated from the Bragg equation

$$\lambda = 2d \sin\theta$$

and thus the compounds and structures present could often be identified by referring to the A.S.T.M. index (1965) or the Inorganic Index to the Powder diffraction file (1971).

3.5.8 THERMOGRAVIMETRIC ANALYSIS (TGA)

A number of samples of pure silica and more commonly samples of the material incorporating nickel compounds were subjected to thermogravimetric analysis.

The instrument employed for these studies was a Du Pont 990 analyser combined with a 951 thermogravimetric unit. The powdered samples (typically a few milligrams) were suspended in a small platinum boat in a stream of air with a flow rate of 50ml/min. The platinum boat was surrounded by a furnace allowing the temperature to be increased up to 1000°C at a set rate. The samples were analysed in the range 0°-1000°C (occasionally 800°C) run at a heating rate of 20°C per minute. The temperature was monitored by a Cr/Al thermocouple. The resulting weight loss was measured by the thermobalance and plotted as a percentage weight loss again temperature.

3.5.9 INFRARED SPECTROSCOPY

Infrared analysis was used to gain information about the structure of the material produced in the reactions, especially the samples containing nickel compounds.

Samples were prepared by drying the material in an oven at

80°C and then grinding the material in an agate mortar and pestle to prepare a powder. Some of this powder was then ground with dry potassium bromide to provide an intimate mixture. The quantity of sample used varied depending on the material but typically 1mg of sample would be dispersed in 300mg of spectroscopic grade potassium bromide. This mixture was then placed in a die and exposed to 8 tons pressure for five minutes to prepare a solid, roughly transparent disc. The transmission infrared spectrum, in the region $200cm^{-1}$ to $4000cm^{-1}$, was then obtained by placing this disc in the sample path and a plain potassium bromide disc in the reference path of a Perkin Elmer model 983 spectrophotometer.

3.5.10 MICROANALYSIS

For the determination of the content of carbon, hydrogen and nitrogen small samples of the product were analysed. This was done by weighing under 1mg of the material into a platinum boat. This was then analysed in a Carlo Erba Elemental Analyser Model 1106. In each case two samples were analysed to minimise the possibility of error. In subsequent calculations the average of the two figures was used.

The chlorine content of the materials was determined by microanalysis using the method described by Cheng (1959).

3.5.11 NICKEL CONTENT DETERMINATION

To determine the nickel content of a material the following method, which is based on the production on nickel bis(dimethylglyoximate) was employed.

A sample of the material to be analysed was accurately weighed into a beaker. To the solid was added 50ml of distilled water and then concentrated nitric acid was added to destroy any complexes present and to bring the nickel into solution in the form of nickel ions. The solution was then brought back to a neutral pH by the addition of concentrated ammonia solution. If the material being analysed contained silica it was then filtered to remove the silica and the filter washed to ensure all nickel ions were in the solution.

Solutions of dimethylglyoxime were prepared by dissolving some in ethanol. The exact quantity dissolved depended on the expected nickel content in the solution being analysed. Once all of the dimethylglyoxime had dissolved the solution was added to the solution containing the nickel ions. This led to the formation of nickel bis(dimethylglyoximate) as a bright red precipitate. This precipitate was then recovered by filtration and dried.

To test if any nickel ions were still in solution some of the filtered solution was added to a concentrated dimethylglyoxime solution. Any nickel present would lead to the formation of a red precipitate.

To make sure that enough dimethylglyoxime had been added to

precipitate all of the nickel ions present solution some of the filtered solution was added to a solution of nickel chloride. If a red precipitate appeared, as it always did, there had been an excess of dimethylglyoxime in solution.

The mass of nickel bis(dimethylglyoximate) formed in the reaction was determined, and the nickel content of this material was the mass of nickel present in the mass of material originally weighed into the beaker.

4. NEUTRAL OR ACID CATALYSED REACTIONS

4.1 INTRODUCTION

As described previously the work discussed within this thesis is mainly concerned with the hydrolysis of silicon alkoxides, normally tetraethylorthosilicate (TEOS). This reaction is catalysed by a number of reagents, most importantly acidic and basic species. Work by a number of authors, which has previously been discussed, indicates that the different catalysts lead to different product types including gels, suspensions or precipitates. Those conditions which lead to the formation of a gel, presence of an acid catalyst or no catalyst, appear to have been studied in more detail than the others. This may be due to more industrial interest but possibly because of the fact that the reaction remains a homogeneous liquid which is necessary for the use of some of the most powerful techniques ie NMR spectroscopy.

Because of the larger base of information on the neutral and acid-catalysed system this system was the first to be studied.

4.2 REACTION PREPARATION

The aim of the work described here was to examine the morphology produced by the hydrolysis and to relate it to the reaction conditions which gave rise to it. Therefore it was necessary to produce a series of reactions which covered a range of reaction compositions to allow comparison between those

compositions. However, as the product of interest in this system is a clear coherent gel it was desirable that the composition which acted as a base for the study, and from which the alterations were made, should produce such a gel. Therefore a composition known to produce such a gel (Segal, 1986) was used as the initial composition.

Based on this composition a series of reactions were prepared to allow the study of reactions in which one of the reagent concentrations had been altered. The compositions of the reaction mixtures are shown in table 4.1.

Composition	TEOS	Water	Ethanol	Acid
A1	1	4.1	4	0
A2	1	2	4	0
A3	1	1	4	0
A4	1	8	4	0
A5	1	4.1	4	$7x10^{-7}$
A6	1	2.01	2.87	0.132
A7	1	3.55	2.87	0.132
A8	1	6.65	2.87	0.132
A9	1	9.74	2.87	0.132

Table 4.1: Molar ratios of reagents in reactions A1 to A9.

The method of preparation of these reactions has been described in the previous chapter. Upon mixing of the reagents the reaction normally formed a clear one phase liquid but in some reactions, those of the A4 composition, there appeared to be a second phase composed of small droplets within the main liquid. This is probably due to the amount of water present exceeding the volume the ethanol can dissolve. These droplets disappear rapidly as the water is used in the hydrolysis reaction and more ethanol is produced.

The second notable feature of the preparation stage of the reactions which contain acid was that the reaction rapidly became hot. This may be due to the heat of hydration of the concentrated acid used but it is more likely to be due to the reaction itself. This belief is supported by the observation that under acidic conditions the reaction is exothermic (Jones and Fischback, 1988)

The reactions were monitored closely and as the reactions proceeded the liquid became more viscous until after some period of time the liquid would not move when the reaction container was tilted or inverted. There is no standard definition of the gel point of the reaction but the point at which the mixture will not move will be used here. The time for the reactions to reach this point are listed in table 4.2. After the point at which the reaction produces a gel the material does not alter in appearance. However after a few weeks the gel appears to shrink leaving a gap between it and the reaction flask. This gap is normally filled with liquid. This is due to syneresis which has been described in detail elsewhere (Scherer, 1988(a)). This type of behaviour has

Composition	Gel Time (days)
A1	6
A2	47
A3	44
A4	5
A5	30
A6	90
A7	21
A8	23
A9	24

Table 4.2: Time Taken to gel for reactions A1 to A9.

been described as a property of polymeric gels but not of colloidal gels (Partlow and Yoldas, 1981). It is not made clear whether such properties would appear in gels made of colloidal particles where the colloidal particles are polymeric in nature.

The first feature noted was that the reaction A1 gelled in six days, in fact three reactions prepared to this composition gelled in six days. When prepared previously in another lab (Segal, 1986) this composition gelled in twenty one days. The only change in method between that used by Segal and that used by the author was a reduction in the scale. Such a change in volume should have no direct affect on the reaction but it does have the effect of increasing the relative surface area in contact with the

glass reaction flask. It is known that in certain polymer reactions the contact with the reaction vessel can affect the rates of reactions (McNeil, 1985). To determine if the area of contact could have an affect on the time taken to gel, two reactions were prepared to the A1 composition, one in a normal reaction flask the other in a flask which contained 200 glass balls of 5mm diameter. Thus one reaction has a far greater contact area with the glass. The reactions both gelled at approximately the same time, thus indicating the area of contact does not have a significant affect on the gel time. This would therefore appear to be an example of the phenomenon well known in this field; reactions appear to behave consistently but differently in different laboratories (LaCourse et al, 1983)

Other than this feature the alteration of the gel time appears to follow a pattern. Decreasing the water concentration at first decreases the gel time and then increases it. This is possibly due to the fact that at high water concentration a decrease lowers the volume in which the gel has to form but does not greatly alter the rate of polymer formation. At lower water concentrations the decrease may actually slow the hydrolysis reaction and therefore increase the time before the gel forms. The addition of acid also appears to delay the gel time. However the results are not absolutely consistent. This may be due to variations in temperature which might affect the reaction.

4.3 INFRARED SPECTROSCOPY

Because of the large amount of water and ethanol present in the reaction mixture it would not be possible to follow the reaction by means of IR spectroscopy. However the IR spectrum of the products may provide information, for example whether there is sufficient organic material remaining within the silica to give rise to absorptions due to organic group vibrations.

The IR spectra of the products were obtained. In most cases the spectra correspond to that of silica, as shown in fig. 4.1. In the case of the spectra of A2 and A6 there were peaks at $2980cm^{-1}$, $2930cm^{-1}$ and $2900cm^{-1}$ although these are more prominent in the spectra of A2 as shown in fig. 4.2. These peaks occur within the region where C-H vibrations would be expected (Williams and Fleming, 1980) although the peak at $2980cm^{-1}$ is in the region where it would be expected to be of a C-H group adjacent to an oxygen atom or to a carbon bonded to an oxygen. This is consistent with FTIR studies (Orcel et al, 1986) which report similar peaks being due to the presence of Si-O-OR groups and the vibrations of the C-H groups within them, or of the whole group.

In the case of A7 the spectrum showed small peaks in the regions described above but not as individually identifiable as those above. It also showed strong absorptions at $1695cm^{-1}$, $1540cm^{-1}$, $1355cm^{-1}$ and $740cm^{-1}$. The peaks in the higher wavenumber region are illustrated in fig. 4.3. These peaks are similar to those reported by Orcel et al (1986) which they assign to the vibrations of carbonyl groups or -COOH groups.

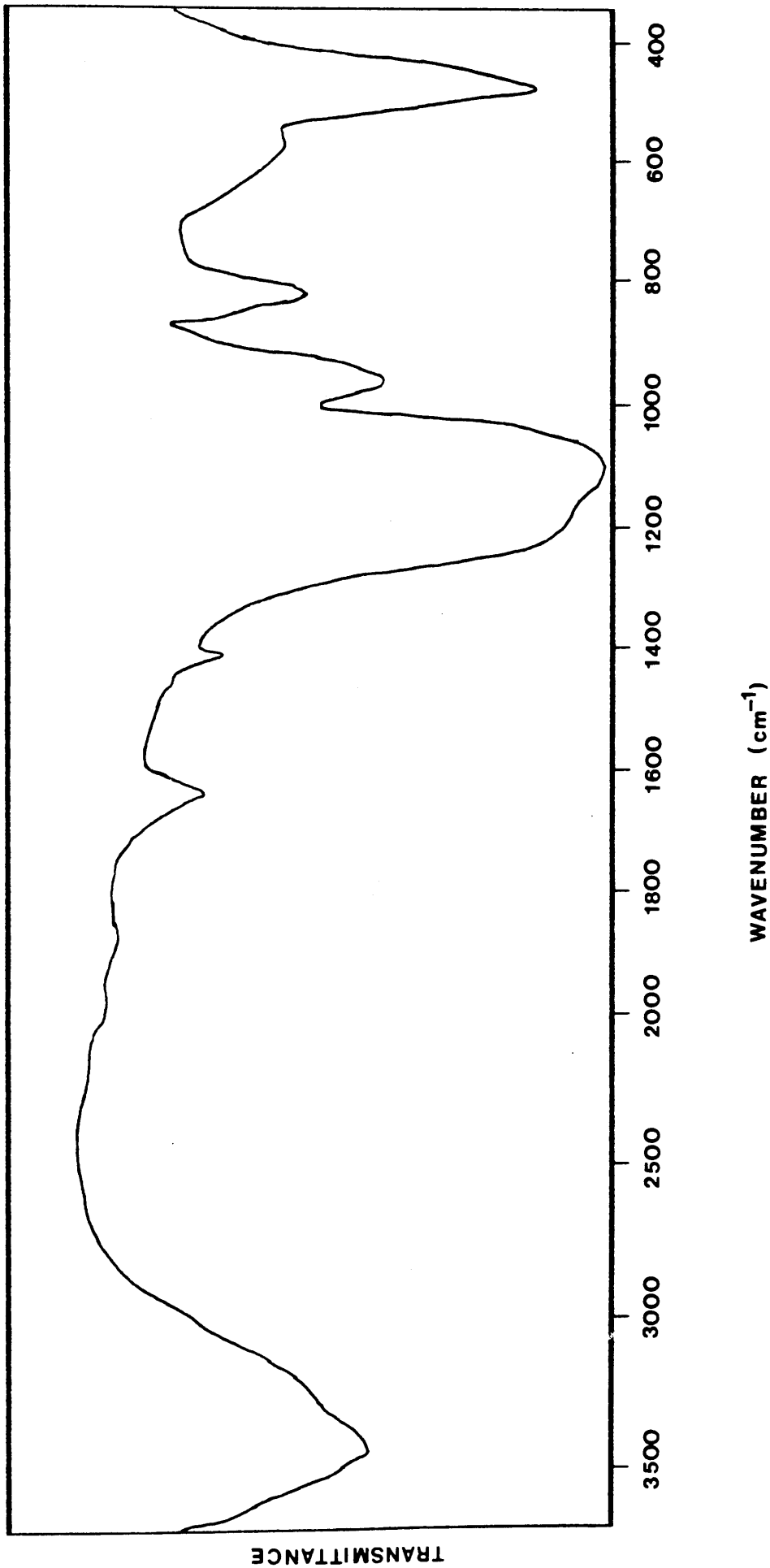

Fig 4.1: IR spectrum of silica

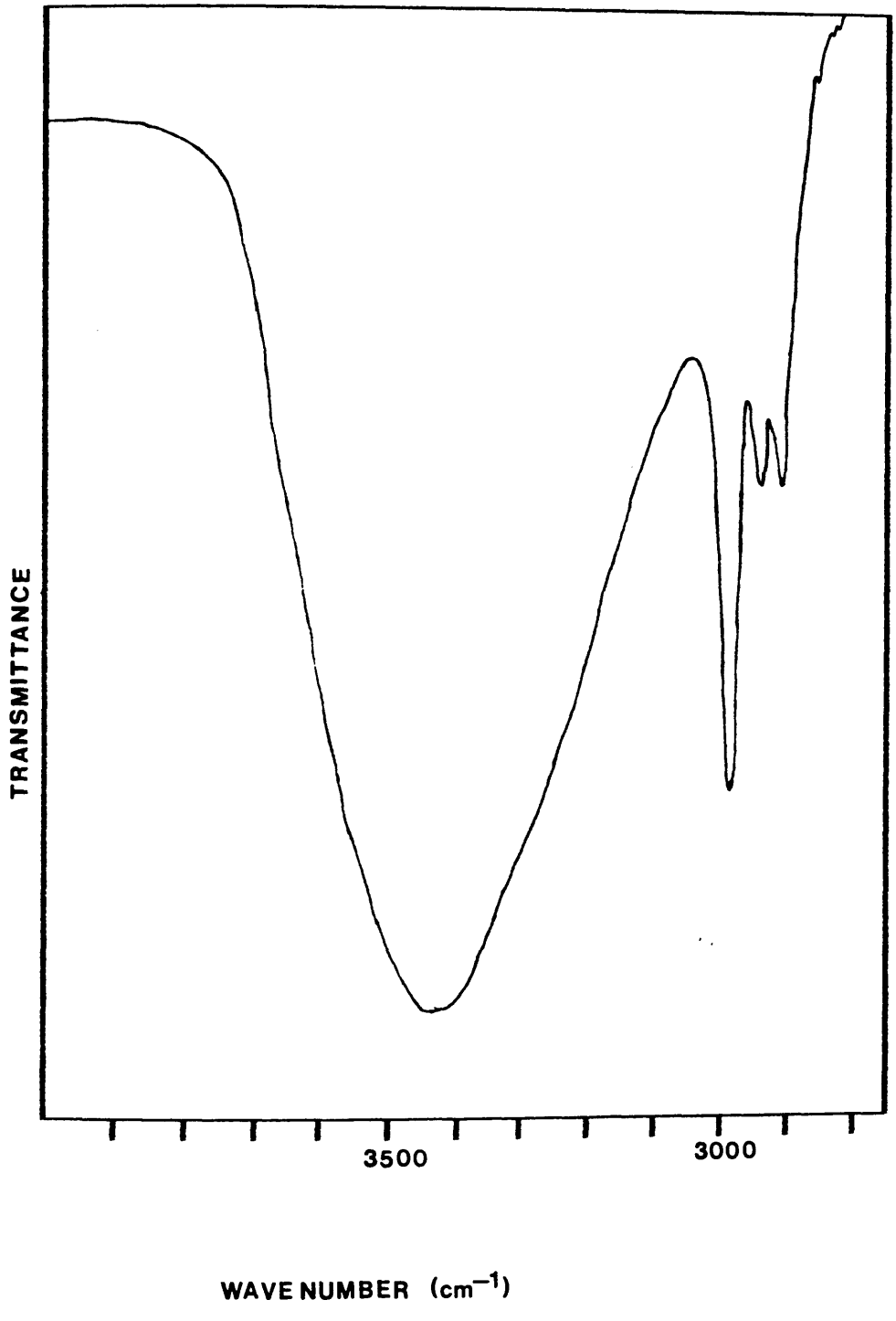

Fig. 4.2: Appearance of C-H vibrations in the IR spectrum of sample A2

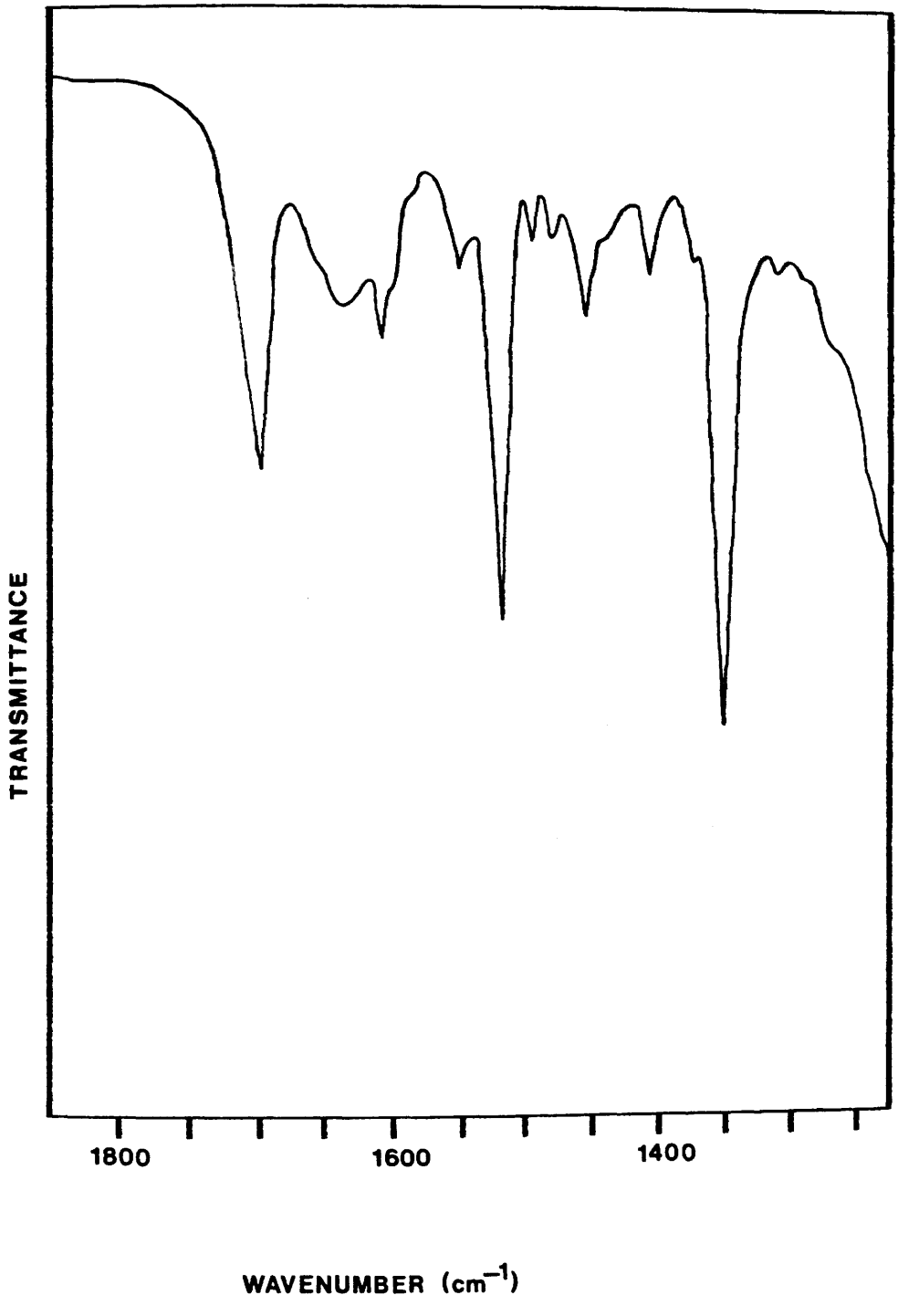

Fig. 4.3: Region of the IR spectrum of A7 showing additional peaks.

The appearance of the peaks in A2 and A6 can be explained in terms of retained alkoxy groups due either to incomplete hydrolysis or to re-esterification of silanol groups. The peaks which appear in A7 indicate the presence of species which were not originally present in the reaction mixture. It would appear that the silica has acted as a catalyst for the conversion of ethanol to ethanal and ethanoic acid. A similar suggestion has been made for reactions carried out in methanol (Orcel et al, 1988). It should also be noted that when the gel A7 had been left long enough for syneresis to occur the IR spectrum was that of silica with no additional peaks. This would support the idea that species producing the peaks were absorbed on the surface of the silica. As syneresis occurred and the surface area reduced they would no longer appear in the spectrum because they would no longer be present on the surface.

The reason why these particular products gave rise to the extra peaks is not clear. It is notable that all of these have a ratio of TEOS : water of less than 1 : 4 which is the required amount indicated by the reaction equations(not taking account of the water regenerated by the condensation reaction). It may also be necessary to dry the product and run the spectrum within a certain period of time before the organic species are no longer apparent, as in the later spectrum of A7.

4.4 X-RAY DIFFRACTION

The x-ray diffraction patterns of some of the dried products were obtained. These patterns showed a very broad band in the region of 2θ angles of 14° to 23° which, taking the estimated maxima, correspond to a lattice spacing of 4.98Å but with extreme broadening. The appearance of such a broad peak in the XRD is a well known feature of glasses (Kingery et al, 1976). A number of reasons for this have been proposed. The first being that the extremely broad peaks are due to crystallites of such a small size that size broadening (West, 1985) causes the peak to become broad. However as detailed by Warren (1937) to obtain such a broad peak the crystallite size would have to be so small as not to be reasonable.

The model of glass structure which is more commonly accepted is that proposed by Zachariasen (1932) which is based on a random network of silica tetrahedra. More recent work (Hoseman et al, 1986) suggests that even within glasses there is significant order and it is this "medium range order" which gives rise to the diffraction.

The similarity between gels and glasses suggests that the observed peak in the XRD may be due to a similar ordering within the gel. Thus, although XRD analysis appears not to be a useful method of studying the variations within the gel structure due to the reaction composition variations, these results indicate that the structure formed is of the type expected and that no significant crystallinity occurs.

4.5 MICROANALYSIS

Microanalysis of the dried gel could give information on the extent of hydrolysis and the amount of carbon and hydrogen due to ethoxide groups remaining within the structure. It is necessary to dry the gel because any retained solvent would distort the results. The microanalysis results for three of the dried products are given in table 4.3. These products were those which indicated the presence of organic material in their IR spectra.

These results indicate that increasing the water content decreases the carbon and hydrogen content in the product. Such a result would be expected as the higher water content would be expected to promote a higher degree of hydrolysis. A further explanation would be that the re-esterification of the silica would be greater in the reactions which have a higher ethanol content in the solvent.

Composition	% Carbon	% Hydrogen
A2	17.18	3.50
A6	9.30	2.79
A7	1.53	0.90

Table 4.3: Microanalysis results for dried reaction products

4.6 THERMOGRAVIMETRIC ANALYSIS

The thermogravimetric analysis of the product may give information about the sample such as the amount of certain types of material retained within the structure. The TGA results for three of the products are shown in figs. 4.4, 4.5 and 4.6. The results are also given in tables 4.4, 4.5 and 4.6. These indicate that there are a number of separate processes occurring as the sample heats which causes mass losses in the sample.

Thermogravimetric analysis has been used by a number of authors (Brinker et al, 1982; Gonzalez-Oliver et al, 1982; Klein, 1985; Duran et al, 1986) to study the conversion of gels to glass. In all cases a number of mass losses were recorded and although not identical the explanations of the mass losses are essentially the same. The losses occur in the sequence; elimination of trapped water and ethanol, desorption of physically adsorbed water, carbonisation of residual alkoxy groups, combustion of carbonaceous material and condensation of hydroxyl groups. In a more detailed description (Brinker et al, 1982) it was stated that the desorption of physically adsorbed water occurs between 100°-150°C, the carbonisation of residual alkoxy groups between 200°-300°C and the combustion of carbon between 275°-400°C.

In the results obtained with gels prepared and examined as described above, it appears that the losses which were observed in the regions from 25°C ending at between 150° and 200°C were due to the loss of trapped solvent and the loss of physically adsorbed water. The losses observed above these which ended at 375°C or

400°C were due to the carbonisation and combustion of the retained alkoxy groups. In the case of A6 the two losses between 150° and 375°C may be due to the two loss processes appearing separately. Losses at higher temperatures were most probably due to the loss of water produced by the condensation of hydroxyl groups.

The losses observed up to 200°C appear to be slightly different but this may be due to slightly different drying conditions as these results are essentially the loss of solvent. The losses observed in the region 200° to 400°C do, however, show a pattern. The loss in this region for A2 is the largest followed by that in A6 and then in A1. This would suggest the alkoxy group content is highest in A2 and lowest in A1. This is in part supported by the microanalysis results which show the carbon content of A2 higher than A6. Although not identical it can also be seen that the total amount of carbon and hydrogen present as determined by microanalysis are close in value to the mass loss obtained in the region 200°-400°C in samples A2 and A6.

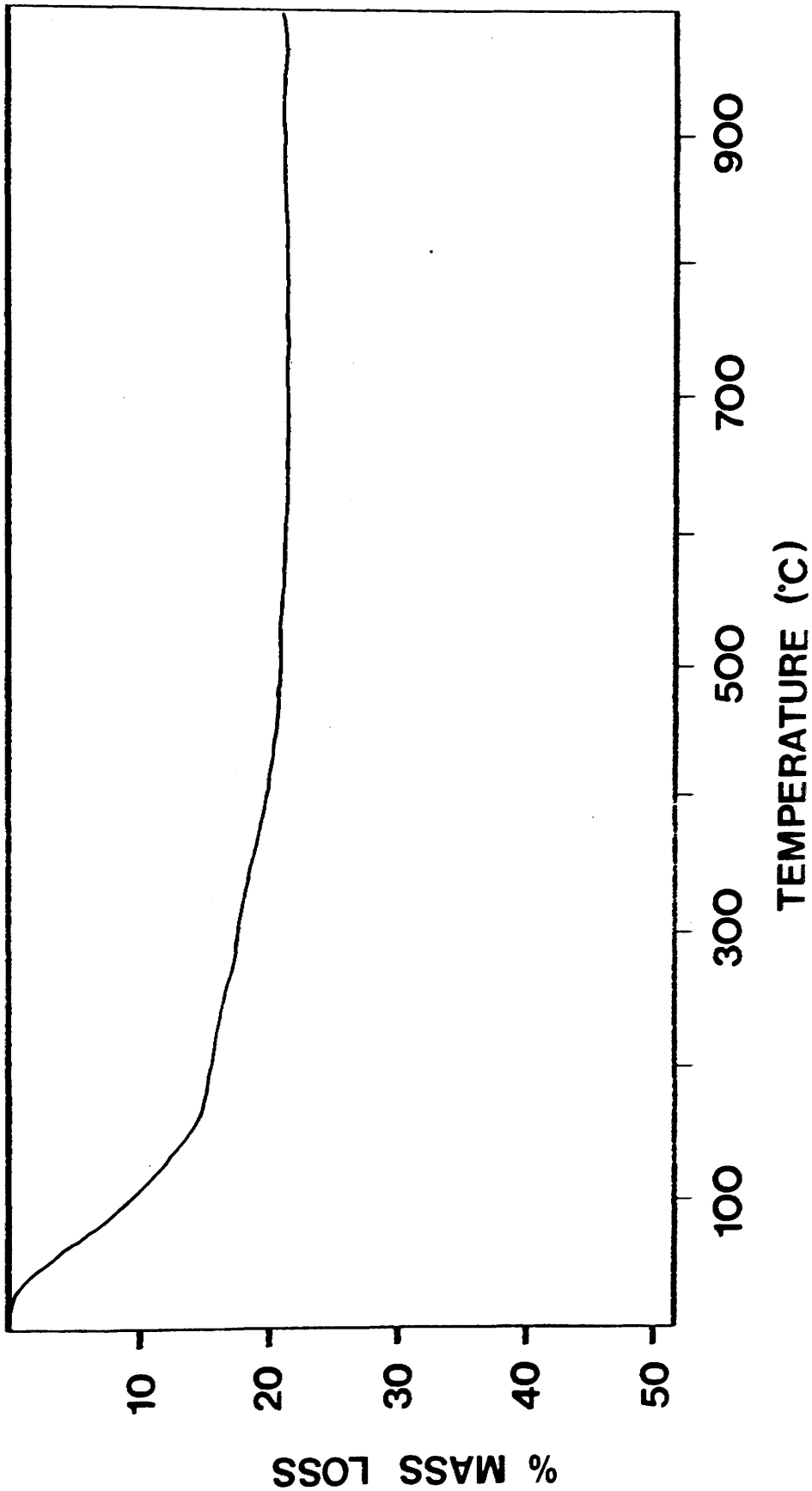

Fig. 4.4: TGA of sample A1

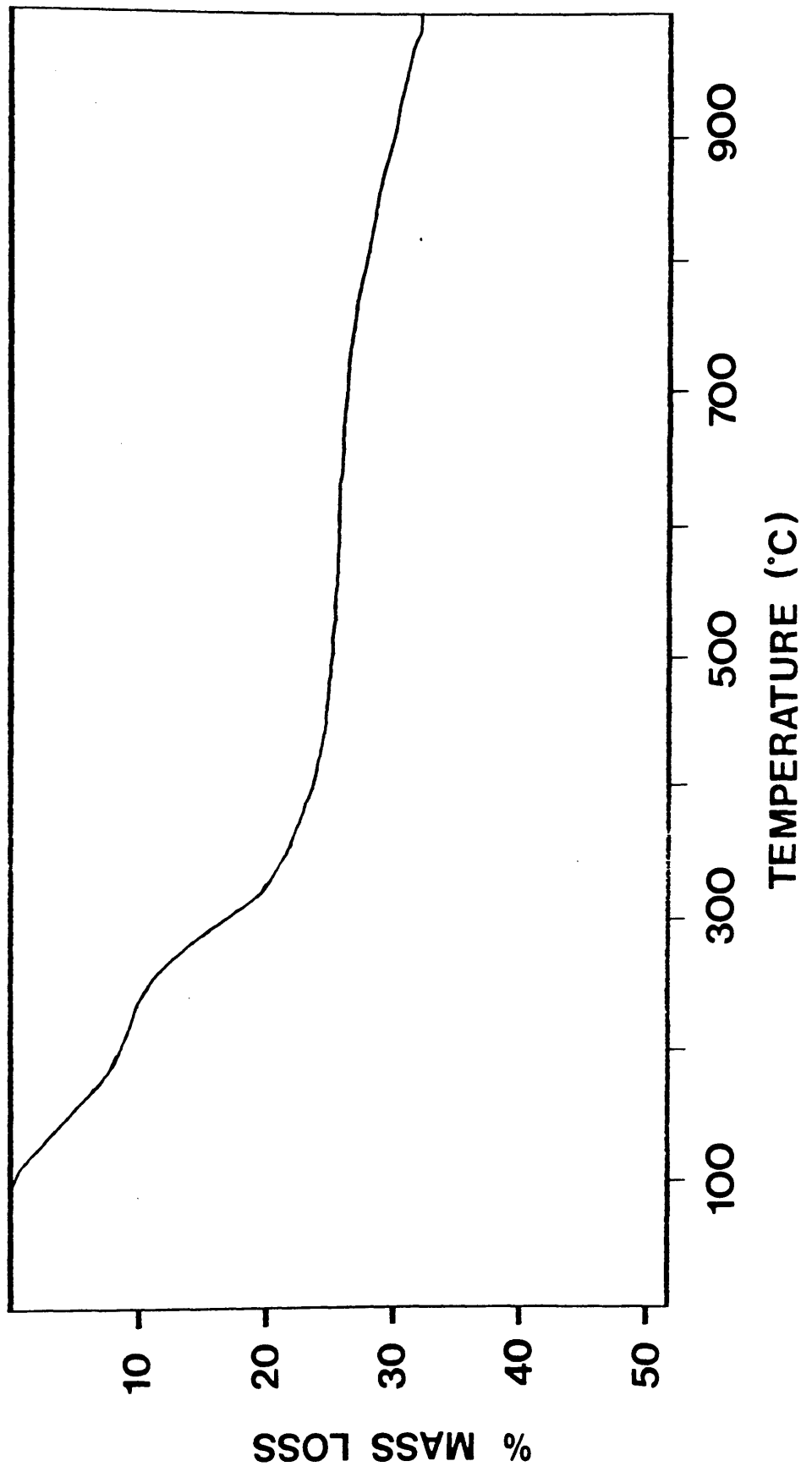

Fig.4.5: TGA of sample A2

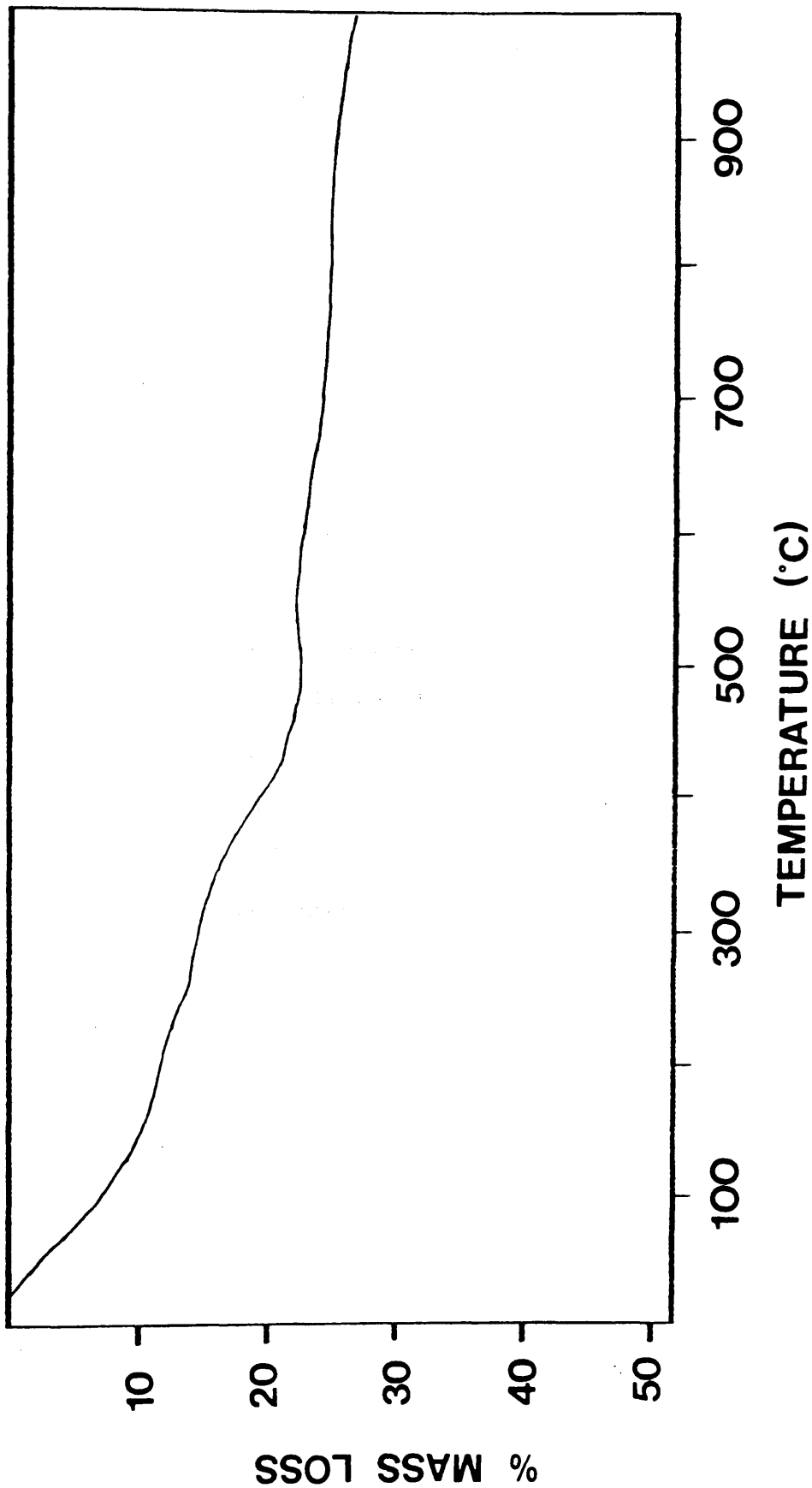

Fig.4.6: TGA of sample A6

The highest water : TEOS ratio is that in A1 which would suggest that there would be a higher degree of hydrolysis. The water : TEOS ratio in A2 and A6 are similar but the reaction A6 had a much lower amount of ethanol present which would possibly lead to a higher degree of hydrolysis. So that the losses due to retained alkoxy groups could be related to the reaction conditions in that they would determine the degree of hydrolysis.

A further possible explanation is that much of the alkoxy group content of the product was due to re-esterification of the silica. The content of ethanol in the solvent increases in the order A1, A6, A2 which could indicate the equilibrium between the alkoxy groups on the silica surface and in the ethanol in the solvent would be more on the side of the alkoxy groups in the same order.

The losses at higher temperatures are due to the loss of silanol groups because of condensation but the reason for the variations within this area are not clear.

4.7 ELECTRON MICROSCOPY

The aim of the investigation carried out is to relate the morphology of the product to the reaction conditions which gave rise to it. It is of interest to study the developing morphology of the products as the reaction proceeds and after the material has gelled. It would also be of interest to study the gelled structure during any processing subsequent to its production.

Temperature Range	Mass Loss
25° to 180°C	15.0%
180° to 400°C	5.0%
400° to 700°C	2.5%

Table 4.4: TGA results for product A1

Temperature Range	Mass Loss
75° to 200°C	9.0%
200° to 375°C	14.0%
375° to 450°C	2.0%
700° to 1000°C	6.0%

Table 4.5: TGA results for product A2

Temperature Range	Mass Loss
25° to 150°C	10.0%
150° to 300°C	5.0%
300° to 375°C	7.5%
475° to 750°C	2.5%
750° to 1000°C	2.0%

Table 4.6: TGA results for product A6

A requirement for such a study is the ability to study the material in a manner which gives an accurate representation of the structures and morphologies present within the reaction at that time. If such a technique exists then it is also necessary that the technique shows differences between reaction conditions; otherwise there is little gain in carrying out the experiment. To determine if a suitable technique exists a number of sampling techniques were carried out during the period of the reaction.

4.7.1 DIRECT SAMPLING

Direct sampling of the reaction mixture took two forms. In the first, small volumes of the reaction mixture (usually less than 5 μl) were removed with a pipette and dropped onto carbon-coated copper electron microscope grids. In the second copper electron microscope grids, which had not been coated, were dipped into the reaction mixture and removed. The first of these could only be carried out before the point at which the reaction formed a gel, the latter could be carried out after this point.

Both of these techniques suffered from a problem which has already been mentioned; gels shrink on drying. The effect of this on the samples prepared by the above techniques is detrimental to the sample. In both cases the specimen shrinks to form a thick area in the region of the copper grid bars. In the case of the grids which had been coated with carbon, the carbon film was torn and drawn back towards the sample attached to the grid bars. It appeared as if the sample had formed a layer of gel across the

grid bars which adhered to the grid bars and carbon film. On drying, the gel shrank and broke across the middle shrinking back towards the grid to which it was attached drawing the carbon film with it. The areas which include the sample appeared thick and little detail could be studied.

One feature which could be observed in these samples was that in the thinner areas of the film small triangular crystals could be seen. Because they were embedded in an amorphous material it was difficult to obtain an electron diffraction pattern. One which could be obtained gave peaks at 4.425Å, 2.1744Å, 1.458Å, and 1.077Å which is similar to that of hydrated copper chloride (A.S.T.M. file 13-145). It is therefore probable that these were crystals of hydrated copper chloride which were created by the reaction of the copper in the electron microscope grids with the hydrochloric acid in the reaction mixture.

Therefore these sampling techniques do not appear to be of use in studying the sample.

4.7.2 DILUTED SAMPLES

The direct sampling methods were not of great use because the samples shrank and formed a small but thick area of sample which could not easily be studied. A possible method of overcoming this problem would be to dilute the sample before dropping it onto the carbon coated grids. In this manner it might be possible that when the silica polymer shrink the area will still be thin enough to study.

In the samples produced in this fashion the sample was diluted with ethanol because this was the reaction solvent. The sample was then dropped onto carbon-coated grids. Because of the low surface tension of the liquid the sample spread from the sample grids onto the copper gauze support on which the grids were placed.

This technique also suffered from a number of problems. The first was that the sample, which spread onto the gauze support, on drying formed a polymer film over the grid and surrounding copper gauze. This made it difficult to remove the grid from the gauze without damaging the sample. The second difficulty was that on drying the silica material had shrunk. This led to it forming areas in the region of the copper grid bars. Again the carbon film had been ripped and drawn back towards the copper grid bars. In this case however, the sample was not too thick to observe any detail. Unfortunately most of the detail observed were wrinkles, tears and folds in the carbon film. This would appear to be due to the polymer adhering to the carbon film and when it shrunk the carbon film was drawn back with it.

It would appear that this type of sampling is not useable.

4.7.3 DISPERSED SAMPLES

To obtain samples of reaction mixture which had gelled it was attempted to disperse the gel in organic solvents by the use of an ultrasonic bath, the aim being that the ultrasonic bath would break small pieces of the gel off forming a suspension which

when dropped onto carbon coated grids would provide a suitable sample for study. In general the solvents used were diethyl ether, chloroform, n-hexane, absolute alcohol and toluene. Although water was normally avoided because it was a reagent it was used in a few cases.

In general the samples produced in this manner appeared as a thick amorphous layer over the grids with little detail observable in it. However there were areas where the layer became thin or broken and some features could be observed. In these areas low magnification of the sample give the impression that it consists of small particles packed together. When examined at higher magnification these actually appear to be three dimensional networks, as shown in plate 4.1, which may have been formed by the necking of small particles but may be due to other formation methods.

One notable feature of this sampling technique is that when the organic solvents, in which the dispersion had been prepared, had evaporated the silica left was in the form of a white powder which gave the appearance that it might be crystalline. X-ray diffraction and IR spectroscopic examination of these materials indicated that there was no significant difference from the gel. It would appear that the different appearance was due to the silica being broken into small particles.

Plate 4.1: Sample of gelled material formed by dispersion in organic solvents showing three dimensional networks.

Magnification = 220×10^3

1cm = 45·45 nm

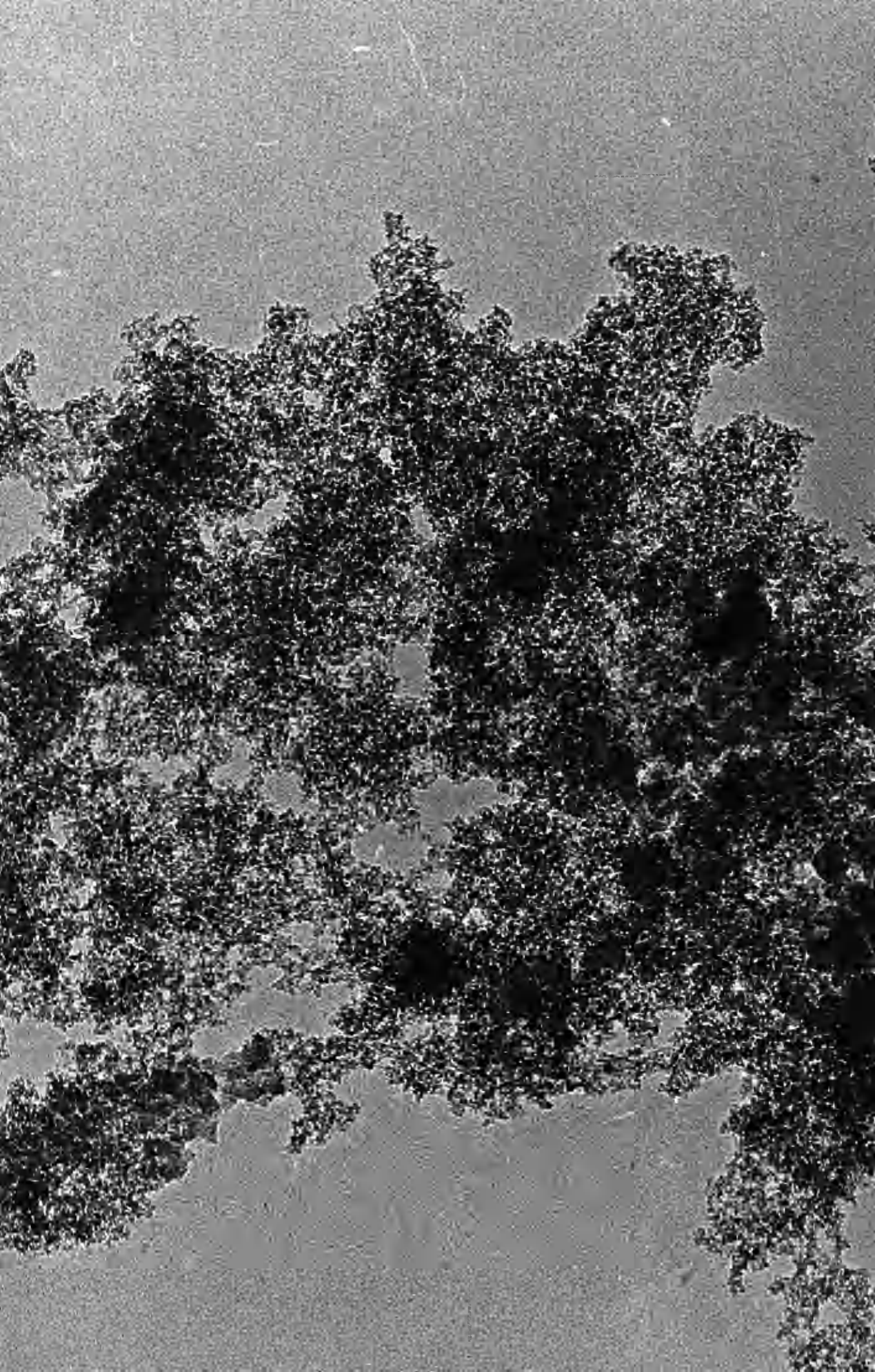

4.7.4 FILM PREPARATION

A technique for sample preparation which has found use in the study of organic polymers is to form a thin layer of the material and float it onto a bath of suitable liquid. Specimens are then obtained by lifting off areas of the film with copper grids. In this technique the thin layer is often formed by the vacuum evaporation of the organic material onto a potassium chloride crystal which is then dissolved in water to leave the thin film (Clark et al, 1979, 1980; Fryer and Holland, 1983) although direct growth onto water has been used (Sabih and Cosslett, 1974). In the present case the formation of the film must take a different route.

The method employed was to carefully pipette some of the reaction mixture onto a petri dish filled with solvent. A number of solvents were used but toluene was the most commonly used. In most of the reactions which were sampled in this fashion the early attempts to prepare a film failed with the reaction mixture dissolving in the solvent or falling to the bottom of the petri dish. At later reaction times however films usually formed and could be picked up to form a sample.

Examination of the films showed that in all cases the sample appeared to be a very porous material with an appearance similar to a honeycomb structure. This type of material is shown in plate 4.2. Similar structures have been observed by Gallagher and Klein (1986) who prepared silica membranes by floating TEOS solutions on sym-tetrabromoethane. They claim that the pores in

Pate 4.2: Sample of reaction mixture prepared by formation of a film on organic solvents showing a honeycomb-like structure.

Magnification = 235×10^3

1cm = 42·55 nm

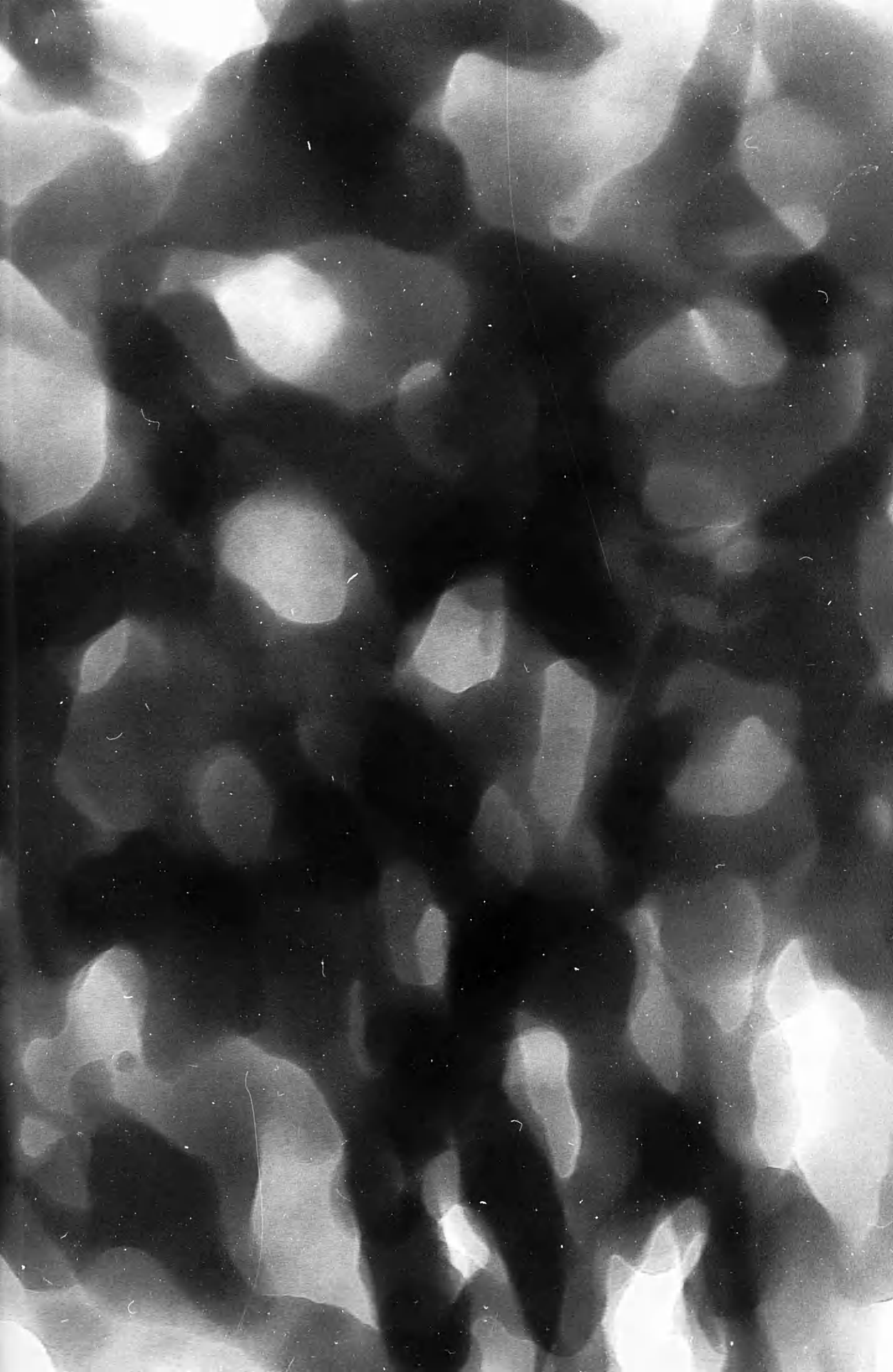

the membrane are caused by evaporation of the ethanol in the solution.

4.7.5 SAMPLES BY CONTACT

To prepare samples suitable for examination in the electron microscope it is necessary to obtain areas of the sample on grids. The sample must be thin enough to study. A possible way of preparing such samples is to touch carbon coated copper electron microscope grids against the surface of the gel. Small areas of the gel would adhere to the carbon film so that when the grid is retracted these areas of the gel will stay on the carbon film. In practice large amounts of the carbon film stayed on the surface of the gel. However examination of the grids showed that a number of areas of the gel appeared on the carbon film which remained on the grid and allowed study.

There were some problems associated with this method of sampling. The main ones being that the amount of sample retained on the grid could be low and that because of damage to the carbon film the areas with the sample were likely to move in the electron beam. However, even with these problems, the technique provided samples which could be examined.

The samples produced in this fashion exhibited a number of different types of morphology. Many of these appeared only a few times and it is therefore not possible to say with certainty that they come from the samples and are not due to contamination. Some of the morphologies were regularly observed and these can be

assumed to be associated with the products being examined and will be mentioned below. In the case of reactions prepared under neutral conditions a number of types of material were observed. These were;

1. Areas of amorphous material of a honeycomb structure which often occurred in circular areas. This type of material is shown on page 4.3.

2. Small particles of roughly spherical shape which formed strands or networks. Also sometimes observed embedded in a film of amorphous material. This type of material is shown in plate 4.4.

3. Regions which could be described as plate-like in appearance which included fibrous material. It is possible that the fibrous regions are the plate-like areas seen from the side. This type of material is shown in plate 4.5.

4. Areas of material which appeared plate-like with the regions at the edge showing a layered structure. The material appears to be amorphous, ie ragged edges and no thickness fringes, but many such areas gave diffraction patterns and some showed Moiré patterns due to overlapping lattice images. This type of material is shown in plage 4.6.

5. Thick layers which could not be studied. However near the edges at some points the material appeared to consist of particles as shown in plate 4.7.

It was noted that the types of morphology which consisted or appeared to consist of particles became more common the higher the water content in the reaction medium.

In the reactions prepared under acidic conditions there were again a number of types of morphology observed but again some were observed so infrequently that they could not be assigned with certainty to the samples. The main types of material observed were;

1. Material which appeared plate-like with the edges appearing layer-like. In the large number of these areas the area gave an electron diffraction patterns.

2. Areas of amorphous material of a honeycomb structure which often occurred in circular areas.

Plate 4.3: Samples of gelled material formed by touch showing amorphous material with a honeycomb like structure.

Magnification = 192×10^3

1cm = 52·08 nm

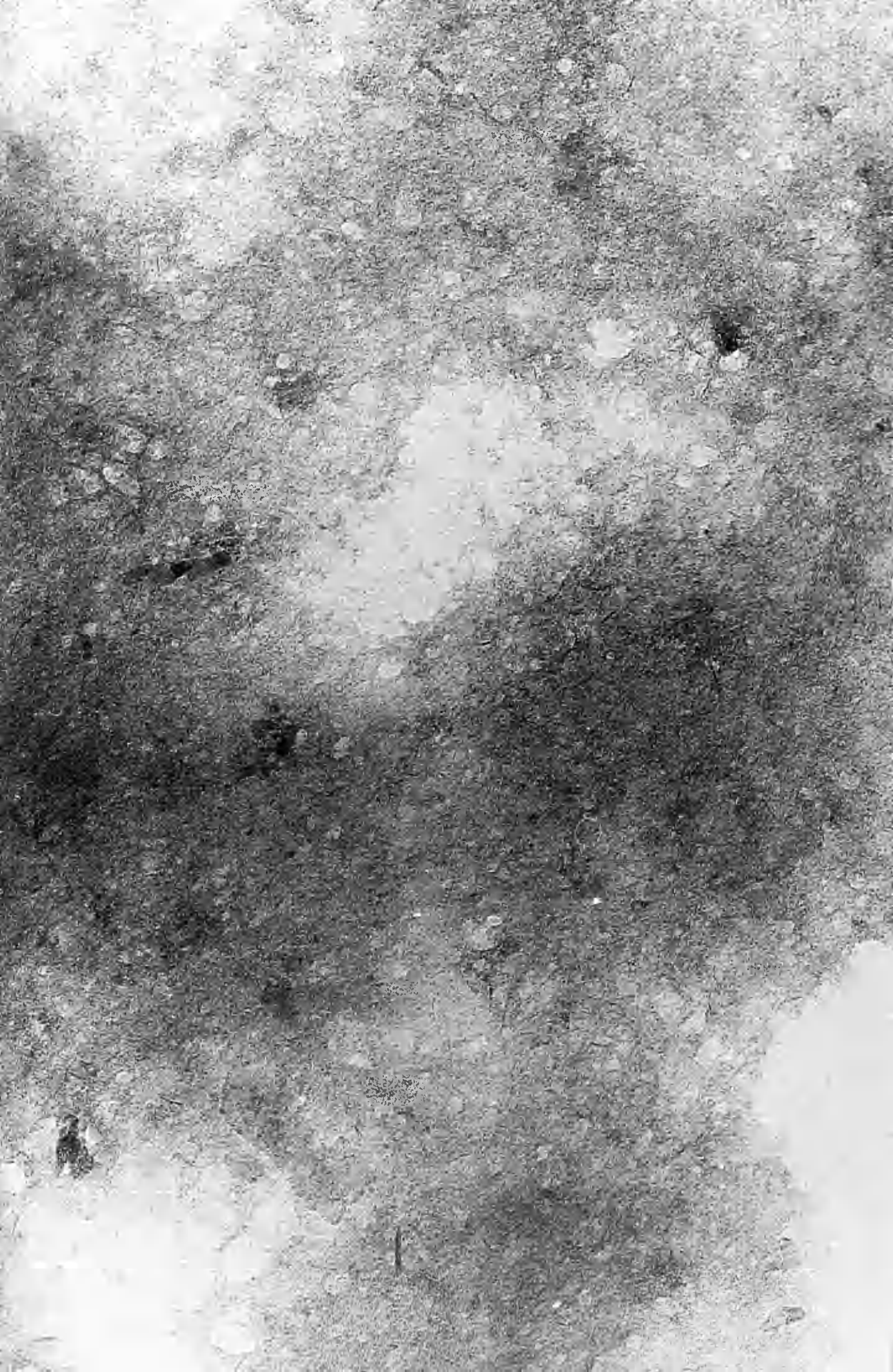

Plate 4.4: Samples of gelled material formed by touch showing networks of small particles.

Magnification = $73{\cdot}5 \times 10^3$

1cm = $136{\cdot}05$ nm

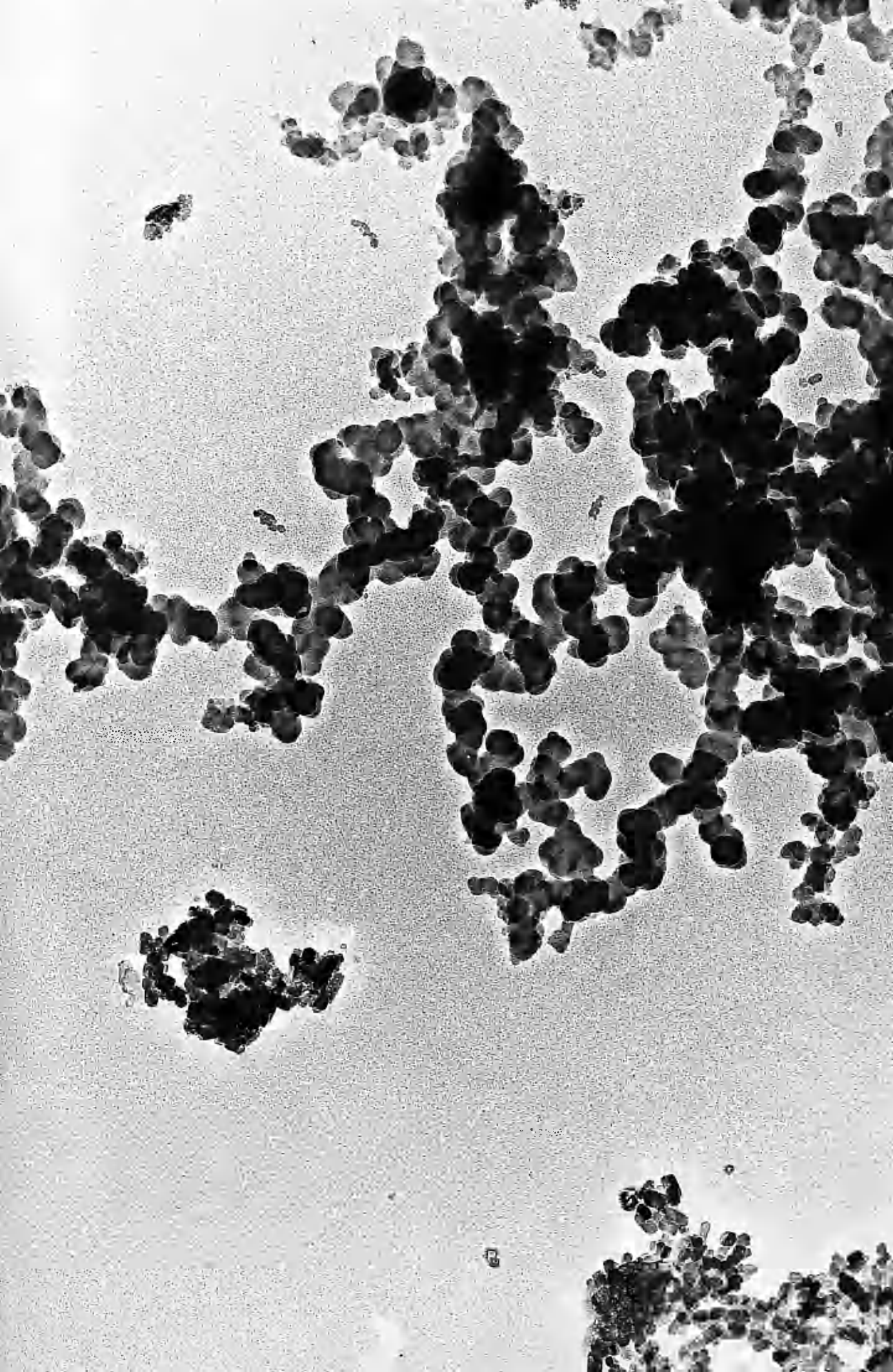

Plate 4.5: Samples of gelled material formed by touch showing material which included regions which could be described as plate-like and fibrous.

Magnification = 115×10^3

1cm = 86·95nm

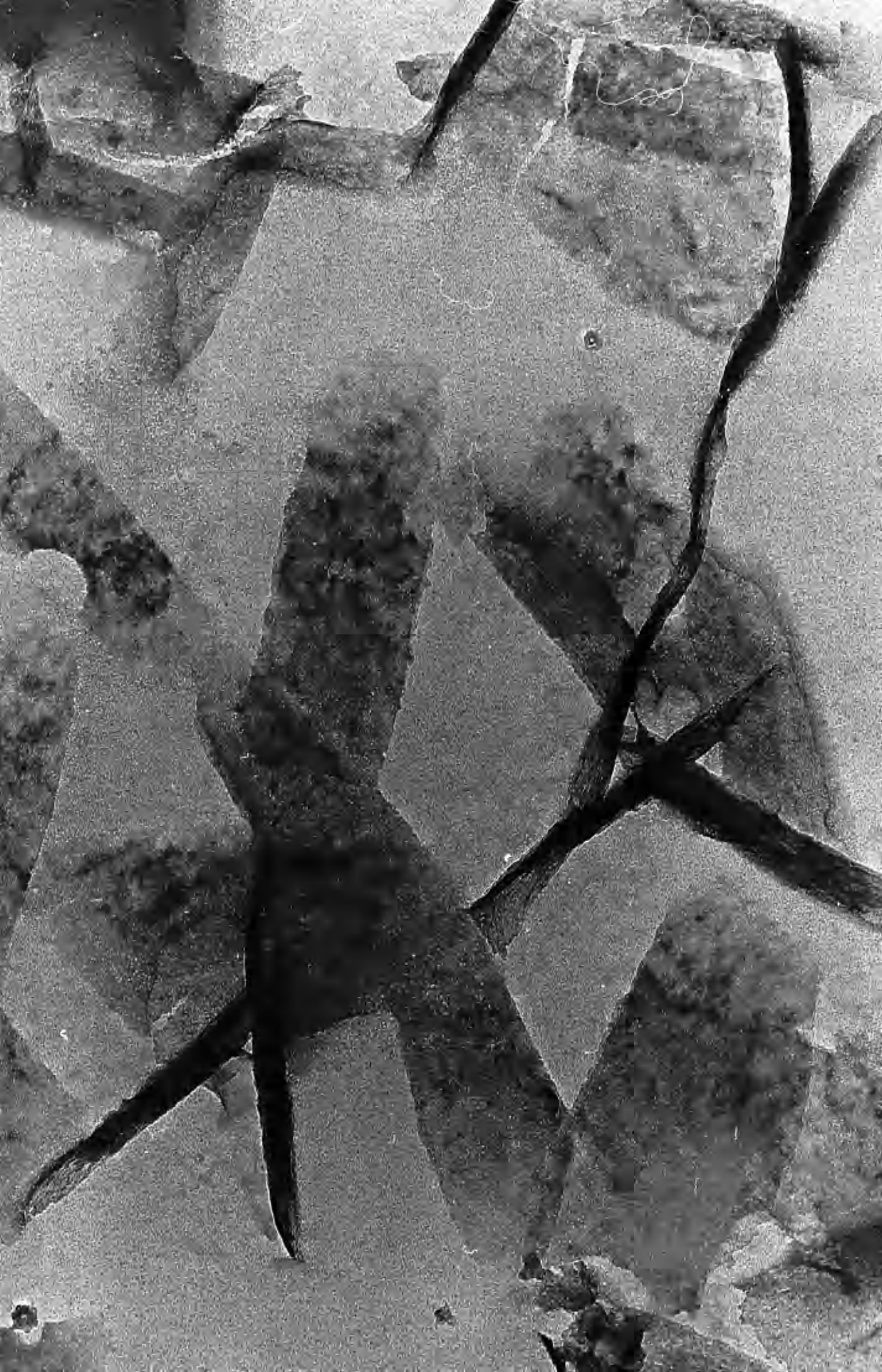

Plate 4.6: Samples of gelled material formed by touch showing material of a plate-like appearance with a layered structure.

Magnification = $652{\cdot}25 \times 10^3$

1cm = $15{\cdot}99$ nm

Plate 4.7: Samples of gelled material formed by touch showing thick layers which appear particulate near the edge.

Magnification = 309×10^3

1cm = 32·36 nm

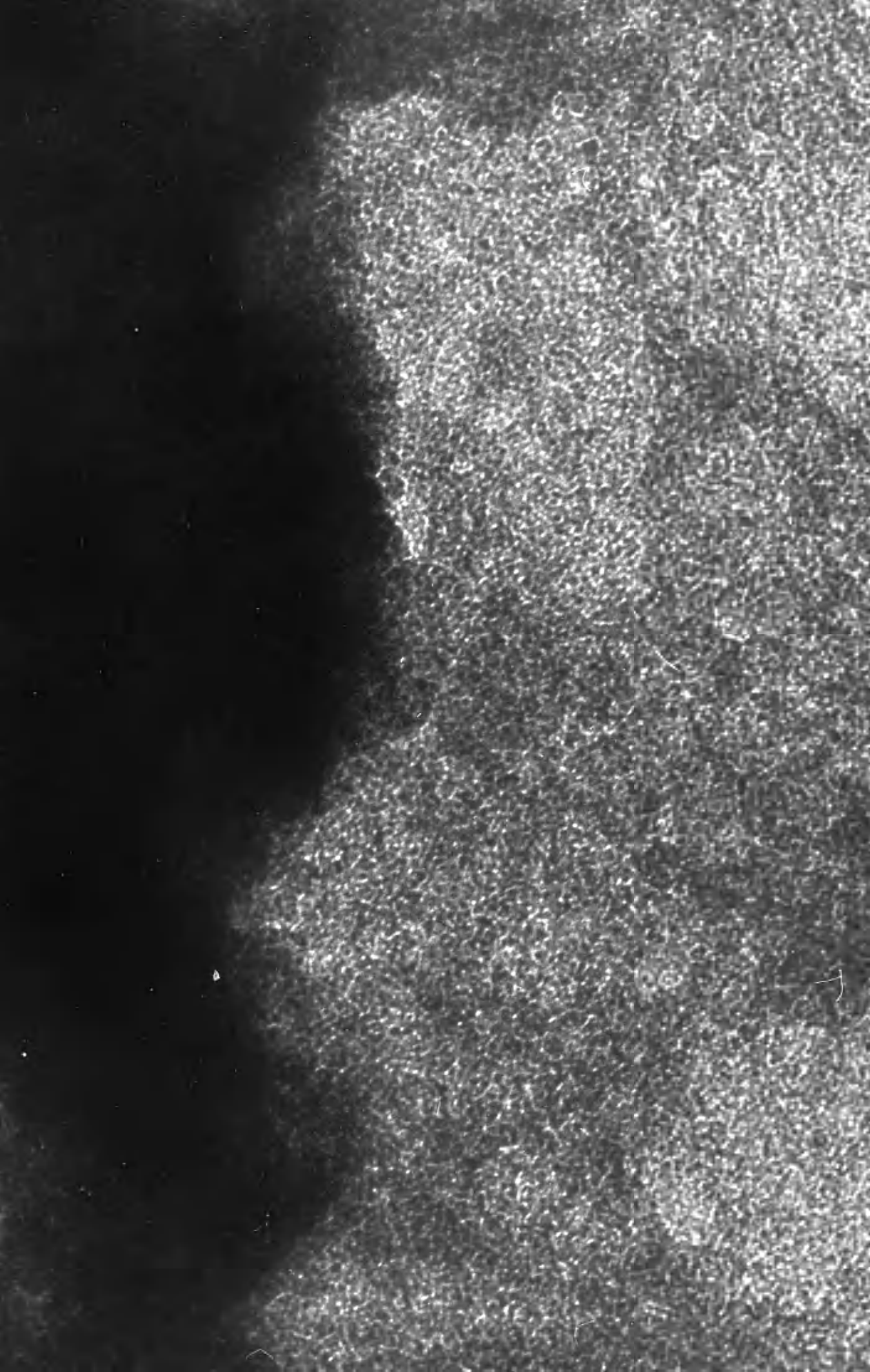

The most common type of material in the acid-catalysed system was the plate-like material which appeared to have a layer-like structure. However there did not appear to be observable differences within the material prepared under different conditions. This layered structure has previously been observed (Strawbridge et al, 1985) and this work also noted the lack of finer detail. Therefore this does not apear to be a suitable method of studying the reactions.

However it must be questioned why so many of the areas observed within the specimens gave diffraction patterns and had a crystalline appearance. The first possible explanation is that the crystalline material was contamination of the grid which was not related to the sample. This is unlikely in view of the amount of material observed and the number of samples in which it was present. However to ensure these results were not due to contamination the diffraction patterns of possible contaminants were compared to those observed in the samples.

The preparation of the grids involves the vacuum evaporation of graphite onto mica to form a film which is removed and floated onto the grids. This could give rise to contamination by graphite or mica (A.S.T.M. files 11-400, 12-187, 15-361, 17-520, 19-117, 19-690, 19-860) but the diffraction patterns do not correspond to these. A further possible source of contamination, especially in the case of reactions prepared with hydrochloric acid, would be copper from the grid bars in the form of copper salts or, although unlikely, copper silicate species.

Therefore the diffraction patterns were compared to those of copper chloride (A.S.T.M. files 6-349, 9-17), hydrated copper chloride (A.S.T.M. file 13-145) and copper silicate species (A.S.T.M. files 3-219, 7-172, 11-248, 11-322, 13-501, 13-507). Again no match was found.

Comparison of the diffraction patterns with those of the types of crystalline silica listed in the introductory chapter shows that although there were a number of similarities none of the patterns obtained in the electron microscope matched them.

In fact the electron diffraction patterns observed within the samples were not all the same, there were variations so that although many were similar very few were identical to a previously observed pattern. Consideration of the electron diffraction pattrens observed showed that peaks corresponding to a number of periodicities were quite common. These are listed in table 4.7.

5.905Å	1.511Å
2.950Å	1.429Å
2.050Å	1.217Å
1.565Å	1.174Å

Table 4.7: Commonly observed diffraction periodicities.

It has already been noted that the patterns obtained do not correspond to possible contaminants or known forms of silica. Although some of the periodicities which appear are similar to those appearing in known silica the patterns did not match.

A possible explanation for the appearance of these crystalline areas is that they are crystalline hydrated silica similar to those reported previously (Iler, 1964; Frondel, 1979). This could explain why so many diffraction patterns were observed, because at least twenty different crystalline hydrated silicas have been identified (Frondel, 1979) all with different diffraction patterns. It has also been noted that the drying conditions can alter the diffraction pattern (Iler, 1964).

A further possible explanation is that a significant amount of order exists in at least some areas of the gel. These areas may actually be crystalline or the stresses involved in the sampling process may be sufficient to convert them to a crystal-like order. The latter explanation may be the correct one if the previous discussion of the XRD results is correct and there is ordering within the gel.

4.7.6 THIN SECTIONS

The difficulties in many of the techniques described above are based on the thickness of the sample. A possible solution to this problem is to take thin sections of the gelled products. This is a method used extensively in biological electron microscopy (Meek, 1970; Lewis and Knight, 1982) to study the

structures within objects which are themselves not suitable for examination.

The types of material observed from samples prepared in this fashion were the same as those observed in samples prepared by touch. This would indicate that this method of sample formation does not shed more light on the morphologies present in the sample. One difference observed between samples produced by touch and those from thin sections was that less crystalline material was observed in thin-sectioned material. The significance of this, if any, is not known.

4.7.7 FREEZE-DRYING

It has been described in the introduction that during the drying of a gel the structure changes by a large extent. It is of interest to be able to study the structure of the gel as it exists in reaction and after drying. However all electron microscopy techniques require a dried specimen. Therefore it is necessary to have a method of drying a sample of gel which does not alter the structure. The problem is similar to the problems faced in biological electron microscopy where drying the samples can distort or destroy the structure of interest. A technique used to overcome this problem was freeze-drying.

A system was improvised to freeze-dry samples. In this small pieces of gel were placed on a glass slide on a block at liquid nitrogen temperature, the whole apparatus being within a chamber which could be evacuated.

The samples prepared in this manner showed types of material which were similar to those observed in samples prepared by touching the gel. Therefore this would not appear to be a technique suited to the study of gels because the added difficulty provides no further information.

4.7.8 STAINED SAMPLES

In many of the above examination methods a problem existed with the ability to see detail within the sample. To a large extent this was due to the low scattering factors of the elements present which led to a low contrast. Again a solution to the problem of low contrast has been developed for biological electron microscopy (Meek, 1970; Lewis and Knight, 1982); staining the sample with a heavy element with a higher scattering factor, thus increasing contrast.

In the case of the gelled material in this project the staining agent, uranium in the form of uranyl acetate, would be in contact with the surfaces of the gel both the outer surfaces and those within the pores. It was therefore possible that the contrast of the sample as a whole would be increased and the pore structure, where more uranium would be located, be increased even more. Thus making the detailed structure within the gel observable. Having stained and washed the gel the recovered gel still had a yellow colouration indicating the presence of uranyl acetate within the gel.

Although there may have been more contrast in the sample

observed there were no new morphologies or details observed by preparing samples in this fashion.

4.8 DISCUSSION

Electron microscopy has been used in a number of studies of the formation of gels by the sol-gel process (Brinker et al, 1984(d); Roy et al, 1984; Tewari et al, 1986; Bailey and Mecartney, 1988; Ruben and Shafer, 1986(a), 1986(b), Mulder et al, 1986). In most of these studies the alterations in the reaction composition were quite large for relatively small alterations in the observed product morphology. In many of these works electron microscopical examination was merely a confirmation of predictions made by other techniques and shows that at high water concentration the material is particulate in nature. However in one of these papers (Ruben and Shafer, 1986(b)) the strand like nature of the product of acid-catalysed systems, predicted by other work (Brinker et al, 1982), was confirmed.

The work carried out in this project shows a similar pattern. Many of the sampling methods provided samples which were not suitable for examination. By this it is meant that although some features could be observed these were fairly infrequent. In a technique such as TEM, where the amount of sample examined is extremely small, results based on the observation of a small proportion of this would not be reliable.

Although the specimens prepared were not suitable for examination in the microscope, in the sense that little detail

could be observed, they still provide information. The observation that the sampling methods provide a film, and diluting the sample produced a thinner film, supports the models which propose a polymerisation process forming linear polymers which link to form a gel which is homogeneous This would also concur with the observation of little internal structure within the areas of this material which could be observed in the microscope. Similarly the observations that samples from reactions with high water concentration seemed more particulate in nature correspond to the predictions that the higher water concentration would lead to the formation of more highly crosslinked polymers.

The preparation of samples by forming a film on top of organic solvents can also be explained in terms of the predictions of the polymerisation theory. The samples form a film because the organic materials in the reaction dissolve in the organic solvent or evaporate. The silica polymers can not evaporate and, if large, can not dissolve in the organic solvent. At early times in the reaction no film forms. This is probably due to the fact the polymers would not be large or greatly interlinked so that there is insufficient structure to form a film and the silica polymers fall into the solvents and the smaller ones may dissolve. At later times in the reaction a film forms on top of the organic solvent because the reaction has had sufficient time to form large interlinked polymers which will not enter the organic solvent. The actual morphology of the film is determined by the way in which the reaction organic materials enter the organic solvent or evaporate to leave the silica.

In the sampling technique which actually gives a sample which can be studied, sampling by touch, a further problem arises; little variation in product morphology is observed with alteration of the reaction conditions. In most of the samples the material appeared to be plate-like with irregular shape. The outer regions of these areas of the sample appear to have a layered structure. These samples also regularly appeared to be crystalline with quite pronounced variation in the electron diffraction patterns. These observations do not alter to a large extent without a large change in the reaction conditions leading to them. Therefore this would not appear to be a technique sensitive enough to study the effects of alterations of the reaction conditions on the product morphology within the acid-catalysed system.

Although the sampling techniques employed showed a few types of morphology these give some information about the product. In earlier chapters a basic outline of the reaction mechanism was given which indicated that under acid-catalysed conditions with a low water concentration the mechanism leads to the formation of linear polymers. Although the basis of this model has not been challenged, other work (Peace et al, 1973; Bunker, 1988) suggest that these linear polymers form rings. It can easily be envisaged how such a structure could lead to the formation of a layered structure and the plate-like appearance of the observed material.

This type of structure may also explain why there were so many areas which appeared crystalline. If the rings in the structure are of about the same size then there is a possibility that a layer polymer will have an affect on the layers on each

side of it. That is, there may be positions which are more stable for the rings to be in, in a layer next to another ring-structured polymer. This could lead to an ordering of the polymer, which could be crystalline or converted to crystallinity by the stresses involved in sampling by touch.

A further, but more speculative, explanation of the crystallinity is that the rings give a regularity to the polymer. Therefore if a bond occurs between a silicon atom in one polymer and one in another then other atoms in that area of the polymers will be in a position to bond together. This "zipping" action could lead to areas of structure.

It was possible that the lack of structure observed in samples was because of changes and shrinkage which occurred during drying or because of the thickness of the sample. These are problems which have occurred and been overcome in biological electron microscopy. To try and overcome these some of the techniques used in biological microscopy, thin-sectioning, freeze-drying and staining of samples, were attempted. Whereas in biological samples there is generally large scale structure which can be observed after the use of these techniques this was not the case in this work. Therefore the use of these techniques did not improve the observations in the microscope.

4.9 CONCLUSIONS

Several reactions were prepared to various compositions with both acid or no catalyst present. These reactions produced gels

which were usually clear and rigid. Examination of these gels by a number of physical techniques showed that little difference could be found between the products of different reactions. It would appear that the differences in the gels are on the molecular level and not detectable with the techniques employed.

Although no differences of great significance were observed in the different reaction products a number of features of interest were noted. The first of these was that the gels appeared to consist of material which forms a layered structure. This would agree with the reaction models which predict the product should be in the form of linear chains or rings. The second feature was that a number of crystalline areas were observed. The reason for the appearance of these regions is not clear but it could indicate a level of structure within the product and again this can be rationalised in terms of an arrangement of rings forming a layered structure with some form of repeat, but this must be considered as extremely speculative.

The final conclusion is that the study of gels of amorphous material is extremely difficult due to the fact the changes in modecular structure would be impossible to determine in a totally irregular material.

4.10 FUTURE WORK

1. Hypercritical drying, as developed by Kistler (1931, 1932), removes the capillary pressure by heating the gel above the critical temperature and pressure of the liquid in the gel. Thus

gels dried in this fashion do not shrink and therefore this may be a method of forming samples of gelled material which accurately represent the structure present in the gel.

2. Combinations of techniques such as thin-sectioning, freeze-drying, hypercritical drying and staining may provide more information about the structures within the products.

3. Analysis of the initial reagents and the final product solvent to determine if the added peaks in the specta of certain products were due to the presence of oxidation products of the alcohol.

4. Preparation and study of gels prepared from material which tends to form a crystalline product may provide more information on the variations in structure due to reaction condition alterations.

5. Investigate the possibility of impregnating the gel with a material which lends itself to study. Then remove the gel by dissolution, possibly with strong base or hydrofluoric acid, and then study the cast left behind.

VOLUME 2

NOVEL ROUTES TO HIGH PURITY OXIDES

BY

JEFFREY ADAMS

being a thesis submitted for the degree of Doctor of Philosophy in the Chemistry Department of the University of Glasgow.

FEBRUARY 1991

VOLUME II

CONTENTS

CHAPTER SIX

NICKEL DEPOSITION

5. BASE-CATALYSED REACTIONS

5.1 INTRODUCTION

The previous chapter dealt, as far as possible, with the examination of reaction products produced under acidic or neutral conditions. The third possible condition for the reactions to be carried out under is base-catalysed. It is reactions produced under such conditions which are the subject of this chapter.

5.2 REACTION PREPARATION

5.2.1 REACTION PLAN

Having observed the difficulties posed in studying silica produced by the acid catalysed hydrolysis of TEOS, the initial aim of producing base-catalysed reactions was to determine whether the products would be suitable for study by electron microscopy. For this purpose reactions were prepared, as described in the experimental chapter, to molar ratios of reagents. These ratios are listed in table 5.1. The results of these experiments, as detailed below indicated the products could be studied by electron microscopy. Therefore a systematic study of the reaction products of the base-catalysed reactions was carried out.

The composition of the reactions prepared under acid catalysis and those base-catalysed reactions described in table 5.1 followed the convention of work in this field (for example Yu

Composition	TEOS	Water	Ammonia	Ethanol
B1	1	3.163	0.102	3.974
B2	1	5.639	0.102	3.974
B3	1	10.593	0.102	3.974
B4	1	15.546	0.102	3.981
B5	1	20.500	0.102	3.981
B6	1	8.116	0.102	3.074

Table 5.1: Molar ratios of base-catalysed reactions B1 to B6

et al, 1982; Brinker et al, 1982, 1984(b), 1986(b)), Schaefer et al, 1984; Chen et al, 1986; Duran et al, 1986; Colby et al, 1986) and were prepared to correspond to molar ratios of reagents. Such a system has the advantage that the quantities of each reagent could be calculated before preparation and the composition would correspond exactly to that desired. However such descriptions lack information about the volume involved and do not clearly represent the concentrations of the reagents. The previous discussion on hydrolysis indicated the product morphology is dependent on the extent and rates of the hydrolysis and condensation reactions. Studies of chemical kinetics (Braley-Smith, 1975; Jones, 1979) indicate that such factors are affected by the concentration of reagents. Taking account of these arguments the investigation of the base-catalysed reactions was carried out in reactions prepared to specific reagent concentrations.

However such a system has the disadvantage that because TEOS and water dissolve in ethanol, to a certain extent, the volume of ethanol required to make up the volume can not be calculated beforehand. As described in the experimental chapter this causes slight errors in the concentrations of reagents, especially water, used in the reactions. Therefore the actual concentrations do not exactly match the desired value. However the variations are small, and very small in comparison to the difference between the different water concentrations used in the study. A list of the accurate compositions of the reaction mixtures is given in table 5.2. In the tables and figures later in this chapter the rounded values will be used for convenience.

The range of reaction compositions listed in table 5.2 allows the comparison of reactions in which only one reagent concentration had been altered. This is illustrated in tables 5.3 and 5.4 which correspond to reactions prepared with 10M water concentration and 5M water concentration respectively. These tables show that different reaction compositions correspond to changes in one reagent. For example composition B7 corresponds to that of B8 except that the ammonia concentration has been increased. Similarly B14 matches the composition of B24 with the exception that the water concentration has been altered.

Composition	TEOS	Water	Ammonia	Ethanol
B7	0.994	10.173	0.034	10.36
B8	0.994	10.164	0.1695	10.842
B9	0.994	10.288	0.339	10.43
B10	0.994	10.09	0.998	10.53
B11	0.994	10.516	1.695	9.79
B12	0.497	10.298	0.0339	12.578
B13	0.497	9.926	0.1695	12.478
B14	0.497	10.370	0.339	12.389
B15	0.497	10.072	0.998	11.973
B16	0.497	10.696	1.695	11.931
B17	0.2485	10.111	0.0339	13.333
B18	0.2485	10.122	0.169	13.333
B19	0.2485	10.144	0.339	13.333
B20	0.2485	10.016	0.998	13.243
B21	0.2485	8.744	1.694	13.694
B22	0.497	5.149	0.0339	14.012
B23	0.497	4.987	0.169	13.667
B24	0.497	5.213	0.339	13.773
B25	0.497	5.09	0.998	13.511
B26	0.497	5.532	1.695	13.480
B27	0.2485	5.096	0.0339	14.878
B28	0.2485	5.167	0.169	15.144
B29	0.2485	5.133	0.339	14.689
B30	0.2485	5.754	0.998	14.420
B31	0.2485	5.611	1.694	14.244

Table 5.2: Molar concentrations of reagents in reaction B7-B31

	Ammonia Concentration				
TEOS	0.034M	0.17M	0.34M	1.0M	1.7M
1.0M	B7	B8	B9	B10	B11
0.5M	B12	B13	B14	B15	B16
0.25M	B17	B18	B19	B20	B21

Table 5.3: Relative positions in reaction plan of compositions with 10M water concentration.

	Ammonia Concentration				
TEOS	0.034M	0.17M	0.34M	1.0M	1.7M
0.5M	B22	B23	B24	B25	B26
0.25M	B27	B28	B29	B30	B31

Table 5.4: Relative positions in reaction plan of compositions with 5M water concentration.

5.2.2 REACTION PATTERNS

The reactions were prepared in the manner described in the experimental chapter. After the initial preparation the observations of the reactions varied depending on the reaction conditions.

In reactions which had compositions with high ammonia and water concentrations (a more detailed list of the concentrationswill be given later) the mixture became cloudy almost immediately upon addition of TEOS. Within a matter of minutes, usually 5-10 minutes, the reaction flask contained a solid which was often foam-like in appearance. This material settled quite rapidly and could be recovered by filtration to give a white powder.

In compositions with ammonia and water concentrations lower than those of reactions of the above description, but not very low, the changes were slower. After the addition of TEOS the reaction mixture became cloudy and gradually became more cloudy until it was a white suspension. In general the reaction became cloudy within 15-20 minutes of the addition of TEOS, although in some cases of higher water and ammonia concentration the change was within 5 minutes. The product could be recovered by removal of solvent in a rotary evaporator, by centrifuging or by allowing the solvent to evaporate. The first of these methods produced white powders which were often free flowing. The latter two produced solids which were hard and often appeared to have an iridescent sheen on the surface.

In the reactions with low ammonia concentration there were no rapid changes of appearance on addition of the TEOS. In those with high TEOS concentrations the mixture became cloudy over a period of several hours and after several weeks formed a loose gel. In cases where the TEOS concentration was low the reactions became slightly cloudy but did not gel. This material could be recovered by allowing the solvent to evaporate to leave an opaque gel.

The only other notable feature of these reactions was that in cases where the amount of water added was high the ethanol was often not sufficient to act as a solvent. In these cases the addition of TEOS caused a separation of phases leading to a two-phase system with the second phase comprising small droplets within the bulk of the reaction mixture. Similar observations were made by Bridger et al (1979) while preparing silica spheres for further theoretical studies. These small droplets rapidly disappeared as the water was used in the hydrolysis, and more ethanol was produced. In one case, reaction B5, the water actually formed a second layer above the ethanol layer. This led to the formation of a layer of silica at the interface of the two layers apparently ceasing or greatly slowing the reaction.

5.3 MICROANALYSIS

The object of the production of the initial reactions B1 to B6 was to determine whether the reactions and products were suitable for examination and study. A requirement for such suitability would be that clear differences could be detected

between samples produced under different reaction conditions. Therefore samples of product produced under different conditions were submitted for microanalysis for the elements carbon and hydrogen. The results are shown in table 5.5.

These results show that a difference does exist and the reaction with the higher water content has a product with a lower carbon content but higher hydrogen content. This result would be expected as the higher water content is likely to produce a higher degree of hydrolysis and have a lower amount of re-esterification.

However these values are extremely low and the differences between results for reaction compositions with widely varying compositions are small. These results also mean the error involved in the measurement is large in relation to the actual value. It was also the case that the low values prevented the analyser from operating properly. This would indicate that the available microanalysis would not be a useful method of studying the reaction products.

Composition	% Carbon	% Hydrogen
B1	1.63	0.72
B6	0.39	0.85

Table 5.5: Percentage content of carbon and hydrogen in products.

5.4 INFRA-RED SPECTROSCOPY

Again, to determine if significant differences within the samples could be detected by IR spectroscopy, the spectra of products B1 to B6 were obtained. However all of the spectra were similar with the only differences being slight changes in the relative intensities of the peaks. The spectra correspond to that of silica as previously described.

5.5 TRANSMISSION ELECTRON MICROSCOPY

5.5.1 INITIAL REACTIONS

In the case of reactions B1 to B6 the object of the examination of the product was to determine if there were significant differences between the samples. The sample preparations and examination methods have been described in the experimental chapter.

The types of material observed altered considerably with changes of the reaction conditions leading to their formation. The product of the reactions B1 and B6 appeared as larger particles which seemed to have been formed by the fusion of the smaller spherical or roughly spherical particles, formed in reactions B3, B4 and B5, and had a rough and irregular shape. This material is hereafter referred to as fused material because of the above description. Micrographs of this material will appear later.

The reactions B3, B4 and B5 gave products which consisted of particles which were spherical or nearly spherical in shape. This type of material will be shown in micrographs in the main discussion following.

The results indicated that a range of product morphologies depending on the reaction conditions exists. Therefore the series of reactions B7 to B31 were prepared to allow systematic study of the products in relation to the reaction conditions.

In such a study it is necessary to determine whether the morphology produced by a set of reactions conditions is reproducible. A series of experiments were designed to test for reproducibility.

5.5.2 REPRODUCIBILITY

As described in the experimental chapter the reactions were carried out a number of times and a representative result quoted. In the case of most of the morphologies studied it could only be seen that the separate reactions produced material which appear similar in nature to those previously prepared to that composition. The reactions which produce spherical particles however offer the opportunity to determine the reproducibility because the actual diameter of the spherical particles offers a direct method of characterisation and comparison. Therefore a reaction composition which, as will be made clear later, produces spherical particles was used to determine how reproducible the results were. The composition used was B14 because this formed

large particles and employed high reagent concentrations which should make any changes more prominent.

The procedure which appeared most likely to affect the reproducibility of the results was the practice of preparing the reactions with part of the ethanol volume and then adding the ethanol necessary to make up the volume of the mixture. After the first preparation of a reaction mixture the volume of ethanol necessary was known and it was thus possible to prepare a reaction with all the ethanol present before the addition of the TEOS and mixing.

To test whether this practice actually had an affect on the reproducibility of the product two reactions were prepared to the B14 composition. In the first reaction, reaction A, the ethanol was added in two parts, one before and one after the addition of the TEOS as described in the experimental chapter. In the second reaction, reaction B, all of the ethanol was added before the addition of the TEOS. After the reaction was complete the size distribution and mean diameter of the particles were determined. These are illustrated in figs. 5.1 and 5.2.

In the reaction where the ethanol was added in two parts the final mean diameter was 388nm (S_n=10.51nm) and in the case where the ethanol was added in one action the final mean diameter was 398nm (S_n=11.57). The particle size distribution shown in figs. 5.1 and 5.2 and the mean diameter figures indicate there was no significant difference in the product sizes or distribution. It would therefore appear that the initial mixing of the reagents does not have a large affect on the product.

To determine how reproducible results were without

altering the method of production two further reactions, reactions C and D, were prepared to the B14 composition. The size distribution of these are shown in figs. 5.3 and 5.4, the mean diameter of the first of these was 371nm (S_n=13.52nm) and the second 526nm (S_n=88.79nm). The latter actually appears to be a bimodal distribution with mean diameters 564nm (S_n=19.26nm) and 333nm (S_n=40.38nm). The last result may be due to the presence of foreign material which caused heterogeneous nucleation. The other results would indicate the reactions are reproducible but there are variations leading to small size differences. Such size variations have been observed by other authors (Bogush and Zukoski, 1987). There is also the possibility of other factors interfering with the reaction to produce results far from the apparent normal. It is possible that the factor which causes the small variations is the temperature which has been shown (Optiz, 1987; Bogush et al, 1988(a)) to cause differences in the product size. In these reactions the temperature was not controlled to a greater extent than the ambient temperature of the laboratory but that based on the above reports any variation would be small.

5.5.3 MATRIX REACTIONS

As has been previously indicated in this chapter, electron microscopical examination of the reaction products showed a number of different types of product morphology. This led to the formation of a matrix of reactions to study the morphology of the products. These reactions showed four different types of morphologies within the products.

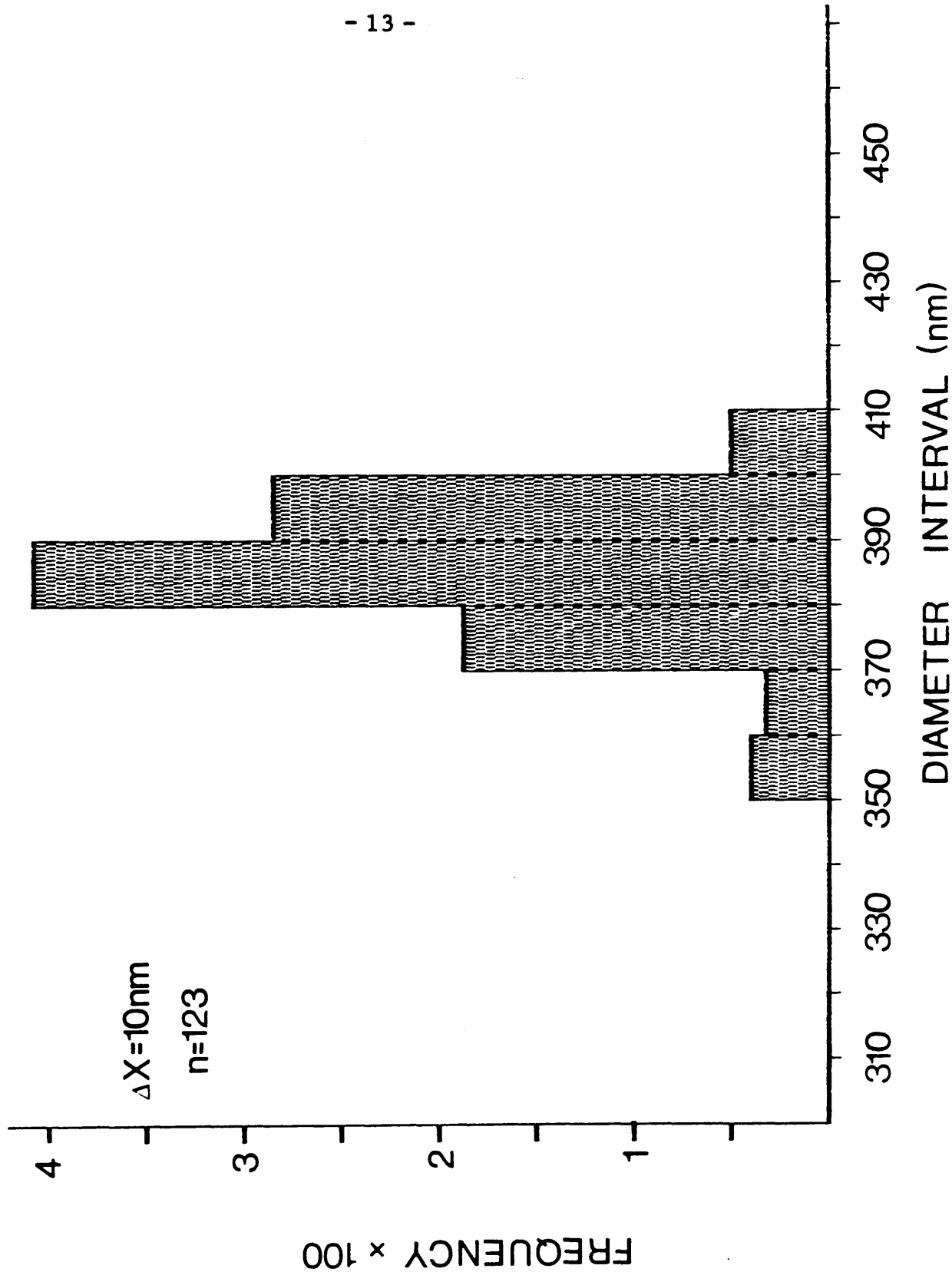

Fig 5.1: Size distribution of product particles in B14 reaction A. Frequency indicates the relative frequency per unit interval in diameter.

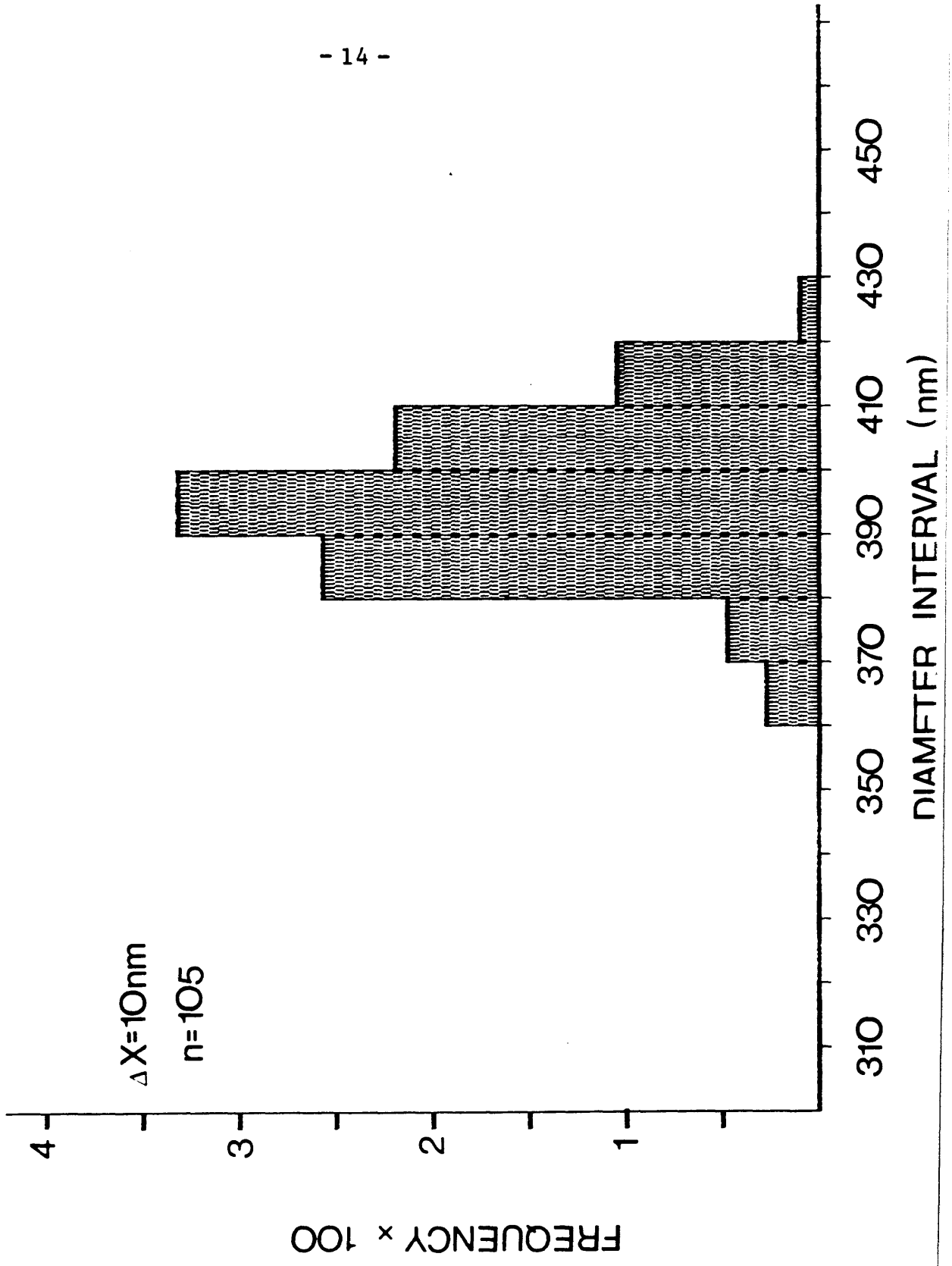

Fig.5.2: Size distribution of product particles in B14 reaction B. Frequency indicates the relative frequency per unit interval in diameter.

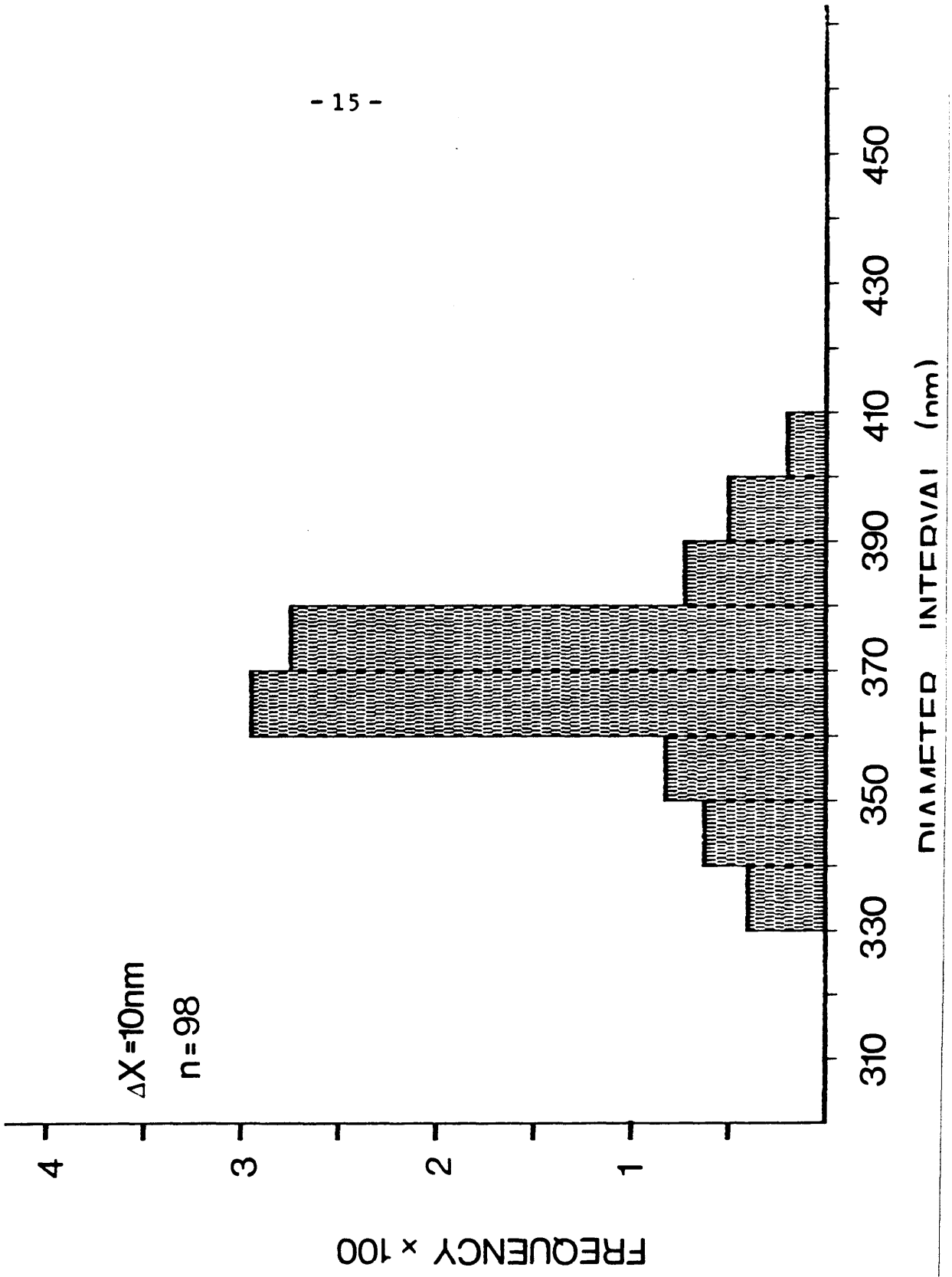

Fig. 5.3: Size distribution of product particles in B14 reaction C. Frequency indicates the relative frequency per unit interval in diameter.

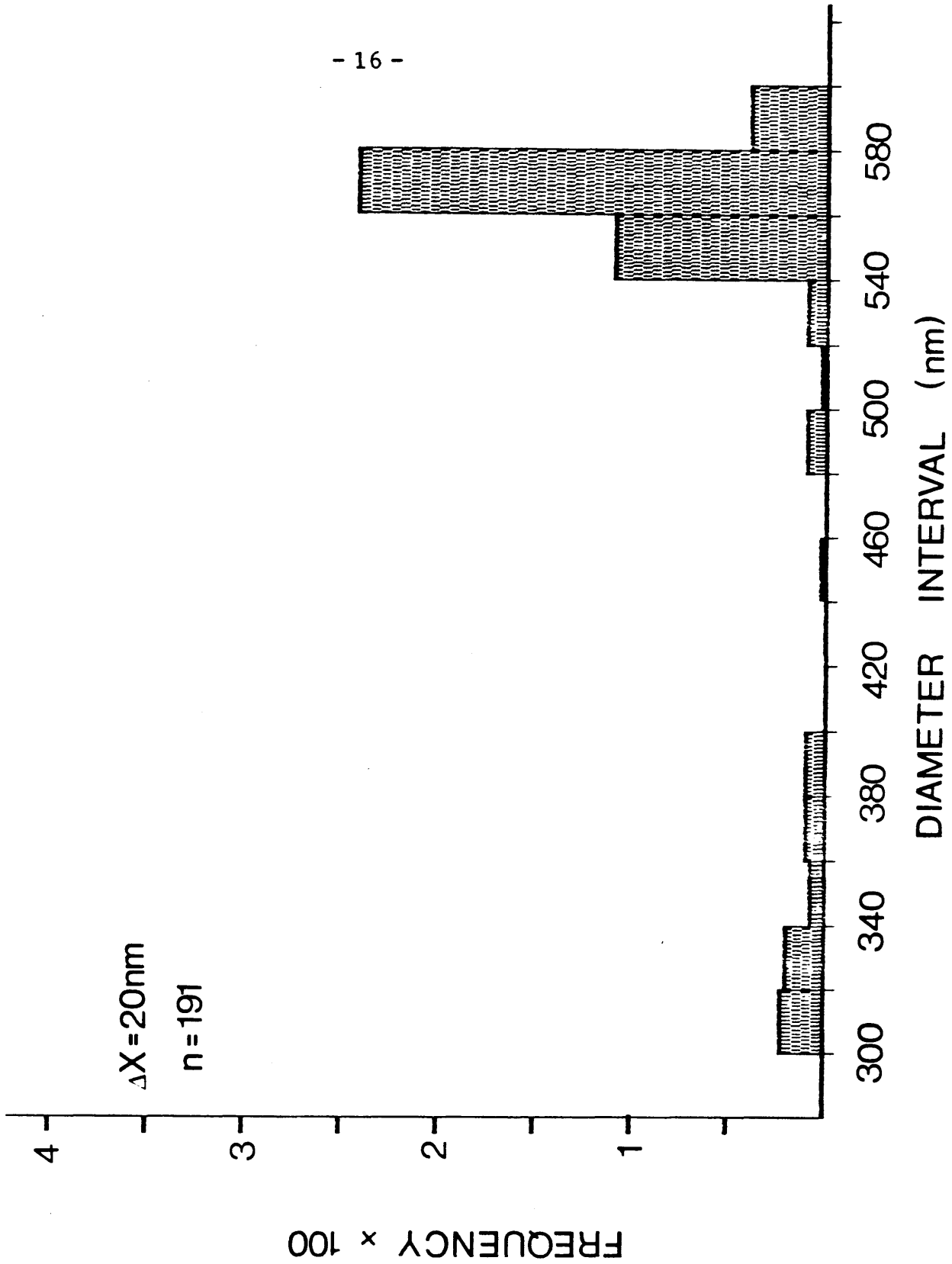

Fig. 5.4: Size distribution of product particles in B14 reaction D. Frequency indicates the relative frequency per unit interval in diameter.

The first of these was the large particles of irregular shape which had the appearance of material made by the fusion of particles. This, as has already been mentioned, has been labelled "fused material". This type of material is shown in plate 5.1. This was the morphology normally observed from reactions in which the solid rapidly appeared and filled the container.

The second type of morphology observed were particles which were roughly spherical in shape. These are shown in plate 5.2. The third type of product were particles which were spherical in shape, as shown in plate 5.3. This type of material has been reported by a number of authors (for example Stöber et al, 1968; Adams et al, 1988; Chatterjee and Ganguli, 1986; Bogush et al, 1988(a)). As can be observed from these plates the particles appear to be monodisperse but in a number of samples the spread of particle sizes was large. In several samples the particles appeared to be of two distinct sizes and in these cases both sizes will be quoted. These bimodal distributions have previously been observed in the silica and other systems (Chatterjee and Ganguli, 1986; Bogush et al, 1988(a)). These latter two types of products are those which form white suspensions in the reaction flask.

The last type of material observed were small particles of irregular but roughly spherical shape which joined or aggregated to form chains and network of irregular shape. This type of material is shown in plate 5.4. These were observed in reactions which formed gel like products. Material of this type has previously been observed by Mulder et al (1986), Iler (1979),

Plate 5.1: Material of the fused morphology.

Magnification = $69{\cdot}75 \times 10^3$

1cm = $143{\cdot}37$ nm

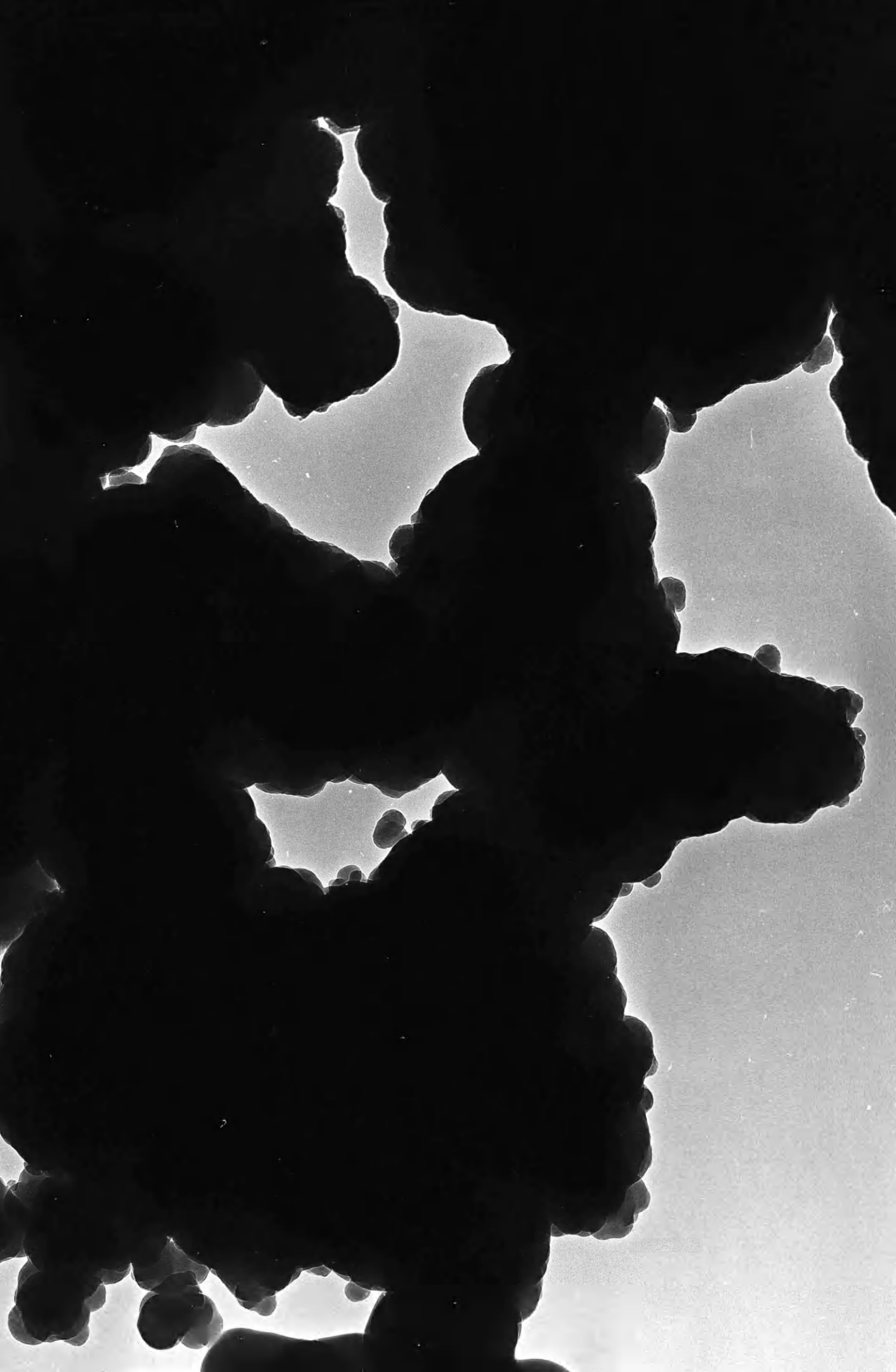

Plate 5.2: Material consisting of roughly spherical particles.

Magnification = 328×10^3

1cm = $30{\cdot}49$nm

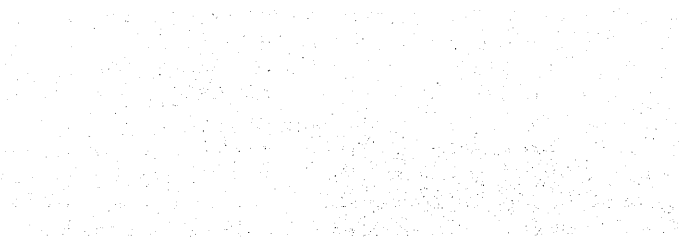

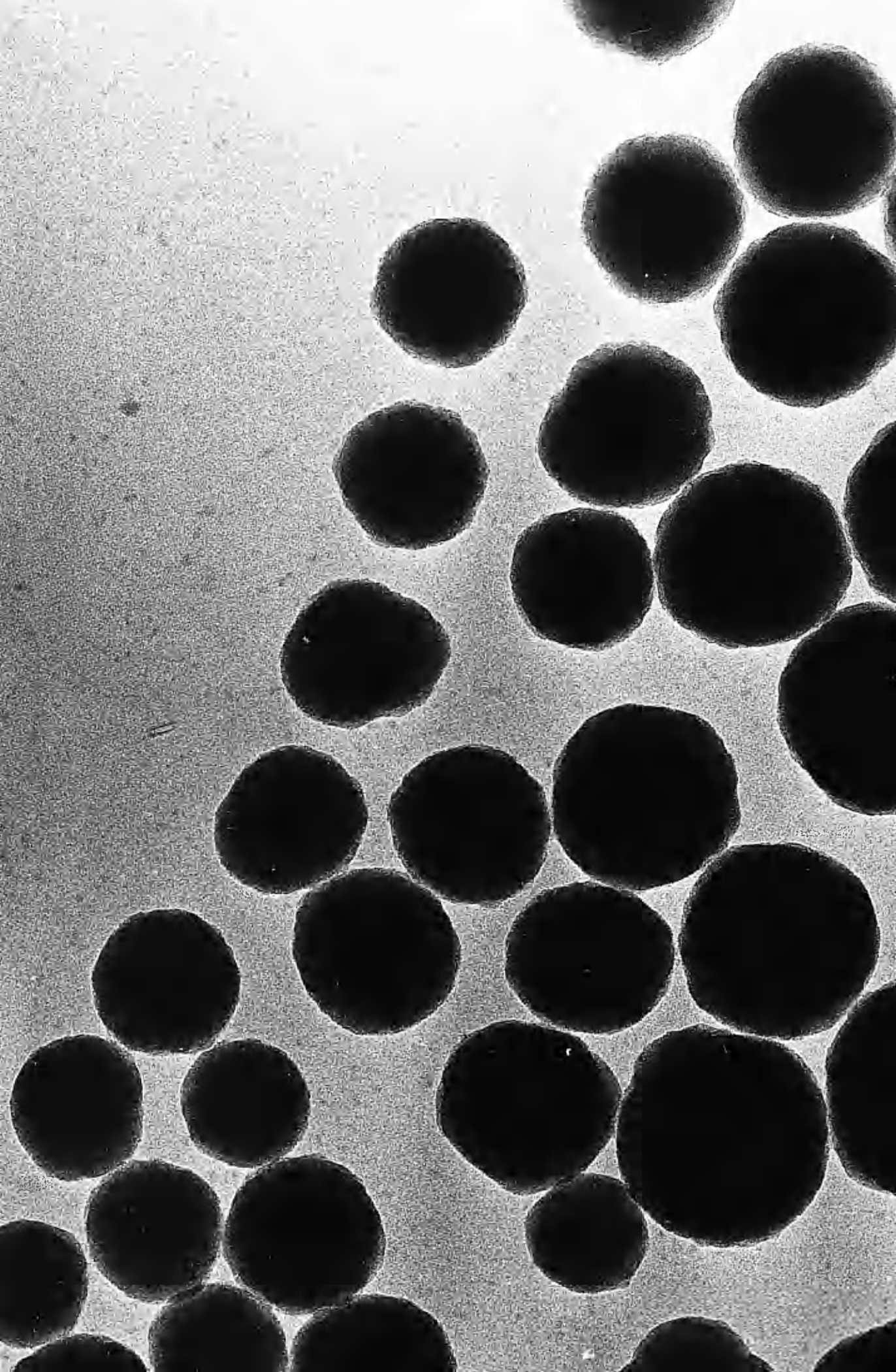

Plate 5.3: Material consisting of spherical particles.

Magnification = 184×10^3

1cm = 54·35nm

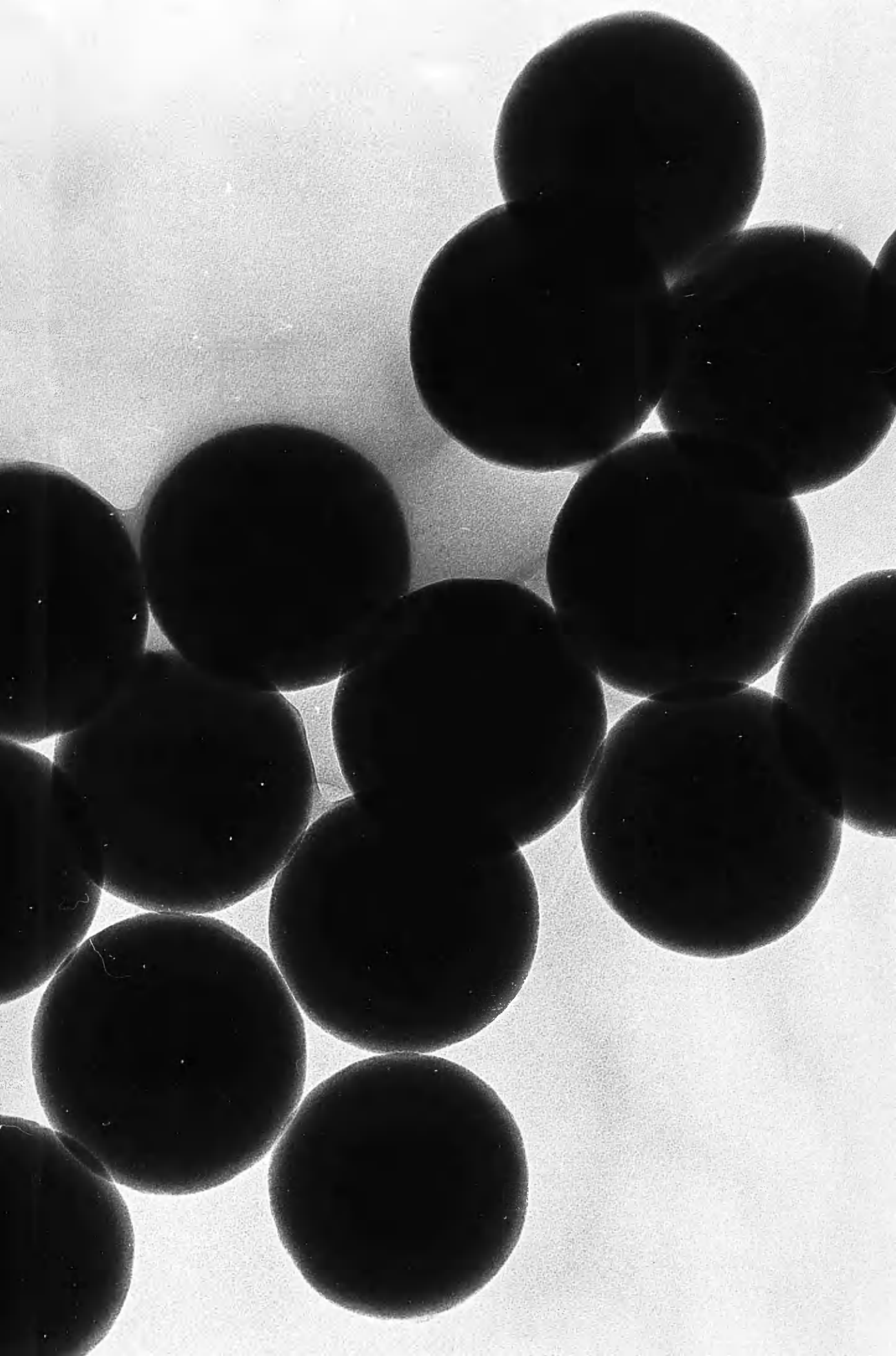

Plate 5.4: Material consisting of small irregularly-shaped particles forming chains.

Magnification = 470×10^3

1cm = $21{\cdot}28$ nm

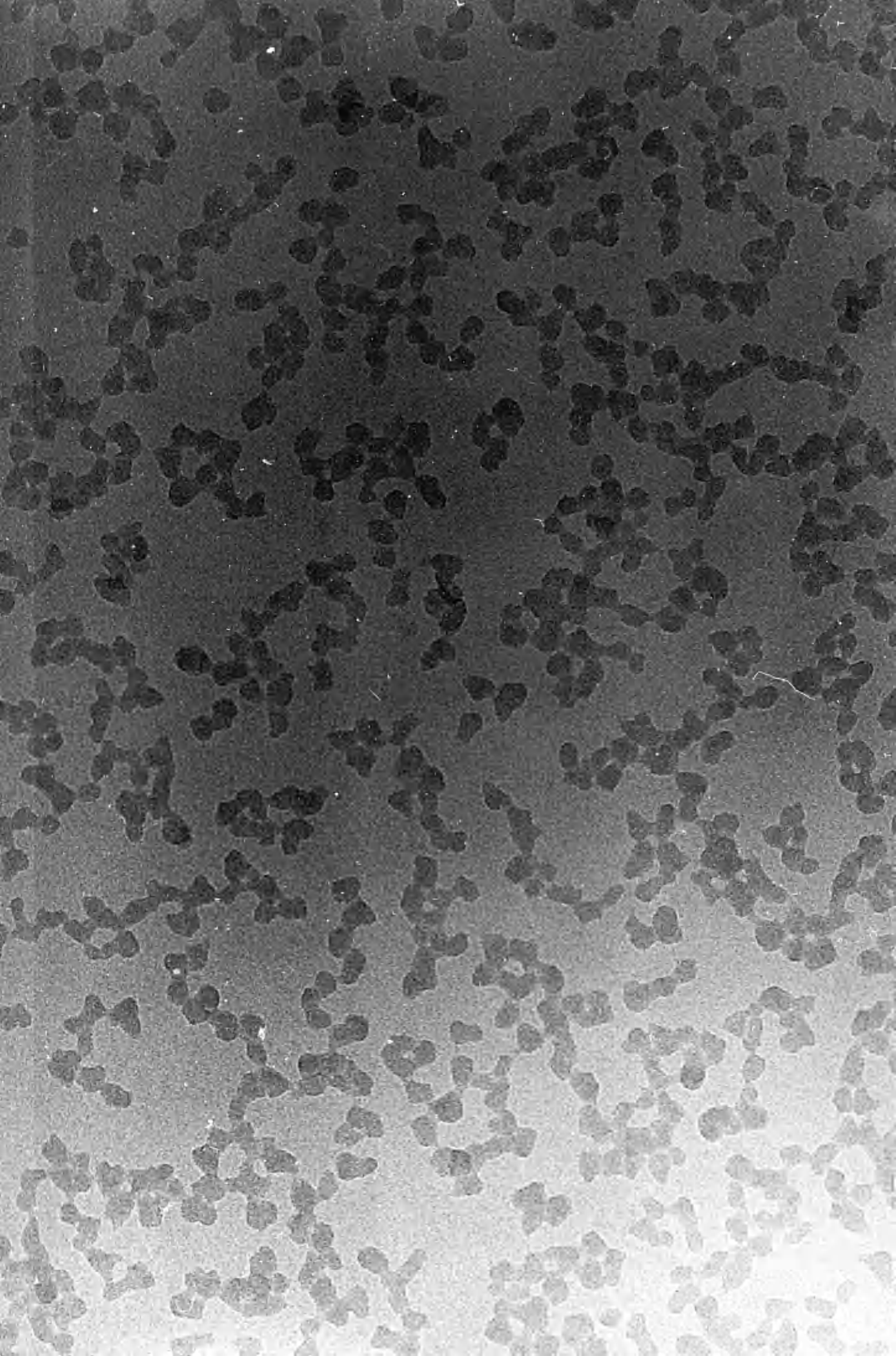

Composition	Mean Diameter (nm)	Standard Deviation (nm)
B8	172	21
B9	139	6
B10	392	69
B13	177/288	16/14
B14	388	11
B15	370	16
B18	167	8
B19	161	7
B20	231	8
B21	279	9
B23	65	13
B24	112	17
B25	132/214	12/13
B26	253	36
B28	53	10
B29	93	24
B30	217	8
B31	282	15

Table 5.6: Size distribution results for reactions producing particulate products.

	Ammonia Concentration				
TEOS	0.034M	0.17M	0.34M	1.0M	1.7M
1M	I	RS 172	RS 139	RS 392	F
0.5M	I	S 177/288	S 388	S 370	F/RS
0.25	I	S 167	S 161	S 231	S 276

where F-fused material, RS-roughly spherical, S-spherical, I-irregular. The figures given are the mean diameters in nanometres.

Table 5.7: Reaction composition and product morphology for reactions with 10M water concentration.

	Ammonia Concentration				
TEOS	0.034M	0.17M	0.34M	1.0M	1.7M
0.5M	I	RS 65	RS 112	RS132/214	RS 253
0.25	I	RS 53	S 93	S 217	S 282

Symbols and figures have the same meaning as in table 5.7

Table 5.8: Reaction composition and product morphology for reactions with 5M water concentration.

Nogami and Moriya (1980) and LaCourse et al (1983). These observations are consistent with the production of small particles which, due to low ammonia concentration and the resultant low surface charge, aggregate to form strands which link to form the gel. Iler (1979) proposed this mechanism for the production of gels at near neutral conditions in the aqueous system.

Having established that there were a number of types of product morphology the occurrence of each morphology, and the size of the particulate morphologies, in relation to the reaction conditions employed to produce them was determined. The results of reactions which produced particles are listed in table 5.6 and the overall results are shown in tables 5.7 and 5.8 which are related to tables 5.3 and 5.4 and show the product type for each reaction composition. The abbreviations used are as explained in table 5.7. Those positions which include two figures indicate a bimodal distribution with the two figures being the mean diameters of the two separate sets of figures making up each peak.

These tables show that there are a number of trends in the appearance of the different product morphologies. The first of these is that the irregular material appears in reactions which have low ammonia concentrations, with the water and TEOS concentrations not appearing to have a noticeable affect on the appearance of this morphology.

The second notable feature is that the fused material only appears in reactions product with high TEOS, water and ammonia concentrations. Between these two extreme situations noted above the produce appears as suspensions of particles with

spherical or near spherical shape. Within this group of products there appear to be a number of trends. These trends are;

1. That increasing the ammonia concentration causes an increase in the diameter of the product particle.

2. Variations of TEOS concentration do not appear to have a set affect on the size of the particles.

3. That increasing the water concentration increases the diameter of the product particles.

These patterns correspond to those observed by Stöber et al (1968) who is generally credited with being first to produce spherical silica particles by the hydrolysis of silicon alkoxides. However this study also indicated that in increasing TEOS, water and ammonia concentration individually, the particle size first increases, reaches a maxima and then begins to decrease. Recent work elsewhere (Optiz, 1987; Bogush et al, 1988(a)) also shows this type of pattern.

It is worthy of note that the concentration of silica suspensions attained for spherical particles in the reactions with the higher TEOS concentration is significantly higher than those previously reported. The 60g/l silica obtained compares to 30g/l prepared by Bogush et al (1988(a)) and the 17g/l prepared by Stöber et al (1968).

Does this information give any indication of the processes which lead to the formation of these particles? In a number of papers (Jean and Ring, 1986(a), 1986(b); Messing et al, 1986(b); Optiz, 1987; Milne, 1986; Harris and Byres, 1988; Brinker, 1988; Segal, 1989(a), 1989(b)) dealing with the formation of spheres from these processes it has been assumed that the nucleation and growth model proposed by LaMer and Dinegar (1950) for the growth of sulphur sols was applicable. If this were the case then such a model should be able to explain the variations in size of the product particles.

In such a system the final size of the particles is determined by the initial number of nuclei produced in the nucleation stage. The numbers of nuclei produced is set at the early stages of the reaction during the nucleation period and it has been stated that the rate of nucleation is determined by the difference in the rate of reaction producing the material and the rate of the reaction removing the material from the solution (LaMer and Dinegar, 1950; Jean and Ring, 1986(a)). In this system these processes are the hydrolysis and condensation reactions. This would suggest that the size of the particles would be determined by the relative rates of the hydrolysis and condensation reactions.

Any attempt to understand the affect of these two reactions on the product morphology is complicated by the fact that the two reactions are linked. Factors which affect one reaction also have an affect on the other. For example the hydrolysis, as previously described, is base-catalysed and increasing the base concentration would increase the rate of

hydrolysis. However the condensation reaction is dependent on the content of deprotonated silanol groups and thus on the base concentration. Similarly an increase in water concentration would increase the rate of hydrolysis but, as a product of one of the condensation reactions, would hinder the condensation reaction. A higher water content in the reaction medium would increase the polarity of the solution and allow the existence of more charged species. This indicates that a direct study of the effects would be difficult if not impossible but it is possible to infer probable effects based on sound chemical and kinetic principles.

The first trend which was noted was the increase in size with increasing ammonia concentration. If the above discussion is correct the change must be determined in the nucleation stage. For such a pattern to occur increasing the ammonia concentration must lower the number of nuclei produced. As stated previously increasing the ammonia concentration will increase the rate of both hydrolysis and condensation reactions. If the effect is more marked on the condensation reaction the rate of production of nuclei would be reduced and a lower number of nuclei produced. This would lead to the production of larger particles as the silica produced would have to be located on a fewer number of particles. However at a certain point the rate of condensation would not be increased further because of the limiting factor of diffusion to the surface. An alteration to the system which would be expected to cause an increase in the rate of condensation can not increase the rate of removal of silica above the rate at which it is arriving at the particle surface. A second possible

limiting factor would be when the surface is saturated with deprotonated silanol groups. When an increase in base concentration can no longer increase the number of deprotonated silanols it could have little affect on the rate of condensation. If this occurs then further increases in ammonia concentration would have a larger affect on the hydrolysis reaction than on the condensation reaction. This would lead to a decrease in the size of the particles. The initial increase in size was observed in the reactions prepared within this study and the maxima and subsequent decrease in size observed elsewhere (Stöber et al, 1968; Bogush et al, 1988(a)).

The second observation made was that the TEOS concentration did not appear to have a set effect on the product particle size. In table 5.6 it can be seen that in several cases the increase in TEOS caused an increase in size but a subsequent increase caused a decrease in size. This pattern corresponds to the results of Stöber et al (1968) and Bogush et al (1988(a)). At first examination these results would not appear to agree with the above model. An increase in TEOS concentration would increase the rate of hydrolysis but have no significant affect on the condensation reaction. This would lead to the production of a larger number of nuclei which would be expected to lead to a smaller size of particle. However although there would be a larger number of nuclei there would also be a larger mass of silica produced which must be accommodated on these particles. These two factors would tend to offset each other and would explain why no set or large change due to alteration of TEOS concentration was observed. Such an explanation is supported by

observations in the titania system (Jean and Ring, 1986(b)) that increasing the alkoxide concentration increases the number of particles. Similarly, in a study of nucleation, Calvert (1986) showed that increasing the rate of addition of material also increased the number of nuclei formed. However the reason for this occurrence of the maxima is not clear.

The last trend which was noted was that increasing the water concentration increased the size of the product particles. As has been described above the increase in water concentration could have a number of effects on the processes occurring. It could increase the rate of hydrolysis, decrease the rate of water condensation or increase the rate of condensation by increasing the polarity of the solution allowing more charged groups to exist. The presence of such high concentrations of water may also increase the content of silanol groups thus tending to increase the rate of condensation.

In the studies carried out the observed trend was that increasing the water concentration caused an increase in particle size. The water concentrations employed, 5M and 10M, were high. In the studies already mentioned the pattern was again that increasing the water concentration caused an increase in size up to a maxima and then a decrease. This could be accommodated in the model if the effects noted above which increase the condensation rate are more marked than the others. If at some point the increase in the rate of hydrolysis becomes more prominent, then a maxima would occur and then a decrease in size. The limiting factor in the increase in condensation could be due

to the saturation in the surface or the limit of diffusion to the nuclei.

The above discussion indicates that although no definite proof exists the pattern and trends observed within the particulate material can be argued to correspond to the nucleation and growth model of LaMer assuming that certain of the processes occurring respond in a particular fashion. However this model predicts that high water and ammonia concentrations would lead to the production of small particles, not the fused morphology observed.

5.5.4 THIN SECTIONS

To obtain information concerning the formation of the spherical particles described above, examination of the internal structure of these particles would be valuable. Therefore thin sections of spherical particles, produced as described above, were prepared as described in the experimental chapter.

Examination of these samples in the TEM showed material of the type shown in plate 5.5. This indicates that there is no internal structure observable. This could mean that there is no internal structure, the internal structure is of a scale too small to be observed or that the thickness of the thin sections prevents or obscures observation of the structure.

Plate 5.5: Area of spherical particles which had been settled and thin sectioned.

Magnification = 910×10^3

1cm = $10 \cdot 99$nm

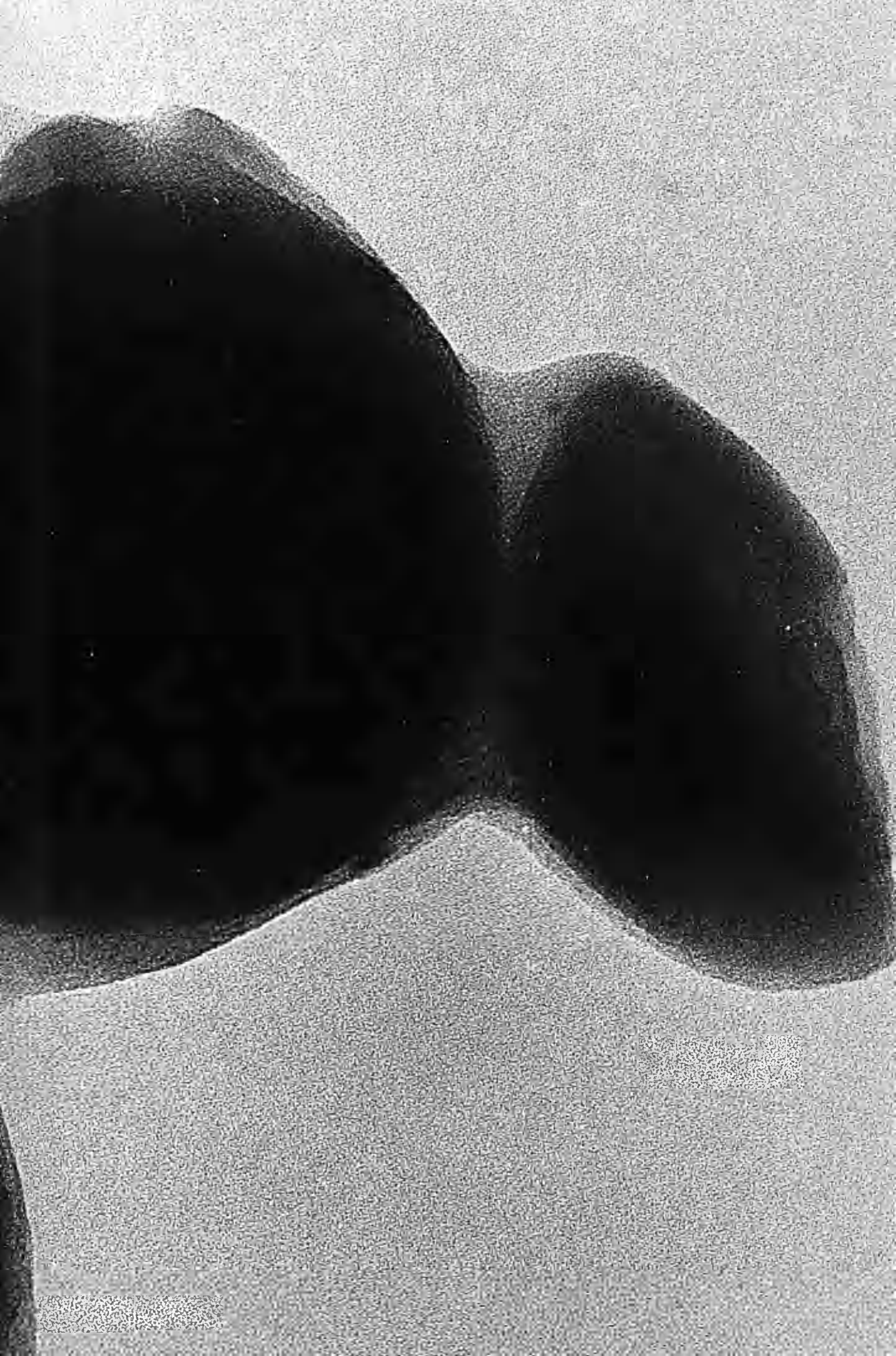

5.6 SCANNING ELECTRON MICROSCOPY

The products of the reactions which formed spherical particles were often hard tile like solids which frequently had a coloured sheen on the surface. The structures of the product which gave rise to these features are of interest, especially considering the packing structures of these particles is one of the main advantages of monodisperse particles.

To observe these structures, samples of the products of reactions which produced spherical particles which had a coloured sheen were examined in the scanning electron microscope. The types of material observed are illustrated in plate 5.6.

The structure observed consists of small spherical particles surrounded by six similar particles in a hexagonal packing arrangement. This arrangement sits on a similar arrangement on the layer below. This structure is analogous to cubic packing in the atomic state but with each subsequent layer being offset by half of the particle diameter. There also appeared to be areas of disorder but these may be caused by the grinding used during the preparation of the sample.

The structures shown in plate 5.6 and the coloured sheen observed in the samples are not a new observation. These features have previously been observed in natural opal (Cole and Monroe, 1967; Jones et al, 1964; Sanders, 1964) and in opal synthetically produced from spherical silica particles (Belova and Fedorovich, 1985). Opal is a mineral consisting of hydrated silica which has been shown to consist of spherical particles of silica which have

Plate 5.6: SEM image of settled spherical particles

Magnification = $41{\cdot}6 \times 10^3$

1cm = $0{\cdot}240\,\mu m$

been proved to be amorphous in the case of precious opal or crystalline, with the α- cristobalite structure, in the case of common opal (Jones et al, 1964). These have packing structures like those shown in plate 5.6 which have been referred to as face-centred cubic (Sanders, 1964) and cubic close-packing (Cole and Monroe, 1967). Belova and Fedorovich (1985) have also noted the presence of areas of tetragonal and hexagonal packing in the same regions of opal. Kose et al (1973) also noted the coexistence of hexagonal and square packing in settled latex spheres. These observations were made from TEM work which are therefore projections. The SEM work illustrated in plate 5.6 indicates that both observations can be seen together and may therefore be the offset cubic close-packing. However it is possible that the material observed is in fact hexagonal or face-centred cubic with the offset being caused by the grinding employed during the sample preparation.

Similar ordered packing structures have also been observed in other cases of spherical particles of silica (Sacks and Tseng, 1984(a); Milne, 1986; Optiz, 1987), titania (Chapell et al, 1986), Alumina (Segal, 1989(a)) and even in polymer/latex spheres (Kose et al, 1973; Kose and Hachisu, 1976; Hachisu et al, 1976; Skjeltorp et al, 1986). The mineral also has a coloured opalescent sheen from the surface because the particles diffract light in a similar manner to the diffraction of x-rays by atomic structures (Sanders, 1964, 1968; Krieger and O'Neill, 1968).

The reason for the formation of such structures in the reactions in this study is based on the charge on the particle. The electrostatic charge on the particles causes a repulsion

between particles. Therefore once a few particles have joined together certain approaches to the group will suffer less repulsion and thus be more favourable (Rees, 1951; Thomas and McCorkle, 1971). This tends to produce linear or possibly planar arrays or rafts of particles (Iler, 1979). It is also the case that the repulsion may prevent particles aggregating as they settle and allow the particles to move within the settled solid to find the optimum position. This process is the explanation favoured by Iler (1965) where it is based on the fact that the aggregation, which is driven by the desire to lower the surface liquid interface, is hindered by electrostatic charge. The repulsion would only be overcome if the particle attached in a position with the maximum number of contact points to other particles. Such an explanation is supported by the fact that these structures are some of the most efficient ways of packing spheres. Hence their occurrence in atomic packing.

5.7 ETHYLAMINE-CATALYSED REACTIONS

To determine the effect of alteration of the base catalysing the reaction, a series of reactions were prepared using ethylamine as the base. A list of the compositions of these reactions is given in table 5.9 and their relative positions within the reaction plan is shown in table 5.10.

Although not as comprehensive as the matrix employed in the study of reactions using ammonia as a base, these compositions allow the examination of the product of reactions with only one reagent altered and comparison with the corresponding reaction

Composition	TEOS	Water	Ethylamine	Ethanol
B32	0.497	10.253	0.0337	12.844
B33	0.497	9.990	0.168	12.044
B34	0.497	10.436	0.336	11.684
B35	0.497	10.768	1.684	10.124
B36	0.2485	10.147	0.0337	13.511
B37	0.2485	10.126	0.168	13.333
B38	0.2485	10.126	0.337	13.333
B39	0.2385	10.085	1.683	11.428

Table 5.9: Molar concentrations of reagents in reaction compositions B32 to B39.

	Ethylamine Concentration			
TEOS	0.034M	0.17M	0.34M	1.7M
0.5M	B32	B33	B34	B35
0.25M	B36	B37	B38	B39

Table 5.10: Relative position in reaction plan of compositions B32 to B39 with 10M water concentration.

Composition	Mean Diameter (nm)	Standard Deviation (nm)
B32	94	19
B36	120	30
B37	311	30

Table 5.11: Size determination results for reaction producing particulate products.

	Ethylamine Concentration			
TEOS	0.034M	0.17M	0.34M	1.7M
0.5M	RS 94	F/S	F	F
0.25M	RS 120	S 311	F	F

Symbols as in table 5.7

Table 5.12: Reaction composition and product morphology for reactions B32 to B39.

employing ammonia as the base.

The types of material observed in these reactions were the same as those observed in the previous reactions using ammonia, with the exception of the irregular material which was not observed. The results of reactions producing particulate products are listed in table 5.11 and the overall results are shown in table 5.12.

This table shows strong similarities to tables 5.7 and 5.8. The main difference appears to be that the transitions between the different types of morphology are at a lower base concentration than the corresponding transition in the ammonia-catalysed system. This would appear to be consistent with the premise that the effect of the catalyst is its basic nature, because ethylamine is a stronger base than ammonia. The actual values of the strengths, the pk_B values, would suggest that the alteration in the transitions should be more marked. However these figures are based on an aqueous system and the system under examination is a mixed ethanol/water system which may alter the figures.

5.8 TIME SAMPLING

5.8.1 FUSED PRODUCT MORPHOLOGY

It has already been noted that the fused material appears to have formed by the fusion of smaller roughly spherical particles. However the porous or particulate appearance in some areas of this material does not support the above explanation of

its formation. Also the fused material does not fit into the nucleation and growth model which would indicate that at high base concentration the product should consist of very small particles.

To obtain more information on the formation of the product with fused morphology a reaction was carried out, to the B38 composition, and samples removed for TEM examination. Samples were removed at times from 2½ to 60 minutes after the addition of TEOS. The most striking feature of the observations made on these samples was that no large spherical or roughly spherical particles were observed. This indicates that the material can not be formed by the fusion of such particles.

The types of morphology observed are illustrated in plate 5.7. These are small particles of diameters in the region 4-10nm, and large aggregates which include large numbers of these particles and material which appear strand like. As the time at which the sample was removed from the reaction increased these materials became less frequently observed. At the same time the fused material became more common. These results appear to indicate the process of formation of the fused material is the formation of a large number of small particles or nuclei which then aggregate to form strand like material and then onto the large particles of the fused material.

This formation process would agree with the nucleation and growth model described above. The model predicts the formation of small particles at the conditions which give rise to the fused morphology. This appears to have occurred, but the small particles then rapidly aggregate to form the fused material. The aggregation of these particles is an indication that the

Plate 5.7: Material present at early times in reactions producing products with the fused morphology

Magnification = 1275×10^3

1cm = 7·84nm

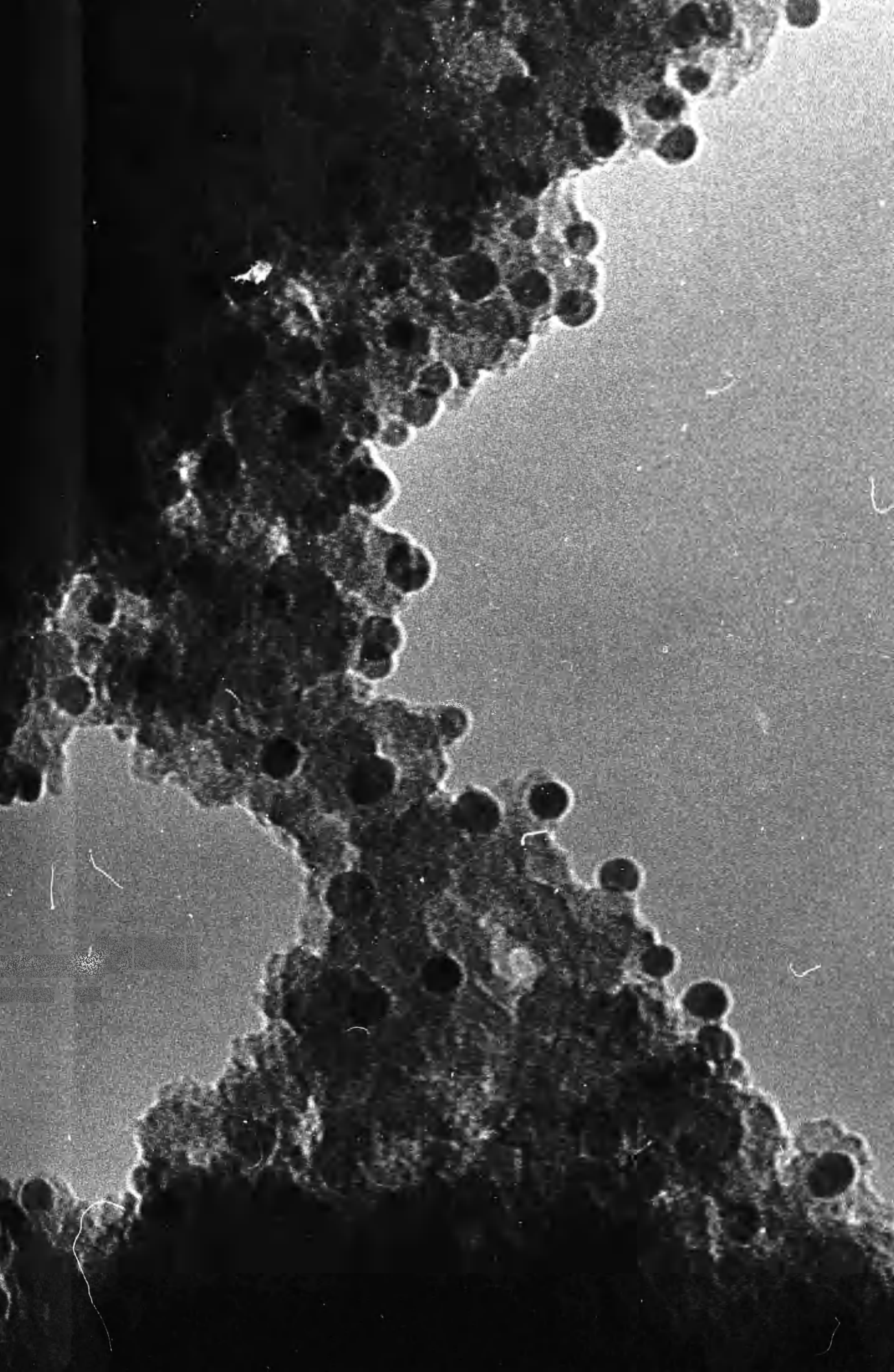

suspension is unstable and a known method of destabilising colloidal dispersions is to increase the ionic strength of the medium (Lyklema, 1982; Everett, 1988). Therefore the increase in charged species in the solution due to the increased ammonia concentration may cause the destabilisation of the particle suspension. This in turn causes the formation of the morphology observed.

5.8.2 SPHERICAL PRODUCT MORPHOLOGY

To obtain more information on the formation of spherical particles a number of reactions were prepared and samples removed during the reaction for TEM examination. The reactions were prepared to correspond to the B13, B14, B19 and B24 compositions thus allowing comparisons between reactions where only the ammonia, TEOS or water concentration had been altered.

In all of these reactions the types of morphology and patterns observed were similar. The samples taken at short times after the addition of TEOS, typically sixty seconds, consisted of small particles of irregular shape forming strands and networks quite similar to those described in previous sections as irregular material. At later sample times the product consisted of roughly spherical particles which have aggregated and necked together, thus making size determination difficult. As the time-lag between the addition of TEOS and the sample being taken increased, particles increased in size and did not tend to aggregate to the same extent. In addition to the above features the samples also included small particles similar to the particles observed in the

irregular material found in the reactions described above. This material also became less frequently observed as the sample time increased, until at 15-30 minutes the observations were rare. The small particles are almost certainly a feature created by the sample preparation technique. At early reaction times the reaction solution will have a high concentration of silica polymer species or alkoxide. When the sample, which has been diluted, is allowed to evaporate on the grid the silica in solution can not evaporate and the alkoxide has a high boiling point so both come out of the solution as a solid. Because of the dilution and the fact the ammonia will rapidly evaporate the precipitation occurs at low basic pH which may in part cause the small particle nature of the precipitate. The small size and low pH will lead the particles to flocculate. As the reaction proceeds and the concentration of silica based species in the solution decreases the appearance of the particles becomes rarer.

The particle sizes measured, where possible, in each sample are listed in tables 5.13 to 5.16 and plotted in fig. 5.5. It must be noted that the spread of particles (the difference between the largest and smallest size) may only be taken as a rough estimate of the true spread of the sizes because of the relatively small number of particles observed. In all cases there appears to be two distinct growth regions. There are a rapid growth region followed by a second region in which the growth is slower. The results have been plotted in a number of fashions which plot diameter against time with one or both as the log and all have shown two regions. These growth patterns are very similar to those shown by LaMer and Dinegar (1950). In a plot of

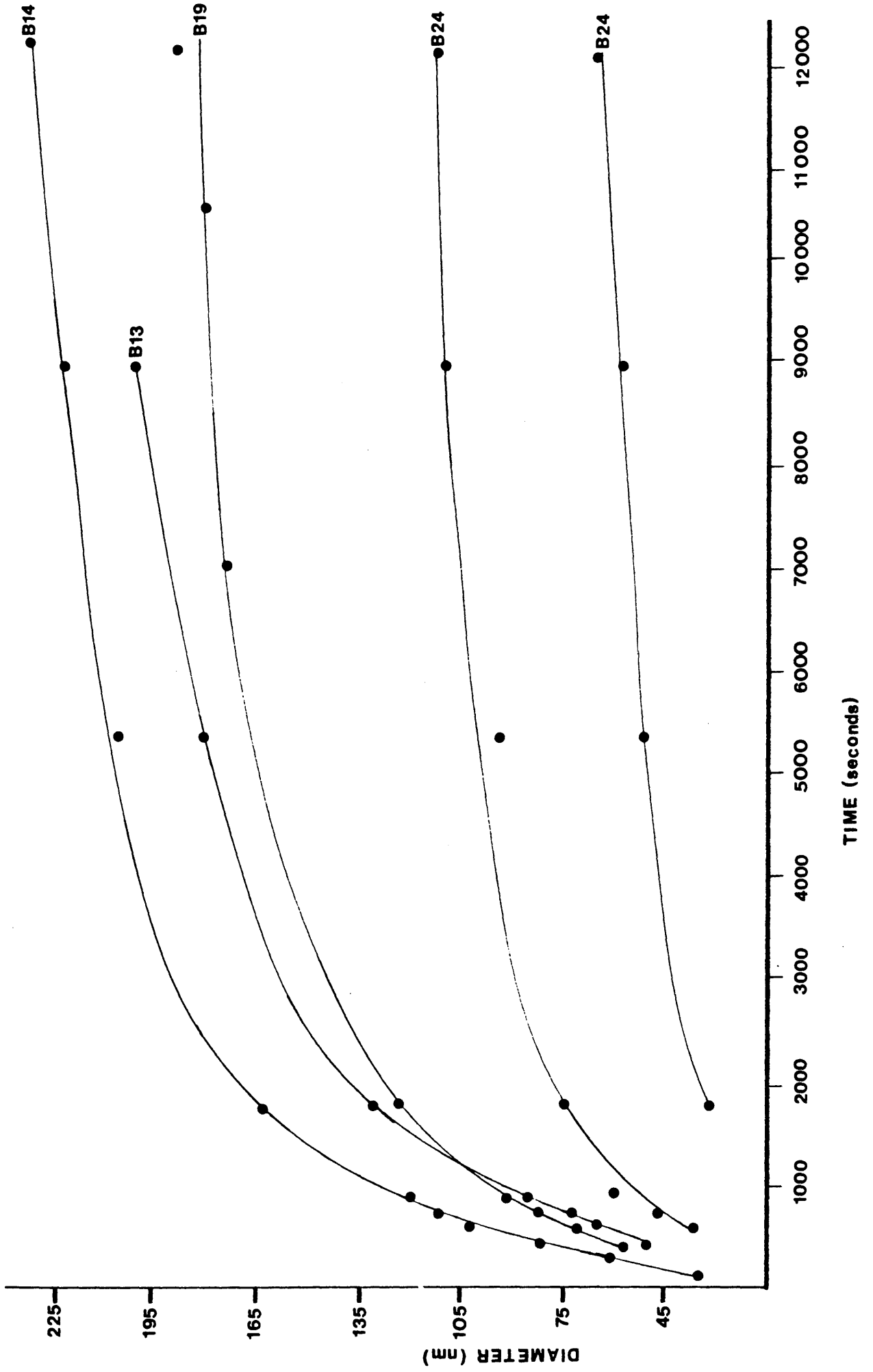

Fig. 5.5: Plot of particle diameter against time for particles in sampled reactions.

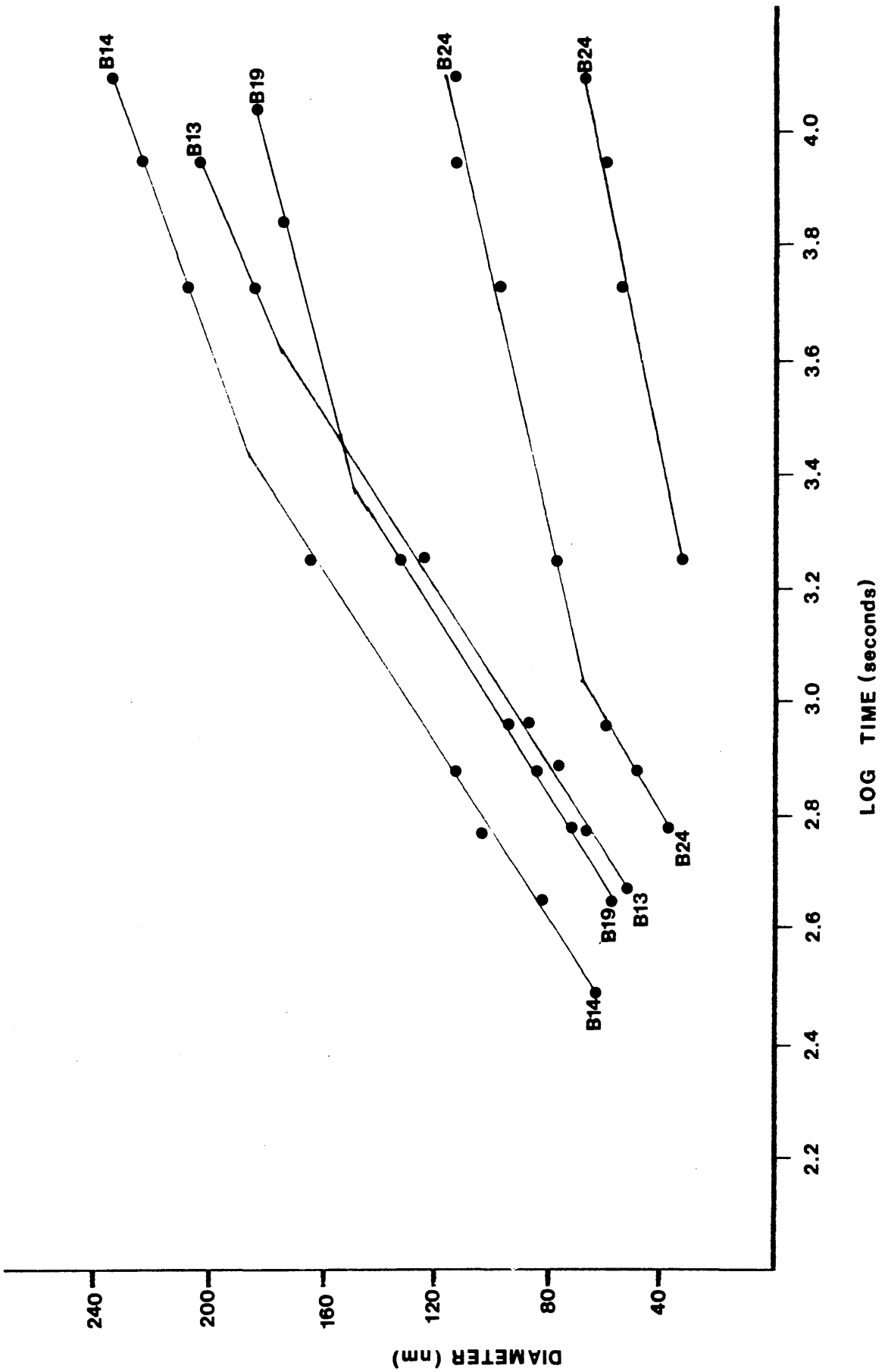

Fig. 5.6: Plot of particle diameter against log time for particles in sampled reactions.

Time(s)	Diameter (nm)	S_n(nm)	Spread (nm)
450	49	8	56
600	66	7	36
750	73	8	45
900	85	6	35
1800	131	9	58
5400	180	8	63
9000	200/100	7/9	37/42

Table 5.13: Mean particle diameter, standard deviation and spread of diameters for time sampled reactions of the B13 compositions.

Time(s)	Diameter (nm)	S_n(nm)	Spread (nm)
300	61	4	25
450	80	5	27
600	102	7	39
750	110	7	39
900	119	6	25
1800	162	7	36
5400	205	5	35
9000	221	8	50
12600	231	6	40

Table 5.14: Mean particle diameter, standard deviation and spread of diameters for time sampled reactions of the B14 compositions.

Time(s)	Diameter (nm)	S_n(nm)	Spread (nm)
450	56	5	27
600	70	5	34
750	82	6	49
900	91	6	25
1800	122	6	30
7020	170	7	32
10560	180	7	50
12600	189	8	43

Table 5.15: Mean particle diameter, standard deviation and spread of diameters for time sampled reactions of the B19 compositions.

Time(s)	Diameter (nm)	S_n(nm)	Spread (nm)
600	37	4	28
750	46	4	24
900	59	5	39
1800	74/32	6/4	34/20
5400	95/52	6/6	26/27
9000	110/57	5/5	17/24
12600	112/66	6/6	21/34

Table 5.14: Mean particle diameter, standard deviation and spread of diameters for time sampled reactions of the B24 compositions.

diameter against log time, as shown in fig. 5.6, the two regions appear to be linear with the gradients of the different reactions in the two regions being very similar. A similar two part growth has been observed in the titania system by Jean and Ring (1986(a)) but here there were more marked, although still small, differences in the gradient in the first region. This may be linked to the more rapid hydrolysis of titanium alkoxides. In the case of B24 where a second set of particles appears during the reaction the growth rate of both sizes appears to be the same. It can also be noted in this plot that the effect of halving the TEOS and halving the ammonia concentration appear to be very similar. In both cases there appears to be a delay in the appearance of the particles and this delay is very similar in both cases. A similar but more marked effect is obtained by halving the water concentration.

An explanation for the above pattern which is in accordance with the nucleation and growth model discussed above is that nucleation occurs then the growth occurs limited by two separate factors. The first factor limiting the rate of growth would be the rate of condensation onto the surface of the nuclei. At a later stage there would be a depletion of the silica in the regions surrounding the nuclei. At this point the growth will be limited by the rate of formation of the silica or by the rate of arrival of the silica at the surface. The hydrolysis of these compounds is believed to be rapid (Bogush and Zukoski, 1987; Balfe and Martinez, 1986; Aelion et al, 1950) so that the most probable limit would be the rate of diffusion to the surface. This is supported by the fact that in B24 the two sizes of particles grow

at the same rate.

The delays in the appearance of the particles also fit in with the model. By lowering the concentration of reagents the time necessary for the hydrolysis to produce enough of the product to reach the critical supersaturation would be delayed. Thus the appearance of the particles was delayed. This behaviour is similar to the induction periods before appearance of solid which have been reported (Jean and Ring, 1986(a), 1986(b); Harris and Byres, 1988). The reason for the longer delay in the reaction with lower water concentration is not clear but it is possible that the effect on the reaction is amplified by an affect on the reaction medium.

It must also be noted that the results from the above experiments in which time sampling was carried out do not correspond to the reactions where no sampling occurred. This difference is apparent in the different products. For example the composition B14 normally formed a product with diameter of 388nm but when sampled the final product had a diameter of 254nm. Similarly the composition B13 typically produced a bimodal distribution with peaks at 178nm and 288nm but when sampled the peaks occurred at 148nm and 255nm. In both cases the change is a decrease in size and this could be due to a decrease in ammonia concentration, which would have such an effect. This loss of ammonia could occur during the sampling process by loss of ammonia vapour from the reaction flask.

5.9 MODIFIED REACTIONS

5.9.1 LITHIUM CHLORIDE ADDITION

The discussion on the time sampled reactions which produced material of the fused morphology suggested that the high ionic strength of the solution led to the aggregation of the nuclei produced by the reaction. To test if this was a valid suggestion, reactions were prepared under conditions which produce spherical particles and these were compared with corresponding reactions with a small amount of lithium chloride added.

The composition chosen was such that the product was spherical particles and the conditions were far from those which gave rise to the fused product morphology. The concentrations used were

5.736×10^{-2}M	TEOS
5.48M	water
14.38M	ethanol
0.391M	ammonia
0.077M	lithium chloride

The concentration of lithium chloride used was quite low so that the alteration to the reaction medium would be small, so the results could be similar to the changes caused by the increase in the ammonia concentration. Because of the need to dissolve the lithium chloride the reaction mixture was stirred by a magnetic

stirrer. So that a comparison could be made the reactions carried out without the addition of lithium chloride were also stirred.

In two reactions carried out without the addition of lithium chloride the products were spherical particles with the mean diameter 184nm (S_n=11.26nm) and 163nm (S_n=14.70nm). When the reactions were carried out in the presence of the low concentration of lithium chloride listed above the product morphology altered to that of the fused type.

It must be noted that work by Pope and MacKenzie (1986(b)) indicates the chloride ion can act as a catalyst for the reaction. However this work was based on the acid-catalysed system and it is not clear if the anion would have a similar affect in a base-catalysed system. It also appears unlikely that the amount of chloride present would have sufficient effect to cause a change in morphology by acting as a catalyst.

Therefore these results would appear to support the premise that the fused material is formed by the aggregation of small particles caused by the lowering of colloidal stability by the depletion of the electrostatic double layer by the increased ionic strength of the reaction medium.

5.9.2 POLYMER ADDITION

As discussed in the section dealing with colloidal dispersions, the stability of such systems arises from a number of factors, most importantly the electrostatic repulsion of the particles. However it was also noted that stability can be caused by other factors including the attachment of polymers to the

surface of the particles. Such steric stabilisation within the system may have an affect on the morphology.

The situation is completed by the fact that addition of polymeric species to silica suspensions may cause flocculation rather than stabilisation (Iler, 1979). However it has been shown that polymers with very large molecular masses tend to prevent aggregation (Dixon et al, 1967). A further complication is the number of polymer types which could be added to the reaction which will attach to the surface. The main types are cationic polymers which are attracted to the negative charges on the surface and nonionic polymers which hydrogen bond to the non-ionised silanol groups on the surface (Iler, 1979).

The addition of charged species to the reaction may have a direct effect on the morphology due to the charge. Therefore a nonionic polymer would be the most suitable type. Such a polymer is polyvinyl alcohol which has been shown to attach to the surface of silica (Iler, 1975). However as the pH, and thus the surface silanol ionisation, increases the hydrogen bonding becomes less successful and the polyvinyl alcohol is partly desorbed by pH 8 (Fleer and Lyklema; 1974). The pH employed in the reactions is in this region so that there should be some polyvinyl alcohol attached to the surface.

To study the effect of the presence of such a polymer on the generation of the product a number of reactions were prepared. The compositions were chosen to match those previously examined which produced spherical particles and fused material as the product. The compositions were prepared to correspond to B14 and B26 reactions with the alteration that in place of adding water an

aqueous solution of polyvinyl alcohol, of high molecular weight, was used. Under normal conditions, without added polymer, these reactions produce spherical particles, mean diameter 388nm, and fused material respectively.

The first difference observed in these reactions was the appearance of a white solid in the reaction corresponding to B14. A similar occurrence may have happened in that matching B26 but in this case the rapid precipitation of silica would have obscured its observation. This was most probably the precipitation of polyvinyl alcohol caused either by the poor solvent effect (Sugimoto, 1987) or the loss of water (in which the polyvinyl alcohol was dissolved) as the hydrolysis reaction proceeds. When the product was recovered both reactions included a solid rubbery material which is believed to be the polyvinyl alcohol which precipitated out of the reaction.

TEM examination of the products indicates that the addition of polyvinyl alcohol did not have a large effect on the morphology produced in the reactions. That corresponding to B26 produced fused material similar to that of B26. The reaction which corresponds to B14 produced spherical particles similar to that in B14. However a small number of small roughly spherical particles which had aggregated into packs were observed.

These results would appear to indicate the presence of a polymer has little affect on the product morphology but the situation is not clear. The amount of polyvinyl alcohol attached to the surface may be low and that present may surround the surface (Iler, 1979) rather than extend out into the medium which may lead to a low steric repulsion. Therefore the lack of

observed effect may be due to a poor steric repulsion rather than the fact that steric repulsion does not have an affect.

5.10 TETRABUTYLORTHOSILICATE REACTIONS

The above discussion indicates the complexity and interaction of the reactions occurring in this system. It has also been stated that separating the hydrolysis and condensation reactions, so that the effect of varying only one could be observed, was not possible. However there is a method of altering the rate of reactions which is common in organic chemistry - alteration of substituent groups. The larger and bulkier the substituent the slower the rate of attack on the central atom. This effect arises because of the increased hindrance to the approach of the nucleophile and the steric crowding which reduces the stability of the penta-coordinate transition state (Jones, 1979). It is also the case that t-butyl groups will lower the polarity of the Si-O bonds by the inductive effect (Jones, 1979; Bradley et al, 1978). This would probably lower the rate of nucleophile attack. Such a view is supported by the work of Aelion et al (1950) which showed that increasing ligand size deceased the rate of hydrolysis. Thus changing the silicate used to one with bulkier alkoxy groups would be expected to slow the rate of hydrolysis, hopefully without having a large effect on the condensation reaction. This is probably true because in base-catalysed systems the hydrolysis rate becomes faster with each alkoxy group which has been hydrolysed. Thus the condensation tends to take place between completely hydrolysed species (Keefer,

1984).

An ideal experiment would be the comparison of reactions using tetra-n-butylorthosilicate and tetra-t-butylorthosilicate, where n and t indicate the primary (normal) and tertiary isomers of the butoxy group, carried out in butanol. However tetra-t-butylorthosilicate is extremely difficult to produce and then only in small quantities (Hyde and Curry, 1955; Narain and Mehrotra, 1967). The tetra-s-butylorthosilicate, where s indicates the secondary isomer of the butoxy group, could be substituted for the tetra-t-butylorthosilicate but the difference may not be sufficient to give a clear result. Such substitution is complicated by the fact that tetra-s-butylorthosilicate is not commercially available and time was not available for its synthesis.

A comparison between the reactions using TEOS and tetrabutylorthosilicate (TBOS) would also be valid but the problem arises that a silicon alkoxide will exchange alkoxy groups with the solvent alcohol (Bradley et al, 1978). This greatly complicates the system by increasing the number of alkoxide species present. The use of ethanol in the reactions using TEOS avoided this problem but to overcome the problem with TBOS would require the use of butanol. In fact it would require the use of butanol of the same isomer as the alkoxy substituent, this added complication is necessary because it has been shown (Harris and Byres, 1988) that altering the solvent of a reaction from n-butanol to t-butanol has a large affect on the resultant product morphology. Changing the solvent of the reaction would so vastly alter the conditions that the comparison would not be valid. In

fact altering the solvent within the same reaction system has been shown to have a great effect on the resultant product (Chatterjee and Ganguli, 1986; Harris and Byres, 1988; Harris et al, 1988; Artaki et al, 1986). Therefore it was necessary to carry out the hydrolysis of both compounds in the same solvent. The risk of substituent exchange affecting the results would be far smaller when the TBOS was dissolved in ethanol because of the steric hindrance to approach. Therefore the reactions were all carried out in ethanol.

A series of reactions were prepared using TBOS with compositions that correspond to reactions previously prepared with TEOS. A list of the reagent concentrations used in these reactions is given in table 5.17 and the relative positions in the reaction plan shown in table 5.18. This shows that the reactions allow comparison of compositions in which only one reagent concentration has been altered.

Although not as comprehensive as the matrix used in the TEOS reactions the results for the particulate products are listed in table 5.19 and the relative positions are shown in table 5.20 and these allow the observation of a number of trends. These were

1. Increasing the ammonia concentration causes an increase in the size of the particles.

2. Altering the TBOS concentration does not have a set effect.

3. Increasing the water concentration decreases the size of the particles.

Composition	TBOS	Water	Ammonia	Ethanol
B40	0.4985	10.1	0.167	11.33
B41	0.4985	10.54	0.338	10.56
B42	0.4985	5.1	0.34	12.61
B43	0.4985	5.34	1.69	11.98
B44	0.249	10.12	1.69	12.26
B45	0.249	5.05	0.169	13.88
B46	0.249	5.17	0.338	14.24
B47	0.249	5.53	1.69	13.51

Table 5.17: Molar concentrations of reagents in reaction compositions B40 to B47.

TEOS	Water	0.17M	0.34M	1.7M
0.5M	10M	B40	B41	----
0.5M	5M	---	B42	B43
0.25M	10M	---	---	B44
0.25M	5M	B45	B46	B47

Table 5.18: Relative positions of compositions B40 to B47 in the reaction plan

Composition	Mean Diameter (nm)	Standard Deviation (nm)
B40	132	37
B41	193	14
B42	232	30
B43	1256	169
B44	562	27
B45	89	7
B46	218	61
B47	1216	207

Table 5.19: Size determination results for particles produced from TBOS hydrolysis reactions.

		Ammonia Concentration		
TEOS	Water	0.17M	0.34M	1.7M
0.5M	10M	S 132	S 193	---
0.5M	5M	---	S 232	S 12576
0.25	10M	---	-----	S 562
0.25	5M	RS 89	S 218	S 1216

Symbols as in table 5.7

Table 5.20: Reaction composition and product morphology for reactions B40 to B47.

TEOS reaction		TBOS reaction	
Composition	Diameter	Composition	Diameter
B13	194nm	B40	132nm
B14	388nm	B41	193nm
B24	112nm	B42	232nm
B26	253nm	B43	1256nm
B21	276nm	B44	562nm
B28	53nm	B45	89nm
B29	93nm	B46	218nm
B31	282nm	B47	1216nm

Table 5.21: Comparison of product size for corresponding TEOS and TBOS reactions.

The first two of these trends are the same as those observed in the case of TEOS the last being the opposite of that observed in the TEOS reactions. This would suggest similar, or the same, processes occurring in both reaction systems.

The aim of the production of these reactions was the comparison of the product of TEOS and TBOS reactions of corresponding compositions. If the system does follow the nucleation and growth model of LaMer and the replacement of ethoxy by butoxy groups has the effect of reducing the rate of hydrolysis then the overall effect would be to increase the size of the resultant particles. To determine if this is in fact the result, the figures comparing the TBOS reactions product size with the size of product in the corresponding TEOS reaction are given in table 5.21. This shows that in except two of the reactions the product size in the TBOS reaction is larger and in some cases much larger than the corresponding TEOS product. However in two of the cases the product is smaller in the TBOS reaction.

A possible explanation for the two results in which the TEOS product was larger than the corresponding TBOS reactions was the affect of the high water content on the polarity of the reaction medium. In the case of tetra-t-butoxy compounds the reaction is likely to be of an S_N1 mechanism and with the low polarity of the reagents compared to the reaction transition state the effect of increasing the polarity of the medium would be to greatly accelerate the hydrolysis reaction (Jones, 1979). Such an affect may have been made more prominent by the decrease in the rate of condensation due to the increased presence of protic material and the increase in the polarity of the

medium (Artaki et al, 1986).

In the case of S_N2 reactions an increase in the polarity of the reaction medium will tend to decrease the rate of hydrolysis (Jones, 1979). This is not to suggest that an increase in water concentration would decrease the rate of hydrolysis. Rather that a change in water concentration has two affects on the reaction; the direct affect on the reaction as a reagent and the indirect affect by changing the polarity of the solvent. In the case of TBOS both of these affects act together so that increasing the water concentration increases the rate of hydrolysis by the direct and indirect affects. In the case of TEOS the affects do not act together. An increase in the water concentration would have the direct affect of increasing the rate of hydrolysis but by increasing the solvent polarity would act to slow the hydrolysis, thus lowering the increase in hydrolysis rate due to the water increase.

These factors when taken together would tend to minimise the difference in hydrolysis rates between TEOS and TBOS. This explanation is supported by the observation that increasing the water concentration decreases the product size and that work by Chatterjee and Ganguli (1986) shows that increasing the polarity of the solvent, where all of the other factors are likely to be unaffected, reduces the particle size. Further support is given by the fact that the differences in product size is largest where the water concentration is low and smallest (or reversed) where the concentration is high. Such an explanation would also explain the fact that under the conditions used, increasing the water concentration decreased the particle size in TBOS reactions and

increased the particle size in TEOS. The effect of the alteration of polarity is reversed in S_N1 and S_N2 reactions (Jones, 1979).

The results of this comparison, although not all larger than TEOS, tend to agree with the expected behaviour if a nucleation and growth model was an accurate interpretation of the processes occurring.

5.11 DISCUSSION

The results presented above show that base-catalysed hydrolysis produces three distinct product morphologies; small particles which aggregate to form a gel, spherical or near spherical particles which form a stable colloidal suspension and large particles of irregular shape which precipitate out of solution. As has already been illustrated the nucleation and growth model proposed by LaMer and Dinegar (1950) can explain the variations in size of the particles in suspension if a few chemically logical assumptions are made. These assumptions relate to the effect of reagent changes on the rates of the hydrolysis and condensation reactions. Based on this model an explanation can be made for the formation of all of the types of product observed.

At low base concentration the condensation reaction, which is dependent on pH due to the requirement for deprotonated silanol groups, will be slow. Therefore the hydrolysis reaction will produce silica in solution and exceed the critical supersaturation. This will lead to the formation of nuclei but because the condensation reaction has a low rate the silica

concentration will stay above the critical supersaturation for a long period, thus producing a large number of particles. These particles will, due to a low pH, have a low surface charge and thus little electrostatic repulsion and will aggregate. This aggregation leads to the formation of a gel. This is essentially the mechanism for the formation of a gel in an aqueous system proposed by Iler (1979).

As the pH increases the rate of condensation and the electrostatic charge on the nuclei will increase. This means that the concentration of silica will rapidly fall below the critical supersaturation and nuclei formation will cease. The nuclei formed will also be stable against aggregation because of the surface charge. Therefore the nucleation and growth model of LaMer would be applicable and the final size of the particles would be determined by the nucleation period and the difference in the rates of hydrolysis and condensation.

Further increases in the water and base concentration increases the dielectric constant of the reaction medium and increases the ionic strength. This means that the nuclei produced by the reaction lose their colloidal stability and rapidly aggregate. When the particles aggregate large areas of the reaction medium would have no nuclei and so more nuclei would form, thus producing more particles to aggregate. The high TEOS concentration would help produce a high silica concentration which would aid aggregation. The high ammonia concentration would also aid the formation of dense particles because at higher pH silica is more soluble (Iler, 1979) thus allowing redeposition to densify the material. This is supported by experiments carried out

increasing the ionic strength by adding an ionic salt.

This interpretation of the results is given more credence by the ability to accurately predict or explain the effect of altering the alkoxide used to TBOS. Also by the fact that the pattern of rates of reactions discussed in the above sections as necessary to give the observed changes are similar to those reported by Brinker (1988). Further support is given by the work of other groups. Work by Chatterjee and Ganguli (1986) studied the effect of altering the solvent of the reaction. Such changes alter the reaction in a number of ways but where these are likely to be small eg when altered from methanol to ethanol or from one isomer to another of the same alcohol the solvent with the higher polarity, as shown by the dielectric constant (Weast, 1972), gives rise to larger particles. This agrees with the predicted behaviour caused by the effect of solvent polarity on the rate of reactions. Increasing the polarity of the solvent would reduce the rate of hydrolysis in S_N2 reactions (Jones, 1979) thus producing larger particles, and at high solvent polarity the stability of the small particles could be lowered in a similar manner to the increase in ionic strength.

Studies of the small angle x-ray scattering (SAXS) of these materials (Keefer, 1986(a), 1986(b)) have also been explained in terms of this model. The variations of size of particles caused by temperature has also been explained in terms of the LaMer mechanism (Tan et al, 1987). Similarly, in a study of nucleation models, Calvert (1986) compared the expected appearance of particles formed by nucleation and those by aggregation and stated his belief that the nucleation model

applied to the formation of the monodisperse particles from alkoxide systems.

Although there are a number of supporters of the nucleation and growth model of LaMer, and a considerable amount of evidence, there are other proposed mechanisms. The main alternative mechanism which has been proposed is based on the formation of small particles which then aggregate to form the larger spherical particles which have been observed. This type of mechanism has been proposed by Van Helden et al (1981) to explain SAXS and ultramicroporosity observations. More recently work by Bogush and Zukoski (Bogush and Zukoski, 1987; Bogush et al, 1988(a), 1988(b)) has led them to propose a particular aggregative growth model. This is the coagulative nucleation and growth model which was first proposed by Feeney et al (1984) for emulsion plymerisation.

The basis of this model is that the reaction produces small particles which are marginally stable due to the presence of the electrostatic repulsion. These particles then coagulate, with a rate dependent on the particle size, to form larger particles. This model was proposed by Feeney et al (1984) to account for particle size distributions observed in the emulsion polymerisation of styrene.

The evidence to support such a mechanism in the formation of silica spheres by the hydrolysis of silicon alkoxides has been published by Bogush et al. This evidence is in two forms: theoretical calculations and experimental observations. The calculations (Bogush and Zukoski, 1987) are base don estimation of the silica concentration above which nucleation will occur. These

led to the conclusion that nucleation carried on for several hours, in fact to a point close to the final size of the particles. The experimental evidence (Bogush and Zukoski, 1987; Bogush et al, 1988(a)) takes the form of the observation of small particles during the time sampling of the reaction and the rough or particular nature of the final particle surfaces in some experiments.

The above experimental evidence has been observed by other workers. The rough surfaces of the particles were observed by Keefer (1986(a), 1986(b)) who suggested that this was due to the blocking of growth sites on the surface by unhydrolysed alkoxy groups. Once an alkoxide group blocks a growth site on a particle it is difficult to remove it because the inversion necessary in the S_N2 mechanism can not occur. The small particles in the sample during the time sampling experiments have been described earlier and were explained as artefacts of the sampling technique. The method of sampling used by Bogush should have minimised the production of particles by the method described earlier but would not prevent it.

A further piece of experimental evidence reported by Bogush et al (1988(b)) was that a reaction mixture filtered through a 25nm filter was clear but then began to scatter light and produced spherical particles. From this they drew the conclusion that the filtering process had removed the nuclei present in the mixture and the formation of particles in the filtered solution indicated that the initial solution contained a large number of sub 25nm particles or that nucleation in the system continued a long period into the reaction; both aspects

correspond to the aggregative nucleation model which they propose. Unfortunately the time at which the filtering occurred was not given and it is not therefore possible to assess the importance of this information. However the nucleation and growth model proposed by LaMer could also explain the observations. Once the reaction mixture was filtered and no nuclei were present the rate of removal of material by condensation would drop. Thus the silica concentration would increase until the critical supersaturation would be reached and nucleation would begin again leading to the formation of particles. Because the nature of the reaction mixture had not been greatly altered these would then grow to form spherical particles, thus giving the observations made. The ability to attain the critical supersaturation in the reaction, even with particles present onto which condensation could occur, at late times in the reaction is shown by the occurrence of bimodal distribution as illustrated in the sampled reactions.

Supporters of the aggregative nucleation model have also quoted work by Santacessaria et al (1986) which shows that titania particles can grow by the aggregation of smaller particles. However as this paper was based on the hydrothermal precipitation of titania from concentrated sulphuric acid it is not comparable to the system under study other than to show such a growth is possible. It should also be noted that particles observed by Santacessaria et al by HREM, which show an internal structure corresponding to smaller particles have not been reported in the silica system. And further, that computer simulations of HREM images of amorphous silica (Schmidt et al, 1985) indicate that

contrast variations giving a similar appearance can occur without there actually being any substituent particles. Therefore the experimental evidence is not conclusive.

The model proposed by Feeney is complex and it is not easy to predict or to compare size variations against reagent concentration alterations which cause them. It is also difficult to explain the formation of the bimodal size distributions in such a system. As detailed in the results section the first of these drawbacks do not apply to the LaMer model. Similarly the second drawback does not apply. If during the course of the reaction, but after the end of the first nucleation burst, the rate of removal of silica from solution drops to a level lower than that necessary to remove the silica produced by the hydrolysis reaction then the critical supersaturation will again be exceeded and the formation of nuclei will begin for a second period. Similarly if the rate of production of silica increased above that being removed from solution, but this is less likely. During the diffusion controlled growth of the particles both those from the first and second nucleation periods grow at the same rate, thus leading to a bimodal size distribution.

The reason for the suggested alteration in the rate of removal of silica material is not clear but it has been shown (LaCourse et al, 1983) that the water, alkoxide and ethanol concentrations and the pH change quite rapidly. This could cause alterations in the rate of reaction or in the reaction medium which might be sufficient to cause the alteration necessary to raise the silica concentration again.

Bogush et al (1988(a)) also makes the point that as the particles grow the percentage standard deviation (percentage of the mean diameter) decreases. From this they conclude the mechanism is self sharpening and that small particles grow faster than large ones. This is consistent with the coagulative nucleation and growth model proposed by Feeney et al (1984). However the work described earlier on time sampled reactions shows that although the percentage standard deviation decreases the actual standard deviation stays almost constant. It is also the case that the spread of particle sizes (the difference between the largest and smallest recorded diameters in a sample) is roughly constant. This could be envisage as arising from the LaMer model of nucleation and growth where a spread of particle sizes arises between the nuclei formed at the beginning of the nucleation burst and those formed at the end. As the particle growth subsequent to the nucleation is diffusion controlled and therefore not dependent on size the spread is maintained throughout the growth of the particles. This interpretation is supported by the time sampling of the reaction which corresponds to the B24 composition. In this case a second set of particles appear during the reaction. The growth rate of these particles is the same as that of the larger particles already present. The independence of growth rate on size is expected in the LaMer mechanism but not in that of Feeney.

Some of the other experiments described above had the aim of differentiating between the two mechanisms. The first of these was to examination of thin sections of the spherical particles in the TEM. The observation of internal particulate appearance would

have been strongly supportive of the Feeney mechanism. However the observation of little internal structure, as occurred, does not disprove the Feeney mechanism because there are a number of factors such as the deposition of silica from solution in the spaces between the particles or the lack of resolution of the technique which could have caused the lack of structure.

The second technique aimed at differentiating between the mechanisms was the inclusion of polymers into the reaction mixture. The aim being that should the polymers infer greater stability to the small particles the production of the spherical particles in the Feeney mechanism could be prevented. Again such an effect would be strongly supportive of the coagulative mechanism but the absence of the effect gives little information. In this case the lack of effect may be due to a poor polymer coverage. This view is supported by the fact that the fused material, which was shown to be produced by aggregation, was not affected by the addition of polymer.

This discussion makes it clear that there is no conclusive experimental proof that either mechanism is an accurate description of the processes occurring during the reaction. However there is the theoretical calculation carried out by Bogush and Zukoski (1987). This calculation was based on the rate of nucleation and suggested that the nucleation should continue for a long period of time. This calculation would tend to support the aggregative nucleation model. However the large amount of evidence gathered can be explained in terms of the LaMer mechanism but not easily in terms of the aggregative mechanism and it is not usual to allow theoretical calculations to override experimental

evidence. There exists the possibility that the model system on which the theory was based does not apply to the system under study or that some factor involved in the calculation is not correct. In the calculation being considered the interfacial energy value used was an assumed value but was within a reasonable range and based on calculations of Weres et al (1981). Therefore the main possible source for error was in the model. The model was that for the rate of nucleation which is based on thermodynamic considerations in the production of nuclei. This model considers the main hindrance to the formation of nuclei, and thus the consideration which sets the supersaturation necessary to form nuclei, as the surface energy of the particles. In this case the polymerisation reaction has a strong tendency for the monomer units to react with large highly crosslinked species rather than other monomers (Keefer, 1984). This will also tend to hinder the formation of nuclei because the monomers will react with the nuclei rather than with each other to form new nuclei. This would increase the supersaturation ratio necessary to produce nuclei and thus invalidate the theoretical calculation suggesting that the nucleation would carry on long into the reaction.

This is not to state that the theoretical calculations carried out are incorrect but to indicate that the system is complex and that there are certain factors which apply in this system which are not generally the case. This raises the possibility that the calculations have omitted to consider a factor which is important. Thus it would not appear that the theoretical calculation is sufficient to show that the aggregative

nucleation model applies although this is a matter which requires more investigation.

5.12 CONCLUSIONS

As the above discussion makes clear the formation of the spherical particles in these reactions can be explained by a number of possible mechanisms. There is no conclusive proof that any of these is an accurate description of the processes occurring and there is evidence to support both of the commonly proposed mechanisms. However the work above shows that the mechanism based on the proposals of LaMer and Dinegar (1950) could explain the alteration of the particle sizes. This can not be seen as proof that the mechanism is the correct one because to an extent the variations in the reaction rates were chosen to fit the observations. But it did make clear that the particle sizes could alter in the observed manner because of chemically sensible variations in the reaction rates. This as yet has not been achieved by the mechanism proposed by Feeney, although this may be due to its greater complexity.

The observations on the growth of the particles, especially the appearance of the second set of particles in one reaction, and the occurrence of the bimodal distributions offer support to the LaMer mechanism which can account for them. Similarly the fact that this mechanism can be extended to explain the irregularly-shaped particles and the fused material lend support to the LaMer mechanism.

The greatest support for the LaMer mechanism comes from the prediction of the results of the exchange of the alkoxide to one with a larger alkoxy group. When a theory can be used to predict as then unknown results it must be taken as evidence of its accuracy. Although the results were not exactly as predicted, in that the particles were not all larger, the differences could be explained in terms of a well known affect which would have been accounted for in a more detailed prediction.

Therefore the conclusions of this work are that the morphology of the materials produced under base catalysis are of three types;

1. Small irregular particles which form chains and networks leading to the formation of a gel.

2. Particles of colloidal dimensions which form a suspension.

3. Large particles of irregular shape which precipitate out of the reaction.

These materials appear because of variations in the reactions. At low base concentrations and resultant low pH the condensation reaction rate would be relatively slow and the silica concentration would exceed the critical supersaturation for a long period, forming a large number of nuclei. The particles thus produced would, due to low surface charge and thus low

electrostatic repulsion, aggregate to form the networks leading to gel formation.

As the base concentration and thus the pH is increased the rate of condensation would increase so that at some point the silica concentration in solution would only exceed the critical supersaturation for a short period. The relatively small number of particles thus produced would then grow to form a colloidal dispersion. The final size of the particles would be determined in the nucleation period by the relative rates of the hydrolysis and condensation reactions. Growth then occurs in two periods, one which is probably reaction limited and then one which is diffusion controlled.

Then as the pH and alkoxide concentrations are increased further the ionic strength of the reaction medium increases leading to the aggregation of the nuclei formed by the reaction leading to the large particles which precipitate out of the solution.

It has also been shown that the addition of an ionic salt to reactions which normally produce spherical particles leads to the formation of fused material which precipitates out of solution. Also it has been shown that the use of alkoxides with bulkier alkoxy groups will generally produce larger particles.

Having formed the spherical particles they settle out of solution to form very dense material which has an iridescent sheen due to the fact the packing arrangement is that found in natural opals which diffract light. Once dry this material forms a dense solid.

5.13 FUTURE WORK

1. Prepare sample of tetra-t-butylorthosilicate, tetra-s-butylorthosilicate and tetra-n-butylorthosilicate and hydrolyse them under conditions allowing comparison of the size of the products to check if the predicted alterations occur.

2. Test whether it would be possible to use other types of polymer added to the reactions to prevent aggregation of the nuclei produced. This may indicate whether small nuclei aggregated in the case of reactions which produce spherical particles.

3. Sinter the compacts of spherical particles to observe the changes in morphology during sintering.

4. Observe the effect of compressing the spherical particles together under pressure.

5. Study the growth of spherical particles by light scattering methods and compare to the measurements made by TEM.

6. Attempt to carry out reactions in a manner which would allow the polarity of the system to be altered without altering the ratio of reagents. This would indicate whether the suggestions of the effect of polarity on morphology and particle size were correct.

7. Prepare reactions and, after sufficient time has passed to allow nucleation to occur, add more base to the reaction. If the nucleation model is correct the number of nuclei has already been produced and the final size would not be altered.

8. Attempt to find methods of detecting the presence of particles of <10nm diameter and monitor the reaction to ascertain if they are present throughout the reaction.

9. Monitor the pH of reactions which were sampled through time and compare to copies which had not been sampled. This would indicate whether the alteration of pH is the factor which causes the alteration in sampled reaction.

10. Attempt to monitor the concentration of silica in solution in reactions which give rise to bimodal distributions to determine if the concentration increases just before the new particles appear.

6. NICKEL DEPOSITION

6.1 INTRODUCTION

As has been previously mentioned, compounds which consist of small particles of nickel deposited on silica are used as catalysts in a number of reactions. In the preparation of catalysts the actual morphology of the support is an important factor. Therefore experiments were carried out to determine if it was possible to form small particles of nickel on, or just beneath the surface of, the spherical particles produced by the hydrolysis of TEOS. This would have several advantages over normal methods of catalyst synthesis. These include (i) the support would be well defined and uniform; (ii) if the metal could be deposited during the growth of the support it could be trapped in the support material just below the outer surface of the support particles. The latter could lead to catalysts where the catalytic site could only be reached by entering pores in the support, thus gaining more control over the catalytic selection. This effect might be aided by the fact that the porosity can be controlled to some extent in these reactions. Catalysts of this form may also have the advantage that, because the metal particles are trapped within the support material, the small particles of metal do not agglomerate into large particles with a loss of catalytic activity. The first step in the production of such materials would be to develop a method of incorporating nickel in the silica particles in a controlled manner.

Attempts were therefore made to deposit nickel within the growing silica structure, preferably at the outer region of the particle. To do this it would be necessary to find a method of depositing the nickel out of a solution; a suitable method would be to precipitate an insoluble nickel compound during the reaction, such as nickel bis(dimethylglyoximate), the precipitation of which is well known as a qualitative method of determining nickel content. The precipitation of this complex has therefore been studied. The structure of this molecule, as determined by x-ray crystallography (Godycki and Rundle, 1953), was shown to be a square planar complex with four dimethylglyoxime molecules surrounding the nickel atom. The method of precipitation employed was homogeneous precipitation (Gordon and Salesin, 1961) which allows much greater control of the morphology of the product and is also likely to cause the material to be deposited on surfaces already present in the solution.

Sol-gel processing has been used previously in the formation of catalyst supports (Cairns et al, 1984; Barten et al, 1987) and homogeneous precipitation has been used to deposit the metal (Geus, 1983; Barten et al, 1987). The use of homogeneous precipitation has been shown to produce catalysts with superior characteristics to those prepared by conventional means (Barten et al, 1987).

The initial reactions to precipitate a nickel complex on to silica used the following reaction composition to produce the silica.

0.2485M	TEOS
10.122M	water
0.169M	ammonia
13.33M	ethanol

This composition, under the conditions described in previous chapters, produces spherical particles with diameters of 167nm (S_n=8nm). The following reactions are classified, in the cases of nickel bis(dimethylglyoximate) deposition, by the anions present and in the other reactions by the complex being deposited.

6.2 CHLORIDE BASED DEPOSITION

The reactions were carried out in the fashion described in the experimental chapter where the ethanol, water, ammonia, hydroxylamine hydrochloride and nickel chloride were placed in a flask and a solution containing TEOS, diacetyl and ethanol was then added. The reactions were prepared on a scale which would produce 6.71g of silica and therefore it was decided that the reaction to produce the nickel should produce the equivalent of 0.671g nickel, a 10% loading if all nickel remains within the silica.

The first reactions of this type, referred to as reaction N1, were prepared in the above fashion. The expected appearance of the reaction was that the reaction mixture in the flask would be pale green in colour, due to the nickel chloride present and, on addition of the solution containing TEOS and diacetyl, the reaction should become red due to the formation of the red nickel bis(dimethylglyoximate). However when the ammonia was added to the

flask (the last reagent of the original set to be added to the flask) the material in the flask became deep blue in colour, then a pale blue precipitate appeared in the flask. On addition of the contents of the vessel containing the TEOS and diacetyl the contents of the reaction mixture became red. The mixture was then allowed to stir for two hours and the product, a red solid, recovered by filtering under vacuum. The mass of product recovered was 2.3575g which is well below the mass expected, 6.71g silica and 3.344g nickel bis(dimethylglyoximate).

In case the reason for the low yield was the short time allowed for the reaction, a second reaction method was used, reaction N2, which followed the same procedure as N1 with the exception that the reaction was allowed to stir for three days before the product was recovered. In this case the mass of product recovered was 13.7742g which is greater than the mass expected from the reaction.

The interpretation placed on the above observations is the following. The initial flask contained ammonia and nickel ions and this lead to the production of the hexamino nickel (II) complex, $[Ni(NH_3)_6]^{2+}$. This resulted in the appearance of the deep blue colour and a lowering of the pH of the reaction mixture because a large amount of ammonia had complexed to the nickel. Then a nickel complex precipitated out of the reaction, observed as the pale blue solid. Subsequently, as the solution containing TEOS and diacetyl was added, the reactions to produce silica and nickel bis(dimethylglyoximate) began. Thus the appearance of the red colour as the nickel still present in solution formed the nickel bis(dimethylglyoximate) compound. The lowering of the pH

could also explain the lower yield in the first reaction because production of silica would be much slower under conditions of lower pH.

To obtain information on the blue precipitate the reaction mixture described above was prepared again but with the variation that the solution of TEOS and diacetyl was not added. The pale blue precipitate was recovered, by filtration under vacuum, and labelled N3.

To determine which reagents are necessary for the production of the blue precipitate two reactions were prepared in the same manner as that above for the isolation of N3. The composition of these reactions being scaled down versions of that used to form N3 except in one case no hydroxylamine hydrochloride was included.

The reaction which included all reagents proceeded in the same fashion as that to produce N3 and a pale blue precipitate was formed. In the reaction which did not include any hydroxylamine hydrochloride the reaction formed a deep blue colour but no precipitate formed. This would indicate the presence of hydroxylamine hydrochloride is necessary to form the precipitate.

6.2.1 THERMOGRAVIMETRIC ANALYSIS

The products of all of the above reactions were subjected to thermogravimetric analysis (TGA). The results of these analyses are shown in figs. 6.1, 6.2 and 6.3 and the data summarised in tables 6.1, 6.2, 6.3.

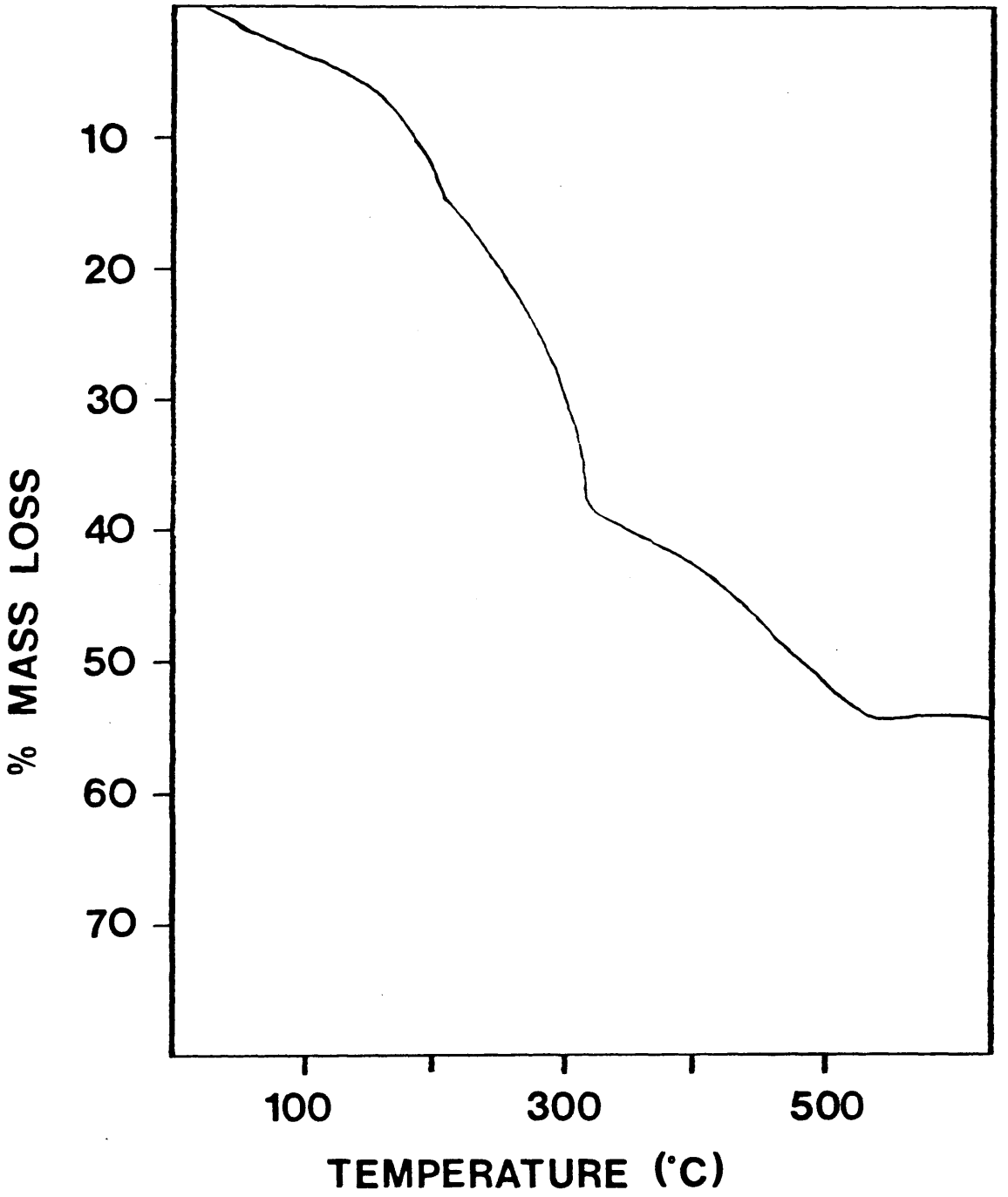

Fig. 6.1: TGA of sample N1.

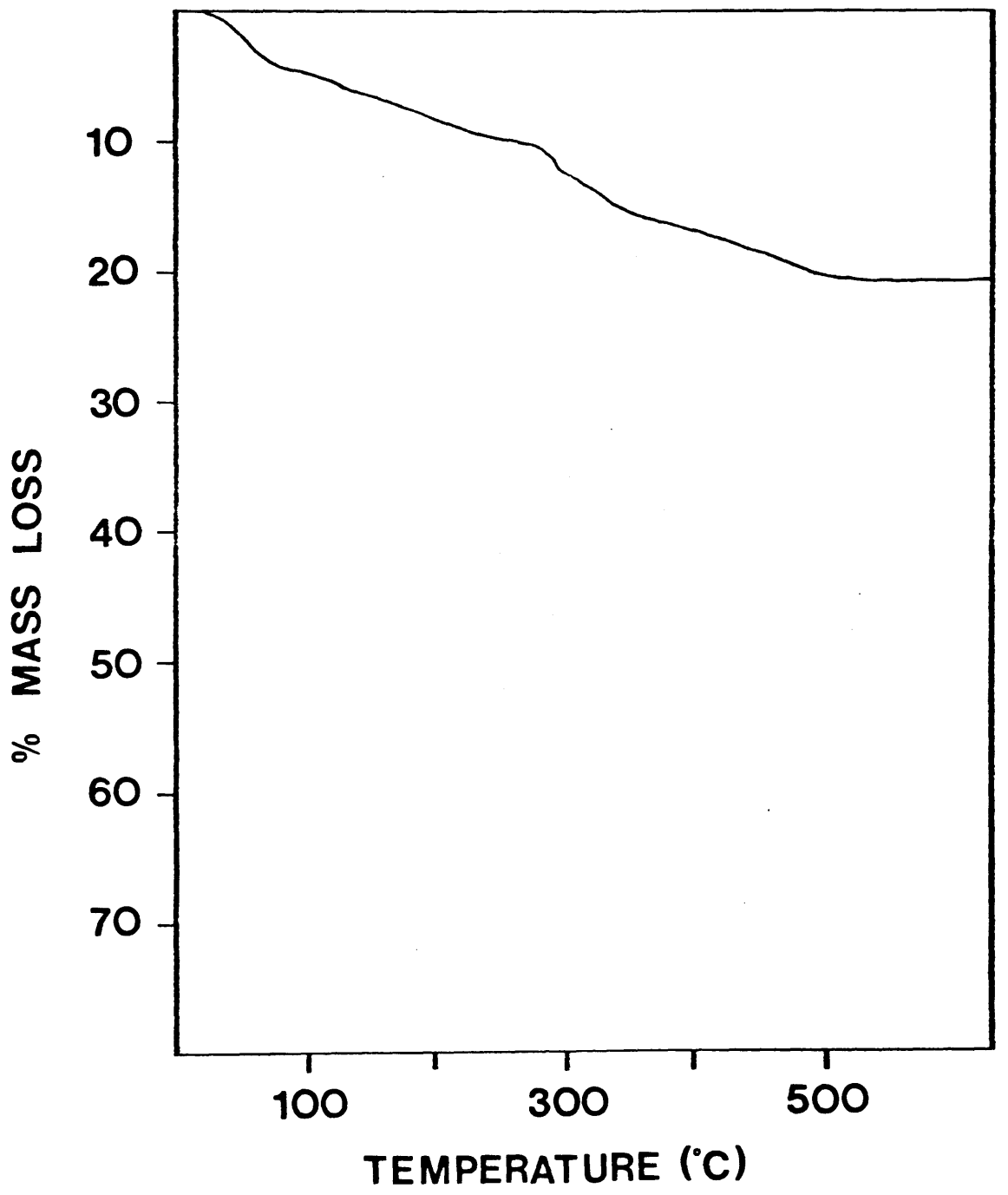

Fig. 6.2: TGA of sample N2.

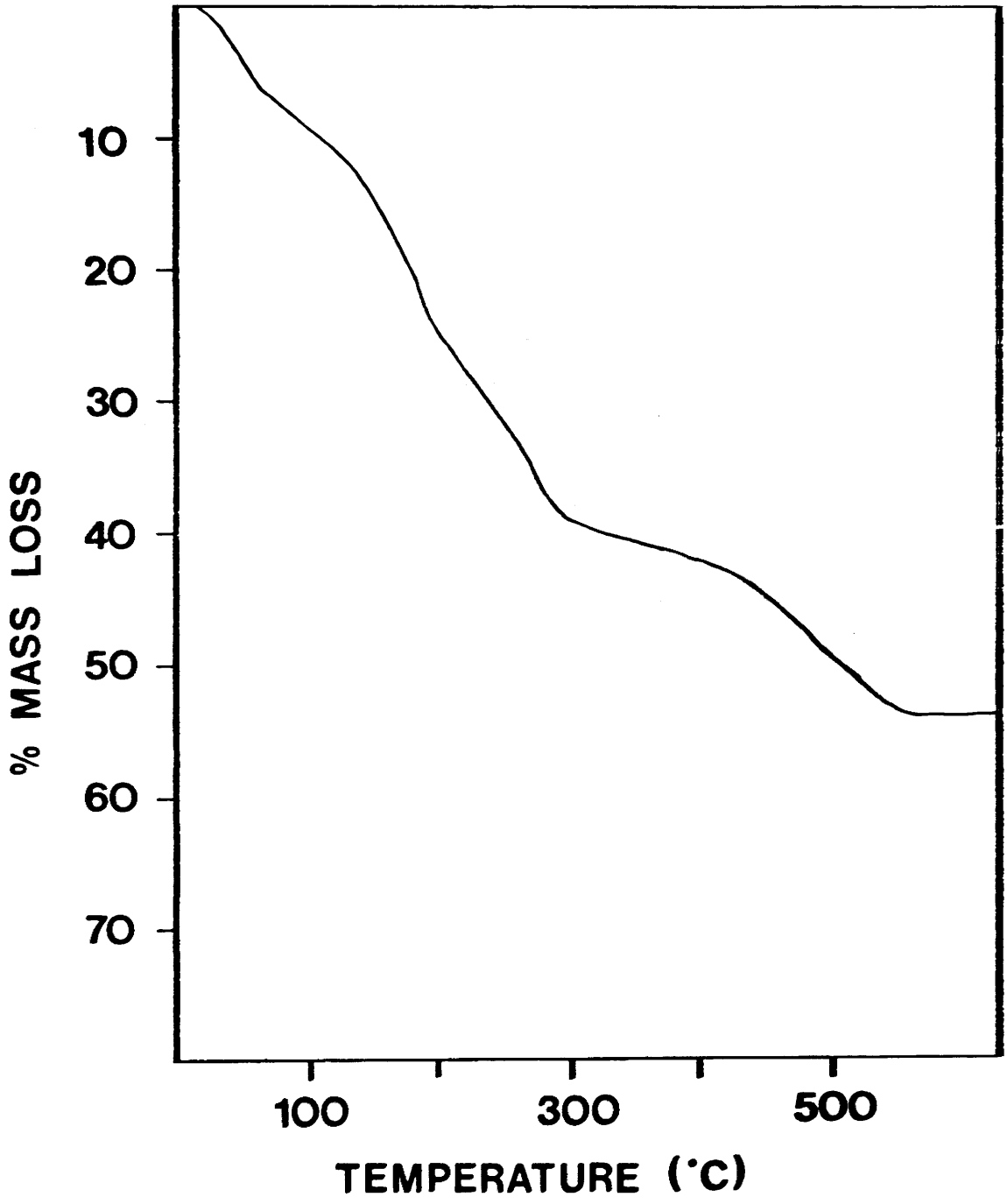

Fig. 6.3: TGA of sample N3.

The most striking features of these results are the similarity of the trace for N1 and N3 and the difference between N1 and N2. However these results could be predicted from observations made during the reactions and the yield of the reactions.

The reaction N1 produced a low yield and a large proportion of this was the blue precipitate which formed in the original flask. It is therefore reasonable to expect the TGA of the product N1 to be similar to that of the blue precipitate N3. In the reaction N2 the yield was much greater due to a larger mass of silica. Therefore the mass losses due to the decomposition processes of the nickel complexes would be a much small percentage of the mass. Thus the difference in the TGA results.

Although similar in appearance the TGA results for N1 and N3 are not identical. The mass loss in the region 300° to 535°C is similar in both cases indicating a similar content of the nickel complex N3. However the mass loss in the region 200° to 300°C is much larger in N1 than would be expected from the results for N3. This is probably due to a decomposition process of the nickel dis(dimethylglyoximate) present in the sample.

If the loss between 310° and 535°C is used to calibrate the comparison between the losses in these samples, by determining the value for 100% N3, then it becomes clear that the loss in the region 215° to 310°C in N1 is 6% higher than accounted for by the N3 present. This extra loss would be due to the presence of a second nickel complex. In the case of N2 the low overall loss makes the identification and end points of each loss process more

difficult and this would explain why fewer loss processes were observed.

TEMPERATURE RANGE	MASS LOSS
25° to 215°C	15.0%
215° to 310°C	22.5%
310° to 535°C	16.5%

Table 6.1: TGA results for reaction product N1.

TEMPERATURE RANGE	MASS LOSS
25° to 100°C	4.0%
100° to 245°C	6.0%
260° to 500°C	11.0%

Table 6.2: TGA results for reaction product N2.

TEMPERATURE RANGE	MASS LOSS
25° to 75°C	6.5%
75° to 200°C	18.5%
200° to 295°C	14.0%
300° to 535°C	14.0%

Table 6.3: TGA results for precipitate N3.

6.2.2 CALCINATION

To discover the effect of heating the reaction products and to determine what occurs during the calcination of the samples a number of calcination reactions were carried out.

Samples of the reaction products N1 and N2 were heated to 450°C to determine the properties and morphology of the final product. This will also allow the determination of the position of the nickel in the final product. Samples of the precipitate N3 were heated to 750°C to determine the final decomposition product of this material. During these reactions the mass losses from the samples were;

reaction product N1	55.6%
reaction product N2	29.0%
precipitate N3	62.2%

The TGA results also indicate that certain decomposition processes which occur during heating end at 200°C and 300°C. Therefore, to determine the decomposition processes occurring, samples of the reaction product N1 and the precipitate N3 were heated to these temperatures in the hope of isolating the intermediate compounds. The mass losses observed in calcining the samples were;

Samples heated to 200°C

reaction product N1	17.8%
precipitate N3	27.9%

Samples heated to 300°C

reaction product N1	30.3%
precipitate N3	38.1%

These mass losses correspond quite well to those expected from the TGA results. The sample of reaction product N1 heated to 200°C appeared pink in colour, the sample heated to 300°C appeared brown in colour. This could indicate the nickel bis(dimethylglyoximate) had not been affected by heating to 200°C but was in some way altered by heating to 300°C. The sample of precipitate N3 heated to 200°C appeared pale green in colour, that heated to 300°C appeared very pale lime green in colour. This may indicate the formation of a chloride compound on heating to 200°C as hydrated nickel chloride is a green compound.

6.2.3 MICROANALYSIS

To determine the compounds which are present in the products and the calcined materials microanalysis was carried out for carbon, hydrogen and nitrogen in all cases, and for chlorine in several of the materials. The results of these experiments are summarised in table 6.4 and the ratio of elements calculated from this data is shown in table 6.5.

The first point that can be made about these results is that the only source of carbon that should be present in the samples is the nickel bis(dimethylglyoximate) precipitate. Therefore the amount of this material present can be calculated.

Compound	% Carbon	% Hydrogen	% Nitrogen	% Chlorine
product N1	7.29	3.56	14.64	NA
product N1(200°)	8.69	2.18	11.29	NA
product N1(300°)	3.94	0.97	3.11	NA
product N2	4.39	1.20	3.90	NA
precipitate N3	nil	3.62	16.87	16.16
precip. N3(200°)	nil	2.27	11.36	27.88
precip. N3(300°)	nil	0.65	1.52	27.68

where the figures in brackets indicate the temperature to which the sample had been heated. The entry NA in a column indicates this analysis was not carried out.

Table 6.4: Microanalysis results for reaction products and precipitates

Compound	Carbon	Hydrogen	Nitrogen	Chlorine
product N1	1	5.86	1.72	NA
product N1(200°)	1	3.01	1.13	NA
product N1(300°)	1	2.95	0.67	NA
loss N1 (0-200°)	1	144.32	31.25	NA
loss N1 (200-300°)	1	1.34	3.04	NA
product N2	1	3.23	0.75	NA
precipitate N3	nil	7.95	2.65	1
precip. N3(200°)	nil	2.89	1.03	1
precip. N3(300°)	nil	0.83	0.13	1
loss N3 (0-200°)	nil	3.19	1.00	nil
loss N3 (200-300°)	nil	2.90	1.03	1

where the figures are given for loss indicate the elemental ratio of the material given off during the temperature range indicated.

Table 6.5: Elemental ratios in reaction products, precipitate and material lost during heating.

Using this assumption the mass of nickel bis(dimethylglyoximate) produced in reaction N1 was 0.5167g and in reaction N2 was 1.8185g. If these amounts are correct then there is an excess of nitrogen and hydrogen present in both samples. In N1 the ratio of excess nitrogen to hydrogen in 1:4.8 in product N2 it is 1:4.9. These would probably be due to the presence of the unidentified blue precipitate. However as the ratio of nitrogen to hydrogen in the precipitate N3 is 1:3 there is still an excess of hydrogen which may indicate the presence of some water.

If the carbon content is used to calculate the amount of nickel bis(dimethylglyoximate) present in the samples of N1 which had been calcined these would be

reaction product N1	0.5167g
N1 heated to 200°C	0.5064g
N1 heated to 300°C	0.1215g

Therefore it would appear that the nickel bis(dimethylglyoximate) is not affected by heating to 200°C, above this temperature the amount falls off quite rapidly. This agrees with the visual observation that the product remained red until it had been heated to above 200°C.

The microanalysis results also indicate the blue precipitate N3 contains nitrogen and hydrogen in the ratio 1:3 which could indicate the presence of either ammonia or hydroxylamine. This idea is supported by the fact that many of the decomposition processes which are observed include the loss of nitrogen and hydrogen in the ratio 1:3. These facts would tend to

indicate the blue precipitate is a nickel complex, probably an amino or hydroxylamino complex, which exists as the chloride salt. However the percentage content of nitrogen, hydrogen and chlorine, which are in the correct ratio for such materials, are too low for any of the common salts.

As the sample N3 is heated the material being lost appears to be ammonia or hydroxylamine, thus leaving the nickel and chlorine behind. This would correspond to the observation that the samples which had been heated appeared green - the same colour as certain nickel chloride compounds.

It was also observed during the microanalysis of N3 that if the material was left on the balance it slowly lost weight. This may indicate that the material is unstable and continuously decomposing.

6.2.4 NICKEL CONTENT

The nickel content of the precipitate N3 was determined by destroying the precipitate and converting the nickel ions to the nickel bis(dimethylglyoximate) precipitate and determining its mass. The nickel content could also be estimated from the calcination and TGA experiments. The mass of material left after calcination or TGA should be nickel oxide and therefore the nickel content could be determined.

The analysis by forming the nickel bis(dimethylglyoximate) compound would indicate the precipitate N3 to contain 30.64% nickel. However the TGA results would indicate the precipitate to be 36.54% nickel and the mass loss during

calcination would indicate the material to contain 29.72% nickel. The reason for the difference is not clear, but if the content of nickel is assumed to be 30.64% and if it is assumed that any percentage mass unaccounted for is oxygen then the precipitate and its calcination products would have the ratios shown in table 6.6.

This illustrates the fact that the ratio of elements does not correspond to those of any simple nickel complexes, which would have either four or six nitrogen atoms to each nickel atom. It may therefore be the case that the material produced as precipitate N3 is in fact a mix of a nickel hydroxylamine complex and a nickel oxide or hydroxide material. The decomposition would appear to occur by the loss of hydroxylamine in the first process and the second loss may include the decomposition of hydroxylamine to form ammonia and hydroxyl groups with the ammonia molecules leaving. Such an explanation would explain why the nitrogen content and hydrogen content did not fall in the proportion expected. It must also be noted that the ratio of nitrogen to hydrogen may be affected by silanol groups, the effect of which would become more prominent as the amount of nitrogen decreases.

Compound	Nickel	Hydrogen	Nitrogen	Chlorine	Oxygen
precipitate N3	1	6.94	2.31	0.87	3.92
precip. N3(200°)	1	3.14	1.12	1.08	1.38
precip. N3(300°)	1	0.77	0.13	0.92	1.53

Table 6.6: Elemental ratios of the precipitate N3 and its calcination products.

6.2.5 X-RAY DIFFRACTION

The x-ray diffraction patterns of N1, N2, N3 and the calcined samples of N1 and N3 were recorded. The patterns which showed definite peaks are recorded in tables 6.7 to 6.11. These give the interplanar d-spacing in Angstroms and the intensity of the peak, I, relative to the strongest peak, I_o. As well as the diffraction patterns and peaks listed in these tables several samples gave diffraction patterns which included very broad peaks. The samples which include silica give broad peaks in the regions 7°-10° and 16°-24° which are probably due to the amorphous silica as discussed in relation to gels prepared under acidic conditions. However the sample of precipitate N3 showed broad peaks in the regions 5°-13° and 14°-22° which would indicate the material was amorphous. The pattern of the precipitate N3 which had been calcined to 750°C also showed the broad peak at 14°-22°. The diffraction pattern of product N1 heated to 300°C also showed broad peak from 12°-23° which would indicate the material was amorphous.

The XRD results outlined above show that both N1 and N2 contain the same crystalline material. This material remains in the sample of N1 which had been heated to 200°C but is not present in the sample which had been heated to 300°C. This is similar to the behaviour expected from nickel bis(dimethylglyoximate) based on previous results. Therefore the XRD of nickel bis(dimethylglyoximate) was determined. A sample of nickel bis(dimethylglyoximate) was prepared by direction reaction of nickel chloride and dimethylglyoxime solutions. The peaks of this

pattern are listed in table 6.12. In this case it was not possible to keep the strongest peak, that at 3.350Å, on scale and still retain the weaker peaks. Therefore the relative intensities are indexed against the second strongest peak, that at 5.918Å. A number of these peaks are similar to those of dimethylglyoxime (A.S.T.M. file 3-435). This may be due to dimethylglyoxime being present in the sample of nickel bis(dimethylglyoximate) or due to a similar crystal structure which might be expected. Comparison of these peaks with those of products N1 and N2 show that the crystalline matter in the products is nickel bis(dimethylglyoximate). This would support the idea that nickel bis(dimethylglyoximate) remains in the sample heated to 200°C but decomposes on heating beyond this temperature.

When the samples are calcined to a sufficient temperature a new crystalline phase appears. The diffraction pattern of this material appears in samples of the N1 and N2 products and the N3 precipitate which had been calcined to above 450°C. The diffraction pattern corresponds to that of the bunsenite form of nickel oxide which is shown in table 6.13. Bunsenite is in fact nickel (II) oxide. Therefore in calcining the samples in air the nickel in the precipitate N3 present in the sample is converted to nickel oxide. It is not clear what occurs to the nickel present as the nickel bis(dimethylglyoximate).

d-value	I/Io
8.889	100
8.346	32
3.246	25
3.048	12

Table 6.7: X-ray diffraction pattern of product N1.

d-value	I/Io
8.980	100
8.385	40
3.255	38
3.058	29

Table 6.8: X-ray diffraction pattern of product N2.

d-value	I/Io
8.889	100
8.346	26
3.238	14
3.048	8

Table 6.9: X-ray diffraction pattern of product N1 heated to 200°C.

d-value	I/Io
2.423	84
2.099	100
1.481	38

Table 6.10: X-ray diffraction pattern of product N1 heated to 450°C.

d-value	I/Io
2.413	OS
2.089	OS
1.477	OS

where OS indicates the peak went over the scale on the chart recorder.

Table 6.11: X-ray diffraction pattern of precipitate N3 heated to 750°C

d-value	I/Io
8.934	29
8.355	6
5.918	100
5.206	44
3.780	17
3.674	5
3.527	7
3.350	OS
3.247	8
3.053	4
2.969	10
2.881	3
2.595	20
2.521	13
2.484	5
2.453	9
2.369	4
2.349	4

where OS indicates the peak went over the scale on the chart recorder.

Table 6.12: X-ray diffraction pattern of nickel bis(dimethylglyoximate).

d-value	I/Io	h k l
2.410	91	(1 1 1)
2.088	100	(2 0 0)
1.476	57	(2 2 0)
1.259	16	(3 1 1)
1.206	13	(2 2 2)
1.0441	8	(4 0 0)
0.9582	7	(3 3 1)
0.9338	21	(4 2 0)
0.8527	17	(4 2 2)
0.8040	7	(5 1 1)

Table 6.13: X-ray diffraction pattern of the bunsenite form of nickel oxide. (A.S.T.M. index file 4-835).

6.2.6 INFRARED SPECTROSCOPY

The infrared (IR) spectra of the products N1 and N2, the precipitate N3 and the calcination products of N1 and N3 are shown in figs 6.4 to 6.11. The peaks at 3450cm^{-1} and at 1640cm^{-1} may be due to water contained within the potassium bromide disc (Williams and Fleming, 1980) but as described later may be due to the sample. The IR spectrum of nickel bis(dimethylglyoximate) is shown in fig. 6.12. As this spectrum is only for purposes of comparison, the exact nature of the vibrations which give rise to the absorptions are not detailed but can be found in several references (Rundle and Parasol, 1952; Orel et al, 1980).

The IR spectra of N3 and its calcination products provide valuable information about the nature of the precipitate and its thermal decomposition. Previous results from microanalysis indicate the precipitate contains nitrogen and hydrogen in a ratio of 1:3 but does not make clear the nature of the complex ie the elements could be present as an ammonia or hydroxylamine complex. The spectrum of the precipitate N3 is similar to that of the hexamino nickel chloride complex (Sacconi et al, 1964) with a number of peaks appearing close to those in $Ni(NH_3)_6Cl_2$. However these peaks do not correspond precisely and the peak at 940cm^{-1} in the N3 spectrum is not explained. Thus it would appear the precipitate is not the amine complex.

Spectroscopic studies of hydroxylamine complexes (Hughes and Shrimanker, 1976) have shown that there are a number of possible hydroxylamine complexes of nickel, with variations of the

number of water and hydroxylamine molecules involved. This work states that hydroxylamine complexes are characterised by peaks at 3400cm^{-1}, 1245cm^{-1} and 940cm^{-1} in the IR spectrum which arise from vibrations of the OH, NH_2 and NO groups within the complex. These corresponds to vibrations in N3. It would therefore appear that N3 is a nickel hydroxylamine chloride complex. However the microanalysis results of N3 do not correspond to any of the complexes listed in the paper by Hughes and Shrimanker (1976). Similarly the IR spectrum of N3 does not exactly match those of the complexes listed by Hughes and Shrimanker. A possible explanation for this is contained within the paper where the production of a grey-blue precipitate is described. This precipitate is non-stoichiometric and converts to a complex containing three water molecules and three hydroxylamine molecules. Therefore it is possible that the precipitate N3 is the same, or a similar, non- stoichiometric hydroxylamine complex.

The spectra of the calcination products of N3 also show peaks which correspond to the hydroxylamine complex, but, with increasing temperature the intensity of these peaks decreases. For example, in the sample heated to 200°C the peaks at 3250cm^{-1}, 1245cm^{-1} and 940cm^{-1} have decreased and in the sample heated to 300°C the peak at 3250cm^{-1} is not clearly distinguishable from the OH vibration peak occurring at 3450cm^{-1}, the peak at 1245cm^{-1} is greatly reduced and the peak at 945cm^{-1} no longer appears. This corresponds to the microanalysis results which suggest the decomposition of N3 occurs by a loss of hydroxylamine between 0° and 200°C and a further loss of hydroxylamine between 200° and 300°C with approximately no hydroxylamine present in the sample

heated to 300°C.

Examination of the spectrum of product N1 and comparison with the spectrum of precipitate N3 and nickel bis(dimethylglyoximate) shows that peaks corresponding to vibrations in both latter compounds appear in N1. This is particularly evident in the region 3000 to 3500cm^{-1}, where the OH and NH vibrations observed in N3 appear, and in the region 1100 to 1250cm^{-1} where two strong bands which appear in nickel bis(dimethylglyoximate) also appear in the N1 spectrum.

The appearance of the peaks indicating the presence of both nickel bis(dimethylglyoximate) and precipitate N3 in the product N1 could have been expected from the visual observations of the reaction ie the appearance of the blue precipitate and the later precipitation of nickel bis(dimethylglyoximate). However the surprising feature of the spectrum of N1 is the absence of peaks. The peaks observed from the vibrations within silica, which appear in previous spectra, do not appear in the spectrum of N1. This would indicate the low yield in the reaction was due to a low final mass of silica produced.

The IR spectra of the products of calcining the material N1 to 200°, 300° and 450°C are also shown. These give information about the decomposition processes occurring in the samples as they were heated. This information supports the observations made at the time of the calcinations and the interpretation of the microanalysis and TGA results.

The spectrum of N1 calcined to 200°C still contains the peaks due to the vibrations of the nickel bis(dimethylglyoximate) molecule. These peaks are not present in the sample which had

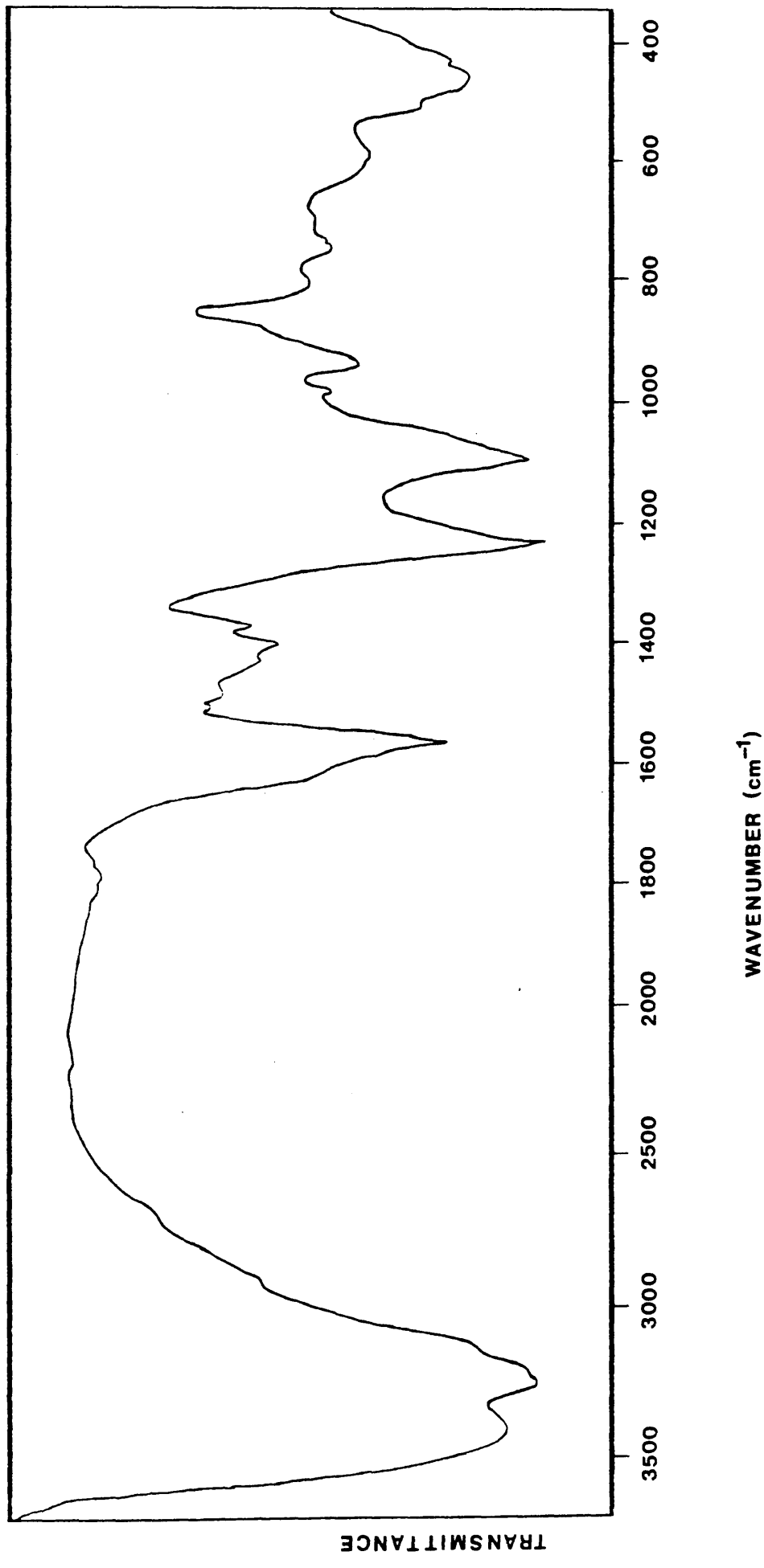

Fig 6.4: IR spectrum of material N1.

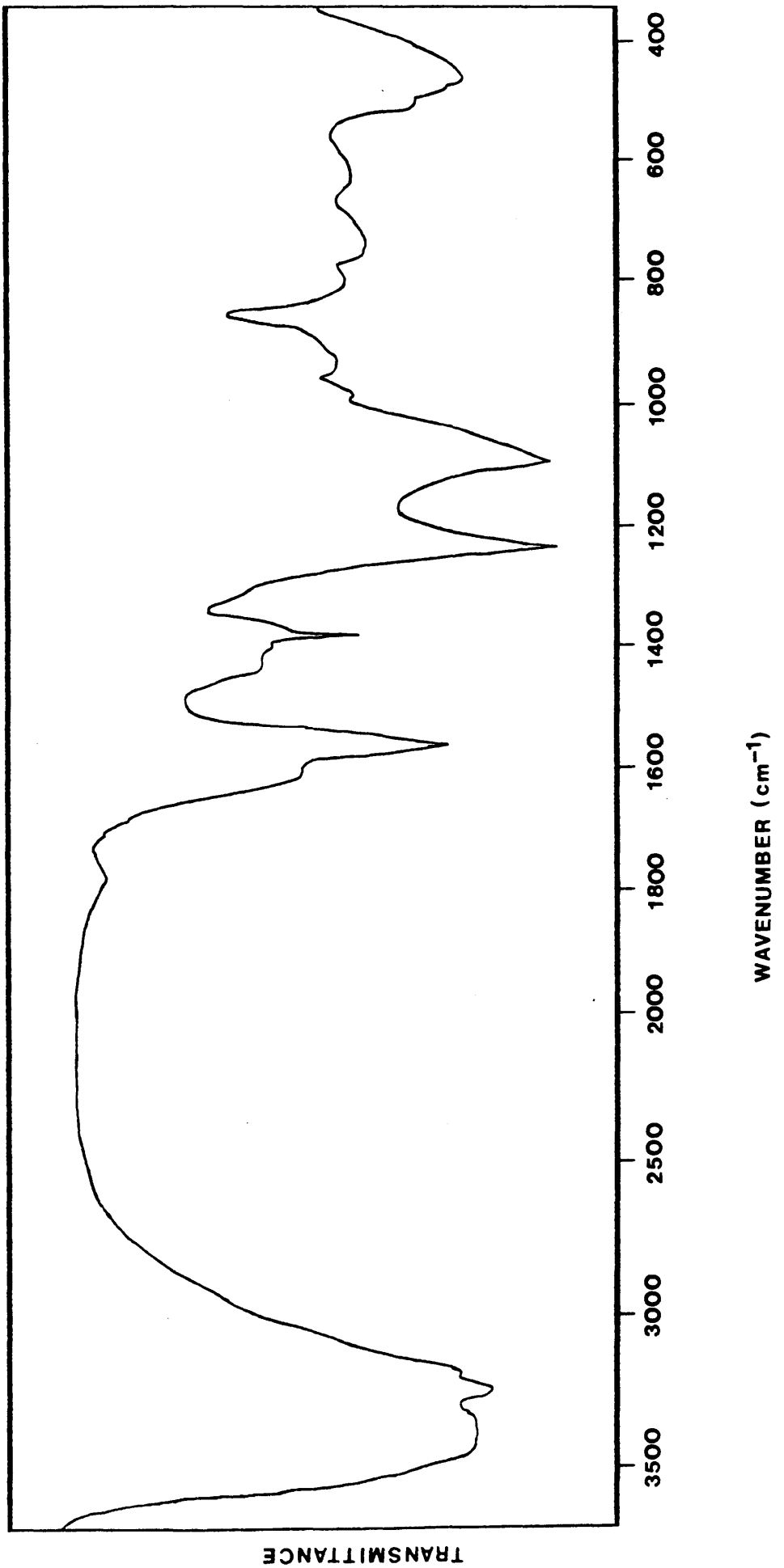

Fig 6.5: IR spectrum of material N1 calcined to 200°C.

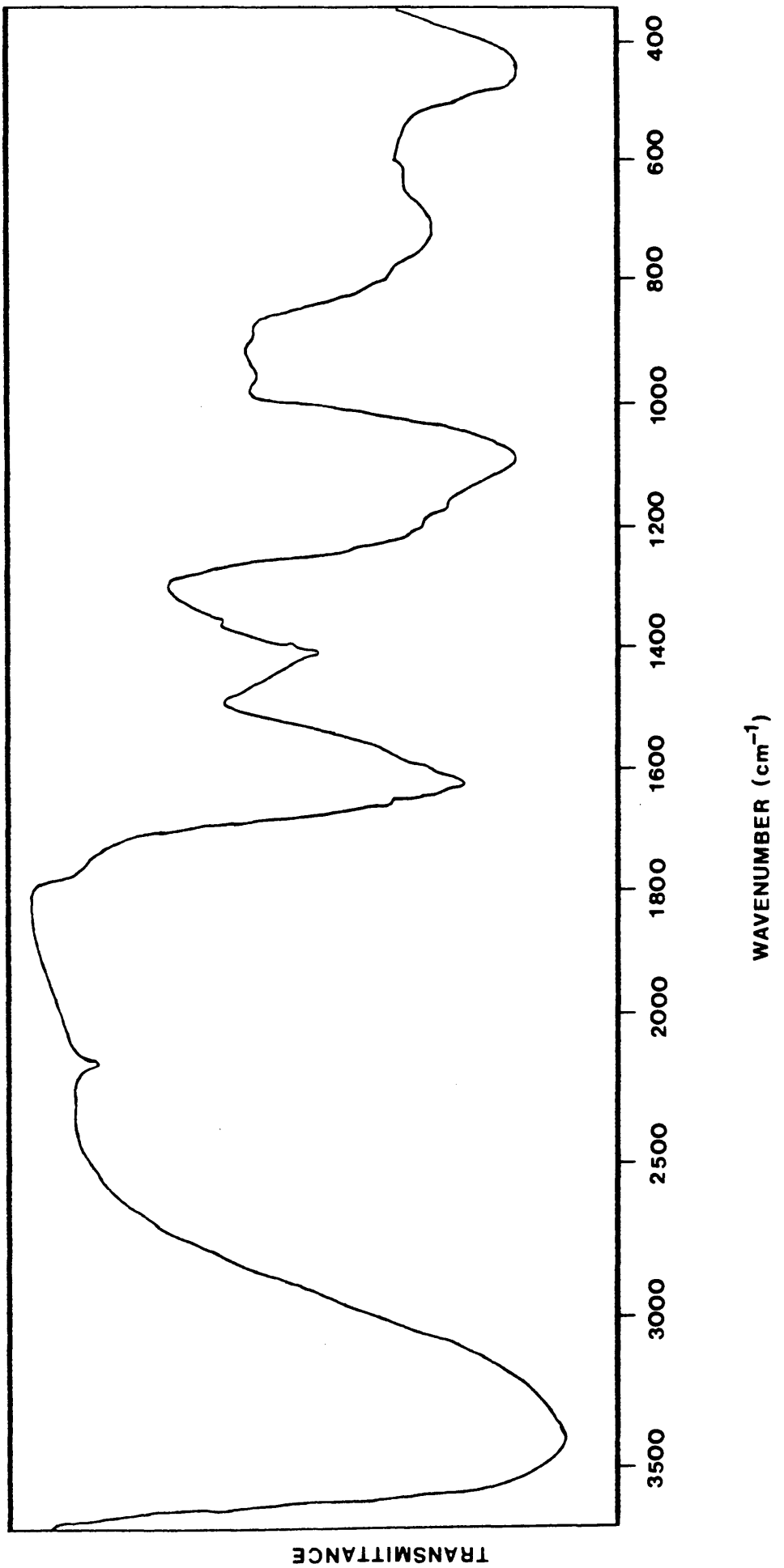

Fig 6.6: IR spectrum of material N1 calcined to 300°C.

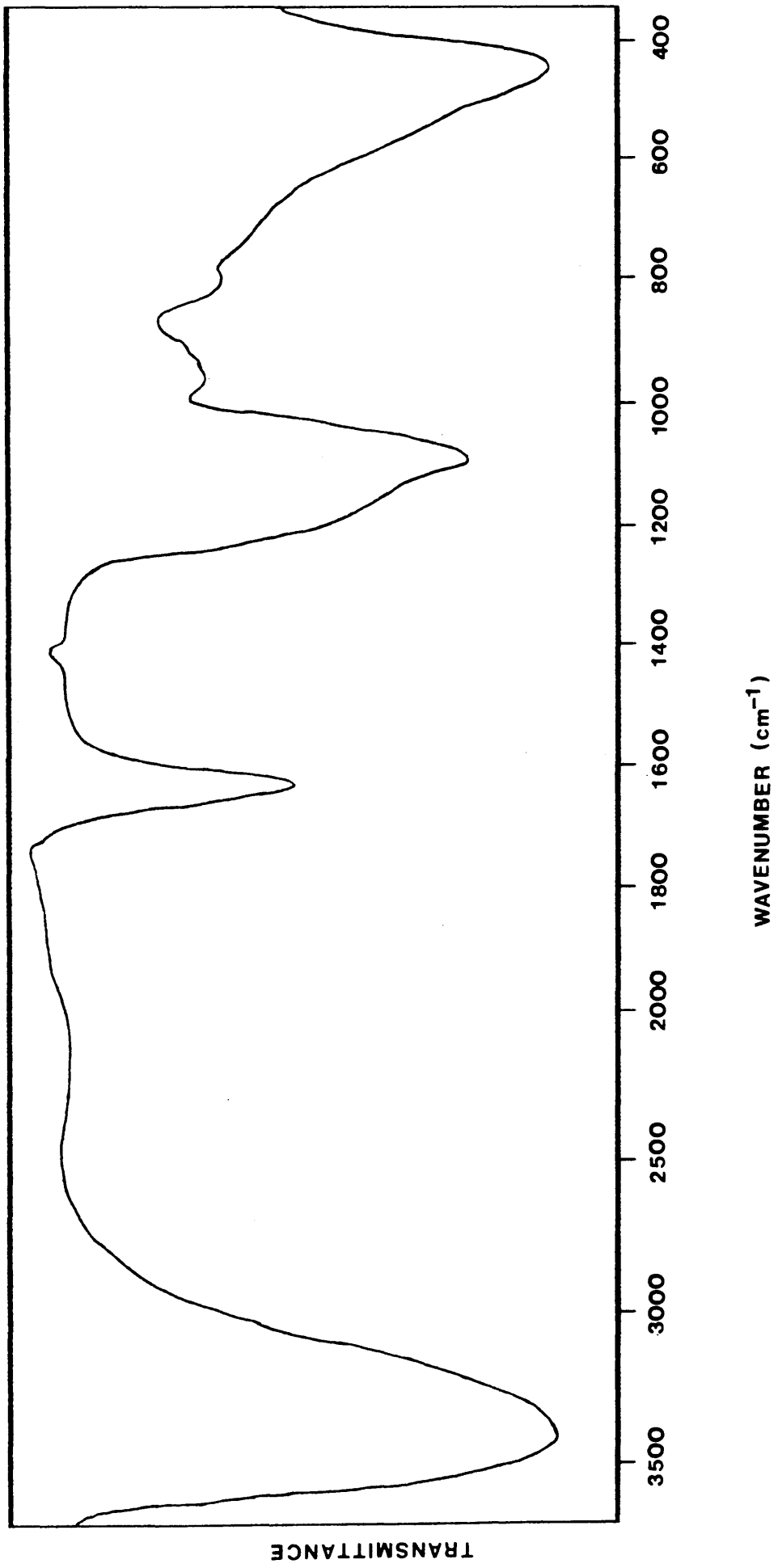

Fig 6.7: IR spectrum of material N1 calcined to 450°C.

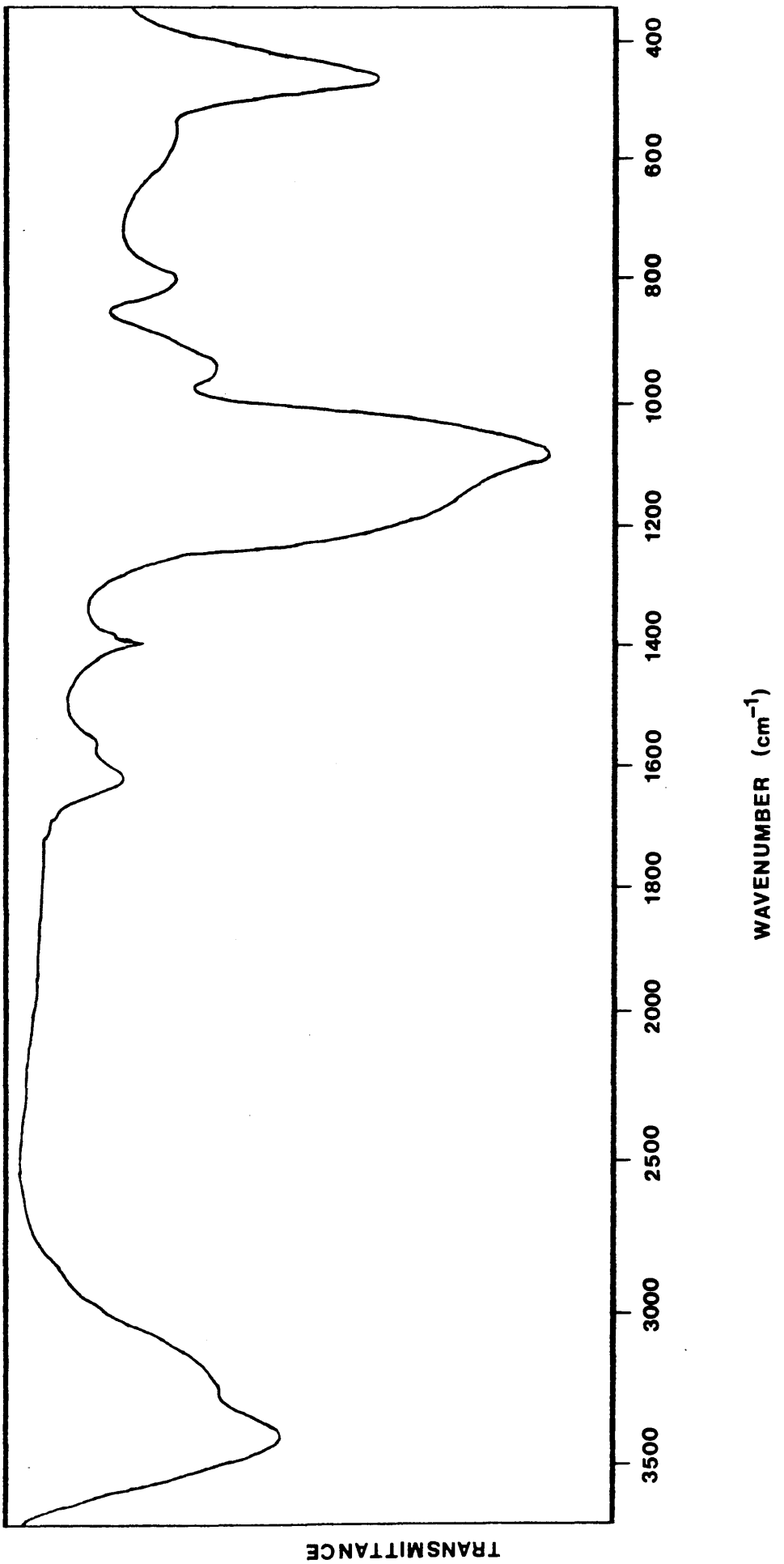

Fig 6.8: IR spectrum of material N2.

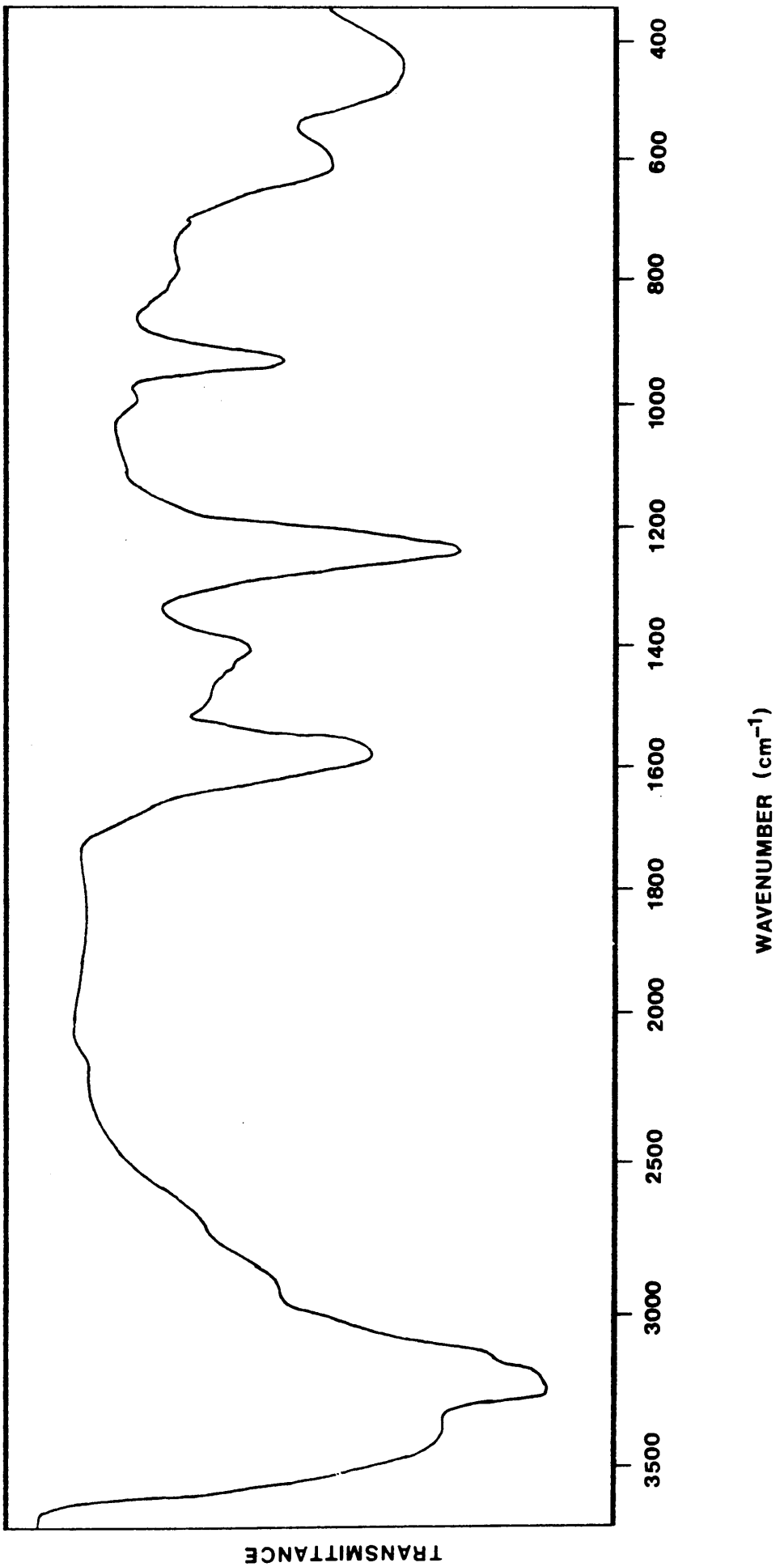

Fig 6.9: IR spectrum of material N3.

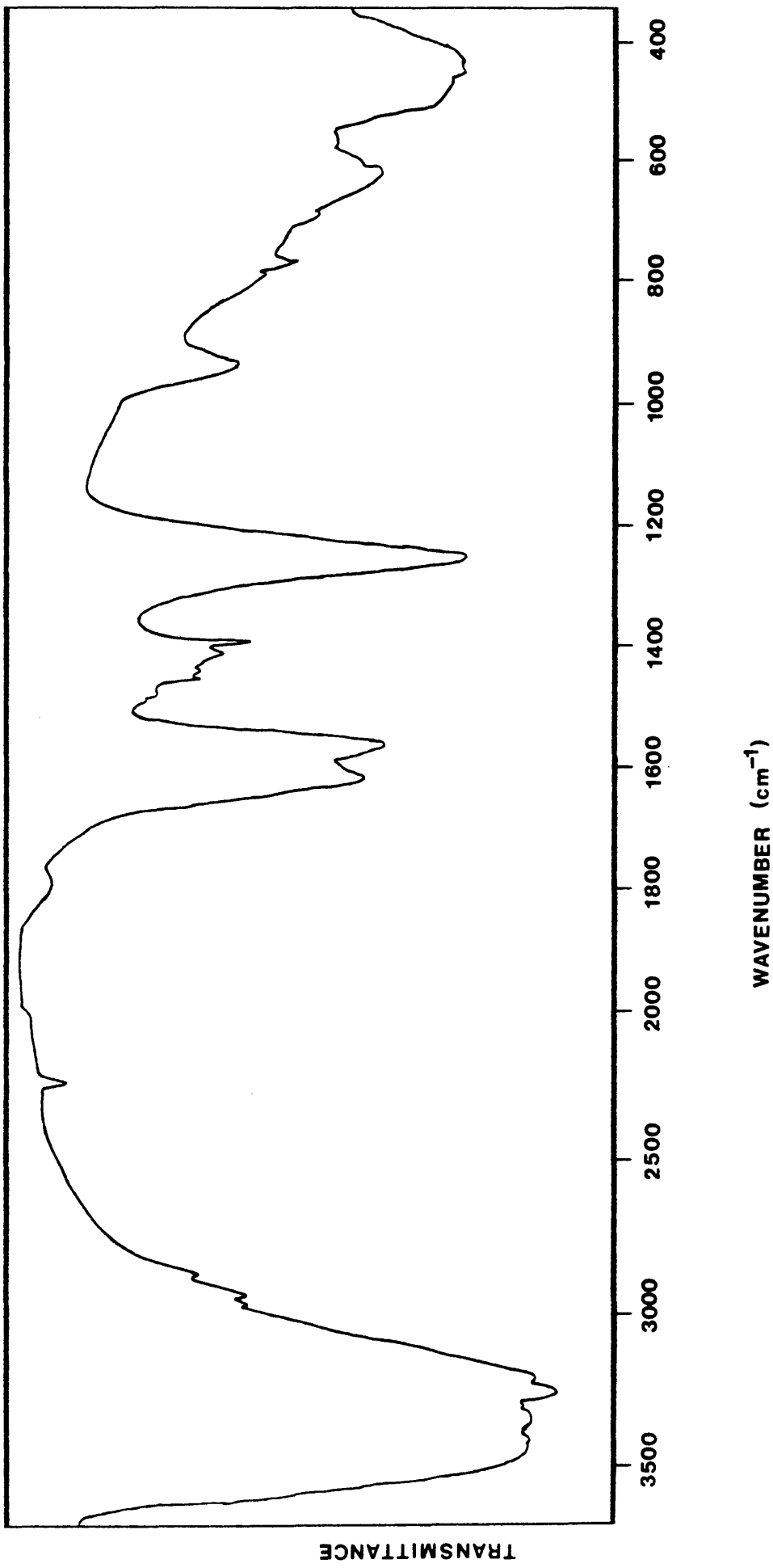

Fig 6.10: IR spectrum of material N3 calcined to 200°C

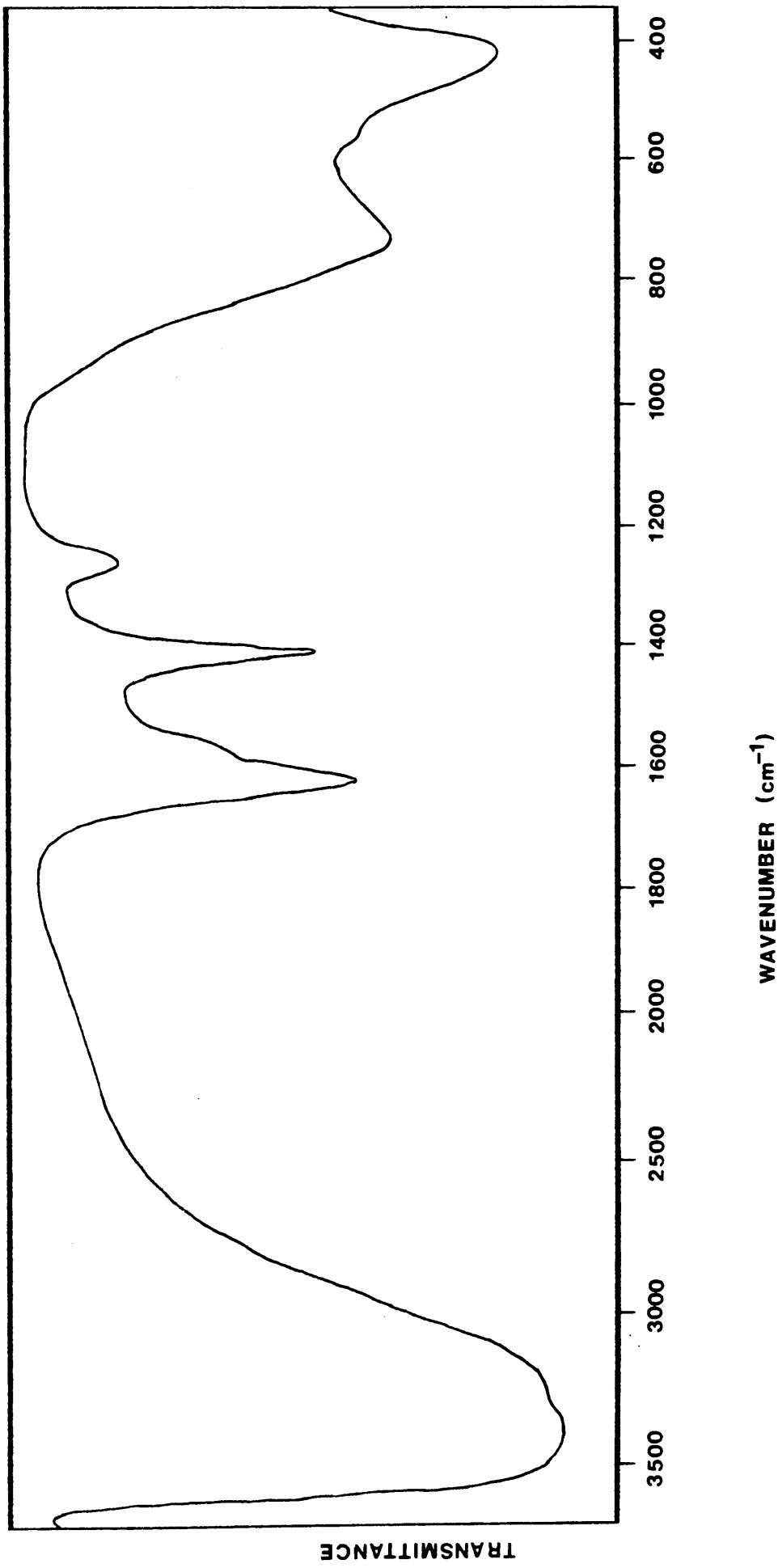

Fig 6.11: IR spectrum of material N3 calcined to 300°C.

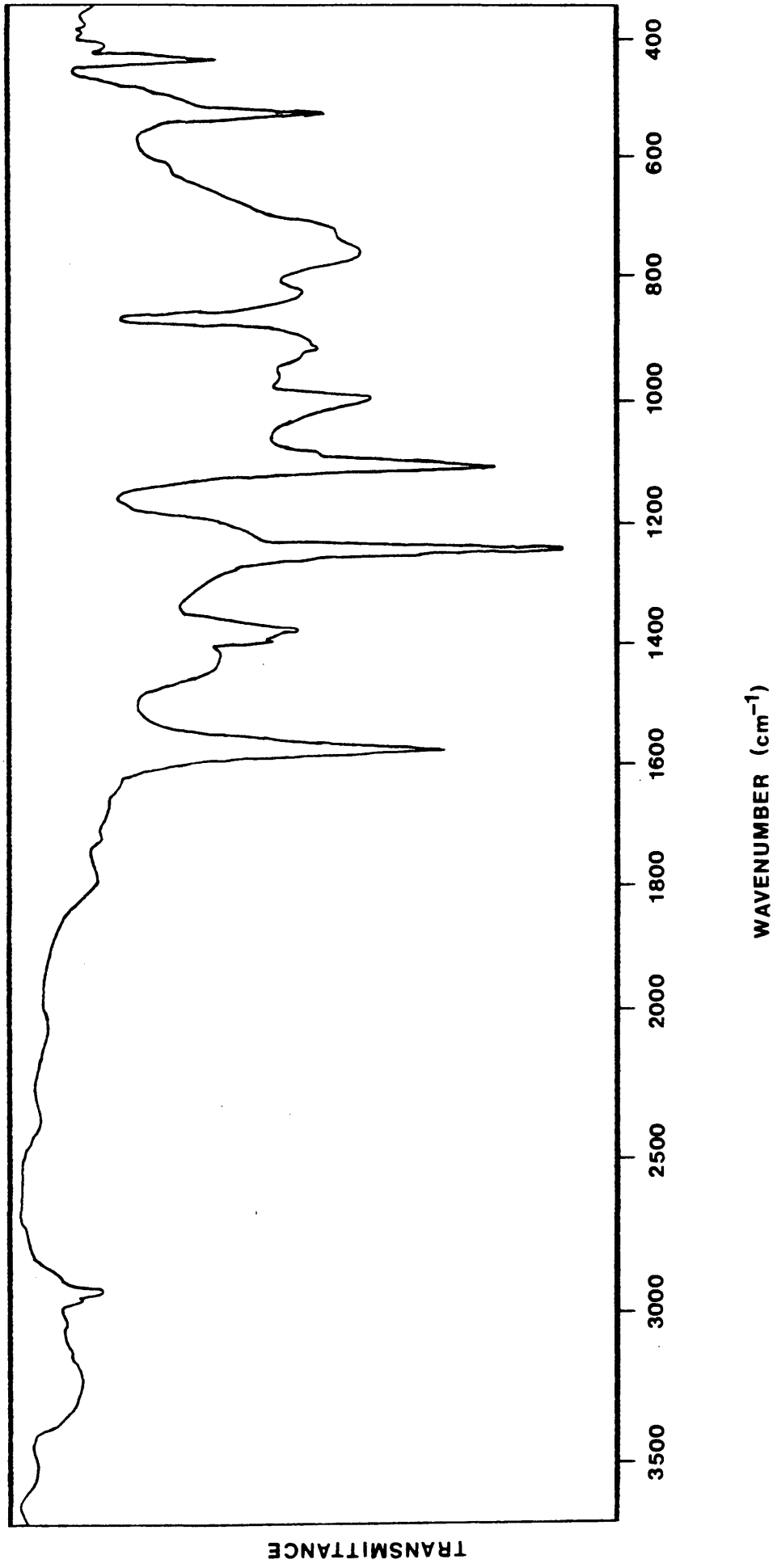

Fig 6.12: IR spectrum of nickel bis(dimethylglyoximate)

been calcined to 300°C. This would support the previously suggested position that the nickel bis(dimethylglyoximate) decomposes between 200° and 300°C. The peaks corresponding to the precipitate N3 alter in a similar manner to that described for the pure material N3.

The spectrum of the product of N1 calcined to 450°C is very similar to that of silica, as seen previously. This could be explained in the following manner. The major components of the product N1 are the nickel complexes and therefore the spectrum of the product shows peaks corresponding to these compounds. Upon heating these complexes decompose to form nickel oxide and thus greatly reduce the fraction of the material they comprise. The silica present in the sample will be unaffected by heating to these temperatures and its fraction will therefore increase. Thus the spectrum of the calcined material will correspond to silica.

The spectrum of the product N2 corresponds to that of silica. The reason for this is the much larger yield of silica from the reaction so that the nickel complexes are a small proportion of the product. Thus the peaks for these compounds will not be observed in the spectrum.

6.2.7 ELECTRON MICROSCOPY

Electron microscopy offers the opportunity to examine the materials produced by the reactions thus allowing the direct observation of the morphology of the silica, the size, occurrence and crystallinity of the nickel present. Because of these abilities TEM has become a valuable method of catalyst

characterisation (Baird, 1982; Smith et al, 1983(b); White et al, 1983).

The reaction product N1 was examined in the electron microscope and consisted of particles which appeared roughly spherical in nature with rough surfaces. These particles had aggregated into chain and flocs which appeared similar to the fused material observed in the pure silica reactions. Most of these particles appeared to have dark regions around the surface or forming the surface. The sizes observed vary within the samples but the outer diameter of the particles appeared to be within the range 185nm to 225nm and the thickness of the outer layer varied between 20nm and 35nm. This type of material is shown in plate 6.1. It is possible that the dark regions on the outer edge of the particles are in fact the solid surface of hollow particles. Many of the regions gave diffraction patterns, a larger number gave no diffraction pattern and in many areas rapidly fading diffraction patterns could be observed. The diffraction patterns which did not fade and could be observed correspond to that of the bunsenite form of nickel oxide.

The reaction product N2 was also examined in the electron microscope. The material consisted of small irregularly shaped particles, of diameters between 10nm and 40nm, aggregated into clusters which were very densely packed in some areas. Within this material there were also a number of crystals many of which appeared hexagonal or nearly hexagonal in shape. The size of the crystals covered a wide range with the larger crystals having a width of 150nm and the smaller crystals having a width of 25nm. The materials observed within this material are shown in

Plate 6.1: Material N1 showing particles with dark outer regions.

Magnification = 188×10^3

1cm = $53{\cdot}19$nm

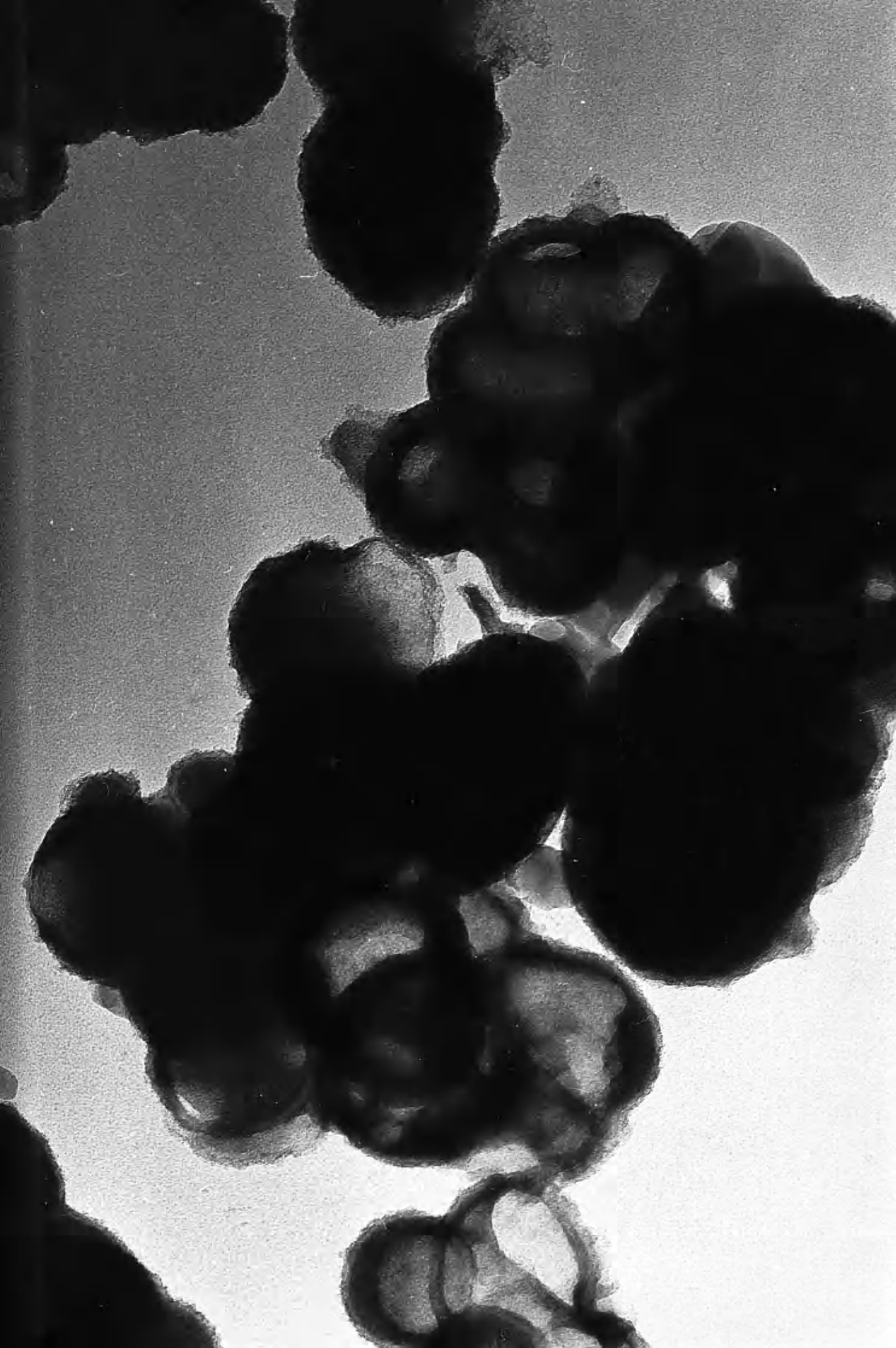

Plate 6.2: Material N2 showing irregularly shaped particles and crystals.

Magnification = 255×10^3

1cm = 39·22nm

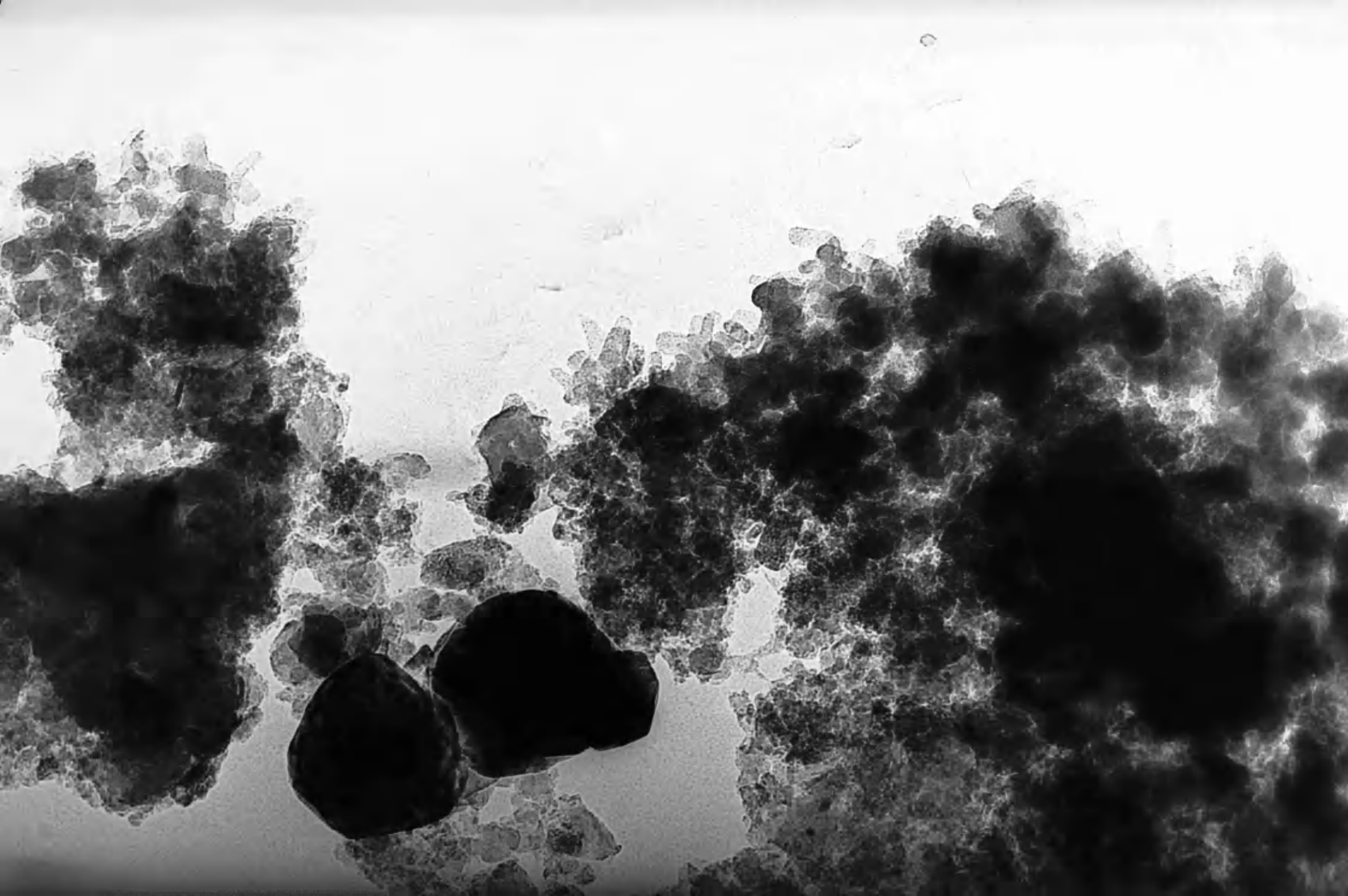

plate 6.2. The areas of crystals gave diffraction patterns which correspond to that of the bunsenite form of nickel oxide. However some areas gave diffraction patterns with much larger interplanar spacing than occur in bunsenite. Also observed were long fibrous particles which did not appear to give diffraction patters.

The sample of N1 which had been calcined to 300°C was examined in the electron microscope and showed a number of morphologies. Most of the sample consisted of roughly spherical particles and such particles which had aggregated and appeared similar to the fused material observed in the pure silica reactions. Many of these particles appeared to have dark surfaces and hollow regions within. Some of these particles also showed breaks in the dark surface region. There were also a number of small crystalline particles which were associated with these particles. These types of material are illustrated in plate 6.3.

The sample of N1 which had been calcined to 450°C was examined. Again the material contained roughly spherical particles and material similar to the previously noted fused material. The diameter of these particles were in the range 160nm to 260nm. In this sample the particles still showed the dark outer region but the internal regions were often not completely hollow, but contained crystalline particles. In a number of cases the crystals actually burst through the dark surface region. Areas were also observed where the shape of the crystals within the hollow particles had altered to match the shape of the inner surface of the particle. Also quite common were areas where the particles appeared hollow and there was a large crystal nearby. The largest crystals observed had widths of 175nm to 360nm but the

smaller, more common, particles found had cross-sections of 10-15nm. In all cases the crystals gave the electron diffraction pattern of bunsenite.

The sample of N2 which had been calcined to 450°C was examined and showed similar material to that in the sample which had not been calcined. That is, the aggregates of irregularly shaped particles and also areas which showed the dark outer layers on particles. Also observed were small crystalline particles which gave the diffraction pattern of bunsenite.

For comparison with the above examinations, the samples of precipitate N3 and its calcination products were examined. The sample of N3 consisted of roughly spherical particles and aggregated roughly spherical particles. Much of the material appeared to have holes or voids in it and appeared to be very porous. The sample also appeared to be beam sensitive. Also observed, but less common, were areas which contained large numbers of small crystalline particles. These crystalline particles gave the diffraction pattern corresponding to bunsenite. The material described is shown in plate 6.4.

The sample of N3 which had been calcined to 750°C was examined in the microscope and consisted entirely of crystals, many of which were hexagonal or approximately hexagonal in shape. All of which gave the diffraction pattern of bunsenite. The size of these crystals, shown in plate 6.5, varied from 35nm up to 140nm. Many of these were beginning to sinter together to form networks.

Plate 6.3: Material N1 calcined to 300°C showing roughly spherical particles with outer layers and crystals

Magnification = $817{\cdot}5 \times 10^3$

1cm = $12{\cdot}23$nm

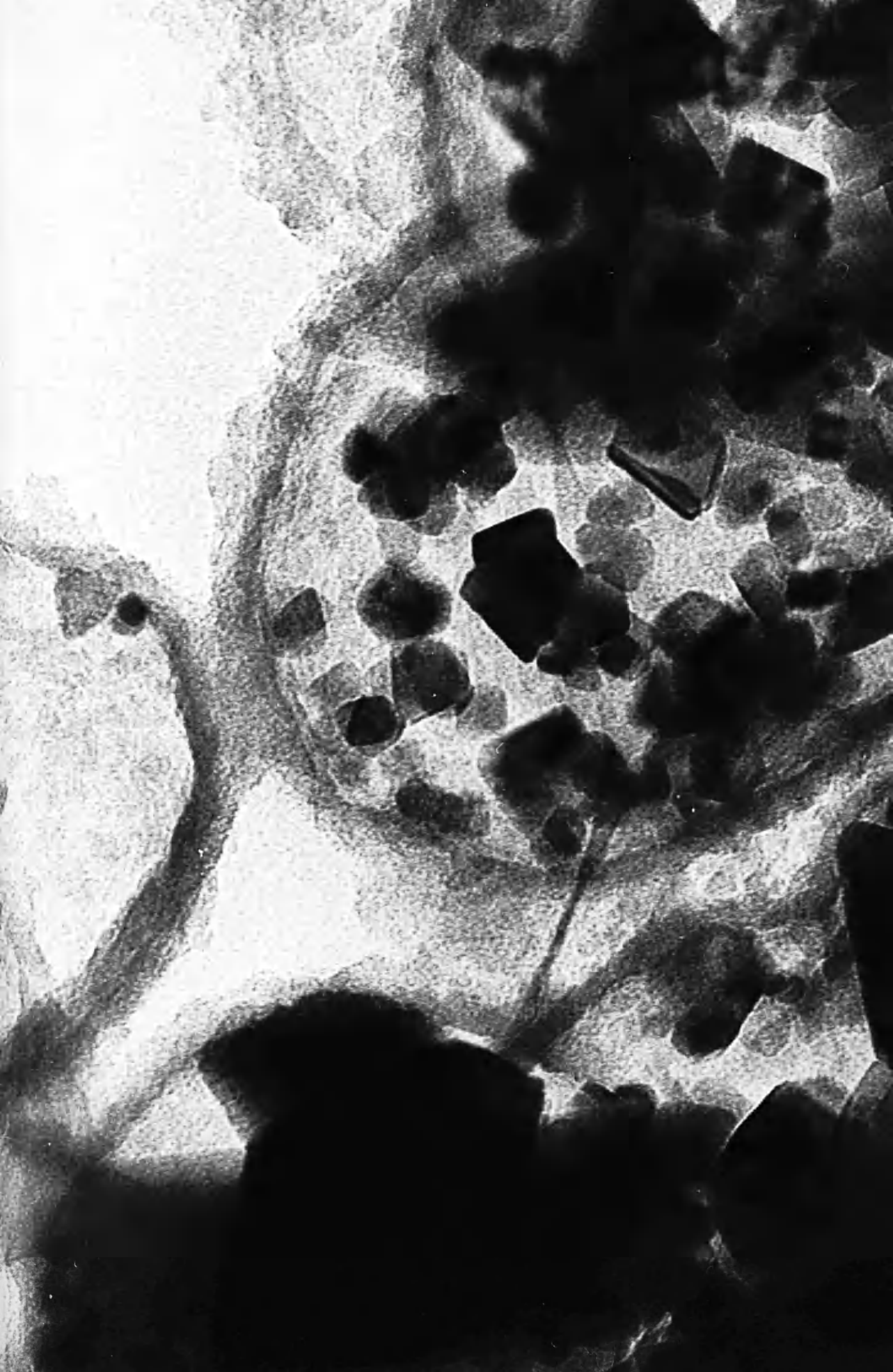

Plate 6.4: Material N3 showing roughly spherical particles and crystalline particles.

Magnification = 450×10^3

1cm = 22·22nm

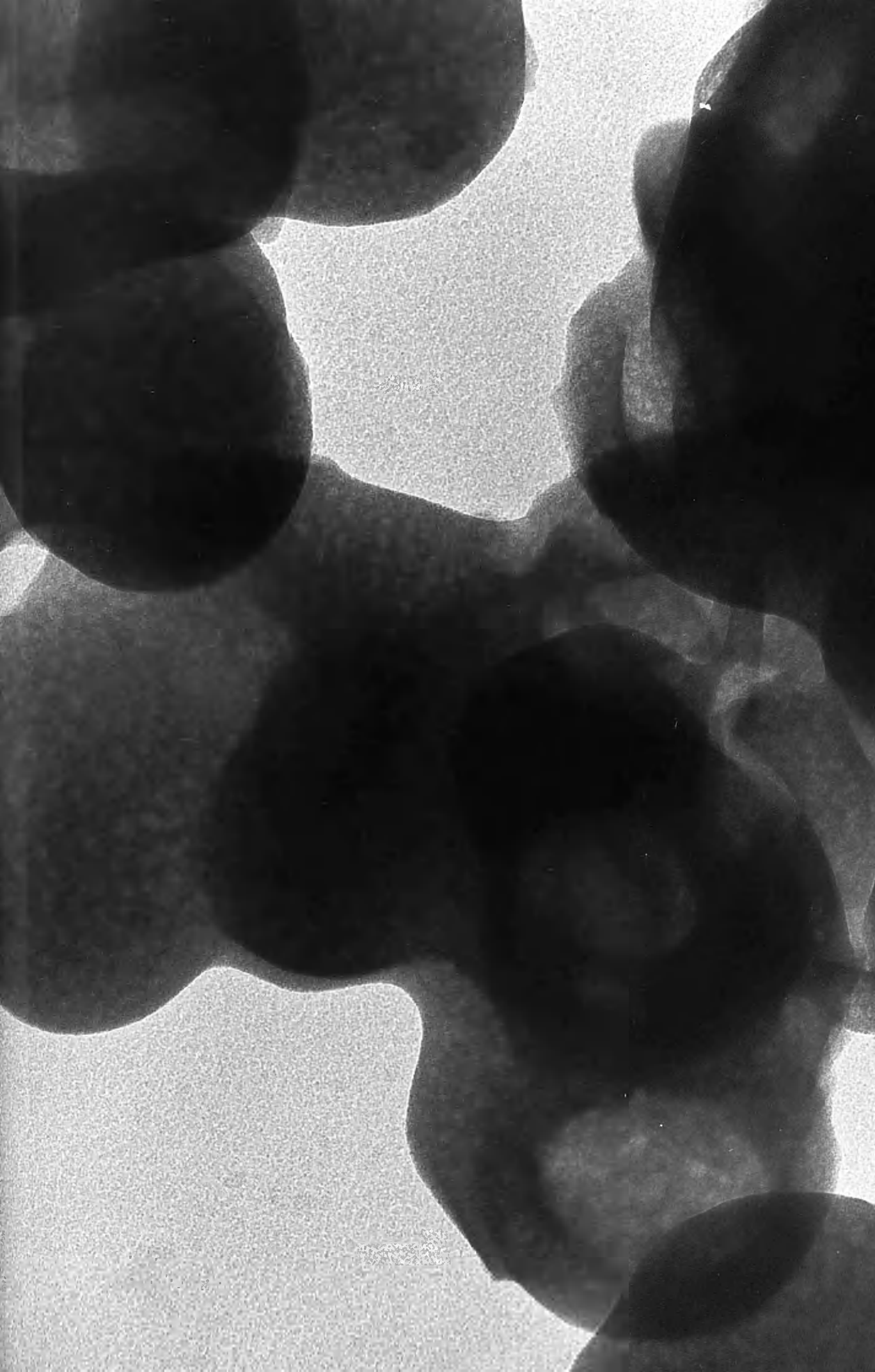

Plate 6.5: Material N3 calcined to 750°C showing hexagonal crystals.

Magnification = 940×10^3

1cm = 10·63nm

6.2.8 DISCUSSION

The observations made during the reactions and the results of analyses described above can be explained in terms of the following model. The original mixing of the reagents in the reaction flask produced a complex mixture which included a hexamino nickel complex, causing the deep blue colour, and an insoluble nickel hydroxylamine chloride complex, the pale blue precipitate. This has the effect of lowering the pH of the solution by removing ammonia molecules. It also provides a large surface area of solid in the reaction flask. The pH reduction will have a direct affect on the reaction producing silica as detailed in chapter 5. The presence of a large surface area of solid may prevent the nucleation of silica particles by acting as a growth site.

The observations of product N1 in the electron microscope show what could be particles composed of two sections; an inner core composed of compounds which decompose in the electron beam and an outer layer which is stable in the beam. Such a situation could be produced by a case in which the silica produced by the hydrolysis of TEOS is deposited on the surface of the particles which were already present in the reaction flask - the blue precipitate. The outer layer of silica would be stable and unaffected by the beam where the inner core of nickel complexes decompose.

While the above situation is possible, electron microscopic examination of the precipitate N3 shows the material

to consist of similar material to that observed in N1. Therefore it may be the case that, due to the extremely low amount of silica produced in reaction N1, the material being observed during the examination of the product N1 is the material N3.

In the case of N2 the observations of the product showed irregularly-shaped particles and small crystals. The small crystals are of the bunsenite form of nickel oxide. These observations can be explained in the following manner. The formation of the nickel complex with ammonia reduced the pH so that the morphology of the silica produced in the TEOS hydrolysis reaction corresponds to the irregular material as observed in the pure silica reactions. The small crystals would be due to the decomposition of the nickel complexes within the product in the electron beam. Also observed in this material are long needle like particles which, on close examination, show a very porous structure. These are almost certainly due to the presence of nickel bis(dimethylglyoximate) which normally has a needle like morphology (Gordon and Salesin, 1961). This type of morphology was not observed in the reaction N1 but this may be due to the very low yield of this material in that reaction. The type of morphology observed in N3 was not observed in N2 but this may be due to the larger yield of silica. The irregular silica particles are similar in appearance to the outer layer of the particles observed in N3. Thus the N3 type particles, which are in much lower abundance in N2, may not be easily distinguished from the irregular silica particles especially if broken up by the grinding used to prepare the samples.

The calcination of the material then decomposes the

nickel complexes which are contained in the product. The decomposition of the N3 begins almost immediately on heating, proceeding via a number of steps which appear to involve the loss of hydroxylamine. The decomposition of nickel bis(dimethylglyoximate) does not appear to begin until the temperature is in excess of 200°C and appears to occur in one step which involves the loss of the dimethylglyoxime molecules. If, as suggested for N1, the particles are coated with a layer of silica then the N3 is contained within the particles, thus the centre of the particles becomes hollow when the nickel complexes decompose. In the samples which had been heated the centre of the particles contain nickel oxide crystals which were formed by the decomposition process. The particles which show holes in the dark outer region or surface layer are those in which the growing nickel oxide crystals rupture the surface layer or perhaps the gas being released during decomposition caused a rupture.

Another explanation of these observations is that the decomposition of the particles of the precipitate N3 initially forms an outer layer of stable material, possibly a nickel oxide. The subsequent decomposition processes convert a material within this outer layer to nickel oxide. The latter processes form the hexagonal crystals observed within the outer layer. The observed ruptures in the surface layer could occur in a similar manner to that described above. This model would explain why the hollow particles were observed in N3 where there was no possibility of an outer layer of silica.

The reason for the materials which had not been calcined, showing crystals of nickel oxide when examined in the electron

microscope could be that the nickel complexes decompose in the beam to produce the same material which was produced during calcination. Such decomposition in the electron beam could also explain why samples which show peaks in the x-ray diffraction do not appear to contain crystalline material when examined in the electron microscope. This explanation is supported by the observation of electron diffraction patterns which faded when areas were exposed to the beam for extended periods in the microscope.

6.3 PERCHLORATE BASED DEPOSITION

The chloride based reactions described above have the problem of the blue precipitate N3 which occurs and makes the positioning of the precipitate deposition difficult. To overcome this problem the reaction was carried out in a manner which would prevent the formation of the precipitate N3. This was based on the premise that the precipitate would not occur if all chloride ions in the reaction were replaced by perchlorate ions. The reactions were carried out as described in the experimental section. A second alteration was based on observations made during the reactions in the chloride based deposition. It was observed that the nickel ions in solution complex with the ammonia molecules present, and thus lower the pH and alter the morphology of the silica produced. To overcome this problem the composition used to prepare the silica was altered to one where the initial ammonia concentration is in the range which produces spherical particles and the concentration remains within the range which

produces spherical particles even when all of the nickel ions present in solution have complexed to the ammonia. The concentrations used were

0.2485M	TEOS
10.144M	water
0.339M	ammonia
13.333M	ethanol

Two reaction methods were employed as described in the experimental chapter. In the first, N4, the reaction leading to the production of nickel bis(dimethylglyoximate) was begun at the same time as the TEOS hydrolysis, and in the second, N5, the start of the reaction to deposit the nickel complex was delayed for one hour after the start of the TEOS hydrolysis so that the precipitate had a sufficient silica surface to grow on and would be close to the surface of the product silica particles.

The reactions followed a similar pattern and colour sequence to the chloride based deposition reaction except that the precipitate N3 did not occur. In fact a small amount of the precipitate N3 occurred in reaction N5, almost certainly due to a small amount of chloride ions which had not been totally removed from one of the reagents. Both reactions produced red solids as the product. The mass of the product in reaction N4 was 8.0874g, an 88.40% yield. The reaction N5 produced a mass of 11.5687g, a yield of 115.93%. The high figure is probably due to the formation of the small amount of the precipitate N3.

6.3.1 THERMOGRAVIMETRIC ANALYSIS

The thermogravimetric analysis of products N4 and N5 are shown in figs. 6.13 and 6.14 and the results are summarised in tables 6.14 and 6.15. The TGA results of N4 show two losses, the first of which may be due to the loss of retained solvent. The second falls within the region which is, from previous experiments, expected to cause the decomposition of the nickel bis(dimethylglyoximate). The results for N5 show three losses. The difference is probably due to the presence of a small amount of the N3 precipitate and in fact the TGA shows similarities to that of N1, which contained N3. However, in the case of N5, the final mass of the material appears to be very low, below the mass of silica expected to be present, and it is possible that some of the material has been blown off the balance by the reaction occurring.

6.3.2 CALCINATION

To determine the affect of calcining the samples, the products N4 and N5 were calcined to 450°C. The mass loss observed during the calcination reaction of N4 was 8.5%. The mass loss during the calcination of the product N5 could not be determined because the material had been sprayed out of the crucible during calcination (even though the crucible was covered with a lid). A similar occurrence during the TGA of this material may explain why a low final weight was observed.

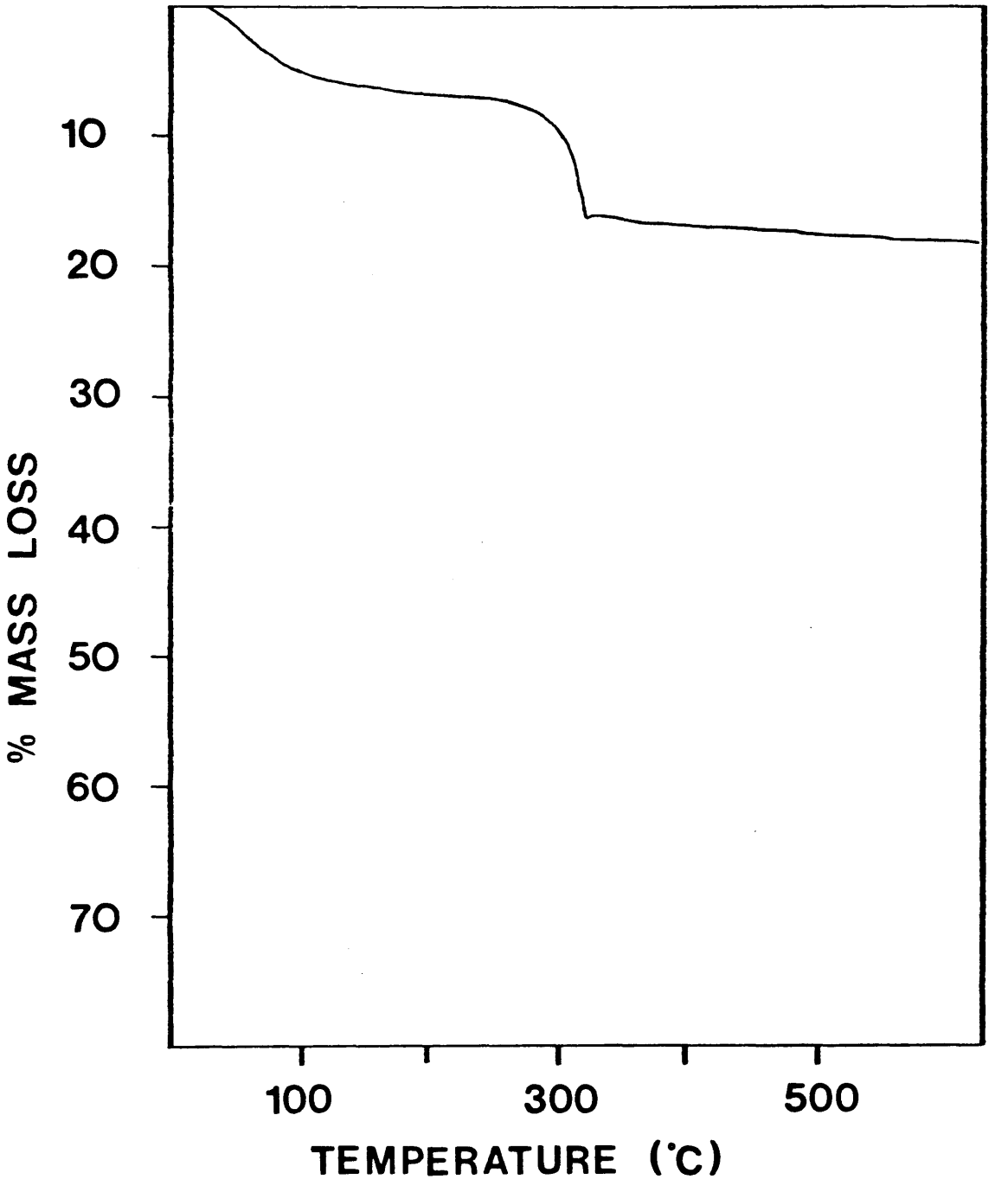

Fig 6.13: TGA of sample N4

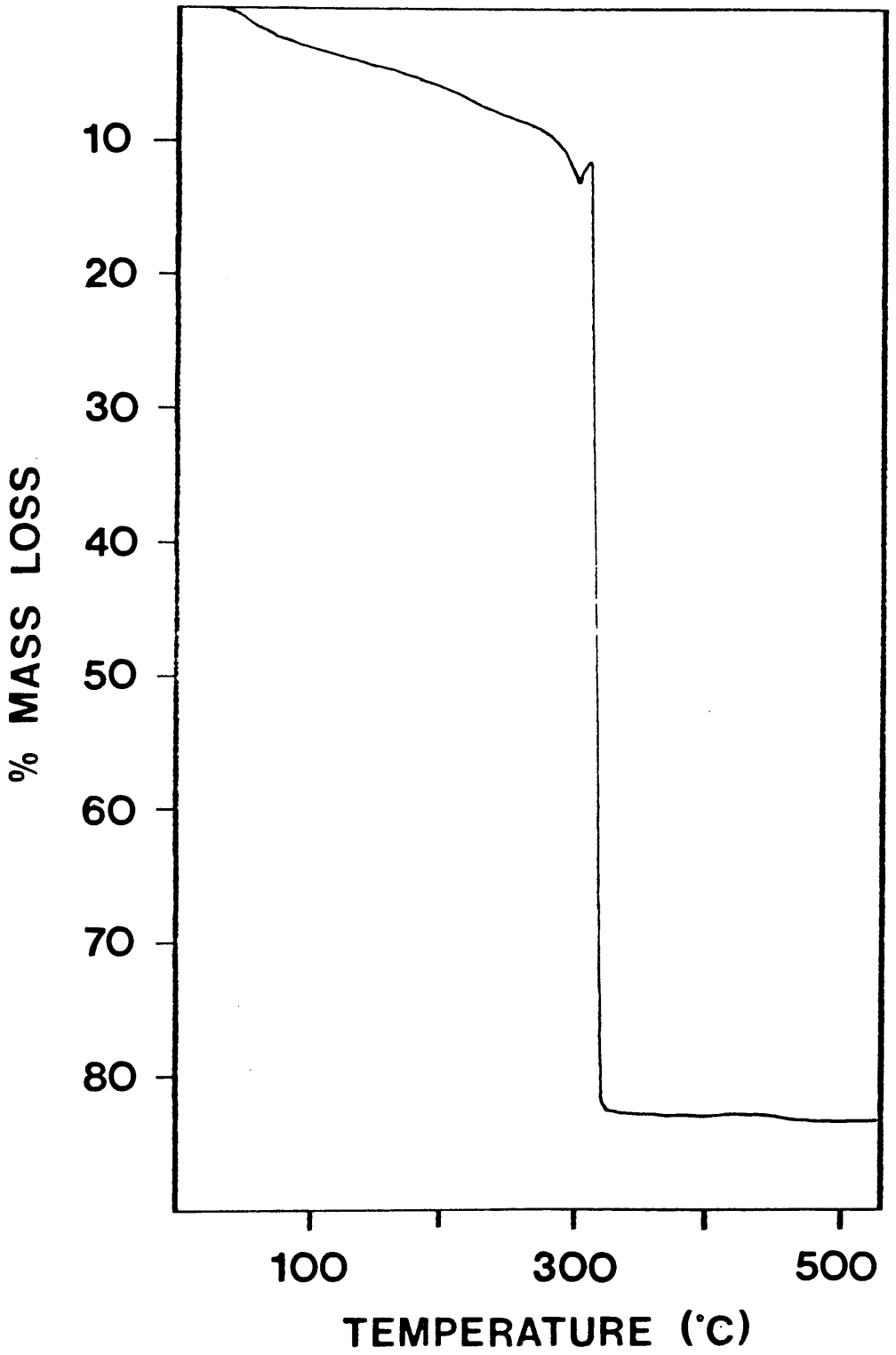

Fig 6.14: TGA of sample N5

Temperature Range	Mass Loss
25° to 150°C	6.5%
250° to 310°C	9.5%

Table 6.14: TGA results for reaction product N4.

Temperature Range	Mass Loss
25° to 75°C	2.5%
75° to 290°C	11.5%
297° to 310°C	71.0%

Table 6.15: TGA results for reaction product N5.

6.3.3 MICROANALYSIS

The microanalysis results for the materials N4 and N5 are shown in table 6.16. Based on the assumption that the only source of carbon in these compound is the nickel bis(dimethylglyoximate) then N4 contains 13.286% of this complex and N5 contains 12.571%. This accounts for almost all of the nitrogen and hydrogen in N4. It can also be seen that the ratio of elements in N4 is 7 carbon to 24 hydrogen to 4 nitrogen. The carbon and nitrogen are almost exactly the ratio in nickel bis(dimethylglyoximate). The hydrogen is higher but this may be due to the presence of water.

In the product N5 the ratio of the elements is 1 carbon to 5 hydrogen to 1 nitrogen. This does not match that of the nickel bis(dimethylglyoximate) complex but this is probably due to the presence of the N3 precipitate.

Compound	% Carbon	% Nitrogen	% Hydrogen
product N4	4.42	2.94	1.28
product N5	4.18	6.66	1.76

Table 6.16: Microanalysis results for products N4 and N5.

If the nitrogen present in the sample, which is not accounted for by the content of nickel bis(dimethylglyoximate), is assumed to be due to the presence of the blue precipitate, and the composition of this precipitate is assumed to correspond to that of the isolated sample of N3, then the percentage content of the blue precipitate can be calculated. Such a calculation indicates the product N5 contains 25.0% by mass nickel hydroxylamine chloride complex, N3. This figure is supported to an extent by comparison of the TGA of the material N5 to that of N3. In the region 75° to 290°C the mass losses in N3 total 32.5% where in the same region in N5 the losses correspond to 11.5%. Although not precisely a quarter of that for N3, as expected from the relative proportion of the precipitate calculated from microanalysis, it is not extremely far away. The difference in results may indicate variations in composition within the sample. The appearance of a smaller number of decomposition processes in N5 compared to N3 may be explained by the fact that the magnitude of the losses in N5 are much smaller and it may therefore not be possible to clearly separate the processes.

6.3.4 X-RAY DIFFRACTION

The x-ray diffraction patterns of products and the calcination products of the reaction N5 were determined. The peaks obtained are described in tables 6.17 and 6.18. In addition to the peaks listed the patterns also showed a broad peak in the range 16°-28° which is due to the presence of silica.

d-value	I/Io
8.934	100
8.346	28
6.632	55
5.810	20
5.735	25
4.600	78
4.049	52
3.936	29
3.738	16
3.633	19
3.255	17
2.747	35
2.600	28

Table 6.17: X-ray diffraction pattern of product N5.

d-value	I/Io
2.411	64
2.085	100
1.475	44

Table 6.18: X-ray diffraction pattern of N5 heated to 450°C.

Comparison of these diffraction patterns with that of nickel bis(dimethylglyoximate), table 6.12, show that a number of the peaks correspond to those of nickel bis(dimethylglyoximate). However there are a number of peaks which are not due to this compound and do not correspond to any of the compounds listed in section 6.4.3 which may be present.

The pattern of the sample calcined to 450°C corresponds to the bunsenite form of nickel oxide, listed in table 6.13. This indicates the decomposition of the nickel containing complexes to nickel oxide at or below this temperature.

6.3.5 INFRARED SPECTROSCOPY

The infrared spectra of the products N4 and N5 are shown in figs. 6.15 and 6.16. These spectra show that both products are composed mainly of silica but features which correspond to nickel bis(dimethylglyoximate) also occur. These are a peak at 1570cm^{-1} in both spectra and an indentation at 1240cm^{-1} in the spectrum of N5. The latter feature is small and is not clear in the reduced spectrum shown in fig. 6.16. The features are small because of the small proportion of nickel bis(dimethylglyoximate) in the products.

6.3.6 ELECTRON MICROSCOPY

The samples of the products N4 and N5 and their calcination products were examined in the transmission electron microscope. The samples of N4 were examined and consisted of

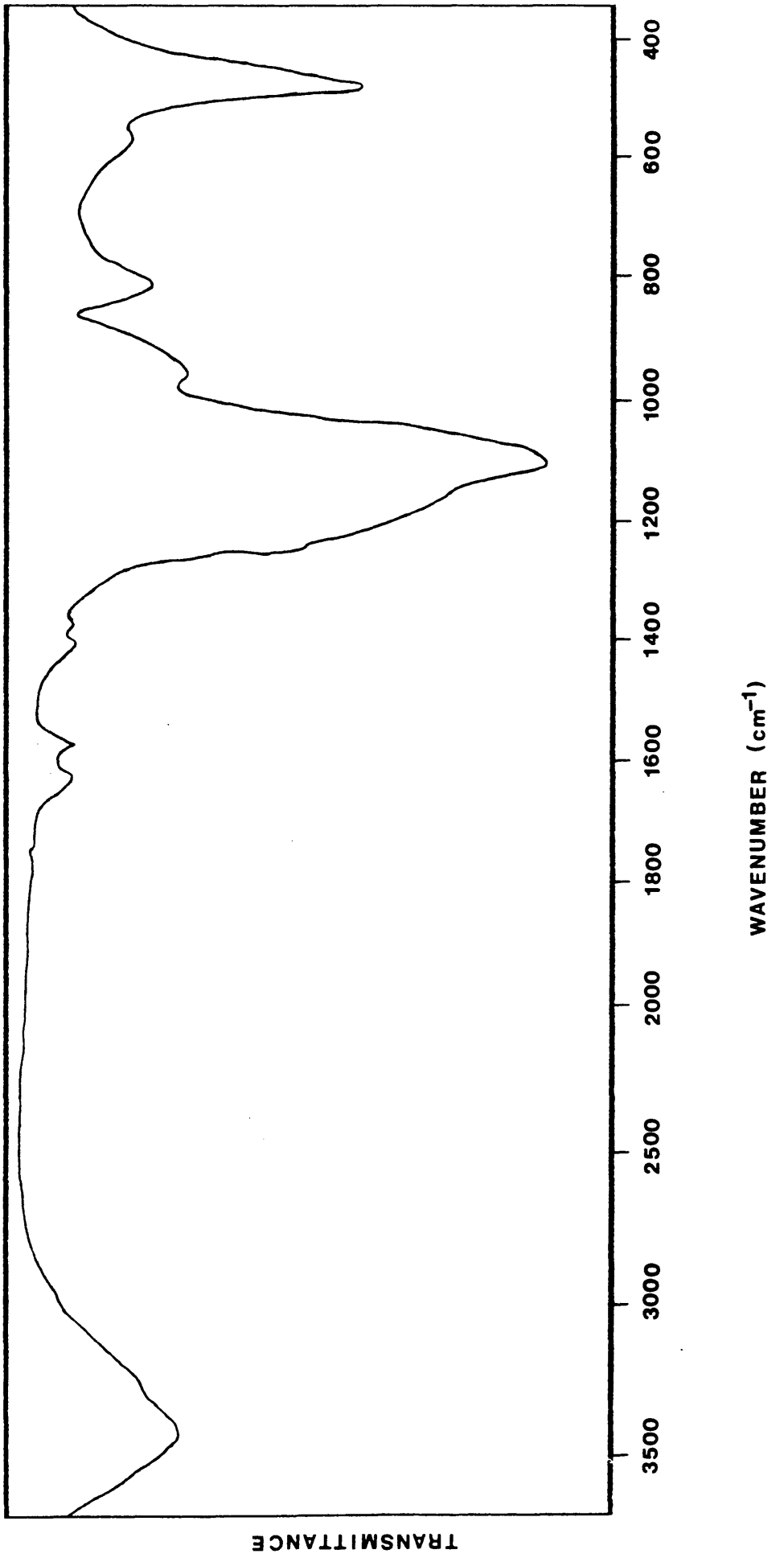

Fig 6.15: IR spectrum of material N4.

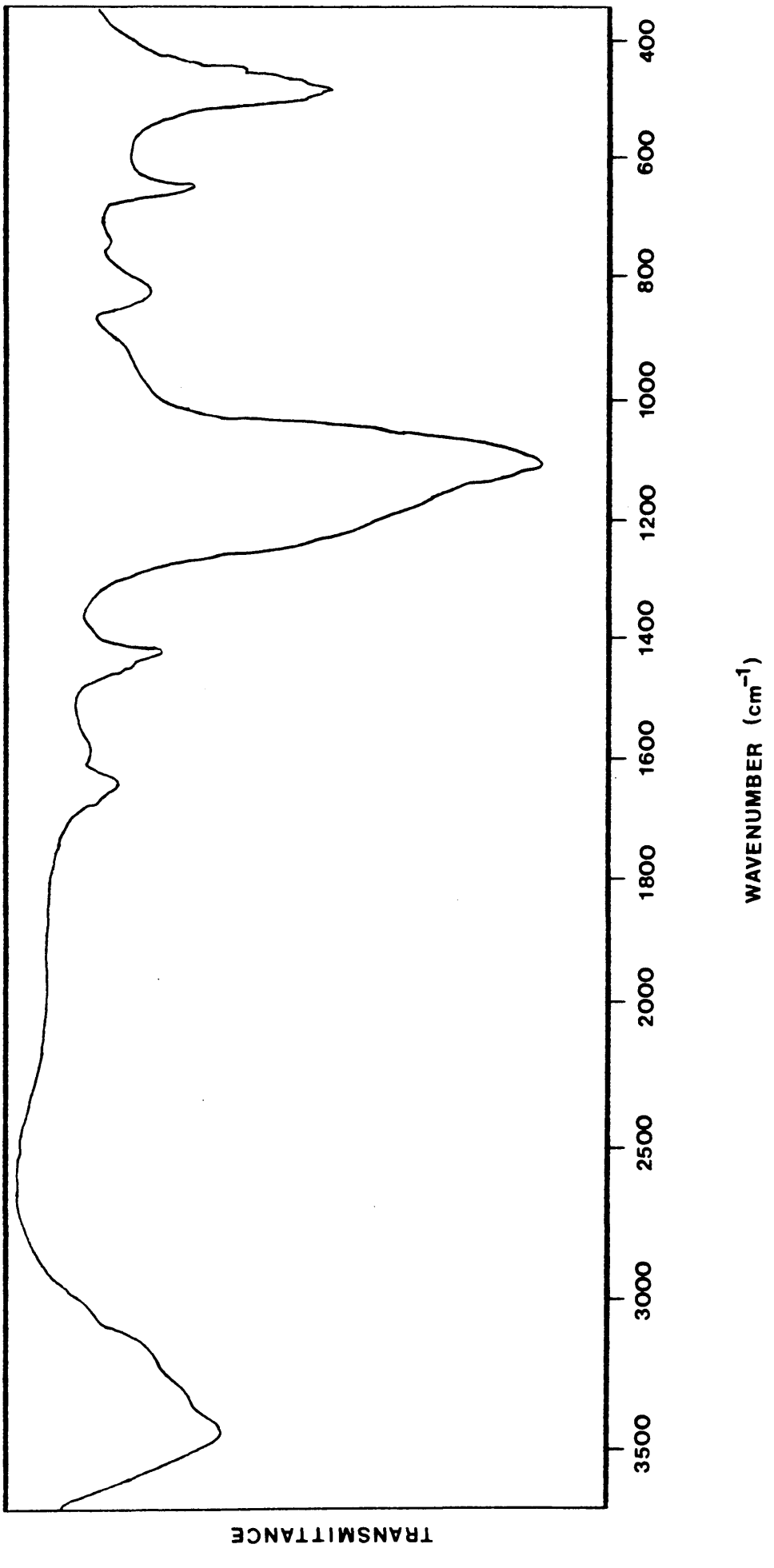

Fig 6.16: IR spectrum of material N5.

roughly spherical particles, fused material and rod or fibre-like particles, shown in plate 6.6. Many areas of the fused material showed holes or voids, similarly some of the roughly spherical particles, those which had fractured, appeared very porous or to include a large number of holes or voids. This type of material is shown in plate 6.7. Examination of the fibre like particles also proved that some of these consisted of a fine network with a large pore volume. It was also noted that several areas appeared to give a diffraction pattern but these rapidly faded. In certain cases part of the diffraction patterns could be recorded before it faded completely. Although not of a high quality they appeared to give peaks corresponding to interplanar spacing d-values of 4.762, 3.288Å and 2.762Å. These are quite close to the diffraction pattern peaks of N5, table 6.17, but not those peaks which correspond to nickel bis(dimethylglyoximate). It would appear that the material giving rise to the diffraction decomposes in the electron beam but it is not clear what this compound is.

The sample of N4 calcined to 450°C was examined in the microscope and the material consisted of large particles of irregular shape but plate like in appearance, see plate 6.8, these are believed to be silica particles. The size of these particles varied with small ones in the range 250-500nm and the larger ones in the range 1.5-2μm. The fragmented appearance may be due to the grinding during sample preparation. On these particles could be observed smaller crystalline particles which appeared to be hexagonal or approximately hexagonal in shape. Most frequently these crystals were in the size range 6-17nm but some as large as 35nm were observed. These are believed to be nickel oxide of the

bunsenite form. Also observed were fibre or rod-like particles which did not give rise to diffraction patterns.

The sample of N5 was examined and consisted of a number of types of material. The first and most common were fragmented particles which were similar in appearance to the fused material observed in previously examined pure silica reactions. Some of these particles contained voids or holes within them. Also observed were fibre or strand like particles, some of which were quite long, extending over a number of grid squares on the electron microscope grids. Some of the fibre like particles appeared crystalline but this appearance faded rapidly when the sample was brought into the electron beam. A number of diffraction patterns were observed but these faded rapidly before they could be recorded. Taking these observations together it would appear that the material forming the needle-like particles is crystalline but rapidly loses this crystallinity when exposed to the electron beam.

The sample of N5 which had been calcined to 450°C was also examined and appeared to consist of fragmented particles which were similar to the fused material observed in the non-calcined samples. These were most commonly in the size range 30-170nm but some of 850nm and above were observed.

On the surface of this material there also appeared small crystalline particles which appeared to be nickel oxide both from their electron diffraction pattern and the x-ray diffraction of the sample. There were also small crystalline particles which could have been on the surface or within the silica structure. This type of material is shown in plate 6.9. It is not possible

Plate 6.6: Material N4 showing morphology similar to the fused morphology observed in silica.

Magnification = $87{\cdot}5 \times 10^3$

1cm = $114{\cdot}29$nm

Plate 6.7: Material N4 showing voids within the structure.

Magnification = 400×10^3

1cm = 25nm

Plate 6.8: Material N4 calcined to 450°C showing large irregularly shaped particles including smaller crystals.

Magnification = 288×10^3

1cm = $34{\cdot}72$ nm

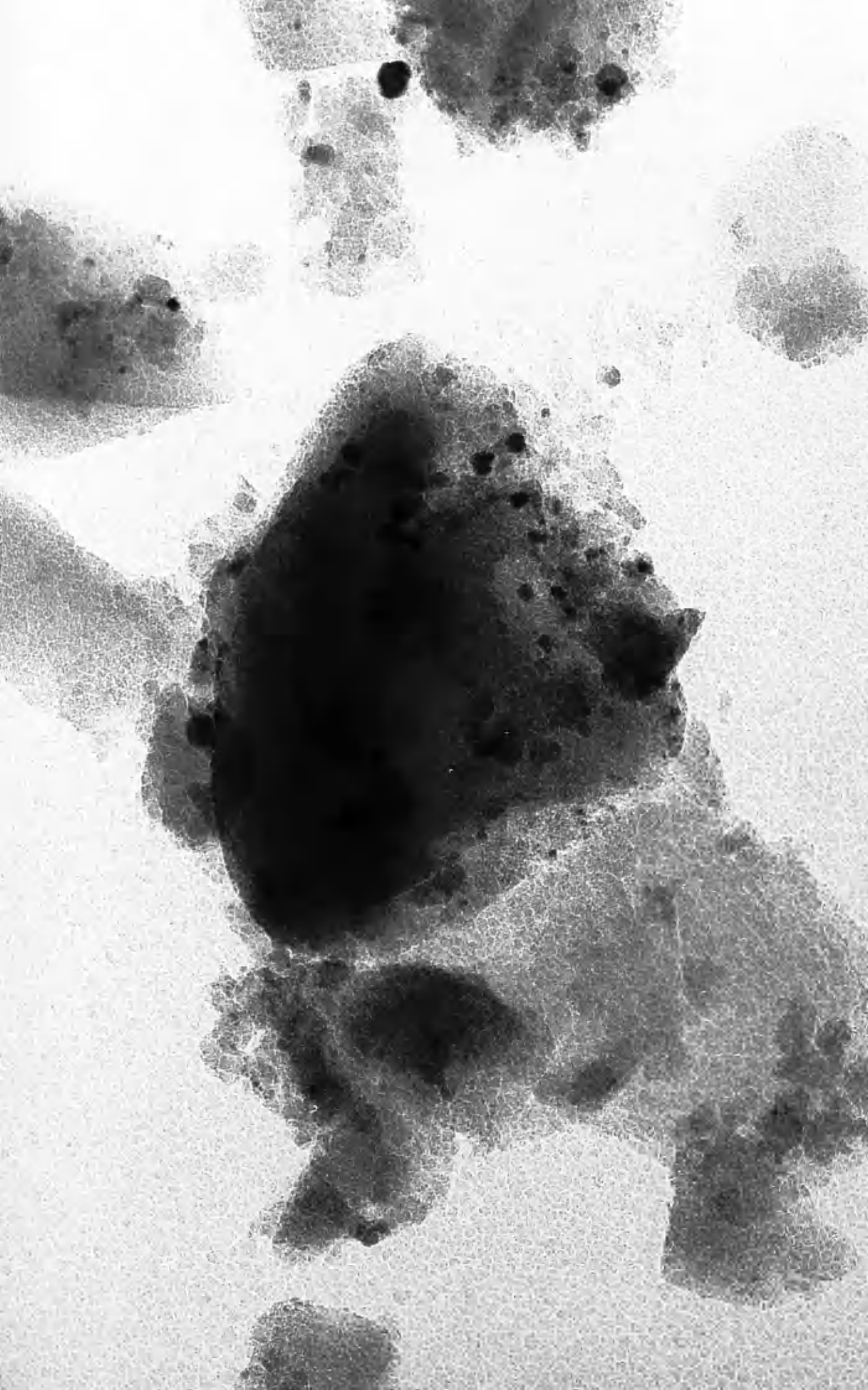

Plate 6.9: Material N5 calcined to 450°C showing crystals on the surface of the silica.

Magnification = 282×10^3

1cm = 35·46nm

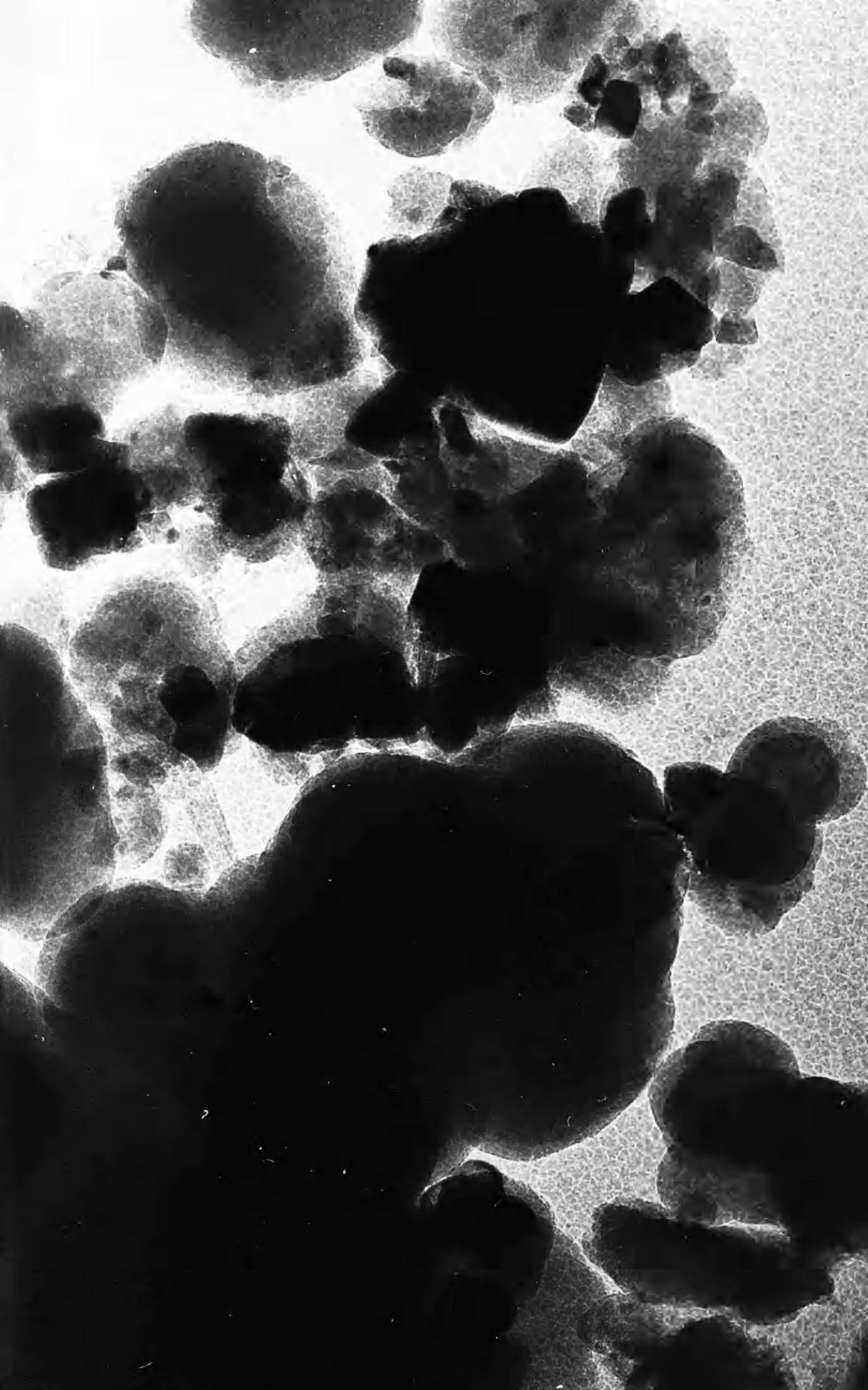

to differentiate between the two, because the image observed in the microscope is a two dimensional projection. The most frequently observed crystal sizes were in the region 5-25nm but there were also a number in the region 50-90nm.

6.3.7 DISCUSSION

The observations made on the samples from the reactions here described, indicate that these reactions produce nickel bis(dimethylglyoximate) in the product. However the observations in the electron microscope indicate that the crystalline material present, which is the nickel bis(dimethylglyoximate), decomposes in the beam. Hence the observation of fading diffraction patterns and the loss of the crystalline appearance of some of the fibrous particles.

This can be explained as follows. The hydrolysis of TEOS produces silica in the form of fused material because of the presence of the ionic salt, nickel perchlorate, in the solution. Within this silica structure, there are areas of the nickel bis(dimethylglyoximate). Therefore when the sample is exposed to the electron beam and this material decomposes the voids within the silica structures are left. Similarly the complex formation reaction produced the fibre like particles, these are the normal morphology of the nickel bis(dimethylglyoximate) (Gordon and Salesin, 1961). However in this case silica is included in the structure, so that when these particles are exposed to the beam and the nickel bis(dimethylglyoximate) decomposes, the shape of the particles is maintained by the silica present. Thus the

appearance of the loss of crystallinity of fibre-like particles but retention of the shape.

The question which arises is what is the nature of the nickel bis(dimethylglyoximate) decomposition. Very little nickel oxide was observed in the calcined samples although more was observed in N5 due to the presence of the blue precipitate. When this is taken in conjunction with the fact that the mass loss in the TGA in the region 250° to 310°C (the temperature range in which the nickel bis(dimethylglyoximate) was expected to decompose) almost exactly match the mass of the nickel bis(dimethylglyoximate) believed to be present in the material from microanalysis it appears possible that the nickel bis(dimethylglyoximate) does not actually decompose but sublimes.

Consulting reference text (Weast, 1972) shows that this is in fact the case. The compound nickel bis(dimethylglyoximate) sublimes at 250°C. This makes this compound unsuitable for the purpose of the reaction because it will leave no nickel in the calcined product but the work on its deposition has provided a valuable base of information to go forward from.

6.4 NICKEL COMPLEX DEPOSITION

The aims of the experiment make it necessary that the complex which is deposited actually decomposes to form nickel or, under an air atmosphere, nickel oxide. The nickel bis(dimethylglyoximate) used above does not fill this requirement but the blue precipitate, N3, which unexpectedly appeared in the early reactions does. Therefore this material is a suitable

substitute for the nickel bis(dimethylglyoximate) and the procedure could be altered to deposit this within the product. To do this, the reactions were prepared to essentially the same composition as the reactions N4 and N5 except nickel chloride replaces nickel perchlorate, the hydroxylamine was used in the hydrochloride form and no diacetyl was used.

Two variations of the reaction were carried out. The first method, N6, starts the formation of the nickel complex at the same time as the reaction to produce the silica. The second method, N7, leaves a period of one and a half hours between starting the reaction to produce silica and the start of the reaction to produce the nickel complex. The delay time was chosen as one which would allow the silica particles to grow to an appreciable size, as determined by the experiments which sampled reactions through time as previously described.

The reactions both produced pale blue solids as the product with the yield being 9.5917g in N6 and 9.3495g in N7. Because the exact nature of the blue precipitate is not known, no percentage theoretical yield can be calculated.

6.4.1 CALCINATION

Samples of both N6 and N7 products were calcined to 450°C to determine what occurs during calcination and to detect the position of the nickel. The mass losses observed during the calcination were

in calcination of N6	14.18%
in calcination of N7	10.51%

In both cases the product of the calcination was a grey solid but with regions appearing green or yellow. The variation in colour may be due to non-stoichiometry in the nickel oxide within the product or due to the presence of nickel chloride, which is yellow, and hydrated nickel chloride which is green.

Based on the mass losses in N3, when calcined in a similar manner, it is possible to estimate the content of nickel complex within the samples. Such a calculation would indicate that N6 contained 37.51% and N7 contains 27.80% of the blue nickel hydroxylamine chloride compound. From the volume of TEOS used it is possible to calculate that 6.17g of silica should have been produced in the reactions. Assuming that the remainder of the product mass was the blue precipitate then the content could be calculated as 30.04% in N6 and 28.30% in N7. Although a good agreement for N7 the values for N6 are not in exact agreement which may indicate variations in composition within the sample.

6.4.2 MICROANALYSIS

The microanalysis results for the products N6 and N7 are shown in table 6.19. These results indicate that the composition of the product is very similar in both cases. Comparison of these results with the microanalysis of N3 would indicate, based on the nitrogen content, that N6 included 26.3% and N7 24.5% of the compound N3. Although slightly lower than the values calculated from the yield of product these values are in the same region as the results previously calculated.

The above results also indicate the hydrogen to nitrogen ratio in these products is higher than in N3. In N6 the ratio N:H is 1:4.07 and in N7 the ratio is 1:4.35 both of which are higher than the 1:3 observed in N3 and expected from the presence of hydroxylamine complexes. This is probably due to the presence of water or silanol groups within the product. The presence of water within the product would explain why the complex content calculated from the product yield would be slightly higher than that calculated from microanalysis results. If the hydrogen unaccounted for by the presence of N3 is assumed to be due to the presence of water then N6 would contain 3.04% by mass and N7 would contain 3.72% by mass water. If the mass of water present is combined with the mass of N3, as calculated from microanalysis, the values are very similar to the mass of product not accounted for by the silica.

	% Carbon	% Hydrogen	% Nitrogen
product N6	nil	1.29	4.44
product N7	nil	1.30	4.20

Table 6.19: Microanalysis results for reaction products N6 and N7.

6.4.3 X-RAY DIFFRACTION

The x-ray diffraction patterns of product N7 and the samples of N6 and N7 calcined to 450°C were obtained. The pattern for product N7 showed only a broad peak between two theta angles of 16° and 28°. This is probably due to the presence of silica.

The d-values and relative intensities of the peaks calculated from the diffraction patterns of N6 and N7 calcined to 450°C are listed in tables 6.20 and 6.21. In both of these patterns there are also broad peaks between two theta angles 7°-10° and 16°-30° which are probably due to the presence of silica, although the broad peak at 7°-10° was observed in the sample of N3.

The peaks which are listed in tables 6.20 and 6.21 indicate that crystalline material is present in these samples. The nature of this material is not completely clear. Both patterns show peaks which correspond to the bunsenite form of nickel oxide, see table 6.13, but also show peaks which do not arise from bunsenite, namely those at 5.574Å, 5.438Å, 4.835Å and 1.734Å. Comparison of these diffraction patterns with those of compounds which could be present, even if an extremely remote possibility, including nickel (A.S.T.M. file 4-850), nickel (III) oxide (A.S.T.M. file 14-481), nickel oxide hydroxides (A.S.T.M. files 6-44, 6-75, 6-141, 6-144, 13-229), nickel silicates (A.S.T.M. files 15-255, 15-384, 15-388, 20-52, 20-791) and nickel silicates (A.S.T.M. files 3-943, 3-1094, 14-429) gives no satisfactory source for the additional peaks. Although the

β-nickel oxide

d-values	I/Io
5.438	99
2.414	61
2.092	100
1.734	33
1.477	42

Table 6.20: X-ray diffraction pattern of product N6 heated to 450°C.

d-values	I/Io
5.574	100
4.835	84
2.414	90
2.092	90

Table 6.21: X-ray diffraction pattern of product N7 heated to 450°C.

hydroxide (A.S.T.M. file 6-141) shows peaks at 4.83 and 2.41Å which correspond to peaks observed in the patterns the other peak of this compound at 1.40Å does not appear and no peak appears in the region of 5.5Å. This would indicate that this material is not present. However comparison with the diffraction patterns of nickel chloride (A.S.T.M. file 1-1134) and hydrated nickel chlorides (A.S.T.M. files 1-200, 1-383, 1-1143) show that these are similar and show peaks which correspond to those in calcined N6 and N5 which do not correspond to bunsenite. Therefore it would appear that these materials contain nickel chlorides. This would explain the presence of chlorine in microanalysis of the calcined samples and the green and yellow colours observed in the samples. Some of these unaccounted for peaks are the same and the paths of formation are probably the same in both samples. A possible explanation for the appearance of these peaks is that during the decomposition of the compound N3 some crystalline intermediates are formed before nickel oxide and that some of these are still present in the samples.

6.4.4 INFRARED SPECTROSCOPY

The infrared spectra of both N6 and N7 are expected to be essentially the same. The spectrum of N6 was obtained and is shown in fig. 6.17. This shows a number of peaks which correspond to those of silica. In addition to these peaks there are peaks at $3440cm^{-1}$ and $1640cm^{-1}$ which can be attributed to vibrations of OH groups either in the specimen or in water held within the potassium bromide disc (Williams and Fleming, 1980). These peaks

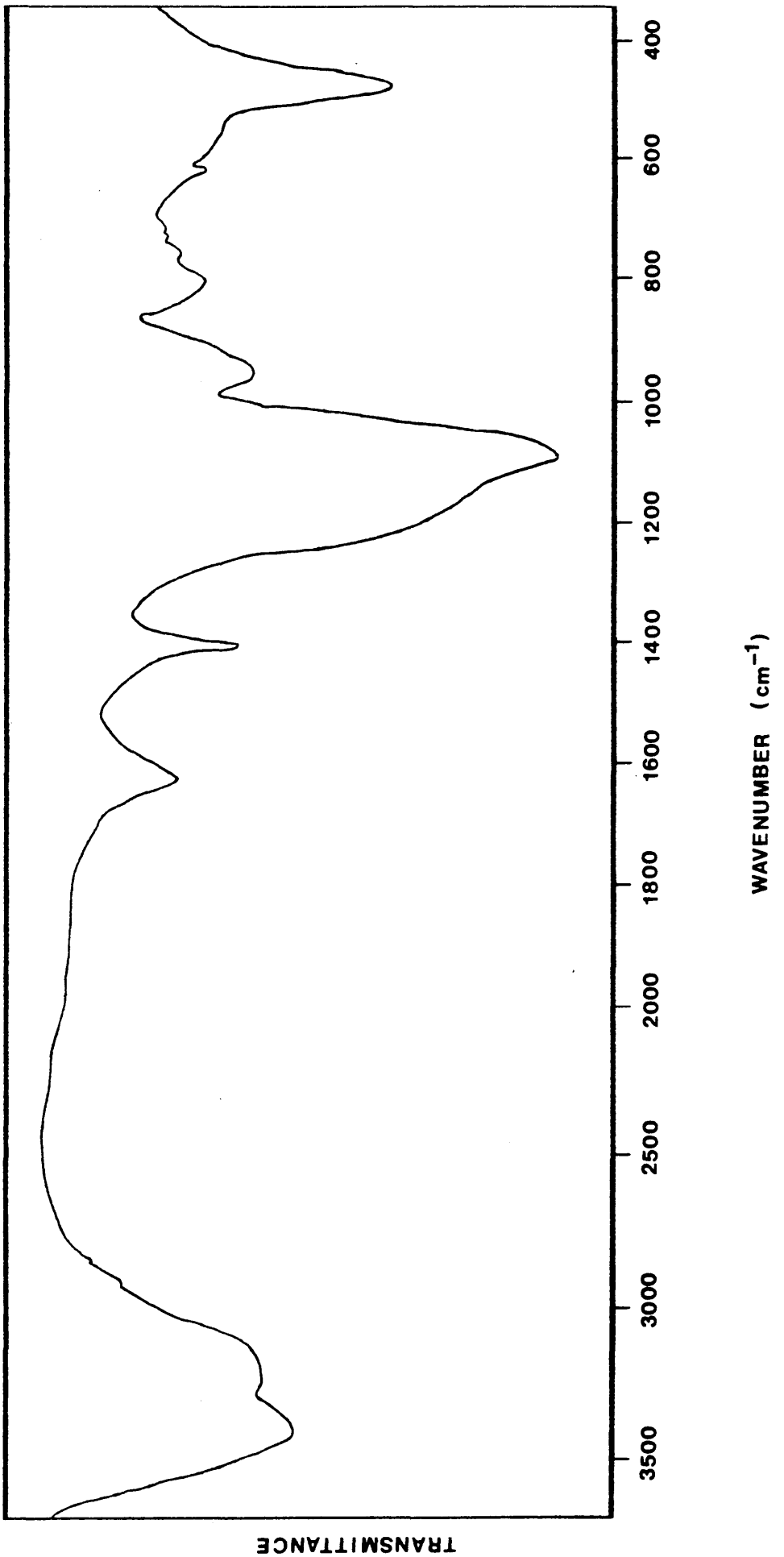

Fig 6.17: IR spectrum of material N6.

occur in the spectrum of N3 due to the vibrations within the hydroxylamine groups. Also present in the N6 spectrum is a peak at 3220cm^{-1} which can be attributed to NH vibrations and is again present in the spectrum of the material N3.

This result is that expected from previous observations of the material - silica with a small amount of N3 included.

6.4.5 ELECTRON MICROSCOPY

Examination of the product N6 in the electron microscope showed it consisted of material of a morphology similar to that of the fused material observed in the base catalysed hydrolysis of TEOS.

On the surface of this material small particles were observed. These small particles appeared crystalline. This type of material is illustrated in plate 6.10. A possible explanation for the observation of crystalline particles in a sample which showed no peaks in the x-ray diffraction pattern is that decomposition of the nickel complex within the electron microscope causes the formation of the crystalline material. The decomposition of the complex may occur as the beam is brought onto the sample or it may be induced by the extreme vacuum maintained within the electron microscope. The process of decomposition which, as mentioned previously, may occur continuously, is based on the loss of volatile species, almost certainly hydroxylamine. Thus exposure to the vacuum within the microscope may greatly accelerate this process.

Samples of the N6 which had been calcined to 450°C were

also examined in the microscope. This sample consisted of fused material as observed in the non-calcined sample but in these samples there appeared to be voids or holes in the material. On the surface of this material were small particles and crystals. The size of these particles and crystals varied but the largest crystals were 200nm across and there were a number at 25nm. There was a much larger number of smaller particles on the surface of the fused material and on the carbon film. This type of material is shown in plate 6.11. The electron diffraction patterns of these areas correspond to the bunsenite form of nickel oxide but there are also other peaks, the main ones being at 2.843Å, 1.715Å and 1.688Å. These peaks do not clearly match any of the diffraction patterns listed in section 6.4.3. It is possible that these peaks are due to the presence of an intermediate. Such an intermediate may not appear in the x-ray diffraction pattern because of a low abundance but would still be detectable in selected area electron diffraction because of the small amount of sample involved.

Examination of the product N7 showed that it consisted of spherical particles, many of which had come together into aggregates. The diameters of these particles were determined, although difficult because of the presence of smaller particles on the surface, and the average figure is 125nm although this was from a small number of particles. The original composition of this reaction mixture corresponds to one which, if allowed to react to produce pure silica, forms particles of diameter 167nm. It would therefore appear that the addition of the reagents necessary for the formation of the nickel complex had an affect on

the reaction producing the silica. The surface of these spherical particles appeared covered with small particles which appeared crystalline. See plate 6.12. The size of these small particles vary but the larger of these particles appear to be in the region of 8nm in diameter and the smaller particles to be 1-2nm in diameter. There also appeared to be even smaller particles which could not be clearly resolved on the surface of the silica. The explanation for the appearance of the crystalline material could be the same as for that in the product N6.

The samples of N7 which had been calcined to 450°C were examined. These consisted of spherical and roughly spherical particles. On the surface of these particles and on the carbon film in the area of the surface were a large number of small particles which appeared crystalline. As shown in plate 6.13. The size of the crystalline particles varied greatly, with some crystals being 150nm across but the vast majority were in the region 5-10nm. The electron diffraction patterns of the areas of these small particles had diffraction patterns similar to that of the bunsenite form of nickel oxide.

6.4.6 DISCUSSION

It would appear, from the above discussion, that the reactions N6 and N7 produce the same material with the major difference being the morphology of the silica. This situation could arise as follows. In reaction N6 the silica was produced in a solution which contained an ionic nickel salt. This alters the morphology of the silica by reducing the electrical double layer

Plate 6.10: Material N6 showing material of a morphology similar to the fused material with small crystalline particles on the surface.

Magnification = $241{\cdot}5 \times 10^3$

1cm = $41{\cdot}41$nm

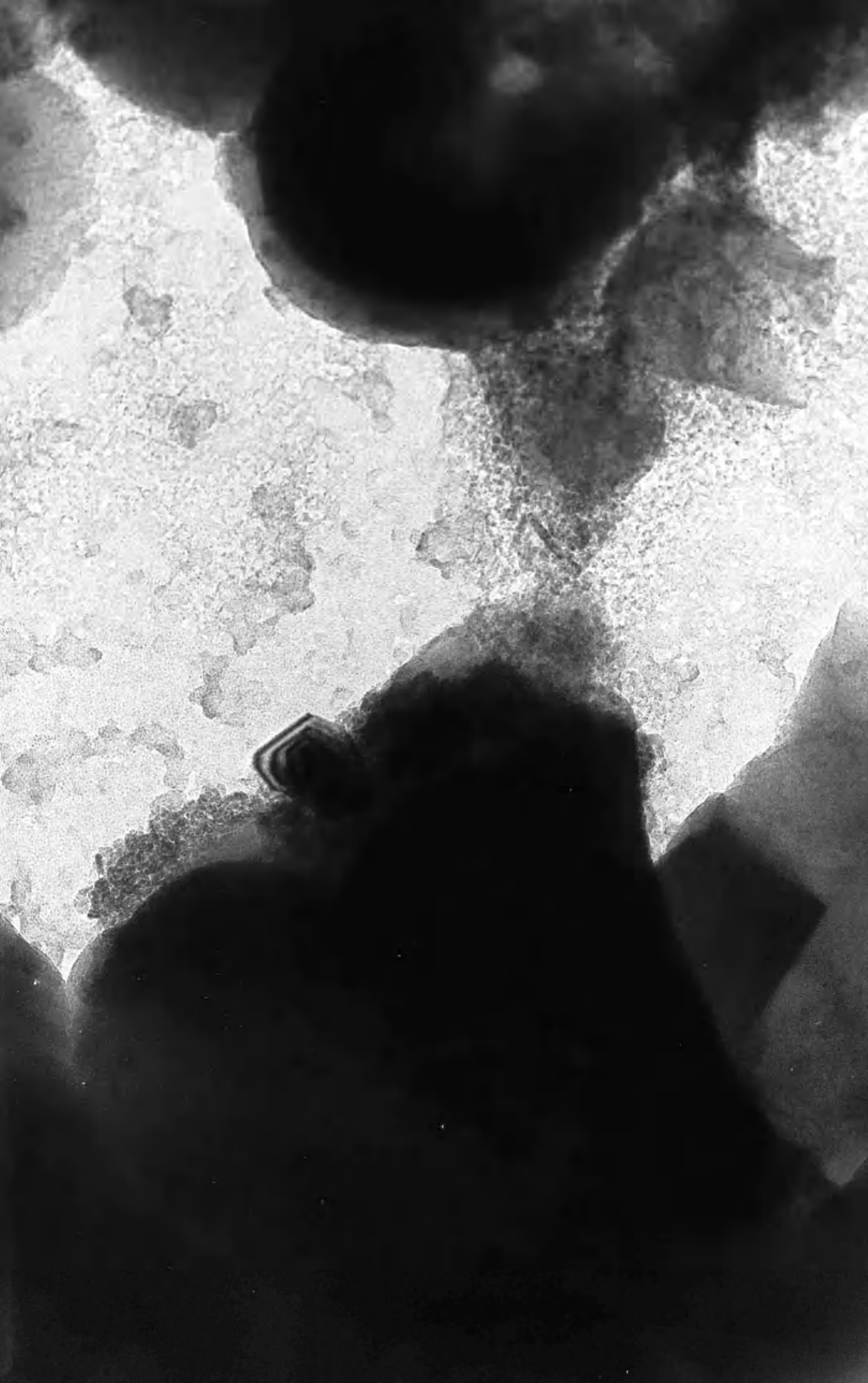

Plate 6.11: Material N6 calcined to 450°C showing fused morphology with voids and crystals.

Magnification = 132×10^3

1cm = $75{\cdot}76$ nm

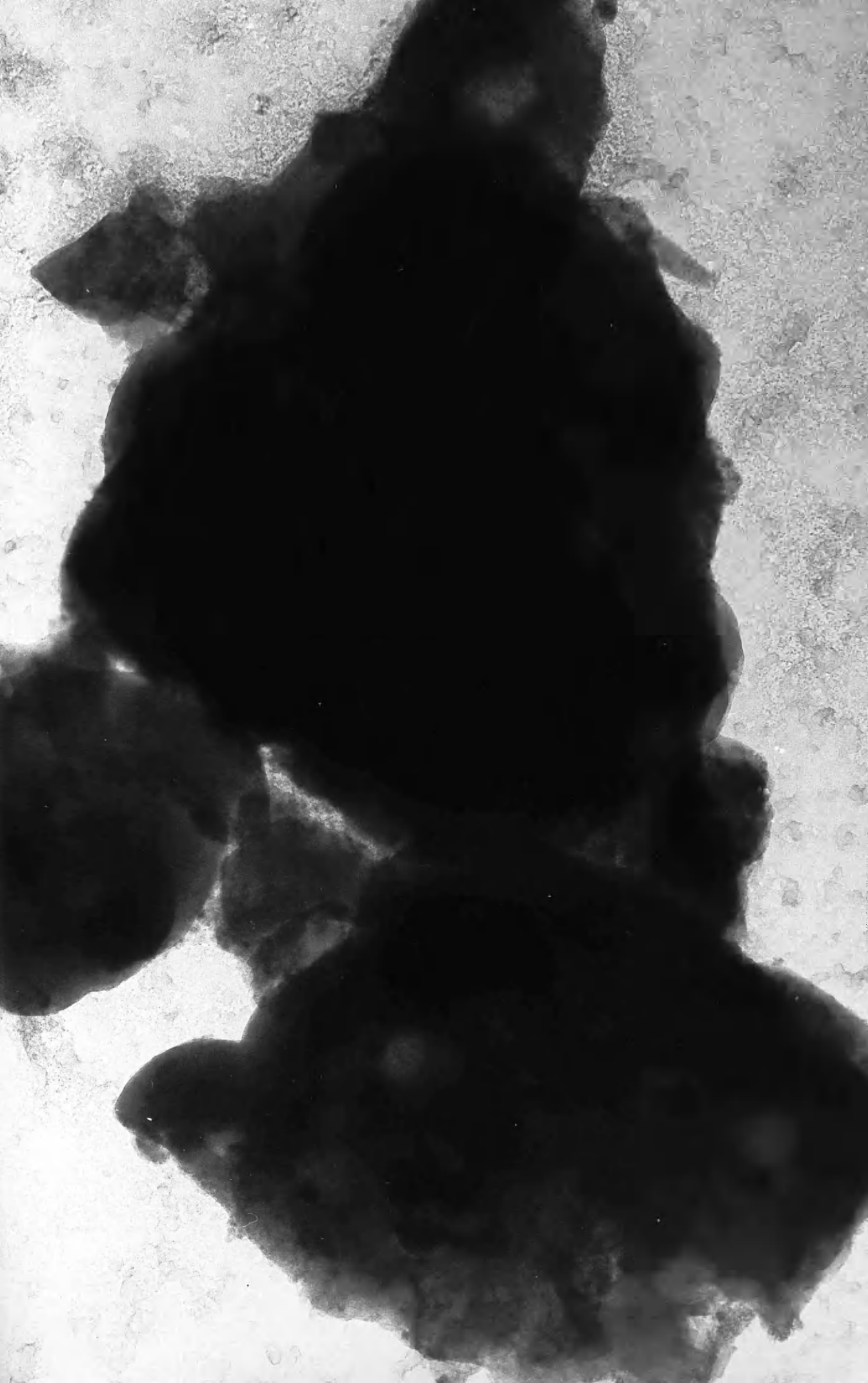

Plate 6.12: Material N7 showing spherical particles with crystalline particles on the surface.

Magnification = 702×10^3

1cm = $14{\cdot}24$ nm

Plate 6.13: Material N7 calcined to 450°C showing spherical particles with crystals on surface.

Magnification = 390×10^3

1cm = 25·64nm

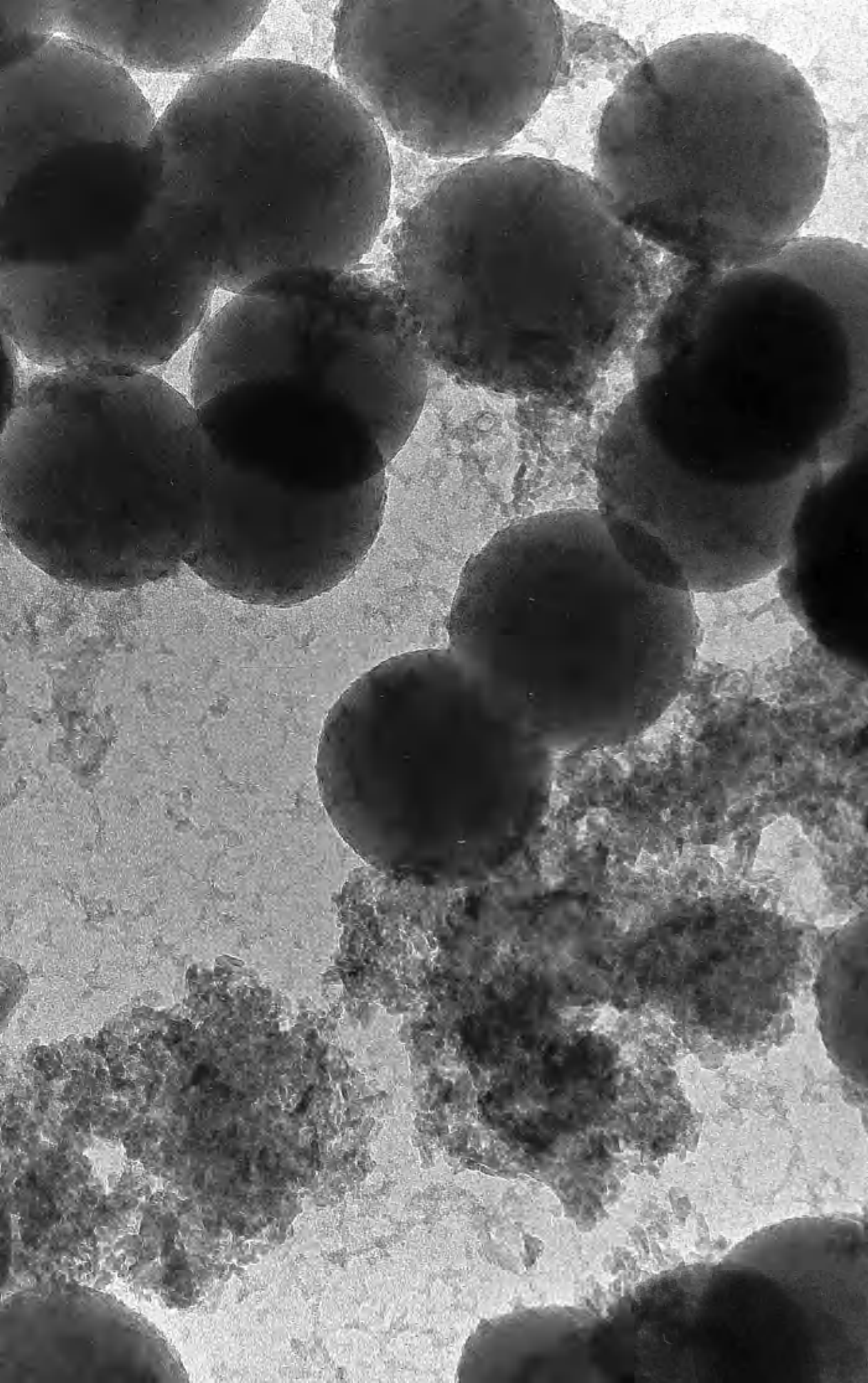

surrounding the particles of silica and allowing them to aggregate in the manner already described for the fused material observed in the base catalysed TEOS reactions. In the reaction N7 the procedure was varied so that the ionic salt was added a considerable time after the beginning of the TEOS hydrolysis reaction. Therefore the silica particles grew under conditions which normally lead to the formation of spherical particles before the ionic salt was added. Thus at the point of the addition of the nickel salt the reaction mixture contained a suspension of colloidal silica particles. The thickness of the electrostatic double layer of these particles was then reduced leading to the aggregation of these particles. This explains why the two reactions produce two different morphologies of silica.

The distribution of the nickel complexes within the sample is not easily determined. In both samples there appeared to be nickel oxide, indicating the prior presence of the nickel complex, on the surface of the silica and in the surrounding area. This indicates that some of the compound was on the surface of the silica or within a short distance of it. The small crystalline particles on the carbon grid in the area of the surface could be particles which were separated form the surface during sample preparation for electron microscopical examination. In the case of reaction N6 there appeared to be voids or holes within the silica which may be caused by the decomposition of the nickel complex. This may indicate the presence of the nickel complex throughout the silica. This interpretation is supported by the fact that the particulate material observed in the reaction N3 was not observed, so that it is reasonable to suggest that none, or

very little, of the blue precipitate formed as particles on its own. Therefore this compound must be included within the material which has been observed within the sample.

This distribution of the material, in N6, would be explained by the reaction producing silica and the nickel compound occurring simultaneously. Thus the nickel compound will be deposited within the silica structure. In the case of N7, the nickel deposition was only begun after the silica particles had grown to a considerable size. Therefore the nickel complex was only deposited near the outer surface of the silica particles. This explains the observations above. It is however not possible to determine whether, in the case of N7, the nickel is deposited in the silica near the surface or just on the surface of the particles.

6.5 CONCLUSIONS

The aim of the experiments described above was the controlled deposition of a source of nickel within the silica produced by hydrolysis of TEOS. In particular, to carry out the deposition in such a manner that the nickel source is positioned a short distance below the outer surface of the spherical silica particles.

The original method employed was the deposition of nickel bis(dimethylglyoximate). This technique illustrated a number of problems which arise. The first is that the presence of the reagents necessary for the production of the nickel bis(dimethylglyoximate) have a direct affect on the overall

composition of the reaction by forming complex molecules. In this case hexamminonickel and nickel hydroxylamine complexes which remove basic species from the solution and thus lower the pH. This in turn alters the conditions under which the TEOS hydrolysis occurs, altering the morphology of the silica produced to small irregular particles and slowing the rate of the production of the silica.

The second problem which arises is that the nickel hydroxylamine complex forms a precipitate which appears to be the chloride form of the complex. The consequences of this are that the nickel containing particles are separated from the silica and larger than would be desirable for the use in catalysis.

The calcination of these samples cause the decomposition of the nickel hydroxylamine chloride precipitate by a process involving a number of steps. These steps are believed to occur by the loss of hydroxylamine to form nickel chloride and nickel oxide of the bunsenite form. This decomposition leads to the formation of hollow particles which have an outer layer and a hollow centre which often includes crystals of nickel oxide.

By altering the conditions in which the reactions are carried out so that no chloride ions are present the formation of the precipitate of nickel hydroxylamine chloride can be avoided. Also adjusting the ammonia content of the reaction to account for that removed by forming a complex with nickel prevents a drop in pH to a region which would be expected to produce a different morphology of silica. However these adjustments cause several other problems to become apparent.

The presence of the ionic salt in the reaction mixture

decreases the electrostatic double layer surrounding the silica particles as they form so allowing them to aggregate and form material of a morphology similar to that of the fused material described in chapter 5. A further problem which can arise in the reactions is that as well as the desired nickel incorporation into the silica there appears to be incorporation of the silica into the nickel complex. This occurs because both materials begin to appear concurrently and so particles of both silica and nickel bis(dimethylglyoximate) are nucleated and some of the other compounds are incorporated by using these as growth sites.

It also becomes clear from the mass losses during calcination and the low content of nickel oxide within the final product that the nickel bis(dimethylglyoximate) deposited within the sample sublimes rather than decomposes to form nickel oxide.

In view of these difficulties the reaction can be carried out to deposit the nickel hydroxylamine chloride precipitate rather than the nickel bis(dimethylglyoximate) originally used. The alteration overcomes the loss of the nickel from the sample and appears to overcome the deposition of silica within the complex. However it does not overcome the alteration of the morphology of the silica produced because the growth of the silica still occurs in a solution containing an ionic salt. By altering the procedure so that the nickel salt is added at a later stage of the reaction the depletion of the electrostatic double layer, which causes the alteration of the morphology, can be delayed and its effect altered from a complete change of morphology to making spherical particles more likely to aggregate. This last alteration also has the effect of positioning the precipitate of

nickel closer to the surface of the silica particles.

Therefore it is possible to produce spherical silica particles with a nickel containing material deposited near or on the surface. This can be calcined to give nickel oxide or almost certainly nickel, if calcined under the correct conditions, near or on the surface of the silica particles.

6.6 FUTURE WORK

1. Examination of thin sections of the product of N7 may show whether the nickel is deposited on or below the surface of the particles of silica.

2. It is possible that by carrying out the reactions in the presence of material such as ethylenediamminotetracetate which complex to nickel the effect of the nickel on the electrical double layer could be minimised.

3. Samples could be calcined in a reducing atmosphere, such as hydrogen or carbon monoxide, to determine if the nickel complexes would be converted to nickel.

4. The surface area of the metal could be determined by absorption of carbon monoxide. This would give a measure of the metal particle size and would indicate how successful the material may be as a catalyst.

5. The material could be used as a catalyst for a reaction and the products determined to calculate the selectivity of the material as compared to conventionally produced catalysts.

6. Investigate other nickel complexes which may be more suitable for deposition within the silica.

7. Attempt addition of additional TEOS to reactions which have produced metal coated particles to form a further silica layer. It is possible that the new silica would not be deposited on the nickel and thus the nickel particles would be position at the bottom of channels within the silica.

8. Try applying vacuum to N3 to determine if this is what caused decomposition.

9. The decompositions of the precipitate N3 could be illuminated by heating the material, and collecting the material given off and identifying the IR spectroscopy.

10. Electron microscopical examination of the beam sensitive samples may be possible using low dose techniques and image processing.

11. Investigate the possible use of nickel alkoxides as the source of nickel. Thus hydrolysis of a mixture of alkoxides may allow the formation of very small nickel oxide particles bonded to the silica.

REFERENCES

Abbé, E. (1873). Arch. Mikrosk. Anat. Entwicklungsmech, 9, 413.

Adams, D.M. (1981). "Inorganic Solids", John Wiley & Sons, Chichester.

Adams, J., Baird, T., Braterman, P.S., Cairns, J.A.A. and Segal, D.L. (1988). In "Better Ceramics Through Chemistry III", (Brinker, C.J., Clark D.E. and Ulrich, D.R., Eds.), Mater. Res. Soc. Symp. Proc. 121, p. 361-366, Mater. Res. Soc., Pittsburgh.

Aelion, R., Loebel, A. and Erich, F. (1950). J. Am. Chem. Soc., 72 5705.

Agar, A. (1960). J. Appl. Phys., 11, 504.

Ahmed, H. (1971). Electron Microsc. Anal. (Nixon, W.C., Ed.), Inst. Phys. Conf. Ser., No. 10, P.30, London.

Allpress, J.G., Hervat, F.A., Moodie, A.F. and Sanders, J.V. (1972). Acta Cryst., A28, 528.

Andrews, K.H., Dyson, D.J. and Keown, S.R. (1967). "Electron Diffraction Patterns", Hilger, London.

Arfsten, N.J. (1984). J. Non-Cryst. Solids, 63, 243.

Artaki, I., Zerda, T.W., Jonas, J. (1986). J. Non-Cryst. Solids, 81, 381.

Ashley, C.S. and Reed S.T. (1986). In "Better Ceramics Through Chemistry II", (Brinker, C.J., Clark, D.E. and Ulrich, D.R., Eds.), Mater. Res. Soc. Symp. Proc. 73, p. 671-677, Mater. Res. Soc., Pittsburgh.

Assink, R.A. and Kay, B.D. (1988). J. Non-Cryst. Solids, 99, 359.

A.S.T.M. Index (1965). Publication P 0, 15 - 151.

Backer, R.H. (1938). J. Am. Chem. Soc., 60, 2673.

Bailey, J.K. and Mecartney, M.L. (1988). In "Better Ceramics Through Chemistry III", (Brinker, C.J., Clark D.E. and Ulrich, D.R., Eds.), Mater. Res. Soc. Symp. Proc. 121, p.367-372, Mater. Res. Soc., Pittsburgh.

Baird, T. (1982). Chem. Soc. Specialist Periodical Reports 36, Catalysis No. 5, 172.

Balfe, C.A. and Martinez, S.L. (1986). In "Better Ceramics Through Chemistry II", (Brinker, C.J., Clark D.E. and Ulrich, D.R., Eds.), Mater. Res. Soc. Symp. Proc. 73, p.27-33, Mater. Res. Soc., Pittsburgh.

Barby, D., Griffiths, T., Jacques, A.R. and Pawson, D. (1977). In "The Modern Inoranic Chemicals Industry", (Thomson, R., Ed.), p.320-354, Royal Society of Chemistry, London.

Barford, N.C. (1967). "Experimental Measurement : Precision, Error and Truth", Addison-Wesley, London.

Barringer, E., Jubb, N., Fegely, B., Pober, R.L. and Bowen, H.K. (1984). In "Ultrastructure Processing of Ceramics, Glasses and Composites", (Hench, L.L. and Ulrich, D.R., Eds.), p. 315-333, John Wiley & Sons, New York.

Barringer, E.A. and Bowen, H.K. (1985). Ceram. Eng. and Sci. Proc., 5, 285.

Barten, H., Janssen, F., Kerkhof, F.V.D., Leferink, R., Vogt, E.T.C., Van Dillen, A.J. and Geus, J.W. (1987). In "Preparation of Catalysts IV", (Delmon, B., Grange, P., Jacobs, P.A. and Poncelet, G., Eds.), p. 103-111, Elsevier, Amsterdam.

Batson, P.E., Chen, C.H. and Silcox, J. (1976). Proc. 34th Ann. Meet. Electron Microsc. Soc. Am., (Bailey, G.W., Ed.), p.534, Claitor, Baton Rouge.

Bednorz, J.G. and Müller, K.A. (1986). K. Phys., B64, 189.

Beetson, B.E.P. (1972). In "Practical Methods in Electron Microscopy", (Glauert, A.M., Ed.), Vol. 1, p.192, North-Holland, Amsterdam.

Belova, L.B. and Fedorovich, L.D. (1985). Inorg. Materials, 21, 710.

Boerchia, A. and Bonhomme, P. (1974). Optik (Stuttgart), 39, 437.

Boersch, H. (1936). Annalen der Physik, (5), 27, 75.

Bogush, G.H. and Zukoski IV, C.F. (1987). Mater. Sci. Res. (Ceram. Microstruct. '86), 21, 475.

Bogush, G.H., Tracey, M.A. and Zukoski IV, C.F. (1988a). J. Non-Cryst. Solids, 104, 95.

Bogush, G.H., Dickstein, G.L., Lee, P., Zukoski, K.C. and Zukoski IV, C.F. (1988b). In "Better Ceramics Through Chemistry III", (Brinker, C.J., Clark, D.E. and Ulrich, D.R., Eds.), Mater. Res. Soc. Symp. Proc. 121, p. 57-66, Mater. Res. Soc., Pittsburgh.

Bouquin, O., Blanchard, N. and Colomban, Ph. (1987). In "High Tech. Ceramics, Part A", (Vincenzini, P., Ed.), Mater. Sci. Mono. (1987), 38A, p. 717-726, Elsevier, Amsterdam.

Bradley, D.C., Mehrotra, R.C. and Wardlaw, W. (1952). J. Chem. Soc., 5020.

Bradley, D.C., Mehrotra, R.C. and Gaur, D.P. (1978). "Metal Alkoxides", Academic Press, London.

Braley-Smith, E., (Ed.), (1975). "Principles of Chemical Processes, Chemical Kinetics, Part 1", Open University Press, Milton Keynes.

Bridger, K., Fairhurst, D. and Vincent, B. (1979). J. Coll. Interf. Sci., 68, 190.

Brinker, C.J. (1988). J. Non-Cryst. Solids, 100, 31.

Brinker, C.J. and Harrington, M.S. (1981). Solar Energy Materials, 5, 159.

Brinker, C.J., Keefer, K.D., Schaefer, D.W. and Ashley, C.S. (1982). J. Non-Cryst. Solids, 48, 47.

Brinker, C.J., Clark, D.E. and Ulrich, D.R.,(Eds), (1984a). "Better Ceramics Through Chemistry", Mater. Res. Soc. Symp. Proc. 32, North-Holland, Amsterdam.

Brinker, C.J., Keefer, K.D., Schaefer, D.W., Assink, R.A., Kay, B.D. and Ashley, C.S. (1984b). J. Non-Cryst. Solids, 63, 45.

Brinker, C.J., Keefer, K.D., Schaefer, D.W., Assink, R.A., Kay, B.D. and Ashley, C.S. (1984c). J. Non-Cryst. Solids, 63, 45.

Brinker, C.J., Drotning, W.D. and Scherer, G.W. (1984d). In "Better Ceramics Through Chemistry", (Brinker, C.J., Clark, D.E. and Ulrich D.R., Eds.), Mater. Res. Soc. Symp. Proc. 32, p. 25-39, North-Holland, Amsterdam.

Brinker, C.J., Clark, D.E. and Ulrich, D.R., (Eds.), (1986a). "Better Ceramics Through Chemistry II", Mater. Res. Soc. Symp. Proc. 73, Mater. Res. Soc., Pittsburgh.

Brinker, C.J., Tallant, D.R., Roth, E.P. and Ashley, C.S. (1986b). J. Non-Cryst. Solds, 82, 117.

Brinker, C.J., Clark, D.E. and Ulrich, D.R., (Eds.), (1988a). "Better Ceramics Through Chemistry III", Mater. Res. Soc. Symp. Proc. 121, Mater. Res. Soc., Pittsburgh.

Brinker, C.J., Bunker, B.C., Tallant, D.R., Ward, K.J. and Kirkpatrick, R.J. (1988b). A.C.S. Symp. Ser. 360, Inorg. Organomet. Polym., 360, 314.

Brown, D.A., Cunningham, D. and Glass, W.K. (1966). Chem. Commun., 306.

Brown, L.M. and Mazdiyasni, K.S. (1970). Inorg. Chem., 9, 2783.

Brown, R.K. and Pantano, C.G. (1984). In "Better Ceramics Through Chemistry", (Brinker, C.J., Clark, D.E. and Ulrich, D.R., Eds.), Mater. Res. Soc. Symp. Proc. 32, p. 361-367, North-Holland, Amsterdam.

Bunker, B.C. (1988). In "Better Ceramics Through Chemistry II", (Brinker, C.J., Clark, D.E. and Ulrich, D.R., Eds.), Mater. Res. Soc. Symp. Proc. 73, p. 49-56, Mater. Res. Soc., Pittsburgh.

Burton, E.F., Sennett, R.S. and Ellis, S.G. (1947). Nature (London), 160, 565.

Busch, H. (1926). Ann. Phys. (Leipzig), 81, 974.

Busch, H. (1927). Arch. Elektrotech. (Berlin), 18, 583.

Buseck, P.R., (Ed.),(1985). High Resolution Electron Microscopy, Proc. Arizona State Univ. Symp. High-Resolut. Electron Microsc., Ultramicroscopy, 18, (1-4).

Cairns, J.A., Segal, D.L. and Woodhead, J.L. (1984). In "Better Ceramics Through Chemistry", (Brinker, C.J., Clark, D.E. and Ulrich, D.R., Eds.), Mater. Res. Soc. Symp. Proc. 32, p. 135-138, North-Holland, Amsterdam.

Cairns-Smith, A.G. (1982). "The Genetic Takeover", Cambridge University Press, Cambridge.

Calvert, P. (1986). In "Better Ceramics Through Chemistry II", (Brinker, C.J., Clark, D.E. and Ulrich, D.R., Eds.), Mater. Res. Soc. Symp. Proc. 73, p. 79-84, Mater. Res. Soc., Pittsburgh.

Carman, L.A. and Pantano, C.G. (1986). In "Science of Ceramic Chemical Processing", (Hench, L.L. and Ulrich, D.R., Eds.), p. 187-200, John Wiley & Sons, New York.

Catone, D.L. and Matijevic, E. (1974). J. Coll. Interf. Sci., 48, 291.

Chappell, J.S., Birchall, J.D. and Ring, T.A. (1986). Proc. Br. Ceram. Soc., 38, 49.

Charbouillot, Y., Ravaine, D., Armand, M. and Poinsignon, C. (1988). J. Non-Cryst. Solids, 103, 325.

Chatterjee, M. and Ganguli, D. (1986). Trans. Indian Ceram. Soc., 45, 95.

Chen, K.C., Tsuchiya, T. and MacKenzie, J.D. (1986). J. Non-Cryst. Solids, 81, 227.

Cheng, F.W. (1959). Microchem. J., 3, 537.

Cheng, Y. and Hench, L.L. (1988). In "Better Ceramics Through Chemistry III", (Brinker, C.J., Clark, D.E. and Ulrich, D.R., Eds.), Mater. Res. Soc. Symp. Proc. 121, p. 593-596, Mater. Res. Soc., Pittsburgh.

Clark, W.K.R., Chapman, J.N. and Ferrier, R.P. (1979). Nature (London), 277, 368.

Clark, W.K.R., Chapman, J.N., MacLeod, A.M. and Ferrier, R.P. (1980). Ultramicroscopy, 5, 195.

Colby, M.W., Osaka, A. and MacKenzie, J.D. (1986). J. Non-Cryst. Solids, 82, 37.

Cole, S.H. and Monroe, E.A. (1967). J. Appl. Phys., 38, 1872.

Cosslett, V.E. (1951). "Practical Electron Microscopy", Butterworth, London.

Cosslett, V.E. (1981a). Contemp. Phys., 22, 3.

Cosslett, V.E. (1981b). Contemp. Phys., 22, 147.

Cosslett, V.E. (1987). Adv. Opt. Electron Microsc., (Barer, R. and Cosslett, V.E., Eds.), Vol. 10, p.215, Academic Press, London.

Cosslett, V.E., Camps, R.A., Saxton, W.O., Smith, D.J., Nixon, W.C., Ahmed, H., Catto, C.J.D., Cleaver, J.R.A., Tims, K.C.A., Turner, P.W. and Ross, P.M. (1979). Nature (London), 281, 49.

Cowley, J.M. (1975). "Diffraction Physics", North-Holland, Amsterdam.

Cowley, J.M. (1979). In "Introduction to Analytical Electron Microscopy", (Hren, J.J., Goldstein, J.I. and Joy, D.C., Eds.), p. 1, Plenum, New York.

Cowley, J.M. and Moodie, A.F. (1957), Acta Cryst., 10, 609.

Crewe, A.V., Eggenberger, D.N., Wall, J. and Welter, L.M. (1968). Rev. Sci. Instrumen., 39, 576.

Dahmen, U., Kim, M.G. and Searcy, A.W. (1987). Ultramicroscopy, 23, 365.

Davison, C. and Germer, L.H. (1927). Phys. Rev., 30, 705.

de Broglie, L. (1924). Philos. Mag., 47, 446.

Dislich, H. (1985). J. Non-Cryst. Solids, 73, 599.

Dislich, H. and Hinz, P. (1982). J. Non-Cryst. Solids, 48, 11.

Dixon, J.K., LaMer, V.K., Cassian Li, Messinger, S. and Linford, H.B. (1967). J. Coll. Interf. Sci., 23, 465.

Doak, G.O. and Freedman, L.D. (1961). Chem. Rev., 61,31.

Dorn, R., Baumgartner, A., Gutu-Nelle, A., Rehm, W., Schneider, R., Schneider, S. and Haupt, H. (1987). Glastech. Ber., 60, 79.

Du Pont Company (1988a). Data Sheet, H-06064.

Du Pont Company (1988b). Bulletin, E-94776.

Duran, A., Serna, C., Fornes, V. and Fernandez Navarro, J.M. (1986). J. Non-Cryst. Solids, 82, 69.

Ebelman, J.J. (1846). Ann., 57, 331.

Ebelman, J.J. and Bouquet, M. (1846). Ann. Chim. Phys., 17, 54.

Eichorst, D.J. and Payne, D.J. (1988). In "Better Ceramics Through Chemistry III", (Brinker, C.J., Clark, D.E. and Ulrich, D.R., Eds.), Mater. Res. Soc. Symp. Proc. 121, p. 773-778, Mater. Res. Soc., Pittsburgh.

Eisenhandler, C.B. and Siegel, B.M. (1966). J. Appl. Phys., 37, 1963.

English, C.A. and Venables, J.A. (1971). Electron Microsc. Anal. (Nixon, W.C., Ed.), Inst. Phys. Conf. Ser. No. 10, p. 40, London.

Ethyl Corpn. (1955). Brit. Patent 727,923.

Etridge, J. and Sugden, S. (1928). J. Chem. Soc., 989.

Everett, D.H. (1988). "Basic Principles of Colloid Science", The Royal Society of Chemistry, London.

Everhart, I.E., Oatley, C.W. and Wells, O.C. (1959). J. Electronics and Control, 7, 97.

Ewell, R.H. and Insley, H. (1935). J. Natl. Bur. Stand., 15, 173.

Feeney, P.J., Napper, D.H. and Gilbert, R.G. (1984). Macromol., 17, 2520.

Fegley, B. and Barringer, E.A. (1984). In "Better Ceramics Through Chemistry", (Brinker, C.J., Clark D.E. and Ulrich, D.R., Eds.), Mater. Res. Soc. Symp. Proc. 32, p. 187-197, North-Holland, Amsterdam.

Ferguson, D.E., Deans, O.C. and Douglas, D.A. (1964). Third United Nations International Conference on the Peaceful Uses of Atomic Energy, Vol.11, A/Conf.28/P/237.

Fleer, G.J. and Lyklema, J. (1974). J. Coll. Interf. Sci., 46, 1.

Fox, J.R., White D.A., Oleff, S.M., Boyer, R.D. and Budinger, P.A. (1986). In "Better Ceramics Through Chemistry II", (Brinker, C.J., Clark D.E. and Ulrich, D.R., Eds.) Mater. Res. Soc. Symp. Proc. 73, p. 395-400, Mater. Res. Soc., Pittsburgh.

Frank, J. (1973). Optik (Stuttgart), 38, 519.

Frondel, C. (1979). Am. Mineral., 64, 799.

Fryer, J.R. (1978). Acta Cryst., A34, 603.

Fryer, J.R. (1979). "The Chemical Applications of Transmission Electron Microscopy", Academic Press, London.

Fryer, J.R. (1983). Mol. Cryst. Liq. Cryst., 96, 275.

Fryer, J.R., Cleaver, J.R.A. and Smith, D.J. (1980). Electron Microsc. Anal. (Mulvey, T., Ed.), Inst. Phys. Conf. Ser., No. 52, p. 287, London.

Fryer, J.R. and Holland, F. (1983). Ultramicroscopy, 11, 67.

Fryer, J.R. and Smith, D.J. (1984). J. Micros. (Oxford), 141, 3.

Gallagher, D. and Klein, L.C. (1986). J. Coll. Interf. Sci., 109, 40.

Geffcken, W. and Berger, E. (1939). Dtsch. Reichspaten 736 411.

Geiss, R.H. (1979). In "Introduction to Analytical Electron Microscopy", (Hren, J.J., Goldstein, J.I. and Joy, D.C., Eds.), p. 43, Plenum, New York.

George, P.D. and Newkirk, E.A. (1960), J. Org. Chem., 25, 1645.

Geus, J.W. (1983). In "Preparation of Catlysts III", (Poncelet, G., Grange, P. and Jacobs, P.A., Eds.), p. 1-33, Elsevier, Amsterdam.

Gladstone, J.H. and Tribe, A. (1881). J. Chem. Soc., 39, 4

Godycki, L.E. and Rundle, R.E. (1953), Acta Cryst., 6, 487.

Gonzalez-Oliver, C.J.R., James, P.F. and Rawson, H. (1982). J. Non-Cryst. Solids, 48, 129.

Goodman, P., (Ed.), (1981). "Fifty Years of Electron Diffraction", Reidel, Dordrecht.

Goodman, P. and Moodie, A.F. (1974). Acta Cryst., A30, 280.

Gordon, L. and Salesin, E.D. (1961). J. Chem. Ed., 38, 16.

Greenwood, N.N. and Earnshaw, A. (1984). "Chemistry of the Elements", Pergamon Press, Oxford.

Grinton, G.R. and Cowley, J.M. (1971). Optik (Stuttgart), 34, 221.

Grivet, P. (1972). "Electron Optics", 2nd Edition, Pergamon, Oxford.

Guglielmi, M. and Carturan, G. (1988). J. Non-Cryst. Solids, 100, 16.

Hachisu, S., Kose, A., Kobayashi, Y. and Takano, K. (1976). J. Coll. Interf. Sci., 55, 499.

Haine, M.E. and Mulvey, T. (1954). Proc. 3rd Int. Conf. on Electron Microscopy, p. 698, London.

Haine, M.E. and Cosslett, V.E. (1961). "The Electron Microscopy", Spon, London.

Hall, C.E. (1966). "Introduction to Electron Microscopy", 2nd Edition, McGraw-Hill, New York.

Hall, C.E. and Hines, R.L. (1970). Philos. Mag., 21, 1175.

Hanzen, K.J. (1971). Adv. Opt. Electron Microscopy, 4, 1.

Hanzen, K.J. and Trepte, L. (1971). Optik (Stuttgart), 32, 519.

Harris, M.T. and Byres, C.H. (1988). J. Non-Cryst. Solids, 103, 49.

Harris, M.T., Byres, C.H. and Brunson, R.R. (1988). In "Better Ceramics Through Chemistry III", (Brinker, C.J., Clark D.E. and Ulrich, D.R., Eds.), Mater. Res. Soc. Symp. Proc. 121, p. 287-292, Mater. Res. Soc., Pittsburgh.

Hawkes, P.A. (1972). "Electron Optics and the Electron Microscope", Academic Press, New York.

Hawkes, P.A. (1985). "The Beginnings of Electron Microscopy", Academic Press, New York.

Heinrich, R.D. (1964). "Fundamentals of Transmission Electron Microscopy", Wiley Interscience, New York.

Hench, L.L. (1986). In "Science of Ceramic Chemical Processing", (Hench, L.L. and Ulrich, D.R., Eds.), p. 52-64, John Wiley & Sons, New York.

Hench, L.L., Orcel, G. and Nogues, J.L. (1986). In "Better Ceramics Through Chemistry II", (Brinker, C.J., Clark, D.E. and Ulrich, D.R., Eds.), Mater. Res. Soc. Symp. Proc. 73, p. 35-47, Mater. Res. Soc., Pittsburgh.

Hermans, M.E.A. (1964). Third United Nations International Conference on the Peaceful Uses of Atomic Energy, Vol. 11, A/Conf.28/P/634.

Hillier, J. and Vance, A.W. (1945). "Electron Optics and the Electron Microscope", Wiley, New York.

Hirsch, P.B., Howie, A., Nicholson, R.B., Pashley, D.W. and Whelan, M.J. (1965). "Electron Microscopy of Thin Crystals", Butterworth, London.

Hobbs, L.W. (1979). In "Introduction to Analytical Electron Microscopy", (Hren, J.J., Goldstein, J.I. and Joy, D.C., Eds.), p. 437, Plenum, New York.

Hobbs, L.W. (1987). Ultramicroscopy, 23, 339.

Holland, F., Fryer, J.R. and Baird, T. (1983). Electron Microsc. Anal. (Doig, P., Ed.), Inst. Phys. Conf. Ser., No. 68, p. 19, London.

Horowitz, H.S., McLain, S.J., Sleight, A.W., Druliner, J.D., Gai, P.L., Van Kavelaar, M.J., Wagner, J.L., Biggs, B.D. and Poon, S.J. (1989). Science, 243, 66.

Hosemann, R., Hentschel, M.P., Schmeisser, V. and Brückner, B. (1986). J. Non-Cryst. Solids, 83, 223.

Hou, L. and Sakka, S. (1989). J. Non-Cryst. Solids, 112, 424.

Hughes, M.N. and Shrimanker, K. (1976). Inorg. Chem. Acta, 18, 69.

Hunter, R.J. (1987). "Foundations of Colloid Science", Vol. 1, Oxford University Press, Oxford.

Hyde, J.F. and Curry, J.W. (1955). J. Am. Chem. Soc., 77, 3140.

Iijima, S. (1977). Optik (Stuttgart), 48, 193.

Iler, R.K. (1964). J. Coll. Interf. Sci., 19, 648.

Iler, R.K. (1965). Nature (London), 207, 472.

Iler, R.K. (1975). J. Coll. Interf. Sci., 51, 388.

Iler, R.K. (1979). "The Chemistry of Silica", John Wiley & Sons, New York.

Iler, R.K. (1986). In "Science of Ceramic Chemical Processing", (Hench, L.L. and Ulrich, D.R., Eds.), p. 3-20, John Wiley & Sons, New York.

Inorganic Index to the Powder Diffraction File 1971 (1971). Joint Committee on Powder Diffraction Standards, Easton.

James, P.F. (1988). J. Non-Cryst. Solids, 100, 93.

Jean, J.H. and Ring, T.A. (1986a). Proc. Br. Ceram. Soc., 38, 11.

Jean, J.H. and Ring, T.A. (1986b). Langmuir, 2, 251.

Jenkins, F.A. and White, H.E. (1981). "Fundamentals of Optics", 4th Edition, McGraw-Hill, Tokyo.

Jones, R.A.Y. (1979). "Physical and Mechanistic Organic Chemistry", Cambridge University Press, Cambridge.

Jones, G.E.M. and Hughs, D.L. (1934). J. Chem. Soc., 1197.

Jones, J.B., Sanders, J.V. and Segnit, E.R. (1964). Nature (London), 204, 990.

Jones, W.M. and Fischback, D.B. (1988). J. Non-Cryst. Solids,101,123

Kawaguchi, T., Iura, J., Taneda, N., Hishikura, H. and Kokuba, Y. (1986). J. Non-Cryst. Solids, 82, 50.

Kay, D.H. (1965). "Techniques for Electron Microscopy", 2nd Edition, Alden Press, Oxford.

Kay, B.D. and Assink, R.A. (1988). J. Non-Cryst. Solids, 104, 112.

Keefer, K.D. (1984). In "Better Ceramics Through Chemistry", (Brinker, C.J., Clark, D.E. and Ulrich, D.R., Eds.), Mater. Res. Soc. Symp. Proc. 32, p.15-24, North-Holland, Amsterdam.

Keefer, K.D. (1986a). In "Better Ceramics Through Chemistry II", (Brinker, C.J., Clark, D.E. and Ulrich, D.R., Eds.), Mater. Res. Soc. Symp. Proc. 73, p. 295-304, Mater. Res. Soc., Pittsburgh

Keefer, K.D. (1986b). In "Science of Ceramic Chemical Processing", (Hench, L.L. and Ulrich, D.R., Eds.), p.131-139, John Wiley & Sons, New York.

Khaskin, I.G. (1952). Dokl. Akad. Nauk SSSR, 85, 129.

Kingery, W.D., Bowen, H.K. and Uhlmann, D.R. (1976). "Introduction to Ceramics", 2nd Edition, John Wiley & Sons, New York.

Kirkaldy, J.F. (1973). "Minerals and Rocks", Blandford Press, London.

Kistler, S.S. (1931). Nature (London), 127, 741.

Kistler, S.S. (1932). J. Phys. Chem., 36, 52.

Klein, L.C. (1985). In "Annual Review of Materials Science", Vol.15, p. 227-248, (Huggins, R.A., Ed.), Annual Reviews Inc., Palo Alto.

Klein, L.C., (Ed.), (1988). "Sol-Gel Technology for Thin Films, Fibres, Preforms, Electronics and Specialty Shapes", Noyes Data Corp., New York.

Klein, L.C. and Garvey, G.J. (1984). In "Better Ceramics Through Chemistry", (Brinker, C.J., Clark, D.E. and Ulrich, D.R., Eds.),Mater. Res. Soc. Symp. Proc. 32, p.33-39, North-Holland, Amsterdam.

Knoll, M. (1935). Z. Tech. Physik, 16, 467.

Knoll, M. and Ruska, E. (1932), Ann. Phys. (Leipzig), 12, 607.

Koetzsch, H.J. (1968). Fr. Addn. Patent 92,060.

Kose, A., Ozaki, M., Takano, K., Kobayashi, Y. and Hachisu, S. (1973). J. Coll. Interf. Sci., 44, 330.

Kose, A. and Hachisu, S. (1976). J. Coll. Interf. Sci., 55, 487.

Kozuka, H., Umeda, T., Jin, J.S. and Sakka, S. (1988). In "Better Ceramics Through Chemistry III", (Brinker, C.J., Clark, D.E. and Ulrich, D.R., Eds.), Mater. Res. Soc. Symp. Proc. 121, p. 639-642, Mater. Res. Soc., Pittsburgh.

Krieger, I.M. and O'Neill, F.M. (1968). J. Am. Chem. Soc., 90, 3114.

Kuo, R.J. and Matijevic, E. (1980). J. Coll. Intef. Sci., 78, 407.

LaCourse, W.C. (1984). In "Better Ceramics Through Chemistry", (Brinker, C.J., Clark, D.E. and Ulrich, D.R., Eds.), Mater. Res. Soc. Symp. Proc. 32, p. 53-58, North-Holland, Amsterdam.

LaCourse, W.C., Ahktar, M. MD., Dahar, S., Sands, R.D. and Steinmetz, J. (1983). J. Can. Ceram. Soc., 52, 18.

LaMer, V.K. and Dinegar, R.H. (1950). J. Am. Chem. Soc., 72, 4847.

Lecloux, A.J., Bronckart, J. and Noville, F. (1986). Coll. Surf., 19, 359.

Lee, B.I. and Hench, L.L. (1986). In "Better Ceramics Through Chemistry II", (Brinker, C.J., Clark, D.E. and Ulrich, D.R., Eds.),Mater. Res. Soc. Symp. Proc. 73, p. 815-822, Mater. Res. Soc., Pittsburgh.

Levy, D., Einhorn, S. and Avnir, D. (1989). J. Non-Cryst. Solids, 113, 137.

Le Poole, J.B. (1947). Philips Tech. Rev., 9, 33.

Lewis, P.R. and Knight, D.P. (1982). "Staining Methods for Sectioned Material", North-Holland, Amsterdam.

Li, R. and Hench, L.L. (1988). In "Better Ceramics Through Chemistry III", (Brinker, C.J., Clark, D.E. and Ulrich, D.R., Eds.), Mater. Res. Soc. Symp. Proc. 121, p. 589-592, Mater. Res. Soc., Pittsburgh.

Lyklema, J. (1982). In "Colloidal Dispersions", (Goodwin, J.W., Ed.), p.47-70, Royal Society of Chemistry, Dorchester.

Lynch, D.F. and O'Keefe, M.A. (1972). Acta Cryst., A28, 536.

McDonald, S., Daniels, C. and Davison, J. (1977). J. Coll. Interf. Sci., 50, 342.

MacKenzie, J.D. (1985). J. Non-Cryst. Solids, 73, 631.

MacKenzie, J.D. (1988). J. Non-Cryst. Solids, 100, 162.

McNeill, I.C. (1985). Private Communication.

Magnan, C., (Ed.), (1961). "Traité de Microscopie Electronique", Herman, Paris.

Marks, L.D. and Smith, D.J. (1983). J. Microsc.(Oxford), 130, 249.

Matijevic, E. (1981). Acc. Chem. Res., 14, 22.

Matijevic, E. (1984). In "Ultrastructure Processing of Ceramics, Glasses and Composites", (Hench, L.L. and Ulrich, D.R., Eds.), p. 334-352, John Wiley & Sons, New York.

Matejevic, E. (1987). In "High Tech. Ceramics, Part A", (Vincenzini, P., Ed.), Materials Sci. Mono. 1987, 38A, p. 441-458, Elsevier, Amsterdam.

Matsuzaki, K. Arai, D., Taneda, N., Mukaiyama, T. and Ikemura, M. (1989). J. Non-Cryst. Solids. 112, 437.

Meek, G.A. (1970). "Practical Electron Microscopy for Biologists", Wiley-Interscience, London.

Mehrotra, R.C. (1953). J. Indian Chem. Soc., 30, 585.

Mehrotra, R.C. and Pant, B.C. (1962). J. Indian Chem. Soc., 39, 65.

Messing, G.L., Kumagai, M., Shelleman, A. and McArdle, J.L. (1986a). In "Science of Ceramic Chemical Processing", (Hench, L.L. and Ulrich, D.R. Eds.), p.259-271, John Wiley & Sons, New York.

Messing, G.L., McArdle, J.L. and Shelleman, R.A. (1986b). In "Better Ceramics Through Chemistry II", (Brinker, C.J., Clark, D.E. and Ulrich, D.R., Eds.), Mater. Res. Soc. Symp. Proc. 73, p. 471-480, Mater. Res. Soc., Pittsburgh.

Milne, S.J. (1986). Proc. Br. Ceram. Soc., 38, 81.

Missell, D.L. (1973). Adv. Electron. Electron Phys., (Marton, L., Ed.), Vol. 32, p.63, Academic Press, New York.

Monsanto Chemical Company (1986). Tech. Bull., 53-40(E)ME-2.

Mukherjee, S.P. and Zarzycki, J. (1976). J. Mater. Sci., 11, 341.

Mulder, C.A.M., Van Leeuwen-Stienstra, G., Van Lierop, J.G. and Woerdman, J.P. (1986). J. Non-Cryst. Solids, 82, 148.

Müller, H.O. (1937). Z. Physik, 104, 475.

Mulvey, T. (1967). Proc. Roy. Microsc. Soc., 2, 201.

Murata, Y., Fryer, J.R. and Baird, T. (1976). J. Microsc. (Oxford), 108, 261.

Muse, L.A. (1972). J. Chem. Ed., 49, A463.

Napper, D.H. (1982). In "Colloidal Dispersions", (Goodwin, J.W., Ed.), p. 99-128, Royal Society of Chemistry, Dorchester.

Narain, R.P. and Mehrotra, R.C. (1967). J. Indian Chem. Soc., 44, 208.

Nelson, R.L., Ramsay, J.D.F., Woodhead, J.L., Cairns, J.A. and Crossley, J.A.A. (1981). Thin Solid Films, 81, 329.

Nogami, M. and Moriya, Y. (1980). J. Non-Cryst. Solids, 37, 191.

Oatley, C.W., Nixon, W.C. and Pease, R.F.W. (1965). Adv. Electron. Electron Phys., (Marton, L., Ed.), Vol.21, p.181, Academic Press, New York.

Optiz, J. (1987). Glastech, Ber., 60, 133.

Orcel, G. and Hench, L.L. (1984). In "Better Ceramics Through Chemistry", (Brinker, C.J., Clark, D.E. and Ulrich, D.R., Eds.),Mater. Res. Soc. Symp. Proc. 32, p. 79-84, North-Holland, Amsterdam.

Orcel, G., Phalippou, J. and Hench, L.L. (1986). J. Non-Cryst. Solids, 88, 114.

Orcel, G., Phalippou, J. and Hench, L.L. (1988). J. Non-Cryst, Solids, 104, 170.

Orel, B., Penko, M. and Hadzi, D. (1980). Spectrochim. Acta, 36A, 859.

Ottewill, R.H. (1982). In "Colloidal Dispersion", (Goodwin, J.W., Ed.), p. 143-164, Royal Society of Chemistry, Dorchester.

Partlow, D.P. and Yoldas, B.E. (1981). J. Non-Cryst. Solids, 46, 153.

Peace, B.W., Mayhan, K.G. and Montle, J.F. (1973). Polymer, 14, 420.

Pohl, E.R. and Osterholtz, F.D. (1985). In "Molecular Characterization of Composite Interfaces", (Ishida, H. and Kumar, G., Eds.), p.157, Plenum, New York.

Pope, E.J.A. and MacKenzie, J.D. (1986a). In "Better Ceramics Through Chemistry II", (Brinker, C.J., Clark, D.E. and Ulrich, D.R., Eds.), Mater. Res. Soc. Symp. Proc. 73, p. 809-814, Mater. Res. Soc., Pittsburgh.

Pope, E.J.A. and MacKenzie, J.D. (1986b). J. Non-Cryst. Solids, 87, 185.

Pope, E.J.A. and MacKenzie, J.D. (1988). J. Non-Cryst. Solids, 101, 198.

Rabinovich, E.M., MacChesney, J.B. and Johnson Jr., D.W. (1986). In "Science of Ceramic Chemical Processing", (Hench, L.L. and Ulrich, D.R., Eds.), p. 208-216, John Wiley & Sons, New York.

Ramsay, J.D.F. and Daish, S.R. (1978). Faraday Discussions of the Chemical Society, 65, 65.

Ramsay, J.D.F. and Avery, R.G. (1986). Proc. Br. Ceram. Soc., 38, 275.

Reed, S. and Ashley, C. (1986). In "Better Ceramics Through Chemistry II", (Brinker, C.J., Clark, D.E. and Ulrich, D.R., Eds.), Mater. Res. Soc. Symp. Proc. 73, p.631-634, Mater. Res. Soc., Pittsburgh.

Rees, A.L.G. (1951). J. Phys. Chem., 55, 1340.

Reid, N. (1974). In "Practical Methods in Electron Microscopy", (Glauert, A.M., Ed.), Vol. 3, p.211, North-Holland, Amsterdam.

Ring, T.A. (1987). MRS Bull., 12, No. 7, 34.

Roy, R. (1956). J. Am. Ceram. Soc., 39, 145.

Roy, R. (1969). J. Am. Ceram. Soc., 52, 344.

Roy, R. (1987). Science, 238, 1664.

Roy, D.M. and Roy, R. (1955). Am. Mineral., 40, 147.

Roy, R., Komarneni, S. and Roy, D.M. (1984). In "Better Ceramics Through Chemistry", (Brinker, C.J., Clark, D.E. and Ulrich, D.R., Eds.), Mater. Res. Soc. Symp. Proc. 32, p. 347-359, North-Holland, Amsterdam.

Ruben, G.C. and Shafer, M.W. (1986a). In "Better Ceramics Through Chemistry II", (Brinker, C.J., Clark, D.E. and Ulrich, D.R., Eds.),Mater. Res. Soc. Symp. Proc. 73, p. 207-212, Mater. Res. Soc., Pittsburgh.

Ruben, G.C. and Shafer, M.W. (1986b). Proc. 44th Ann. Meet. Electron Microsc. Soc. Am., (Bailey, G.W., Ed.), p.448, San Fransisco Press, San Fransisco.

Rudberg, E. (1934). Phys. Rev., 45, 764.

Rundle, R.E. and Parasol, M. (1952). J. Chem. Phys., 20, 1487.

Ruska, E. (1980). Microsc. Acta., Suppl. 5 : The Early Development of Electron Lenses and Electron Microscopy, (Mulvey, T., Transl.), Hirzel, Stuttgart.

Sabih, S.M. and Cosslett, V.E. (1974). Phil. Mag., 30, 225.

Sacconi, L., Sabatini, A. and Gans, P. (1964). Inorg. Chem., 3 1772.

Sacks, M.D. and Tseng, T.Y. (1984a). J. Am. Ceram. Soc., 67, 526.

Sacks, M.D. and Tseng, T.Y. (1984b). J. Am. Ceram. Soc., 67, 532.

Sakka, S. (1984). In "Better Ceramics Through Chemistry", (Brinker, C.J., Clark, D.E. and Ulrich, D.R., Eds.), Mater. Res. Soc. Symp. Proc. 32, p.91-99, North-Holland, Amsterdam.

Sakka, S. (1985). J. Non-Cryst. Solids, 73, 651.

Sakka, S. and Kamiya, K. (1982). J. Non-Cryst. Solids, 48, 31.

Sanders, J.V. (1964). Nature (London), 204, 1151.

Sanders, J.V. (1968). Acta Cryst., A24, 427.

Santacesaria, E., Tonello, M., Storti, G., Pace, R.C. and Carra, S. (1986). J. Coll. Interf. Sci., 111, 44.

Satterfield, C.N. (1980). "Heterogeneous Catalysis in Practice", McGraw Hill, New York.

Sax, N.I. (1984). "Dangerous Properties of Industrial Materials", 6th Edition, Van Nostrand Reinhold, New York.

Schaefer, D.W. and Keefer, K.D. (1984). In "Better Ceramics Through Chemistry", (Brinker, C.J., Clark, D.E. and Ulrich, D.R., Eds.), Mater. Res. Soc. Symp. Proc. 32, p. 1-14, North-Holland, Amsterdam.

Scherer, G.W. (1985). J. Non-Cryst. Solids, 73, 661.

Scherer, G.W. (1986a). J. Non-Cryst. Solids, 87, 199.

Scherer, G.W. (1986b). In "Better Ceramics Through Chemistry", (Brinker, C.J., Clark, D.E. and Ulrich, D.R., Eds.), Mater. Res. Soc. Symp. Proc. 73, p. 225-230, Mater. Res. Soc., Pittsburgh.

Scherer, G.W. (1987). Yogo-Kyokai-Shi, 95, 21.

Scherer, G.W. (1988a). In "Better Ceramics Through Chemistry III", (Brinker, C.J., Clark, D.E. and Ulrich, D.R., Eds.), Mater. Res. Soc. Symp. Proc. 121, p. 179-186, Mater. Res. Soc., Pittsburgh.

Scherer, G.W. (1986b). J. Non-Cryst. Solids, 99, 324.

Scherzer, D. (1949). J. Appl. Phys., 20, 20.

Schlichting, J. and Neumann, S. (1982). J. Non-Cryst. Solids, 48, 185.

Schmidt, H. (1984). In "Better Ceramics Through Chemistry", (Brinker, C.J., Clark, D.E. and Ulrich, D.R., Eds.), Mater. Res. Soc. Symp. Proc. 32, p.327-335, North-Holland, Amsterdam.

Schmidt, V., Hillerbrand, R., Albrecht, R., Neumann, W. and Muller, B. (1985). Ultramicroscopy, 17, No. 4, 357.

Schmidt, H. and Seiferling, B. (1986). In "Better Ceramics Through Chemistry II", (Brinker, C.J., Clark, D.E. and Ulrich, D.R., Eds.),Mater. Res. Soc. Symp. Proc. 73, p. 739-750, Mater. Res. Soc., Pittsburgh.

Schrödinger, E. (1926). Ann. Physik. 81, 109.

Schubert, V., Rose, K. and Schmidt, H. (1988). J. Non-Cryst. Solids,105,165.

Scott, K.T. and Woodhead, J.L. (1982). Thin Solid Films, 95, 219.

Segal, D.L. (1980). Atomic Energy Research Establishment Report, AERE R 9721.

Segal, D.L. (1984). J. Non-Cryst. Solids. 63, 183.

Segal, D.L. (1985a). Atomic Energy Research Establishment Report, AERE M 3519.

Segal, D.L. (1985b). Atomic Energy Research Establishment Report AERE R 12018.

Segal, D.L. (1986). Private Communication.

Segal, D.L. (1989a). "Chemical Synthesis of Advanced Ceramic Materials", Cambridge University Press, Cambridge.

Segal, D.L. (1989b). Chem. Brit., 25, 151.

Segal, D.L. and Woodhead, J.L. (1986). Br. Ceram. Proc., 38, 245.

Seitz, F. and Koehler, J.S. (1956). Solid State Phys., 2, 303.

Sharma, R., Barry, J. and Eyring, L. (1987). Ultramicroscopy, 23, 453.

Shiihavam, I., Schwartz Jr., W.T. and Post, H.W. (1961). Chem. Rev., 61, 1.

Shukla, B.S. and Johari, G.P. (1988). J. Non-Cryst. Solids, 101, 263.

Skjeltorp, A.T., Ugelstad, J. and Ellingsen, T. (1986). J. Coll. Interf. Sci., 113, 577.

Sidgwick, N.V. (1924). J. Chem. Soc., 125, 2672.

Sixtus, K. (1929). Ann. Physik, 3, 1017.

Smith, K.C.A. and Oatley, C.W. (1955). J. Appl. Phys., 6, 391.

Smith, D.J., Camps, R.A., Freeman, L.A., Hill, R., Nixon, W.C. and Smith, K.C.A. (1983a). J. Microsc. (Oxford), 130, 127.

Smith, D.J., White, D., Baird, T. and Fryer, J.R. (1983b). J. Catal., 81, 119.

Smith, D.J., Camps, R.A., O'Keefe, M.A., Saxton, W.O. and Woods, G.J. (1985). Ultramicroscopy, 18, 63.

Smith, D.J., McCartney, M.R. and Bursil, L.A. (1987). Ultramicroscopy, 23, 299.

Spence, J.C.H. (1980). "Experimental High-Resolution Electron Microscopy", Clarendon, Oxford.

Stark, J.G. and Wallace, H.G. (1982). "Chemistry Data Book", 2nd Edition, John Murry, London.

Stöber, W., Fink, A. and Bohn, E. (1968). J. Coll. Interf. Sci. 26, 62.

Strawbridge, I., Craievich, A.F. and James, P.F. (1985). J. Non-Cryst. Solids, 72, 139.

Sugimoto, T. (1987). Adv. Coll. Interf. Sci., 28, 65.

Tan, C.G., Bowen, B.D. and Epstein, N. (1987). J. Coll.. Interf. Sci., 118, 290.

Tewari, P.H., Hunt, A.J., Lofftus, K.D. and Lieber, J.G. (1986). In "Better Ceramics Through Chemistry III", (Brinker, C.J., Clark,D.E. and Ulrich, D.R., Eds.), Mater. Res. Soc. Symp. Proc. 121, p. 195-205, Mater. Res. Soc., Pittsburgh.

Thomas, I.L. and McCorkle, K.H. (1971). J. Coll. Interf. Sci., 36, 110.

Thomson, G.P. and Reid, A. (1927). Nature (London), 119, 890.

Tohge, N. and Minami, T. (1989). J. Non-Cryst. Solids, 112, 432.

Turova, N.Y., Novoselova, A.V. and Semeneko, K.N. (1959). Zh. Neorg. Khim., 4, 997.

Uhlmann, D.R., Zelinski, B.J.J. and Wnek, G.E. (1984). In "Better Ceramics Through Chemistry", (Brinker, C.J., Clark, D.E. and Ulrich, D.R., Eds.), Mater. Res. Soc. Symp. Proc. 32, p. 59-70, North-Holland, Amsterdam.

Ulrich, D.R. (1988). J. Non-Cryst. Solids, 100, 174.

Van Helden, A.K., Jansen, J.W. and Vrij, A. (1981). J. Coll. Interf. Sci. 81, 354.

Visca, M. and Matijevic, E. (1979). J. Coll. Interf. Sci., 63, 308.

Von Ardenne, M. (1938). Z. Physik, 109, 553.

Vorankov, M.G., Mileshkevich, V.P. and Yuzhelevski, Y.A. (1978). "The Siloxane Bond", Consultants Bureau, New York.

Wang, S.H. and Hench, L.L. (1986). In "Science of Ceramic Chemical Processing", (Hench, L.L. and Ulrich, D.R., Eds.), p.201-207, John Wiley & Sons, New York.

Warren, B.E. (1937). J. Appl. Phys., 8, 645.

Watt, I.M. (1985). "The Principles and Practice of Electron Microscopy", Cambridge University Press, Cambridge.

Weast, R.C., (Ed.), (1972). "Handbook of Chemistry and Physics", Chemical Rubber Co., Cleveland.

Wells, A.F. (1984). "Structural Inorganic Chemistry", 5th Edition, Clarendon Press, Oxford.

Wenzel, J. (1985). J. Non-Cryst. Solids, 73, 693.

Weres, O., Yee, A. and Tsao, L. (1981). J. Coll. Interf. Sci., 84, 379.

West, A.R. (1985). "Solid State Chemistry and its Applications", John Wiley & Sons, Chichester.

Whelan, M.J. (1959). Inst. Metals, 87, 392.

White, D., Baird, T., Fryer, J.R., Freeman, L.A. and Smith D.J. (1983). J. Catal., 81, 119.

Williams, D.B. (1984). "Practical Analytical Electron Microscopy in Materials Science", Verlag Chemie International, Deerfield Beach.

Williams, R.C. and Fisher, H.W. (1970). J. Mol. Biol., 52, 121.

Williams, D.H. and Fleming, I. (1980). "Spectroscopic Methods in Organic Chemistry", 3rd Edition, McGraw-Hill, Maidenhead.

Wischnitzer, S. (1981). "Introduction to Electron Microscopy", 3rd Edition, Pergamon, New York.

Wolfe, R.J. and Joy, D.C. (1971). Electron Microsc. Anal. (Nixon, W.C., Ed.), Inst. Phys. Conf. Ser., No. 10, p.34, London.

Woodhead, J.L. (1972). Silicates Industriels, 37, 191.

Woodhead, J.L. (1974). Brit. Patent, 1 342 893.

Woodhead, J.L. (1975). Brit. Patent, 1 412 937.

Woodhead, J.L. (1984). J. Mater. Ed., 6, 887.

Woodhead, J.L. and Segal, D.L. (1984). Chem. Brit., 20, 310.

Wu, E., Chen, K.C. and MacKenzie, J.D. (1984). In "Better Ceramics Through Chemistry", (Brinker, C.J., Clark, D.E. and Ulrich, D.R., Eds.), Mater. Res. Soc. Symp. Proc. 32, p. 169-174, North-Holland, Amsterdam.

Yamane, M., Caldwell, J.B. and Moore, D.T. (1986). In "Better Ceramics Through Chemistry II", (Brinker, C.J., Clark, D.E. and Ulrich, D.R., Eds.), Mater. Res. Soc. Symp. Proc. 73, p. 765-768, Mater. Res. Soc., Pittsburgh..

Yoldas, B.E. (1977). J. Mater. Sci., 12, 1203.

Yonezawa, A., Nakagawa, S. and Suzuki, M. (1977). Proc. 35th Ann. Meet. Electron Microsc. Soc. Am., (Bailey, G.W., Ed.), p.62, Claitor, Baton Rouge.

Yu, P., Liu, H. and Wang, Y. (1982). J. Non-Cryst. Solids. 52, 511.

Zachariasen, W.H. (1932). J. Appl. Phys., 54, 3841.

Zarzycki, J. (1986). In "Science of Ceramic Chemical Processing", (Hench, L.L. and Ulrich, D.R., Eds.), p.21, John Wiley & Sons, New York.

Zelinski, B.J.J. and Uhlmann, D.R. (1984). J. Phys. Chem. Solids, 45, 1069.

Zworykin, V.K., Hillier, J. and Snysder, R.L. (1942). Bull. ASTM, 117, 15.

Zworykin, V.K., Morton, G.A., Rambery, E.G., Hillier, J. and Vance, E.W. (1945). "Electron Optics in the Electron Microscope", Wiley, New York.